Modelling FKRP and Fukutin Deficiency in Zebrafish

A thesis submitted for the degree of Doctor of Philosophy at Newcastle University

November 2012

Alasdair John Wood

Institute of Genetic Medicine

Abstract

Deficiency in fukutin-related protein (FKRP) or fukutin results in aberrant glycosylation of α-dystroglycan, a key receptor for basement membrane proteins. There is a broad spectrum of disorders associated with FKRP and fukutin deficiency, ranging from limb-girdle muscular dystrophy to congenital disorders such as muscle eye brain disease and Walker-Warburg syndrome (WWS). fkrp and fukutin were knocked down in the zebrafish with antisense morpholino oligonucleotides (MO). The fkrp, fukutin and dystroglycan MOs each produced a spectrum of comparable phenotypes. With each MO producing a comparable morphant phenotype on morphological examination, it was hypothesised that inferences could be made about similarities and differences in the fkrp, fukutin dystroglycan axis during zebrafish development. The morphants had abnormal muscle fibres, including disruptions of the vertical myosepta and sarcolemma. Disorganised retinal layering in the eyes was found in both fukutin and fkrp morphants. Dysplasia of the lens was observed in most fukutin morphants and some of the fkrp morphants with a severe phenotype. Structural changes in basement membranes at 1-3 days post fertilisation (dpf) were investigated. The perturbation observed across the inner limiting membranes may account for the lens dysplasia. Cell density of the granular epithelium in the photoreceptor cell layer was found to be lower in both morphants with the least density in fukutin knock-downs, which may result from a disruption of the external limiting membrane. This leads to the conclusion that fkrp and fukutin are essential for membrane integrity in the eye and muscle of developing zebrafish. A transgenic zebrafish line expressing enhanced green fluorescent protein (EGFP) in vascular endothelium from the fli-1 promoter was used to investigate early vascularisation. In all morphants, including dystroglycan knock downs, the intersegmental vessels failed to reach the dorsal longitudinal anastomotic vessel at 1dpf. Additionally, in the fkrp and fukutin morphant the eye vasculature was abnormal. Interestingly, no change was observed in the eye vasculature of the dystroglycan morphants suggesting that fkrp and fukutin may modify proteins other than α-dystroglycan in the eye.

Acknowledgements

MRC | Centre for Neuromuscular Diseases

3

Contents

List of Figures

List of Tables

List of Abbreviations

ACHR	Acetylcholine receptors
BLAST	Basic local alignment search tool
bp	Base pairs
BSA	Bovine serum albumin
BM	Basement membrane
CoMO	Control morpholino
CoDA	Context dependant assembly
CMD	Congenital muscular dystrophy
CK	Creatine Kinase
DG	Dystroglycan
DGC	Dystrophin associated glycoprotein complex
dH$_2$O	Distilled Water
dNTP	Deoxyribonucleotide triphosphate
DMD	Duchenne muscular dystrophy
dpf	Days post fertilisation
E(#)	Embryonic stage (mice)
EBD	Evans blue dye
ECM	Extracellular matrix
EDTA	Ethylenediaminetetraacetic acid
EGF	Epidermal growth factor
EGFP	Enhanced green fluorescent protein
ELM	External limiting membrane
ENU	*N*-ethyl-*N*-nitrosourea
ES (cell)	Embryonic stem (cell)
FCMD	Fukuyama congenital muscular dystrophy
FKRP	Fukutin related protein
GCL	Ganglion cell layer
GFAP	Glial fibrillary acidic protein

H&E	Hematoxylin and eosin
HEPES	4-(2-hydroxyethyl)-1-piperazineethanesulfonic acid
hpf	Hours post fertilisation
IFN	Interferon
IL	Interleukin
ILM	Inner limiting membrane
INL	Inner nuclear layer
IPL	Inner plexiform layer
LG	Laminin globulin domain
LGMD	Limb girdle muscular dystrophy
MD	Muscular dystrophy
MEB	Muscle eye brain disease
MO	Antisense morpholino oligonucleotide
MTJ	Myotendinous junction
NMJ	Neuromuscular junction
nNOS	neuronal Nitric oxide synthase
OMIM	Online Mendelian inheritance in man
ONL	Outer nuclear layer
OPL	Outer plexiform layer
OPEN	Oligomerized pool engineering
PBS	Phosphate buffered saline
PBST	Phosphate buffered saline Tween-20
PCR	Polymerase chain reaction
PFA	Paraformaldehyde
PPM	Parts per million
PTU	1-phenyl-2-thiourea
RGC	Retinal Ganglion Cell
rpm	Revolutions per minute
RT	Room temperature

SDS	Sodium dodecyl sulphate
SEM	Scanning electron microscopy
shRNA	Short hairpin RNA
TALEN	Transcription activator-like effector nuclease
TBS	Tris buffered saline solution
TBST	TBS Tween20
TEM	Transmission electron microscopy
Tet	Tetracycline
TF	Transcription factor
TG	Transgenic
TGF-β	Transforming growth factor-β
TNF-α	Tumour necrosis factor-α
TRE	Tetracycline response elements
VEC	Vascular endothelial cell
WWS	Walker Warburg Syndrome
ZFN	Zinc Finger Nuclease
ZIRC	Zebrafish International Resource Centre
ZMP	Zebrafish mutation project

Chapter 1   Introduction

1.1 Muscular Dystrophy

The muscular dystrophies (MDs) are a heterogeneous group of inherited conditions characterised by progressive muscle weakness and wasting (Walton and Nattrass, 1954; Bushby, 1994). The latter occurs as a consequence of degeneration, fatty infiltration and fibrosis of muscle tissue (Bushby, 1994; Kornegay *et al.*, 2012). Duchenne muscular dystrophy (DMD) is one of the most common forms of MD and in spite of better standards of care over recent times, it remains associated with a bleak prognosis with most patients dying in their early twenties due to cardio-respiratory complications (Sejerson and Bushby, 2009; Kuru, 2011; Kwon *et al.*, 2012). Nevertheless, there have recently been promising developments in new therapies such as exon skipping which is currently being trialled in several centres including Newcastle (Mann *et al.*, 2001; Kinali *et al.*, 2009; Foster *et al.*, 2012). One would hope that similar therapies will become available in other forms of MD, including the dystroglycanopathies, which like most MDs remain without treatment (Godfrey *et al.*, 2011; Kuga *et al.*, 2011; Muntoni *et al.*, 2011). The aim of this thesis is to gain a better insight into MD by investigating the pathology associated with dystroglycanopathy in zebrafish models (Bassett and Currie, 2003; Guyon *et al.*, 2003; Bassett and Currie, 2004; Guyon *et al.*, 2007).

It was hypothesised that by knocking down the secondary dystroglycanopathy genes *fkrp fukutin* and comparing to primary dystroglycanopathy, as modelled by *dystroglycan* knockdown, the function of these genes with respect to the primary function of dystroglycan could be delineated.

1.1.1 Duchenne Muscular Dystrophy

DMD is an X-linked recessive disorder, affecting 1/3600 male births (Cowan *et al.*, 1980). Frame shifting or nonsense mutations in the DMD gene (Hoffman *et al.*, 1987) on the X-chromosome p21.2-21.1 result in absence of dystrophin expression and a DMD phenotype (OMIM: 310200), however mutations which preserve the open reading frame result in partial protein expression and a milder form of disease, Becker muscular dystrophy BMD (OMIM: 300376) (Nicholson *et al.*, 1993). DMD is named after the neurologist Guillaume Duchenne de Boulogne who was the first clinician to accurately describe the disease in a case report, in the 1861 edition of his book "Paraplegie hypertrophique de l'enfance de cause cerebrale" (Semmola, 1834; Conte G,

1836; Emery, 1993). DMD is still characterised clinically based on these early descriptions that include progressive proximal weakness, pseudo-hypertrophy of the calves and elevated serum creatine kinase (CK) levels, a marker of skeletal and cardiac muscle breakdown (Bach, 2000; Manzur and Muntoni, 2009).

1.1.2 Limb Girdle Muscular Dystrophy (LGMD)

Before genetic testing became available, myopathies were classified based on their clinical presentation (Broglio *et al.*, 2010; Rocha and Hoffman, 2010). The LGMDs were delineated from facioscapulohumeral muscular dystrophy (FSHD), myotonic dystrophy and metabolic myopathies based on the distinct proximal wasting and weakness observed around the shoulder and hip girdles (Walton and Nattrass, 1954; Deufel and Gerbitz, 1991; Reifer and Sobel, 1998; Tawil and Van Der Maarel, 2006). Within the LGMD subgroup, there is a wide range of variation in terms of disease onset and progression (Rocha and Hoffman, 2010). LGMDs are classified into autosomal dominant (type 1) or recessive (type 2) forms, the former being much rarer (Walton and Nattrass, 1954). There are at least eight forms of dominant LGMD, for some of which the gene has not yet been identified (Rocha and Hoffman, 2010; Kaplan, 2011; Reilich *et al.*, 2011). Sixteen forms of autosomal recessive LGMD have been identified to date (Kaplan, 2011). Mutations in FKRP and fukutin both have been associated with autosomal recessive limb-girdle forms (Table 1.1). The sequence in which the disorders appear in the alphabetical list is based on the order in which they were discovered (Bushby, 2009; Kaplan, 2011).

1.1.3 Congenital Muscular Dystrophy (CMD)

Since infants born with hypotonia and weakness could have any one of a number of conditions, a muscle biopsy is helpful in reaching a diagnosis of CMD (Bertini *et al.*, 2011). CMD is differentiated from the clinically similar conditions such as the congenital myopathies by higher serum CK levels and evidence of degeneration/regeneration cycles in the myofibres, whereas the congenital myopathies have developmental defects in myofibre formation (North, 2011; Sparks and Escolar, 2011; Nance *et al.*, 2012). A final molecular diagnosis is important for refining the particular subtype of CMD. All of the CMDs have an autosomal recessive pattern of inheritance and can be divided into three groups: disorders of post translational modification of α-dystroglycan (secondary

dystroglycanopathies), abnormality of endoplasmic reticulum proteins and disorders of the basal lamina (Mendell *et al.*, 2006; Rocha and Hoffman, 2010).

Protein	Gene Symbol	Gene Location	Disease	IH	OMIM	Reference
Cytoskeletal Proteins						
Dystrophin	DMD	Xp21.2	DMD BMD	XR XR	300377 300376	(Monaco *et al.*, 1986)
Basement Membrane Receptors						
Dystroglycan	DAG1	3p21.31	LGMD	AR	128239	(Hara *et al.*, 2011)
Integrin	ITAG7	12q13.2	CMD	AR	600536	(Mayer *et al.*, 1997)
Dystroglycan Post Translational Modifiers						
Fukutin	FKTN	9q31	FCMD LGMD2M	AR AR	253800 607440	(Toda *et al.*, 1993) (Godfrey *et al.*, 2006)
FKRP	FKRP	19q13.3	LGMD2I MDC1C MEB WWS	AR AR AR AR	607155 606612 253280 236670	(Brockington *et al.*, 2001b) (Brockington *et al.*, 2001a) (Mercuri *et al.*, 2006)
POMT1	POMT1	9q34.1	WWS LGMD2K	AR AR	236670 609308	(Beltran-Valero de Bernabe *et al.*, 2002) (Balci *et al.*, 2005)
POMT2	POMT2	14q24.3	WWS MEB	AR AR	236670 253280	(van Reeuwijk *et al.*, 2005) (Mercuri *et al.*, 2006)
POMGnT1	POMGnT1	1p34-p33	MEB	AR	253280	(Hehr *et al.*, 2007)
LARGE	LARGE	22q12-q13	MDC1D	AR	608840	(Longman *et al.*, 2003)
ISPD	ISPD	7p21.2	WWS	AR	614631	(Roscioli *et al.*, 2012; Willer *et al.*, 2012)
Extracellular Matrix Proteins						
Laminin	LAMA2	6q22	MDC1A	AR	156225	(Patton *et al.*, 2008)

Table 1.1: Dystroglycan associated proteins and the diseases associated with mutations in the genes

The table is divided into mutations in proteins of the cytoskeleton, basement membrane receptors, modifiers of dystroglycan post translational processing and extracellular matrix proteins, all of which have been associated with MD. The table gives the protein, its gene symbol, genomic location, disease, mode of inheritance: (IH, AR: autosomal recessive, XR: X-linked recessive), OMIM and a reference describing the clinical phenotype. DMD and BMD account for ~10% each of MD in the Northern Region of the United Kingdom with a prevalence of ~7-8/100,000. There has only been one case in the world with a mutation in the DAG1 gene (Hara *et al.*, 2011). In the Northern region ~6%, 2.5/100,000 of patients were diagnosed with LGMD of total MD in the region interestingly 19% were diagnosed with LGMD2I. 2%, 0.8/100,000 of the

population in the North East with MD had CMD and the majority of these patients were diagnosed with MDC1A 1.6% 0.6/100,000 (Norwood *et al.*, 2009).

1.2 Dystrophin

The disease causing gene in DMD was localized to Xp21 by genetic linkage analysis and cytologically through manifesting females with balanced translocations (Davies *et al.*, 1983; Aldridge *et al.*, 1984; Brown *et al.*, 1985; Francke *et al.*, 1985; Boyd and Buckle, 1986). Subsequently, the DMD gene was identified from cloned cDNA (Monaco *et al.*, 1985), the protein product was isolated shortly after by Hoffman *et al.* (Monaco *et al.*, 1986; Hoffman *et al.*, 1987). Campbell and Kahl purified a dystrophin associated membrane bound glycoprotein known today as dystroglycan and together the discovery of the two proteins allowed rapid progress in the field of MD, (Campbell and Kahl, 1989; Ervasti and Campbell, 1991). These discoveries and subsequent characterisation of the dystrophin-associated glycoprotein complex (DGC) forms the basis of our current understanding of MD (Sciandra *et al.*, 2003; Gumerson and Michele, 2011). Dystrophin is a predominantly hydrophilic, rod shaped protein consisting of 3684 amino acids, with a molecular weight (MW) of 427kDa and an approximate length of 150nm (Hoffman *et al.*, 1987; Pons *et al.*, 1990). The protein can be split into four domains: the actin binding domain at the N-terminus, the rod domain, the cysteine rich domain and the carboxy terminal domain (Koenig and Kunkel, 1990; Winder *et al.*, 1995; Rybakova *et al.*, 1996; Sadoulet-Puccio *et al.*, 1997; Norwood *et al.*, 2000; Harper *et al.*, 2002; Bohm and Roberts, 2009; Le Rumeur *et al.*, 2010).

While screening a batch of C57BL/10ScSn mice the spontaneously occurring *mdx* mouse was identified, initially studied as a biochemical variant at the PK locus (Bulfield *et al.*, 1984). Elevated pyruvate kinase and raised serum CK indicated the mice had muscle necrosis analogous to DMD patients (Banks and Chamberlain, 2008). Breeding experiments showed an X-linked segregation. The *mdx* mouse carries a point mutation in exon 23 of the *Dmd* gene and is an effective null for dystrophin protein expression at birth (De la Porte *et al.*, 1999). A feature of the model is that exon 23 is prone to skipping and over time many fibres revert, similar to the revertant fibres found in humans (Thanh *et al.*, 1995; Yokota *et al.*, 2006). Utrophin upregulation, differences in mouse immune systems when compared to humans and longer telomerase length in mice, also

all account for the diminished phenotype severity compared to human DMD (Brockdorff *et al.*, 1987; Kipling, 1997; Gillis, 2000).

1.3 The Dystrophin Associated Glycoprotein Complex (DGC)

Dystrophin forms an integral part of a stable protein complex at the muscle cell membrane: the dystrophin-associated glycoprotein complex (DGC; Haenggi and Fritschy, 2006). The main function of the DGC in muscle is to form a link between cytoskeletal actin and laminin in the extracellular matrix (ECM; Ervasti and Campbell, 1991; Lapidos *et al.*, 2004; Figure 1.1). The DGC is essential for stabilising the sarcolemma *i.e.* the plasma membrane that encloses a muscle fibre, during muscle contraction (Ibraghimov-Beskrovnaya *et al.*, 1992; Petrof *et al.*, 1993). Dystrophin binds to the actin cytoskeleton and to β-dystroglycan at the sarcolemma (Jung *et al.*, 1995; Ishikawa-Sakurai *et al.*, 2004). Dystroglycan spans the sarcolemma, anchoring the DGC complex to the muscle specific basement membrane and acts as a linker between internal and external components. Dystroglycan stabilises the sarcoglycan complex within the sarcolemma (Lim and Campbell, 1998; Crosbie *et al.*, 1999; Durbeej *et al.*, 2000). In healthy muscle correctly glycosylated α-dystroglycan binds laminin-α2 and various other ligands such as agrin, neurexin and perlecan (Noonan *et al.*, 1991; Campanelli *et al.*, 1994; Gee *et al.*, 1994; Sugiyama *et al.*, 1994; Denzer *et al.*, 1997; Hohenester *et al.*, 1999; Sugita *et al.*, 2001; Michele *et al.*, 2002). Other intracellular components of the DGC include the syntrophins and dystrobrevin (Froehner *et al.*, 1997; Sadoulet-Puccio *et al.*, 1997; Adams *et al.*, 2004; Fuentes-Mera *et al.*, 2006; Bohm and Roberts, 2009; Figure 1.1). Dystrophin and the DGC are also associated with nitric oxide synthase (nNOS; Crosbie, 2001). Nitric oxide synthase catalyzes the synthesis of the potent signalling molecule nitric oxide from L-arginine (Thomas *et al.*, 2003; Kobayashi *et al.*, 2008). Elevation of local calcium levels leads to calmodulin binding NOS and NO synthesis (Walsh, 1994). NO has been shown to be important in muscle for metabolism, inflammation, vasodilatation and contractility (Reid, 1998; Wang *et al.*, 2001).
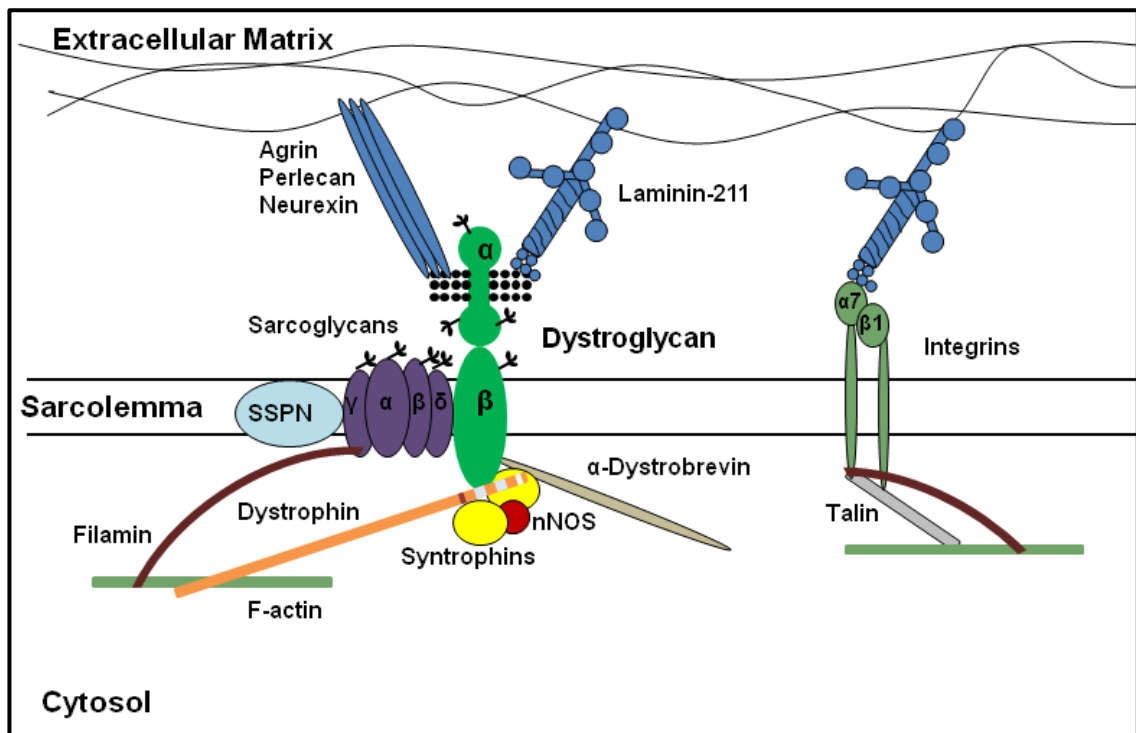
Figure 1.1: Schematic representation of the DGC
Depicts dystroglycan and integrin interaction with ligands both within the DGC and the ECM. The DGC forms a link between intracellular F-actin and laminin-211 in the extracellular matrix. The black circles on dystroglycan represent the *O*-glycosylated mucin domain of α-dstroglycan and the black branched structures represent *N*-glycosylation sitses also found on the sarcoglycans and β-dystroglycan (Cohn and Campbell, 2000; Barresi and Campbell, 2005).

1.3.1 Dystroglycan

Dystroglycan is the central component of the DGC (Ervasti and Campbell, 1991; Figure 1.1). The dystroglycan gene (DAG1) on chromosome 9p21 has two exons split by a large intronic segment which contain an 895 codon open reading frame encoding both alpha and beta peptides (Ibraghimov-Beskrovnaya *et al.*, 1993; Gorecki *et al.*, 1994). The propeptide is translated from a single mRNA and proteolytically cleaved into the core protein of the heavily glycosylated extracellular α-dystroglycan and the transmembrane β-dystroglycan (Ibraghimov-Beskrovnaya *et al.*, 1992; Holt *et al.*, 2000). After post translational cleavage of the precursor polypeptide the two subunits are independently targeted to either the plasma membrane or the extracellular space respectively, where they re-assemble into a complex held together by a relatively weak non-covalent interaction (Bozzi *et al.*, 2006). Mutating the cleavage site inhibits post-translational processing leading to dystrophic changes in a mouse model (Jayasinha *et al.*, 2003).

The β-dystroglycan PPXY motif interacts with the WW domains of dystrophin (Rentschler *et al.*, 1999). Extracellularly the central *O*-glycosylated mucin domain of α-dystroglycan binds the LG domain of the extra-cellular matrix (ECM) protein laminin, linking the ECM to the intracellular cytoskeleton of the skeletal muscle syncytium (Figure 1.1; Jung *et al.*, 1995). α-Dystroglycan is extensively post-translationally modified by *O-* and *N-* linked glycosylation (Brancaccio *et al.*, 1995; Brancaccio *et al.*, 1997) in the Golgi complex. The glycosylation state of α-dystroglycan is tissue specific and variable, resulting in a range of α-dystroglycan glycoforms, differing in molecular weight and glycan composition (Moukhles *et al.*, 2000; McDearmon *et al.*, 2001). The first major glycoform (cranin) was identified in brain and has a molecular mass of 120kDa (Smalheiser and Schwartz, 1987). In skeletal muscle the major glycoform is 36kDa larger than that found in brain as a result of tissue specific *O*-glycosylation (Ibraghimov-Beskrovnaya *et al.*, 1993; Barresi and Campbell, 2005).

1.3.2 Glycosylation

In eukaryotes many cellular proteins and almost all extracellular proteins are post-translationally modified to contain glycans (Spiro, 2002; Moremen *et al.*, 2012). These carbohydrate moieties can have widely diverse functions, from altering protein stability and conformation to defining molecular recognition (Endo, 1999). Glycosylation is generally considered to be the most complex post translational modification because of the large number of steps in the process, usually requiring a number of enzymes (Spiro, 1973). The enzymes which drive glycosylation are segregated into different compartments including the rough endoplasmic reticulum, cristernae of the Golgi apparatus, cytoplasm and nucleus (Opat *et al.*, 2001; Spiro, 2002).
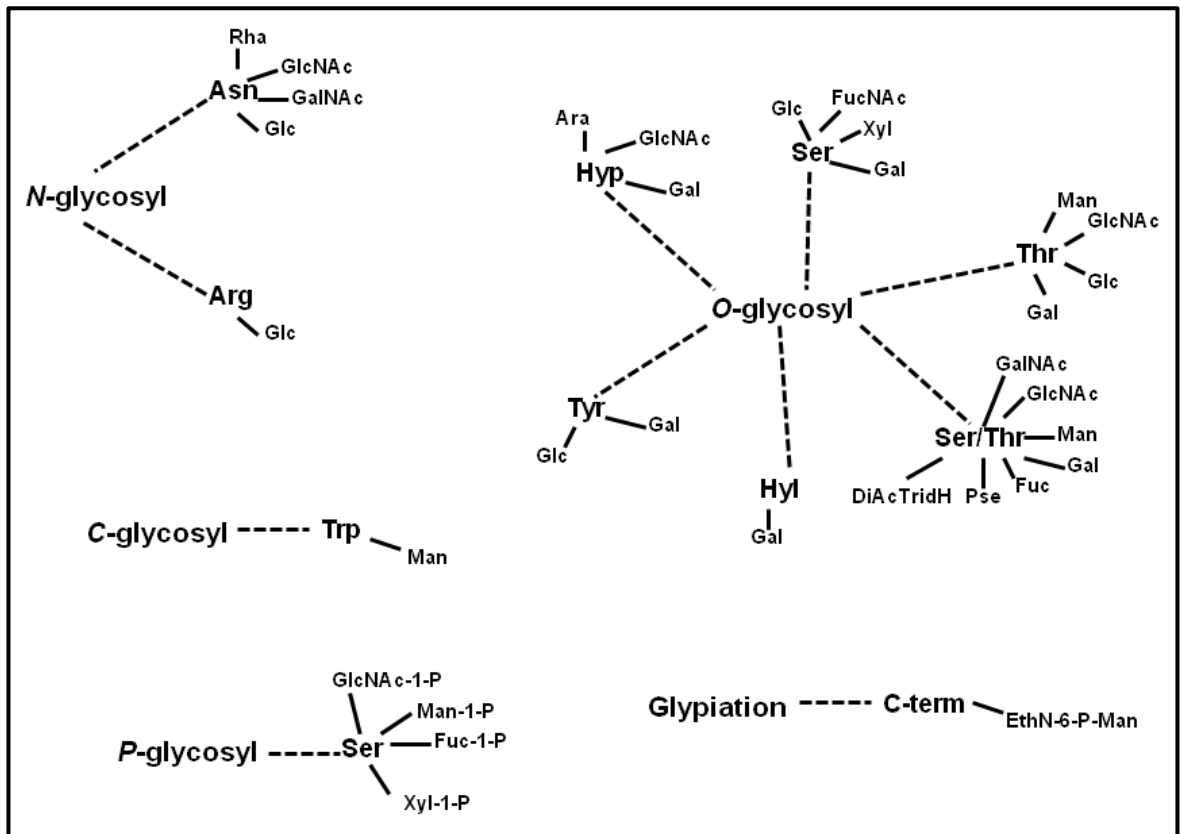
Figure 1.2: Schematic of the five types of sugar-peptide bond
The schematic highlights how different types of glycosylation, O-glycosylation, N-glycoslation phosphor-glycosylation, C-linked glycosylation and glypiation can produce a range glycotopes at the first glycosylation event, (Spiro, 2002).

Sugar chains are classified into one of two major classes, O-glycans and N-glycans. There are three other less relevant classes of glycans: phosphor-glycans, C-linked glycans and glypiation which will not be discussed here (Spiro, 2002; Figure 1.2). O-glycans are attached to the hydroxyl group of serine, threonine, tyrosine, hydroxylysine or hydroxyproline residues. N-linked glycans attach to the amine group of asparagine or arginine residues. O-linked glycosylation occurs predominantly in the Golgi whereas N-linked glycosylation occurs with greatest frequency in the lumen of the endoplasmic reticulum (ER) (Schwarz and Aebi, 2011; Stalnaker et al., 2011). The secondary dystroglycanopathy genes are all involved in the O-glycosylation of α-dystroglycan are found in the ER (POMT1, POMT2) and the Golgi (POMTGnT1, fukutin, FKRP and LARGE; Takada et al., 1988; Esapa et al., 2002; Brockington et al., 2005; Keramaris-Vrantsis et al., 2007; Goder and Melero, 2011; Lynch et al., 2012; Figure 1.3).
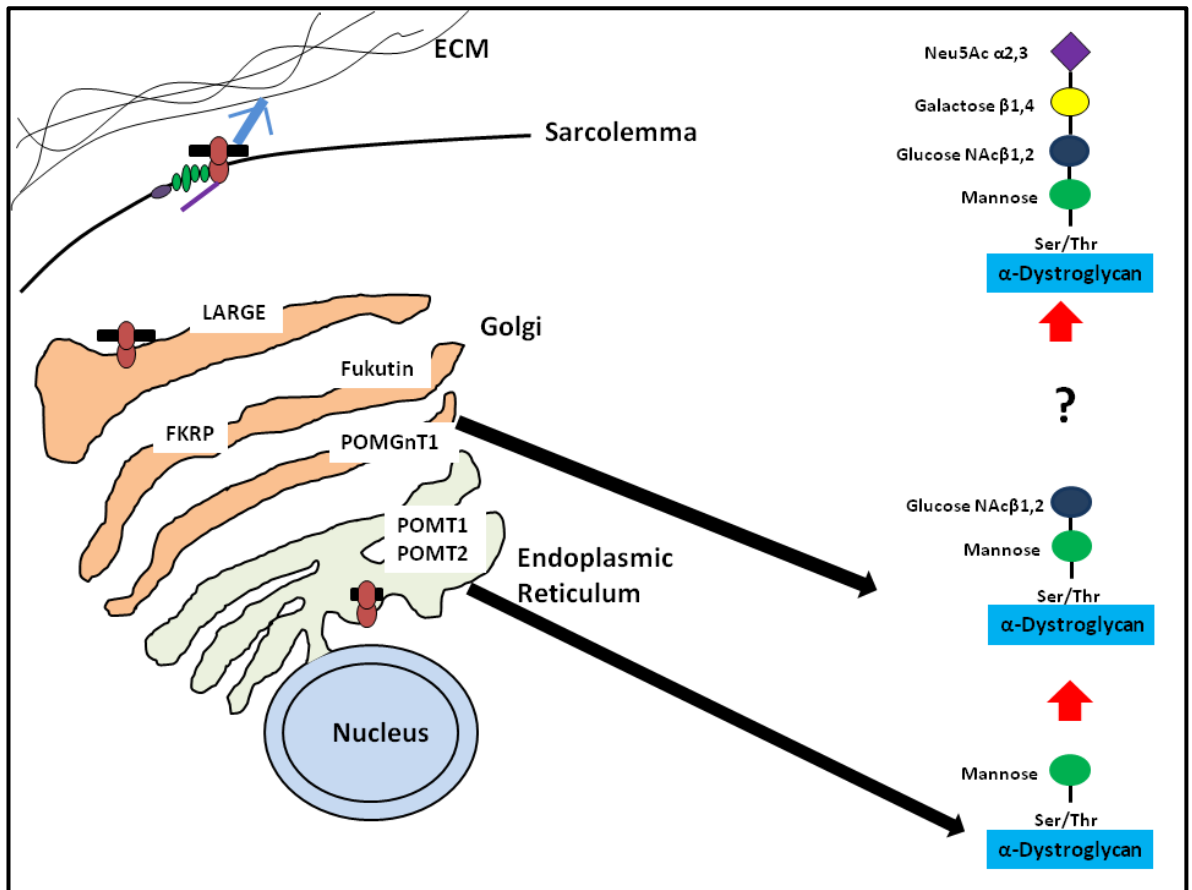
Figure 1.3: Cellular localisation of secondary dystroglycanopathy proteins and how they relate to the glycosylation of α-dystroglycan
As α-dystroglycan moves through the ER and Golgi complex glycans are bound to form the classical glycan tetramer of the mucin domain. The POMT1 and POMT2 complex mannosylate α-dystroglycan and glucose is bound by POMGnT1 to the mannose. It is currently unknown which glycosyltransferases are responsible for the final two glycosylation events, (Manya *et al.*, 2004; Barresi and Campbell, 2005).

N-linked glycosylation and the *O*-mannosylation of α-dystroglycan always requires the participation of the lipid dolichol phosphate (Burda and Aebi, 1999). Dolichol-phosphate-mannose (DPM) is synthesised by DPM synthase (DPM1) catalysing a reaction between guanosine diphosphate mannose (GDP-man) and dolichol phosphate on the cytosolic side of the ER lumen (Richards and Hemming, 1972; Maeda and Kinoshita, 2008; Figure 1.4). Putative flippase machinery presumably translocates DPM onto the luminal side of the ER (Rush and Waechter, 1995). DPM is subsequently utilized as a donor substrate by the POMT1 and POM2 complex for the *O*-mannosylation of α-dystroglycan (Kim *et al.*, 2004; Manya *et al.*, 2004).

Interestingly, there is a reported case of CMD that results in both *N*-linked and *O*-linked glycosylation deficiencies of dystroglycan, caused by a missense mutation (p.L85S) in the highly conserved coiled-coil domain of the *DPM3* gene

(Lefeber *et al.*, 2009). DPM3 is anchored to the ER membrane via this coiled-coil domain and is important for tethering cytoplasmic DPM1to the DPM complex. The associated hypomannosylation of α-dystroglycan results in laminin-211 failing to bind to α-dystroglycan, providing an explanation for the CMD phenotype in the patient (Lefeber *et al.*, 2009).
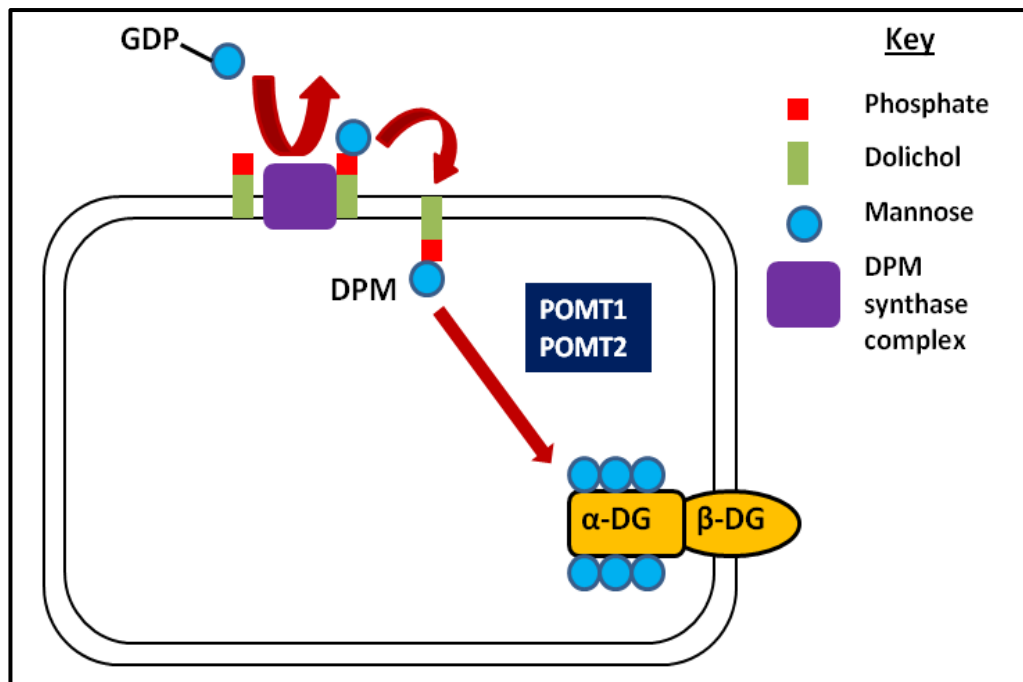
Figure 1.4: Schematic of the *O*-mannosylation of α-dystroglycan
For mannose to be incorporated into α-dystroglycan it must be bound cytosolically to the lipid dolichol phosphate and the DPM synthase complex first. Putative flippases transport DPM into the ER lumen and the POMT complex binds the mannose to α-dystroglycan (Manya *et al.*, 2004; Lefeber *et al.*, 2009). *N.B.* It is unclear at present whether the α and β dystroglycan subunits are cleaved before or after the initial mannosylation of α-dystroglycan.

1.3.3 α-Dystroglycan Structure

Under an electron microscope α-dystroglycan appears as a 20-30nm long dumbbell shaped molecule, the N-terminus being the wider end (Bozic *et al.*, 2004). α-Dystroglycan can be divided into four regions, a signal peptide, the N-terminus, the central mucin domain, and the C-terminus (Hall *et al.*, 2003; Figure 1.5). The first domain is a signal peptide made up from the first 29 amino acids of the propeptide, is principally hydrophobic and targets the alpha peptide to the Golgi complex (Barresi and Campbell, 2005; York and Nunberg, 2006). The 30kDa N-terminus of α-dystroglycan has one potential *N*-glycosylation site and the C- terminus has two *N*-glycosylation sites (Holt *et al.*, 2000).

α-Dystroglycan is heavily *O*-mannosylated with high abundance of the uncommon Neu5Ac(α2-3)Gal(β1-4)GlcNAc(β1-2)Man-Ser/Thr tetramer (Chiba *et al.*, 1997; Sasaki *et al.*, 1998). *O*-glycosylation accounts for the mass differences between dystroglycan in skeletal muscle and other tissues (Yoshida-Moriguchi *et al.*, 2010; Kuga *et al.*, 2012a). The final 41kDa and 242 amino acids of the dystroglycan propeptide is β-dystroglycan containing only one *N*-glycosylation site (Brancaccio *et al.*, 1995; Brancaccio *et al.*, 1997).
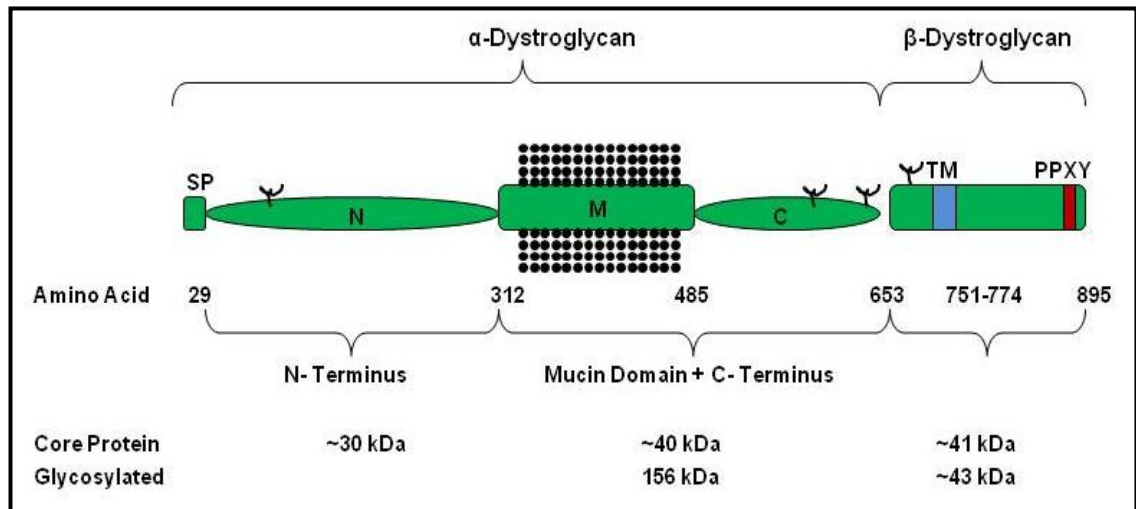
Figure 1.5: **Dystroglycan domain organization.**
Circles indicate O-linked sugar chains. Branches indicate N-linked sugar chains. SP, signal peptide; TM, transmembrane domain; The PPxY motif within the ZZ domain is the site where dystrophin binding occurs. Molecular masses at the bottom refer to the protein mass in the absence (core protein) and presence of post-translational glycosylation, adapted from Barresi and Campbell, 2005.

1.3.4 Deglycosylation of Dystroglycan

Glycosylation of α-dystroglycan is fundamental for binding important extracellular matrix proteins. If the *N*-linked glycans are removed using *N*-glycanases there is no impact on the ligand binding activity of dystroglycan. Conversely *O*-sialoglycopeptidase, which deglycosylates α-dystroglycan's *O*-linked glycans, completely abolishes the ligand binding activity. This indicates that the *O*-linked glycosylation sites are essential for the role of α-dystroglycan as an extracellular matrix receptor (Ervasti and Campbell, 1993). The accurate glycosylation of α-dystroglycan is important for the Ca^{2+} dependant binding of ligands such as laminin, perlecan or agrin in muscle and neurexin in nerves (Campanelli *et al.*, 1994; Gee *et al.*, 1994; Sugiyama *et al.*, 1994; Sasaki *et al.*, 1998; Sugita *et al.*, 2001). All the ligands that bind the *O*-mannosylated mucin domain of α-dystroglycan, do so through a conserved laminin-G (LG) like

domain (Timpl *et al.*, 2000). The *O*-glycans on α-dystroglycan are necessary to bind LG domains (Hohenester *et al.*, 1999; Tisi *et al.*, 2000). There is a report of a small leucine-rich repeat proteoglycan known as biglycan that binds N-linked glycosylation site in the carboxy-terminal of α-dystroglycan (Bowe *et al.,* 2000).

1.3.5 The Functional Diversity of Dystroglycan

Dystroglycan has diverse roles from cell signalling to supporting the architecture of the cell nucleus (Johnson and Kramer, 2012). This raises the question: where does the functional diversity in dystroglycan arise from? As mentioned earlier the two dystroglycan subunits are targeted independently to the sarcolemma (Ibraghimov-Beskrovnaya *et al.*, 1992; Holt *et al.*, 2000). *In vitro* studies found that at the sarcolemma the two dystroglycan subunits are held together by relatively weak non-covalent interactions (Bozzi *et al.*, 2006). However it remains unclear what advantage lies in separating the two subunits: one possibility is that the separation is important for post translational modification of each subunit individually (Bozzi *et al.*, 2009). The ectodomain of β-dystroglycan demonstrates plasticity which enables the protein to establish low affinity interactions and thus change its conformation (Bozzi *et al.*, 2003; Yatsenko *et al.*, 2007). β-Dystroglycan is known to bind several signalling molecules, including mitogen-activated protein kinase, caveolin-3 and growth factor receptor bound protein-2 (Spence *et al.*, 2004). The functional diversity in dystroglycan may therefore be possible through a combination of conformational plasticity in the ectodomain of β-dystroglycan and differences in α-dystroglycan glycosylation patterns afforded by independently processing the subunits (Bozzi *et al.,* 2009).

1.3.6 Dystroglycan as a Bacterial and Viral Receptor

The *O*-glycan sugar residues, in particular the *O*-mannosyl sugars on α-dystroglycan, act as receptors for bacteria and viruses, such as Lassa fever virus and lymphocytic choriomeningitis virus (Cao *et al.*, 1998; Rambukkana *et al.*, 1998; Imperiali *et al.*, 2005). *Mycobacterium leprae* uses α-dystroglycan bound to laminin-211 as a co-factor to infect Schwann cells (Kunz *et al.*, 2005). There is also mounting evidence that it is not the *O*-mannosyl glycans on α-dystroglycan but the glycosylation by LARGE of α-dystroglycan that is required as a recognition site prior to arena-viruses prior to infection (Rojek *et al.*, 2007). It is possible that an element of functional redundancy in the post-translational

modification of the α-dystroglycan mucin domain that affords a selective advantage against viruses and bacteria. Small changes in α-dystroglycan *O*-glycosylation may maintain binding with ECM ligands but prevent parasitic invasion (Herson *et al.*, 2012).

1.3.7 Integrins

Patients with a congenital myopathy have been identified with either deletions resulting in frameshift mutations or a 21-bp insertion caused by a splice site mutation in the integrin-α7 (ITAG7*)* gene (Vachon *et al.*, 1997; Mayer, 2003). The homozygous integrin-α7 null mouse shows progressive MD soon after birth. The MD associated pathology is variable amongst muscle groups, with the soleus and diaphragm affected to the greatest extent. The key change observed on histopathology is impaired myotendinous junction (MTJ; Mayer *et al.*, 1997).

Integrins are a major family of cell surface receptors, which influence the development of skeletal muscle by transducing signals through muscle cell contact with the ECM and cell-cell interactions (Figure 1.1; Tuckwell *et al.*, 1993; Boettiger, 2012). Integrins occupy a similar position in the sarcolemma to dystroglycan and may have overlapping roles (Ribeiro *et al.*, 2011). Integrins are heterodimeric proteins which are comprised of α and β subunits, non-covalently bound in a divalent cation dependant process (Hynes, 1992). There are approximately 24 combinations of integrin dimers (to date,18α and 8β subunits have been identified) which form various combinations of subunit associations (van der Flier and Sonnenberg, 2001). Splice variants however account for an even greater diversity in integrin structure (Nishiuchi *et al.*, 2006). α-Integrins have shorter intracellular and longer extracellular portions of their transmembrane structure, while the β-subunit has the opposite configuration (Fu *et al.*, 2012). The specificity of integrins to ligands is determined predominantly by the α-chain (Mayer, 2003).

Integrins are important for focal contacts at the neuromuscular junction (NMJ), MTJ and the sarcolemmal membrane (Schwander *et al.*, 2004; Welser *et al.*, 2009). α4, β1 or β7 subunits are expressed to the greatest extent during development and in adult skeletal muscle the most important integrin interaction is between laminin-211and integrin-α7 (Belkin and Stepp, 2000; Bajanca and

Thorsteinsdottir, 2002). Integrins are dynamically expressed dependant on stage of development (Burkin and Kaufman, 1999; Carson and Wei, 2000). Intracellular filamin and talin bind integrin, forming a link between the ECM and the intracellular cytoskeleton (Calderwood *et al.*, 2001; Moore *et al.*, 2012a). The interaction between integrins and the ECM has been shown to be important for influencing intracellular signalling (Nieves *et al.*, 2010).

1.4 Extracellular Matrix

Muscle ECM forms a small fraction of total muscle mass in comparison to contractile material, but has a large influence on muscle function. For instance it is thought that the ECM bears most of the passive load *i.e.* any force on relaxed muscle (Trotter, 1993). Stiffness and reduced limb motion on clinical examination might therefore reflect a disruption to ECM functionality. With any pathological change in muscle there will also be at least a small associated degree of excess ECM deposition, a hallmark of fibrosis (Mann *et al.*, 2011).

There are three main subdivisions of ECM in muscle: endomysium, perimysium and epimysium (Purslow, 2010). The endomysium is a highly ordered network surrounding individual muscle fibres (Trotter and Purslow, 1992). The ability of the endomysium to bear weight results from its capacity to elastically deform in a nonlinear fashion as the muscle fibre relaxes (Trotter, 1993; Purslow and Trotter, 1994) while mechanical strength comes from the geometry of the collagen fibres. The perimysium surrounds bundles of fibres. The perimysial collagen filaments are arranged in dense transverse and longitudinal bands connecting muscle fibres at discrete perimysial plates (Rowe, 1981). The epimysial layer surrounds the muscle and is continuous with tendons. A similar "crimp" pattern is seen on scanning electron microscopy (SEM) in muscle and tendons (Jarvinen *et al.*, 2002). This is not surprising considering the epimysium fuses with tendon to insert into the bone (Gillies and Lieber, 2011).

1.4.1 Laminins

Mutations in the LAMA2 gene result in congenital muscular dystrophy 1A (MDC1A; Kuang *et al.*, 1998). Similar to the patients, the spontaneous *Lama2 dy/dy* mouse model presents with peripheral neuropathy and MD (Xu *et al.*, 1994). The MD is as a result of a failure of laminin to form the basement membrane scaffolds necessary for supporting the DGC (Xu *et al.*, 1994;

Miyagoe-Suzuki *et al.*, 2000). Evans blue dye (EBD) can be used as an *in vivo* tracer and an assay for sarcolemmal stability with a discoloration of skeletal muscle indicating a damaged sarcolemma. In normal muscle EBD is unable to cross the sarcolemma following intraperitoneal injection, and is therefore not detected in the sarcoplasm on muscle sections (Lin *et al.*, 2011). EBD has been injected into the mdx mouse, a mouse model for DMD, and the *dy/dy* mouse model of MDC1A. EBD uptake is a frequent finding in the *mdx* mouse but not the *dy/dy* mouse. This indicates that dystrophin deficiency is associated with sarcolemmal instability while laminin-α2 deficiency is not (Straub *et al.*, 1997). In another study disorganisation of the costameric lattice was found in the *dy*^{2J} mouse, a variant of the dy/dy mouse with a splice site mutation, whereas longitudinal striations and M-line defects were observed in the *mdx* mouse (Yurchenco and Cheng, 1994). Together the findings suggest that there is a different mechanism for pathology in MD associated with dystrophin mutations compared to those associated with deficiencies in LAMA2.

Laminin is a heterotrimeric protein consisting of a heavy α-chain and two lighter chains (β & γ), capable of binding three major receptor types: dystroglycan, heparin sulphate based proteoglycans and integrins (Durbeej, 2010). The hetrotrimer is joined by the coiled-coil domains of the three individual polypeptide chains. The α-unit extends beyond the coil-coiled domain to form the laminin globular (LG) domain and is composed of five self folding repeats (LG domains 1-5). The calcium containing LG4 and LG5 domains bind the N-terminus of skeletal muscle α-dystroglycan (Bork *et al.*, 1996; Brancaccio *et al.*, 1997; Timpl *et al.*, 2000). Laminin can be subdivided into fifteen types in mammals consisting of different combinations of the 5α, 3β and 3γ chains (Koch *et al.*, 1999). Laminin-111 (old nomenclature; laminin-α1, β1, γ1) is the isoform expressed during embryogenesis, whereas laminin-211 (merosin or old nomenclature; laminin-α2, β1, γ1) is the type found in mature skeletal muscle (Aumailley *et al.*, 2005).

1.4.2 Basement Membranes

Basement membranes (BM) are specialised ECM, visible on electron microscopy as 50-100nm electron dense sheets found basolaterally to epithelium, endothelium and muscle fibres. The main functions of BMs are to provide structural support and influence cell behaviour. The four major

components of BM's are laminin, collagen IV, perlecan and nidogen/enactin (Noonan *et al.*, 1991; Olsen, 1999; Nicole *et al.*, 2000; Poschl *et al.*, 2004; Kohling *et al.*, 2006). Laminins and collagens both self assemble into super structures held together by perlecan, nidogen and enactin, strengthening and stabilising the BM (Yurchenco and Patton, 2009). Heterogeneity and specificity of BMs arise from various combinations of laminin chains, agrin, fibulin, type XV collagen, type XVIII collagen as well as many other proteins (Prockop and Kivirikko, 1995; Denzer *et al.*, 1997; Xie *et al.*, 2008). The specific composition of BMs in various tissues relates to their unique functions (LeBleu *et al.*, 2007).

1.5 Dystroglycanopathy

1.5.1 Primary Dystroglycanopathy

The first homozygous missense mutation (Thr192/Met) in the DAG1 gene was reported in a woman with LGMD and cognitive impairment (Hara *et al.*, 2011). *In vivo* and *in vitro* studies demonstrated that the missense mutation caused loss of post-translational modification of dystroglycan by LARGE, which prevented laminin binding and reduced receptor function (Zhang *et al.*, 2011). Despite a spectrum of mutations found across numerous other genes that cause secondary dystroglycanopathy with various pathogenic mechanisms (Hara *et al.*, 2011), this is so far the only mutation to be identified in the highly conserved *DAG1* gene (Hewitt, 2009; Godfrey *et al.*, 2011; Muntoni *et al.*, 2011).

1.5.2 Secondary Dystroglycanopathies

Aberrant glycosylation of dystroglycan is associated with several forms of MD, ranging from mild limb girdle MD to severe congenital forms (Figure 1.6; Yoshioka and Kuroki, 1994). The hypoglycosylation of α-dystroglycan can result from mutations in one of at least seven genes. These genes encode known *O*-linked glycosyltransferases, xylosyltransferases, glucuronyltransferase or phosphorylation proteins. These proteins are: Protein O-mannosyl transferase (POMT)1, POMT2, protein O-mannose β1,2-N-acetylglucosaminyltransferase (POMGnT1), acetylglucosaminyltransferase-like-protein (LARGE), fukutin, fukutin related protein (FKRP) and the recently identified isoprenoid synthase domain (ISPD), see (Table 1.1) for further details.

Primary defects in this enzymatic pathway have also provided insights into the role of known or putative glycosyltransferases. The first sugar residue to be added to the carbohydrate moiety on α-dystroglycan is an *O*-mannose-glycan catalysed by POMT1. This mannose residue is bound to the core of α-dystroglycan by POMT2 which works in a complex with POMT1 (Manya *et al.*, 2004). POMTGnT1 then adds the second sugar residue *N*-acetylglucosamine through a β1,2 linkage to the mannose group using uridine 5′-diphosphate *N*-acetylglucosamine as a donor substrate (Zhang *et al.*, 2002). The final two sugar residues on the tetrasaccharide are galactose and sialic acid, but the nature of the glycosyltransferases responsible for adding them remains unknown (Barresi and Campbell, 2005; Figure 1.3). LARGE has recently been shown to be a bifunctional glycosyltransferase with both xylosyltransferase and glucuronyltransferase activity responsible for transferring repeating units of [-3-xylose-α1,3-glucuronic acid-β1-] onto α-dystroglycan (Inamori *et al.*, 2012), and plays a role in the phosphorylation of mannose residues on α-dystroglycan (Yoshida-Moriguchi *et al.*, 2010; Kuga *et al.*, 2012a). The exact role LARGE, POMTGnT1, FKRP and fukutin play in phosphorylation of mannose remains unclear. Interestingly, overexpression of LARGE reinstates laminin binding activity to α-dystroglycan when dystroglycan is in a hypoglycosylated state (Barresi *et al.*, 2004; Kuga *et al.*, 2012a). There is always a loss or reduction of immunoreactivity of IIH6 in patient cells with mutations in any of the secondary dystroglycanopathy genes and diminished bands on western blots. Tests that utilise IIH6 antibody are therefore invaluable in the diagnosis of dystroglycanopathy.

1.5.3 Fukutin

Fukuyama congenital muscular dystrophy (FCMD; OMIM: 253800) was first reported in Japanese patients in 1960 (Toda and Kobayashi, 1999). In the Japanese population 87% of FCMD can be accounted for by an ancestral retrotransposon insertion of a SINE-VNTR-Alu in the 3′ UTR untranslated region of exon 10 in the FKTN gene, on chromosome 9q31-33 (Toda *et al.*, 1993; Kobayashi *et al.*, 1998; Colombo *et al.*, 2000; Taniguchi-Ikeda *et al.*, 2011). The result is a reduction in the expression levels of FKTN mRNA. FCMD affects cardiac, skeletal muscle, eye and brain (Toda and Kobayashi, 1999). FCMD often presents in infancy with hypotonia, weakness and mental

retardation (Fukuyama *et al.*, 1981; Toda, 2009). Homozygous nonsense mutations and compound heterozygotes, *i.e.* patients with the common insertion and a missense mutation, are often associated with more severe CMDs such as muscle eye brain disease (MEB; OMIM: 253280) and Walker-Warburg syndrome (WWS; OMIM: 236670; de Bernabe *et al.*, 2003; Vuillaumier-Barrot *et al.*, 2009). A milder allelic variant was found outside the Japanese population which presented with a LGMD-like phenotype and was termed LGMD2M (OMIM: 607440; Toda and Kobayashi, 1999; Godfrey *et al.*, 2006).

The human fukutin protein is 461 amino acids long (53.7kDa) and encoded for by a 10 exon, 6.8kb transcript located on chromosome 9q31 (Aravind and Koonin, 1999; Breton and Imberty, 1999). In the human adult *FKTN* mRNA expression levels are highest in the brain, liver and kidney with lower expression levels in skeletal muscle and heart (Esapa *et al.*, 2002). Fukutin localises to the medial Golgi of normal rat kidney fibroblasts, a finding which is consistent with its hypothesised role in the glycosylation of α-dystroglycan. Towards the C-terminus there is a DXD domain which is present in a large number of glycosyltransferases, supporting the hypothesis that fukutin is involved in glycosylation. Also supporting this hypothesis is the resemblance of fukutin to RP688, a member of the Fringe family of proteins, known to function as glycosyltransferases in the intracellular parasitic bacterium *R.prowazekii* and T07D3.4, T07A5.1 proteins in *C.elegans* (Aravind and Koonin, 1999). Interestingly, a yeast protein involved in phosphorylation of mannose residues also belongs to the fukutin family of proteins (Aravind and Koonin, 1999). Recently fukutin has been shown to be important in the post-phosphoryl modification of mannose residues on α-dystroglycan (Kuga *et al.*, 2012a).

1.5.4 Fukutin Related Protein

The first mutations in the *FKRP* gene were identified in congenital muscular dystrophy type 1C (MDC1C; OMIM: 606612) and LGMD2I patients (OMIM: 607155; Brockington *et al.*, 2001a; Brockington *et al.*, 2001b; Brockington *et al.*, 2002). LGMD2I is a condition on the less severe end of the spectrum which predominantly affects the shoulder and hip girdles (Figure 1.6). LGMD2I is frequently caused by a homozygous or compound heterozygous missense mutation in the *FKRP* gene (826 C>A; L276I), prevalent in the Northern European population (with an estimated allele frequency of 1:400), as a result of

a founder effect (Brockington *et al.*, 2001b; Frosk *et al.*, 2005). Nonsense mutations in the same gene produce conditions at the more severe end of the spectrum such as MEB and WWS. WWS is thought to be the most severe of the CMDs and patients with this condition rarely survive longer than a year (Van Reeuwijk *et al.*, 2010; Figure 1.6). WWS is defined clinically by agenesis of the corpus callosum, cobble stone lissencephaly, cerebellar hypoplasia and structural eye defects (Mercuri *et al.*, 2003; Muntoni and Voit, 2004; Mercuri *et al.*, 2006).

Fukutin Related Protein was first identified by distant homology to fukutin using database search tools and shown to be responsible for congenital muscular dystrophy (CMD) with hypoglycosylated α-dystroglycan (Aravind and Koonin, 1999; Breton and Imberty, 1999; Brockington *et al.*, 2001a). The 12kb *FKRP* gene located on chromosome 19q13.32, has three non-coding exons and a single 3.8kb coding exon, with a 1485bp open reading frame. *FKRP* encodes a 495 amino acid protein that contains a catalytic domain, a DXD motif and a type II transmembrane domain frequently associated with Golgi proteins (Aravind and Koonin, 1999; Esapa *et al.*, 2002; Keramaris-Vrantsis *et al.*, 2007). A LicD domain resides within the catalytic domain and is thought to be important for phosphorylcholine metabolism (Zhang *et al.*, 1999). Early evidence pointed to FKRP functioning as a glycosyltransferase, although recent work would suggest that FKRP, similar to fukutin, is involved in the post-phosphoryl modification of the mannose residue on α-dystroglycan (Kuga *et al.*, 2012a). Northern blot analysis revealed the highest expression levels of the *FKRP* transcript in adult heart and skeletal muscle with lower expression levels observed in brain, lung, pancreas, kidney and liver (Brockington *et al.*, 2001a; Brockington *et al.*, 2001b; Brockington *et al.*, 2002; Esapa *et al.*, 2002).
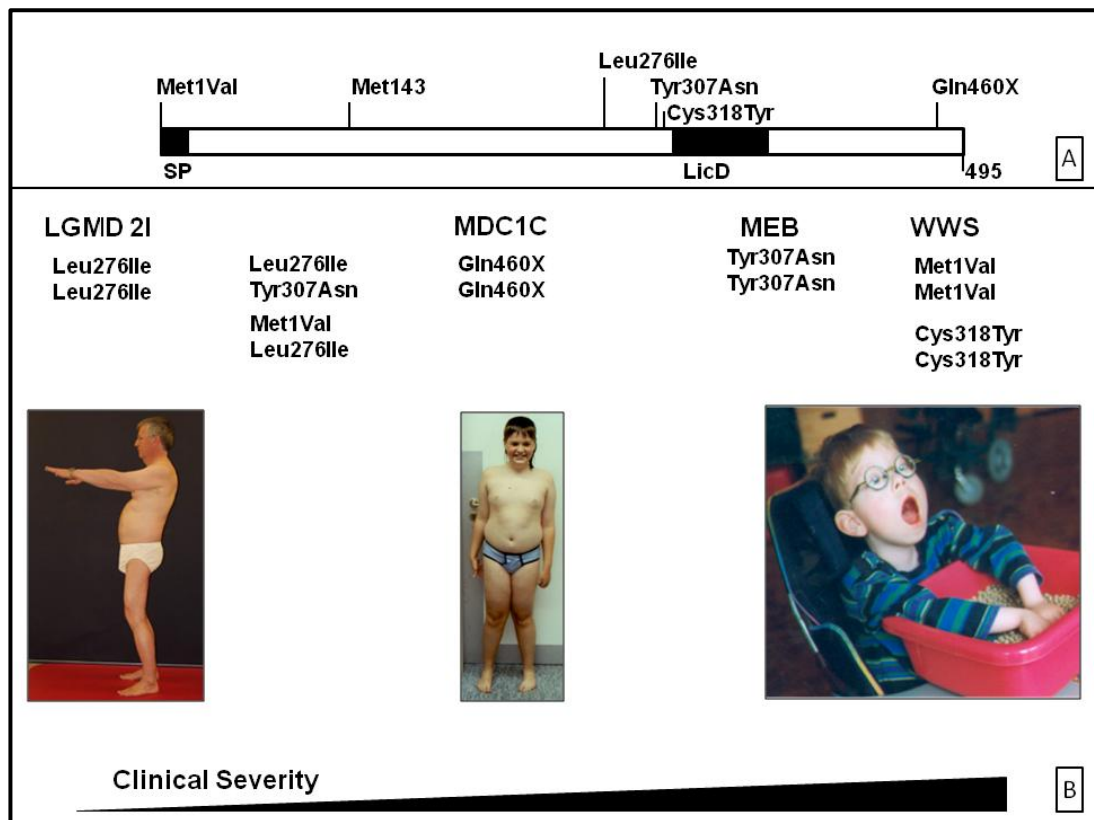
Figure 1.6: Common mutations in *FKRP* with associated severity of clinical phenotype; a genotype-phenotype correlation
A, Representation of FKRP protein, position of mutations along the peptide, LicD domain (Pfam domain PF04991) important in proteins involved in phosphorylcholine metabolism. Mutations at the signal peptide (SP) prevent FKRP being targeted correctly to the Golgi (Esapa *et al.*, 2002). **B,** Mutations linked to clinical severity ranging from LGMD2I to WWS, including representative patient photographs kindly donated by Professor Volker Straub, (Van Reeuwijk *et al.*, 2010). The patient on the left demonstrates that LGMD2I patients can be of considerable age whereas the MDC1C patient (middle) is a lot younger and would in most cases have a lower life expectancy while the CMD patient on the right is much younger. There is an inverse relationship with disease severity, with the lefthand patient being less severely affected despite being older, while the right-hand patient is most severely affected despite being the youngest. Note the patient on the left has muscle wasting particularly around the hip girdle, the middle patient has signs of pseudo-hypertrophy of the limb girdles and finally the patient on the right is clearly very disabled. Out of the three the right hand patient is the only one who is non-ambulant, and note that this patient also displays visual impairment.

1.6 DGC Mouse Models

Over recent years many mouse models that mimic the CMDs associated with dystroglycanopathy have been described in the literature (Hewitt, 2009; Godfrey *et al.*, 2011). The DGC mouse literature is too large to cover in great detail here, therefore the most important mouse models for our discussion are described and discussed below (Durbeej and Campbell, 2002). A summary of other relevant models is provided in Table 1.2, the table highlights some of the key

features of the models, for instance the dystroglycanopathy phenotype of muscle, eye and brain involvement is limited to the secondary dystroglycanopathy mice (Kelly *et al.*, 1994; Grewal *et al.*, 2001; Takeda *et al.*, 2003; Liu *et al.*, 2006; Ackroyd *et al.*, 2009; Ackroyd *et al.*, 2011). Because of the difficulty in generating viable dystroglycan deficient mice, often only one feature of the primary dystroglycanopathy such as muscle weakness or brain abnormalities is modelled in any given mouse strain using tissue specific promoters, with the exception of the MORE-DG null mouse which has features analogous to each aspect of MEB disease (Williamson *et al.*, 1997; Cote *et al.*, 1999; Cohn *et al.*, 2002; Moore *et al.*, 2002; Satz *et al.*, 2008; Satz *et al.*, 2009).

Mouse	Gene	Protein	Phenotype	Reference
Cytoskeletal Proteins				
mdx[*]	*Dmd*	Dystrophin	MD	(Bulfield *et al.*, 1984)
mdc[3CV]	*Dmd*	Dystrophin	MD	(Cox *et al.*, 1993)
Transmembrane Proteins				
Dag1^{-/-}	*Dag1*	DG	EL	(Williamson *et al.*, 1997)
Dag1^{-/-} SM chimera	*Dag1*	DG skeletal muscle	MD	(Cote *et al.*, 1999)
Dag1^{-/-}MCK/cre	*Dag1*	DG skeletal muscle	MD	(Cohn *et al.*, 2002)
Dag1^{-/-} GFAP/cre	*Dag1*	DG brain	ND	(Moore *et al.*, 2002)
Dag1^{-/-} MORE	*Dag1*	DG epiblast	MD,ND, RLD	(Satz *et al.*, 2008)
Dag1^{-/-} Nestin/cre	*Dag1*	DG eye	RLD	(Satz *et al.*, 2009)
Itag7^{-/-}	*Itag7*	Integrin	MD	(Mayer *et al.*, 1997)
Secondary Dystroglycanopathy Proteins				
Fkrp[KD]	*Fkrp*	FKRP	MD, RLD, ND	(Ackroyd *et al.*, 2009; Ackroyd *et al.*, 2011)
Fcmd^{-/-}	*Fktn*	Fukutin	EL	(Kurahashi *et al.*, 2005)
Fcmd^{-/-} chimera[**]	*Fktn*	Fukutin	MD, ND, RLD	(Takeda *et al.*, 2003)
Fcmd[-/hp]	*Fktn*	Fukutin	MD (not severe)	(Kanagawa *et al.*, 2009a; Taniguchi-Ikeda *et al.*, 2011)
myd[*]	*Large*	LARGE	MD, ND, RLD	(Grewal *et al.*, 2001)
enr[*]	*Large*	LARGE	MD, ND, RLD	(Kelly *et al.*, 1994)
Pomt^{-/-}	*Pomt1*	POMT1	EL	(Willer *et al.*, 2004)
Pomgnt1^{-/-}	*Pomgnt1*	POMTGnT1	MD, ND , RLD	(Liu *et al.*, 2006)
ECM Proteins				
dy/dy[*]	*Lama2*	Laminin-α2	MD, PN	(Sunada *et al.*, 1994)
Dy[2J*]	*Lama2*	Laminin-α2	MD	(Straub and Campbell, 1997)

Table 1.2: Overview of DGC Mouse models
Mouse models of DGC components including cytoskeletal, transmembrane, secondary dystroglycanopathy, ECM proteins. MD: muscular dystrophy, EL: embryonic lethal, RLD: retinal layering defect, ND: neuronal migration defect, PN: peripheral neuropathy, DG: dystroglycan, [*] spontaneously occurring mouse model, [**] high percentage chimera.

1.6.1 Reichert's Membrane and the Dystroglycan Null Mouse

Divergent morphology is first observed from embryonic day E6.5 in the dystroglycan null *Dag1*[neo2] mouse (Williamson *et al.*, 1997). By E7.5 the *Dag1*-null mice begin to show signs of developmental failure, with indistinct features and smaller size in comparison to their normal litter mates. By E10.5 the

embryos are largely resorbed with only a small embryonic mass still visible. At E5.5, the cylinder stage, the gross morphology was similar between *Dag1*-null and wild type embryos with one noticeable exception, the presence of red blood cells in the yolk sac cavity in approximately a quarter of the *Dag1*-null mice. Therefore red blood cells were able to cross a perturbed Reichert's membrane, which normally functions as a barrier between the maternal blood and the yolk sac in the *Dag1*-null mice (Inoue *et al.*, 1983). ECM proteins laminin and collagen IV were found to be abnormally distributed at the membrane in *Dag1*-null mice (Hogan *et al.*, 1980; Smith and Strickland, 1981; Salamat *et al.*, 1993). Parietal endoderm cells were able to differentiate normally, indicating that the disruption of Reichert's membrane is the primary pathological event in these mice during the early stages of development (Salamat *et al.*, 1995). A toxic effect is hypothesised to cause the early embryonic lethality, since loss of Reichert's membrane structure and function exposes the uterine environment to maternal blood (Hogan *et al.*, 1984; Williamson *et al.*, 1997).

1.6.2 DG Skeletal Muscle Chimera

The embryonic lethality observed in the *Dag1*-null mice limited the utility of null alleles at this locus and therefore tissue specific strategies for interrupting this gene have been adopted (Williamson *et al.*, 1997). Targeting vectors were used to disrupt the *Dag1* gene in embryonic stem cells (Cote *et al.*, 1999; Kornegay *et al.*, 2012). On ultrastructural analysis the mice were found to have normal sarcolemma, however on histological analysis all the hall marks of MD including central nucleation and phagocytosis were found (Gumerson and Michele, 2011; Kornegay *et al.*, 2012). Immunohistological analysis found reduced expression of the sarcoglycan complex, while laminin-α2 had a normal expression pattern. The myoneural synapses did not form correctly in the DG skeletal muscle chimera mouse, a finding not recapitulated in dystrophin or utrophin deficient mice, and a similar finding was observed in dystroglycan deficient *Drosophila* (Deconinck *et al.*, 1997; Grady *et al.*, 1997; Cote *et al.*, 1999; Bogdanik *et al.*, 2008).

Another muscle specific dystroglycan model the MCK-DG-null mouse has a similar phenotype to the DG skeletal muscle chimera mouse (Cohn *et al.*, 2002). Interestingly, dystroglycan expression was found to be almost completely absent from about 4 weeks, however after ten weeks dystroglycan was re-

expressed. The targeting strategy did not remove dystroglycan from the stem cell niche and therefore by a process of regeneration the mouse muscle was able to acquire dystroglycan positive cells. If the animals were exposed to18 and 25 Gy of irradiation inactivating the satellite cells the mice had complete absence of dystroglycan at the sarcolemma which persisted for 10 weeks and also developed a severe dystrophic phenotype (Cohn *et al.*, 2002).

1.6.3 MORE DG Null Mouse

The MORE-DG null mouse was designed to delete dystroglycan from the epiblast only, thereby bypassing the pathology associated with loss of dystroglycan from Reichert's membrane (Williamson *et al.*, 1997). To create the MORE-DG null mouse, a mouse carrying a floxed *Dag1* allele was crossed with the Mox2-Cre mouse expressing Cre recombinase specifically in the epiblast (Tallquist and Soriano, 2000; Cohn *et al.*, 2002). The principal aim was to recapitulate the WWS phenotype found in patients (Kanoff *et al.*, 1998) since previous models had been proven to be unsuitable for this purpose (Williamson *et al.*, 1997; Cote *et al.*, 1999; Cohn *et al.*, 2002; Moore *et al.*, 2002). The MORE-DG null mice were all found to have muscle, brain and eye pathology with disrupted basement membranes (Cohn *et al.*, 2002; Satz *et al.*, 2008).

Microphthalmia is most commonly bilateral in WWS patients, with unilateral phenotypes reported in less than 10% of the total cohort and a similar ratio is found in the MORE-DG null mouse (Kanoff *et al.*, 1998; Satz *et al.*, 2008). In WWS patients the eye problems are associated with lens and iris tissue herniation through the cornea. The mice were frequently missing lenses and, Descemet's membrane a BM lying between the stroma and the epithelial layer of the cornea, was also found to be disrupted with a periodic acid Schiff stain. Hematoxylin and eosin (H&E) stained sections highlighted abnormal neuroepithelium and ectopic cells internal to the inner limiting membrane (ILM). When laminin expression at the ILM was investigated a discontinuous pattern was found, indicating discontinuity of the ILM itself maybe providing a mechanism by which ectopic cells appear in the anterior chamber (Satz *et al.*, 2008). These abnormalities are consistent with findings in WWS and therefore the MORE-DG null mouse is a good model for investigating early eye pathology analogous to that found in WWS (Yoshioka and Kuroki, 1994; Kanoff *et al.*, 1998; Beltran-Valero de Bernabe *et al.*, 2002; Balci *et al.*, 2005).

1.6.4 Nestin-Cre/DG Null Mouse

The majority of MORE-DG null mice die two days after birth before the eye can fully develop (Satz *et al.*, 2008). An alternative dystroglycan deficient mouse model, for the purpose of investigating eye function is therefore required. Floxed dystroglycan mice were crossed with mice containing rat nestin enhancer that controls the expression of Cre recombinase to produce the Nestin-Cre/DG null mouse (Satz *et al.*, 2009). The Nestin-Cre transgene is useful for deleting particular genes from the retina as early as E9.5. Dystroglycan was found to be absent in corneal endothelium, lens, iris, ciliary epithelia and the retina in the Nestin-Cre/DG null mice. ILM disruption in the Nestin-Cre/DG null mice was shown to lead to a reduction in the number of retinal ganglion cells. Interestingly, staining of core DGC components at the ILM lead to the conclusion that dystroglycan is required early on in development but possibly not for later maintenance of the ILM. The Nestin-Cre/DG null mouse had impaired performance when attempting visual tasks such as water-maze and visual cliff tests. Interestingly, removing the last 15 amino acids of the β-dystroglycan tail affects the physiology of the retina similarly. The implication is the last 15 amino acids of β-dystroglycan may have a role to play in targeting dystroglycan to specific locations within the retina (Satz *et al.*, 2009).

1.6.5 FKRP Mutant Mice

The FKRP^{Tyr307Asn} mouse had no discernible phenotype (Ackroyd *et al.*, 2009), which highlights differences between humans and mice, since in the same substitution at the homologous amino acid in the human *FKRP* gene is known to cause MEB disease (Beltran-Valero de Bernabe *et al.*, 2004; Mercuri *et al.*, 2006; Sveen *et al.*, 2006). Maintenance of the neomycin cassette in intron 2 of the mouse (FKRP-Neo^{Tyr307Asn}) reduced *Fkrp* transcript levels to 80% of wild type. The nomenclature for the FKRP-Neo^{Tyr307Asn} has subsequently been simplified to FKRP^{KD} mouse (Ackroyd *et al.*, 2011), a mouse that dies shortly after birth with a classic MEB phenotype. Muscle fibre density was reduced in the gastrocnemius and soleus muscles with oedematous infiltration. The mice had virtually absent IIH6 and laminin-α2 expression in muscles. The abnormalities in the eye included microphthalmia and perturbations in both retinal layering and inner limiting membrane (ILM), as indicated by ectopic nuclei in the vitreous humor. Reductions in laminin-γ1 and perlecan staining at

the ILM in Fkrp deficient mice confirmed BM pathology. Dystroglycan expression as determined by GT20 antibody was present in both wild type and Fkrp deficient mice. In the brain reduced IIH6 and laminin-α2 staining was associated with aberrant pial layering and disorganised radial glia with glial end feet not correctly attaching to the pial BM (Ackroyd *et al.*, 2009; Ackroyd *et al.*, 2011).

Subsequent studies showed abnormal laminin-α1 deposition under the pial BM. This is significant because it is the end feet of the radial glia which attach to the laminin-α1 and aberrantly positioned glia don't project correctly across the cortex, therefore providing a possible mechanism for the disruption to radial glia scaffolds and loss of cortex partitioning (Ackroyd *et al.*, 2011). A similar process occurs in the eye with abnormal deposition of the laminin-α1 and γ1chains in the eye at the ILM. The result is aberrant binding of the Müller glia with the inner limiting membrane (Halfter *et al.*, 2005). These findings suggest alternative modes of action of Fkrp in the brain and eye when compared to muscle. It is clear that Fkrp is important for maintenance of an α-dystroglycan laminin-α2 interaction in muscle whereas in eye and brain laminin-111 seems to interact with an unknown ligand as the key interaction for stabilizing cells to basement membranes (Ackroyd *et al.*, 2009; Satz *et al.*, 2009). A critical finding was the developmental stage dependant regulation of *Fkrp* transcripts. Higher expression in brain when compared to muscle in the newborn mouse was an interesting finding since muscle is often considered to be the major pathological change in FKRP deficiency (Ackroyd *et al.*, 2009; Ackroyd *et al.*, 2011).

1.6.6 Fukutin Chimera Mouse

Since the Fukutin null mouse was found to be embryonically lethal (Kurahashi *et al.*, 2005), a chimera was sought to overcome the problems associated with perturbations to Reichert's membrane. Vectors were used that targeted both alleles of the *Fktn* gene in ES cells and replaced exon 2 with a neomycin or puromycin resistance gene (Horie *et al.*, 2002). The extent of the chimerism was tested by glucose phosphate isomerase isozyme and related well to the coat colour in the fukutin chimeras (Takeda *et al.*, 2003). Premature death in the mice corresponded with the extent of chimerism: only 48% of highly chimeric but 94% of low chimeric mice survived to 21 months. Non-progressive muscle abnormalities, as determined by behaviour were first observed at one

month of age. Chimeric mice clasped when suspended by the tail and had an abnormal gait. Muscle fibres of the chimeras were necrotic, with mononuclear cell infiltration, increased interstitial connective tissue and basophilic regenerating fibres at 1 month after birth. Glycosylated α-dystroglycan was greatly reduced at the sarcolemma while β-dystroglycan and laminin-α2 were normally localised. Immunoblotting confirmed the findings and laminin overlay showed a reduced binding affinity between α-dystroglycan and laminin-α2 (Takeda *et al.*, 2003).

Disorganization of the laminar structures in the cerebral and cerebellar cortices as well as the hippocampus was observed in the brain of the fukutin deficient chimeric mouse (Takeda *et al.*, 2003). Over migration in the monolayer (layer I) and of the cortical neurons resulted in the normal six layer structure appearing unordered in the chimeric mice. Laminin immunostaining revealed meningeal basement membrane abnormalities in the chimeric mice including perturbations and granular deposits. However, not all basement membranes were disturbed, including that of the parenchyma that surrounds blood vessels in the brain. Loss of *b*-wave on electroretinography demonstrated eye anomalies in the fukutin deficient mice. The corneas were opaque as result of granular tissue, inflammation and degeneration with vascular infiltration. Lens abnormalities, eyeball formation anomalies including detached retina and loss of the laminar structure were also observed in these mice (Takeda *et al.*, 2003).

1.6.7 Fukutin Retrotransposon Mouse

There was an attempt to generate a mouse that better represented patients with FCMD. First *Fktn* exon 10 in mouse ES cells was replaced with exon 10 containing the retrotransposon insertion analogous to that found in FCMD patients (Colombo *et al.*, 2000; Taniguchi-Ikeda *et al.*, 2011), and targeted ES cells were injected into mouse blastocysts. The *fukutin* $^{hp/hp}$ had *FKTN* transcript levels 5-10% of normal levels. These animals were then mated with the fukutin-null mouse to create a compound heterozygote *fukutin*$^{hp/-}$ that better represents the compound heterozygote patients, who generally show the most severe pathology (Vuillaumier-Barrot *et al.*, 2009). Despite hypoglycosylation of α-dystroglycan in these mouse models the MD pathology is mild. Leading to the conclusion that a small amount of residual fukutin prevents MD in these fukutin deficient mice (Kanagawa *et al.*, 2009a; Taniguchi-Ikeda *et al.*, 2011).

1.6.8 Mouse Model Summary

The dystroglycanopathy mouse models are often embryonically lethal and infertile whereas knockout mice models of other DGC components, often with secondary defects to other proteins within the DGC, are frequently viable and fertile (Durbeej and Campbell, 2002). The mouse models highlight the critical importance of correctly glycosylated dystroglycan in mouse development. As a consequence of the hypoglycosylation of α-dystroglcan and subsequent loss of ligand binding much of the early embryonic lethality is attributable to perturbations in the basement membranes particularly Reichert's membrane (Williamson *et al.*, 1997; Willer *et al.*, 2004; Kurahashi *et al.*, 2005). Despite strategies that attempt to either bypass the early embryonic development (Cote *et al.*, 1999; Cohn *et al.*, 2002; Moore *et al.*, 2002; Satz *et al.*, 2008; Satz *et al.*, 2009), or models that directly relate to human mutations (Ackroyd *et al.*, 2009; Kanagawa *et al.*, 2009a), no individual mouse model is comprehensive in modelling every aspect of human dystroglycanopathy, leading the field to look towards other model systems (Hewitt, 2009; Godfrey *et al.*, 2011).

1.7 The zebrafish as a Model for MD

1.7.1 Danio rerio

The zebrafish (*Danio rerio*) is a small freshwater tropical fish becoming an increasingly popular model in the field of biological research (Parichy, 2006). There are several reasons for the increasing popularity of zebrafish in research such as their quick generation time, relatively low maintenance costs, optically transparent embryos, ease of gene manipulation and their regenerative potential. The optical transparency and *ex-utero* development are particularly advantageous features for developmental biologists due to ease of access for imaging studies (Kimmel *et al.*, 1995). These properties are also increasingly being adopted in high throughput pipelines for drug discovery (Lessman, 2011). Importantly there is good coverage of the zebrafish genome. One major drawback of the zebrafish is that many of the genes are duplicated as a result of an ancestral genomic duplication event (Westerfield, 2000).

Importantly, zebrafish do not require Reichert's membrane for normal development. Zebrafish therefore bypass the embryonic lethality seen in mice

associated with deficiencies in dystroglycan, making a case for zebrafish as a model in secondary dystroglycanopathy research (Parsons *et al.*, 2002a).

1.7.2 Zebrafish in Muscle Research

Recently *FKRP* and *fukutin* have been knocked down in zebrafish to study their importance in early embryonic development (Thornhill *et al.*, 2008; Kawahara *et al.*, 2010; Lin *et al.*, 2011; Wood *et al.*, 2011b). Zebrafish show precocious locomotor development, *i.e.* there is force generated by the muscles even before 1 day post fertilisation (dpf), since the embryos can be seen moving within the chorions (Bassett and Currie, 2003; Dowling *et al.*, 2009). The somites are axial muscles that develop from segmented axial mesoderm and eventually give rise to the myotome *i.e.* zebrafish skeletal muscle. The muscle fibres differentiate along the anterior–posterior axis to span an entire somite. The distinctive somite chevron seen by 1 dpf is separated dorsally and ventrally by a myoseptum which is essentially extracellular matrix (Bassett and Currie, 2004; Moore *et al.*, 2008).

The *sapje* fish illustrates some of the key benefits and limitations of working with zebrafish. The *sapje* fish is a model for DMD and has a nonsense mutation in exon 3 of the zebrafish *dmd* gene (Parsons *et al.*, 2002a). There is muscle degeneration in the *sapje* fish because the myofibres fail to adhere to the MTJ *i.e.* in adult fish where muscle is joined to tendon and during development where muscle joins myoseptum (Law and Tidball, 1993; Ridge *et al.*, 1994; Law *et al.*, 1995; Snobl *et al.*, 1998; Bassett *et al.*, 2003). Zebrafish are excellent model systems for investigating both congenital disorders and more importantly for DMD research studies looking at early pathological changes in disease. Using zebrafish for initial drug screens with findings validated in mammalian systems may prove to be a useful complementary strategy to develop therapies for DMD (Tanabe *et al.*, 1986; Lessman, 2011). There is an argument therefore for being selective in choice of animal model, based on their purpose and being prepared to alternate between model systems when appropriate.

Several systems have proved to have great utility for modelling a single aspect of dystroglycanopathy. *Drosophila* are one example, with mutations in the *rt and tw* genes which are homologues of POMT1 and POMT2 respectively having effects on embryonic muscle development and alignment of the adult

cuticle (Martin-Blanco and Garcia-Bellido, 1996). *Drosophila,* despite being used extensively to study the eye during development, lacks the basement membranes within the eye and is therefore less suitable as a model than zebrafish, which have analogous eye basement membranes to humans (Thornhill *et al.,* 2008; Paulk *et al.,* 2012). Simarly *Caenorhabditis elegans* have been useful in MD for pathway discovery, particularly muscle specific pathways, however the system lacks the brain and eye basement membranes present in zebrafish (Chamberlain and Benian, 2000; Gupta *et al.,* 2011). Cellular systems such as patient cell lines or the mouse C2C12 line, have long since been useful models in MD research for: localisation studies, first principle development such as testing novel therapies and to test new antibodies (Favreau *et al.,* 2008; Negroni *et al.,* 2011; Lynch *et al.,* 2012). None of these systems have the complexities of the muscle, eye and brain including the basement membranes required to study dystroglycanopathy from a holistic perspective. Zebrafish have all the facets important for studying dystroglycanopathy, combined with all the advantages of zebrafish over murine models. Zebrafish are therefore an ideal model system to undertake research into FKRP and fukutin deficiency.

1.7.3 Somatogenesis

Somatogenesis is a complex process, starting as early as the onset of gastrulation. However before any muscle progenitors are seen, the embryo undergoes a reorganisation of cells in the blastodisc, occurring during the blastula stage of development. In the process of epiboly at 4 hpf cells intercalate by radial rearrangement, thinning the blastoderm by spreading over the egg (Solnica-Krezel, 2005). The blastoderm coverage of the yolk sack relates to a percentage that can be used to stage the embryo (*i.e.* % epiboly). The first signs of muscle progenitors are seen as early as $5_{1/4}$ hpf at the onset of gastrulation (synonymous with 50% epiboly; Table 1.3 & Figure 1.7A). At this stage the different territories for specific organs are not clearly demarcated and progenitors are intermingled (Figure 1.7B; Kimmel *et al.,* 1990). At 5 hpf the cells at the margins begin to internalize forming the hypoblast, the precursor of endoderm and mesoderm. During the gastrulation process blastocyst self reorganization transforms the endoderm and mesoderm layers into a tri-laminar

structure: mesoderm, ectoderm and endoderm, (Figure 1.7B-C; Kimmel *et al.*, 1995; Shih and Fraser, 1996; Saude *et al.*, 2000; Schier and Talbot, 2005).

Shield cells are the equivalent in zebrafish of organizer cells in amphibians or Hensen's node cells in chick (Stickney *et al.*, 2000). The shield (thickening of epiblast and hypoblast at the animal pole) establishes at approximately 6 hpf on the dorsal side of the embryo and gives rise to the notochord and prechondral plate. The paraxial mesoderm, formed from the cells around the margins of the early gastrula, is important for notochord development. The axial mesoderm is derived from the shield and the paraxial mesoderm. However it is the convergence of the paraxial mesoderm cells in the midline that forms the notochord, contributing to the anterior posterior extension of the embryo. The notochord precursor cells during this stage of development begin to express signalling molecules such as sonic hedgehog (Holley and Nusslein-Volhard, 2000), influencing the patterning of the paraxial mesoderm (Kimmel *et al.*, 1990; Kimmel *et al.*, 1995; Schier and Talbot, 2005).

Stage	hpf	Description
Blastula		
Sphere	4	Straight border between yolk and blastodisc.
Dome	$4_{1/3}$	Beginning of epiboly yolk bulges towards animal pole.
30% epiboly	$4_{2/3}$	The blastoderm even thickness situated 30% between the animal and the vegetal pole.
Gastrulation		
50% epiboly	$5_{1/4}$	The blastoderm even thickness situated 50% between the animal and the vegetal pole.
Germ- Ring	$5_{2/3}$	50% epiboly; Germ ring visible at animal pole.
Shield	6	50% epiboly; Shield becomes visible at animal pole.
75%-epiboly	8	Thickening of dorsal side, hypoblast, epiblast and evacuation zone all become visible.
90%-epiboly	9	Segmental plate distinguishable from brain and notochord rudiments.
Bud	10	100% epiboly; Tail bud becomes prominent, neural keel separates from notochord rudiment. Midsagital groove in anterior neural keel.
Segmentation		
1-somite	$10_{1/3}$	First somite furrow becomes visible.
5-somite	$11_{2/3}$	In the polster prominent phase, optic vesicle and Küpffer's vesicle first appear.
14-somite	16	Somites appear v shaped, brain neuromeres and otic placode form.
20-somite	19	Muscle twitches, eye lens, rhombic flexure become visible for the first time, otic vesicle and hindbrain neuromeres become increasingly prominent, tail extension. All somites present, sideways tail flexures; Prim 3.
26-somite	22	

Table 1.3: Important stages for early somite development in zebrafish
Zebrafish developmental stages defining the terminology used throughout thesis to describe development of the embryo from the blastula stage to the end of the segmentation period. Adapted from Kimmel *et al.*, 1995.
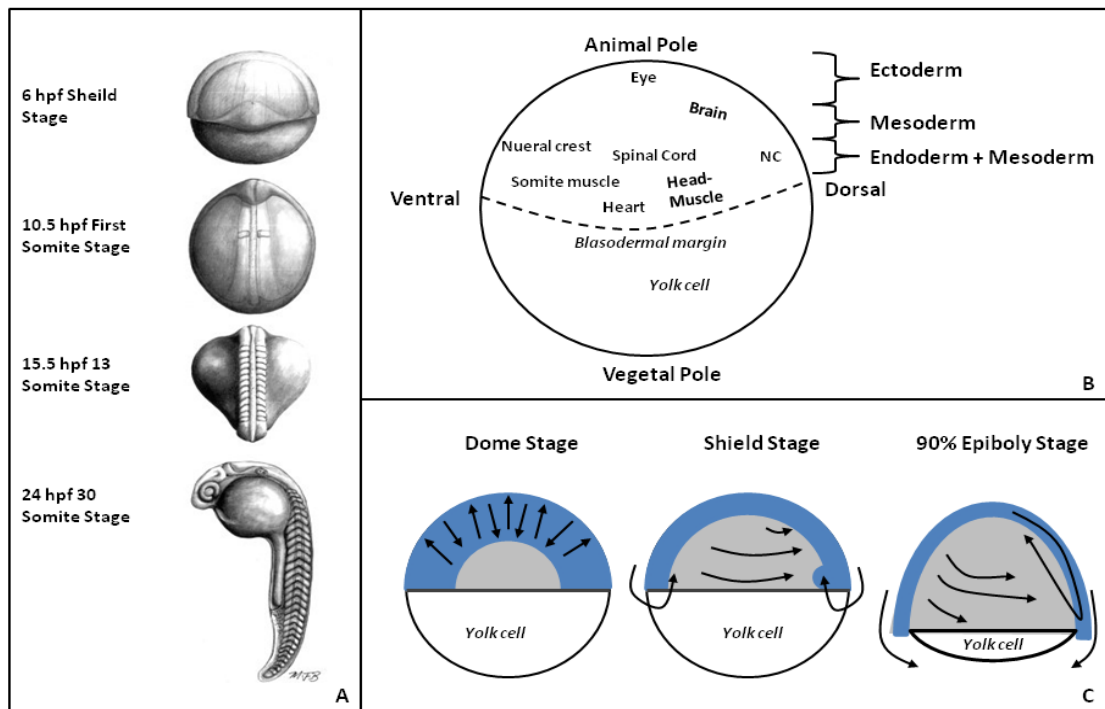
Figure 1.7: Schematics of early somite development in zebrafish
(A) Key stages in embryogenesis, important in the segmentation and patterning of the paraxial mesoderm, adapted from Stickney *et al.*, 2000. **(B)** Fate map of a 50% epiboly stage embryo, adapted from Kimmel *et al.*, 1995. Fates are not completely defined at this stage despite the germ layers being organized along animal-vegetal axis. **(C)** Cell movements during gastrulation, adapted from Stickney *et al.*, 2000. Cells intercalate radially during the dome stage. Marginal cells internalise and migrate towards the animal pole, lateral mesoderm cells converge dorsally during the shield stage. The 90% epiboly stage is concerned with internalization, convergence and extension of the embryo (Schier and Talbot, 2005).

The process of segmentation begins with the first segment at around 10.5 hpf. By 24hpf 30 somite pairs bracket the notochord (Figure 1.7A & Figure 1.8). Importantly for making inferences about human disease, the development of somites in zebrafish is very similar to that of mammals (Kimmel *et al.*, 1995). Somites develop in a bilateral symmetrical process beginning with mesenchymal cells from the rostral region of the presomitic mesoderm. A proportion of the mesenchymal cells alter their adhesion properties to become epithelial cells. A specialised epithelial layer forms around a proportion of the remaining loosely organised presomitic mesenchymal cells *i.e.* muscle precursors, every 30 minutes, in an anterior posterior progression, and once bound they are referred to as a single somite. This formation of uniformly sized blocks of presomitic mesodermal cells occurs at regular intervals in a process termed segmentation (Stickney *et al.*, 2000).

Precise regulation of the timing of segmentation is required to maintain uniformity of the somites which has lead to the hypothesis that a molecular clock might exist (Palmeirim *et al.*, 1997; Forsberg *et al.*, 1998; McGrew *et al.*, 1998). The expression pattern of *her1* which controls size and position of the presomitic mesoderm supports the molecular clock model in zebrafish (Holley *et al.*, 2000). Also thought to support the molecular clock hypothesis is the expression of the Notch family of transmembrane proteins. Notch activates transcription machinery thought to be specifically involved in control of the segmentation process (Agathon *et al.*, 2003). The *Notch1a* mutant zebrafish has no somite boundaries and myoD expression that is not restricted to posterior domain of the somites, as seen in wild type embryos at a similar stage of development (Takke and Campos-Ortega, 1999).
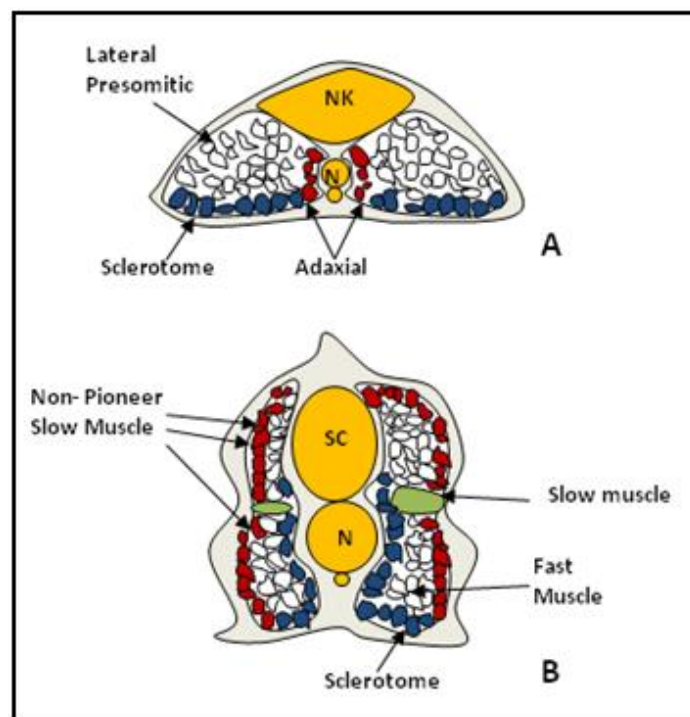
Figure 1.8: Detail of the myotome of zebrafish embryos
At **(A)** 13hpf and **(B)** 24hpf. The cells marked in blue are the precursors of the sclerotome *i.e.* the somitic structure that eventually becomes the vertebrae. The adaxial cells at 13hpf (shown in red) become non-pioneer slow muscle by 24hpf. The notochord in the centre of the embryo provides developmental cues and structural support during development. Neural keel: NK, notochord: N and spinal cord: SC, adapted from Stickney *et al.*, 2000.

1.7.4 Muscle Organisation

The transverse tubule system (T-tubules) are an extension of the sarcolemma penetrating deep into the myofibre allowing the rapid depolarization of the membrane to be synchronously transmitted to the entire contractile unit. A triad

is formed by two terminal cristernae which are enlargements of sarcoplasmic reticulum flanking a specialised area of the T-tubules. At the periphery of the fibre adjacent to the sarcolemma lie the myonuclei. Myonuclei are centrally located with higher frequency in MD when compared to the peripheral location in healthy individuals (Anderson, 1991). Centrally located myonuclei act as a useful assay for regeneration in damaged muscle (Cohn and Campbell, 2000).

1.7.5 Notochord Development

The notochord is an embryonic mid line structure that arises from the dorsal organiser in Chordates (Harland and Gerhart, 1997). The notochord has both a signalling and a structural role. The notochord is positioned centrally in two of three embryonic axes (dorso-ventral and lateral), important for secreting factors which control development of the central nervous system, angiogenesis and somatogenesis. Initially the notochord has a structure closely resembling cartilage and therefore serves as the axial skeleton. Later the notochord ossifies to become the vertebral column in adult fish. In zebrafish embryonic and larval development the structure is also important for locomotion (Figure 1.7 & Figure 1.8; Stemple, 2005).

1.7.6 Embryonic Origin of Zebrafish Eye

The earliest signs of eye development can be traced to the onset of gastrulation at $5^{1/4}$ hpf. The first sign of brain development in zebrafish is the dorsal ectoderm becoming the neural ectoderm (Kimmel *et al.*, 1995), a process controlled by signals from the underlying axial mesoderm. Molecular cues from the notochord induce the adjacent ectoderm to form the neural plate. The neural plate is visible at 10hpf as a thickening on the dorsal side of the embryo (Chow and Lang, 2001) which results from a change in shape of the cells (the cells become columnar forming pseudostratified epithelium) and not from proliferation. The anterior neural plate is comparable to the proencephalon *i.e.* an anterior part of the brain that develops from the anterior part of the neural-tube and is regionalised early in gastrulation. Several homeobox containing gene families (Sox3, Rx, Pax6 & Otx2) are expressed in the neural ectoderm at this stage of development, all are essential for eye development (Grindley *et al.*, 1995; Boncinelli and Morgan, 2001; Purcell *et al.*, 2005). These regulatory genes are important for controlling the fate of neural progenitors which eventually become the optic primordium (Chuang and Raymond, 2002).

Subsequent patterning is controlled by developmental pathways including canonical regulators such as BMP, Hedgehog, Wnt and Fgf family members. (Rubenstein and Beachy, 1998; Wilson and Rubenstein, 2000; Schier, 2001).
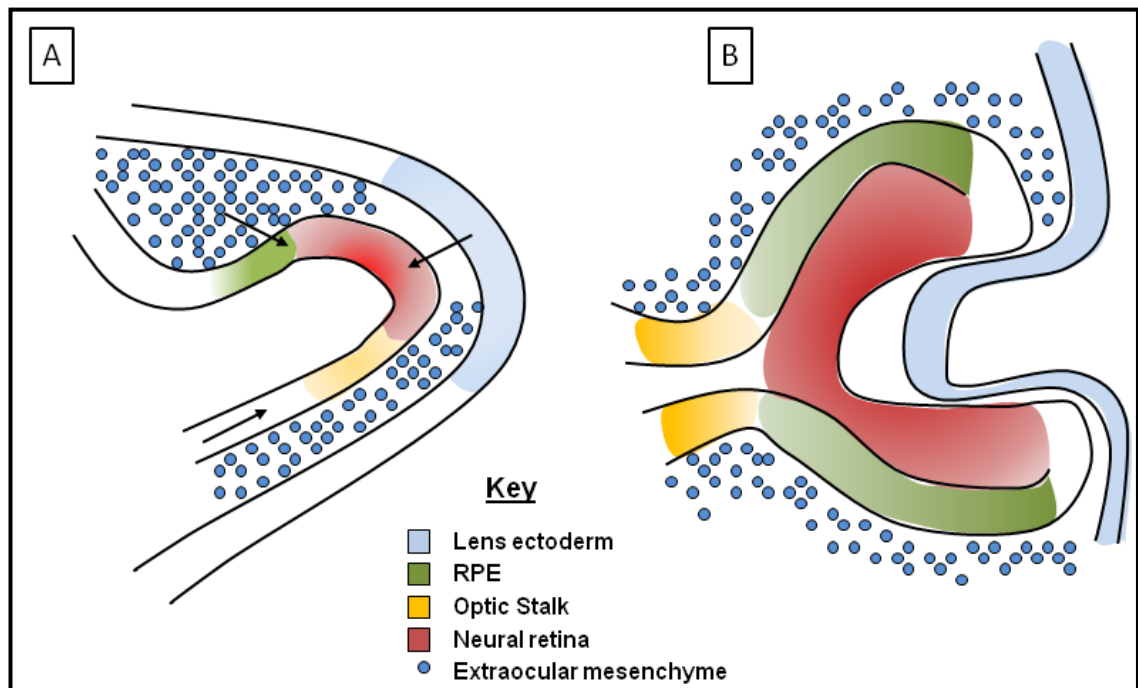
Figure 1.9: Early eye development in vertebrates
A, Arrows show factors from extra-ocular mesenchyme, optic stalk and surface ectoderm regulating the patterning of retinal layering. **B**, Lens vesicle and optic cup formation. The lens placode (lens ectoderm) invaginates the distal optic vesicle (neural retina). RPE: retinal pigmented epithelium. Adapted from Fuhrmann., 2008.

The zebrafish eye forms from the neuroepithelium, surface ectoderm and the extra ocular mesenchyme. The interaction between these three layers co-ordinates the single eye field formation in the midline of the anterior neural plate. Signalling from ventral midline structures underlying the neural plate splits the eye field bilaterally. The inner layer of the optic cup forms the neural retina and the retinal pigmented epithelium forms the outer layer (Figure 1.9). Peripheral structures such as the iris and ciliary body develop from the margins of the two layers. The optic fissure is a ventral fissure in the developing optic cup, through which blood vessels pass to the enclosed mesenchyme, derived from a narrowing of the optic stalk (Figure 1.9). The optic stalk is an evagination of the neural tube, from which the optic cup develops. At its extremity the optic stalk persists as the optic nerve. The lens ectoderm forms an enclosed cellular mass that eventually separates and becomes the adult lens (Rembold *et al.*, 2006; Fuhrmann, 2010).

1.7.7 Adult Zebrafish Eye

The adult zebrafish eye is a complex organ, which shares a great deal of structural homology with the mammalian eye. The adult eye is formed of many different cell types arranged into distinct retinal layers. Precise developmental control is required to form this complex structure in adult zebrafish (Mohideen *et al.*, 2003), which includes the three basement membranes of the eye, important for influencing the fate of the cells that surround them. These membranes are: the internal limiting membrane (ILM), external limiting membrane (ELM) and Bruch's membrane. Disruption of any of these membranes will alter retinal layering, as seen in the MORE DG and FKRP[KD] mouse models (Avanesov and Malicki, 2004; Young *et al.*, 2006; Figure 1.10).
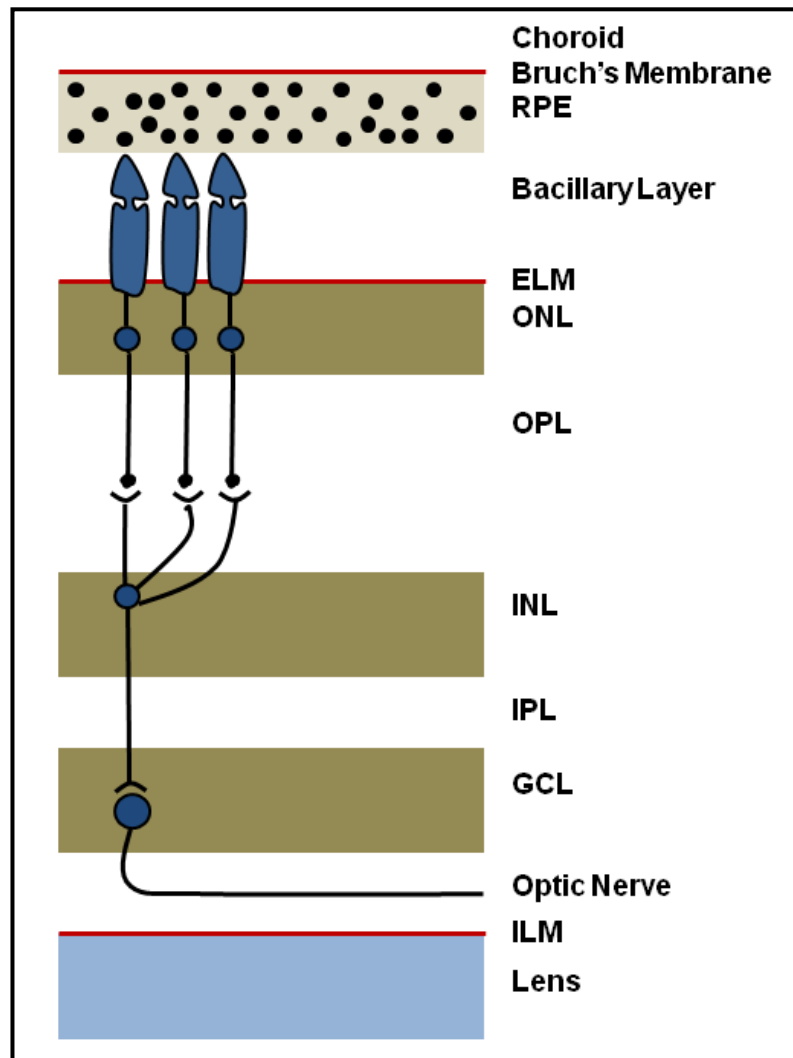
Figure 1.10: Schematic of retinal layering and basic neuronal circuitry
The eye is a highly complex structure made from neuronal layers, pigmented epithelium, the lens and three basement membranes: inner limiting membrane, external limiting membrane and Bruch's membrane. RPE: retinal pigmented epithelium, ELM: external limiting membrane, ONL: outer nuclear layer, OPL: outer plexiform layer,

INL: inner nuclear layer, IPL: inner plexiform layer, GCL: ganglion cell layer, ILM: inner limiting membrane. Adapted from Young *et al.*, 2006.

1.7.8 Vasculogenesis

The "vascular hypothesis" of MD predicts that muscle necrosis associated with MD is caused by chronic muscle ischemia and so a causative vascular pathology has long been sought after in MD (Cazzato, 1968; Demany and Zimmerman, 1969; Mendell *et al.*, 1972; Jerusalem *et al.*, 1974). Nitric oxide synthase (nNOS) is closely associated with the DGC and also involved in the regulation of vasodilation, and is therefore a candidate for the central mediator of the "vascular hypothesis" (Crosbie, 2001; Sharma *et al.*, 2010; Verma *et al.*, 2010; Lombard, 2011; Dabire *et al.*, 2012).

Angioblasts are the precursors of endothelial cells not yet incorporated into blood vessels, originating from the ventrolateral mesoderm (Ellertsdottir *et al.*, 2010). *In situ* aggregation of angioblasts into blood vessels is referred to as vasculogenesis. The sprouting of vessels from existing vessels is termed angiogenesis (Moiseeva, 2001). These processes are integral to all organs making them useful for comparing structural changes within specific organs.

The zebrafish TG*(fli-1:EGFP)* or fli-1 was designed to investigate early vascular development in zebrafish replacing former models that required the injection of fluorescent carboxylated latex beads into wild type fish (Lawson and Weinstein, 2002; Figure 1.11). The transgenic model expresses enhanced green fluorescent protein (EGFP) driven by the fli-1 promoter in the vascular endothelium, cranial neural crest derivatives, a presumptive hemangioblast lineage, and a small subset of myeloid derivatives (Isogai *et al.*, 2001).
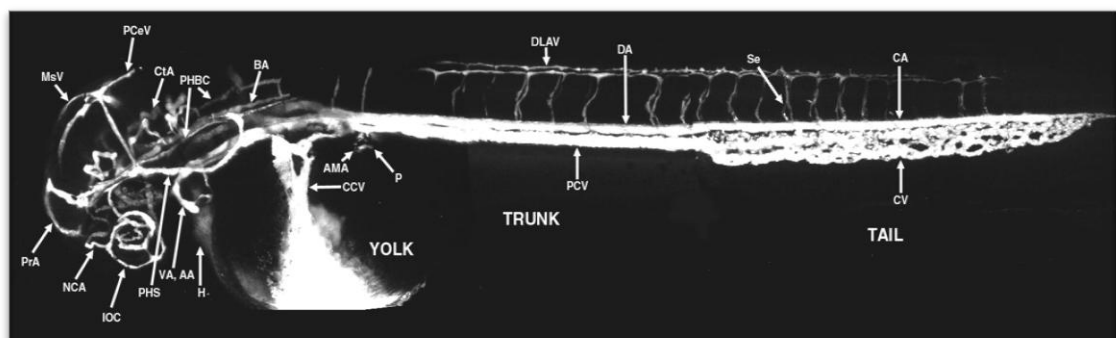
Figure 1.11: Vascular anatomy of 2dpf zebrafish
Embryo injected with fluorescent carboxylated latex beads, produced from confocal projections. Se: intersegmental vessel, DA: dorsal aorta, DLAV: dorsal longitudinal anastomotic vessel, PCV: posterior cardinal vein, CA: caudal artery, CV: caudal vein,

IOC: inner optic circle, Image is an unaltered copy from Isogai *et al.*, 2001; Lawson and Weinstein, 2002.

The first signs of zebrafish eye vasculogenesis are seen at 24-29 hpf. The optic artery branches from the primitive internal carotid artery, entering the eye ventrally through the optic fissure. The optic artery later becomes the hyaloid artery running from the back of the eye through the hyaloid canal to the ILM. By 60 hpf the hyaloid artery has formed a loop around the lens, exiting through the hyaloid canal and eventually the optic fissure as the optic vein. These internal vessels are referred to as the hyaloid vessels, the external vessels that supply the retina are known as the optic vessels (Isogai *et al.*, 2001; Alvarez *et al.*, 2007; Fadool and Dowling, 2008; Gore *et al.*, 2012; Figure 1.11).

1.8 Current Approaches for Generating Stable Zebrafish Mutant Lines

To date there are no stable mutant zebrafish lines modelling any of the dystroglycanopathies. All studies investigating dystroglycanopathies have been carried out using morpholino antisense-oligonucleotides (MOs). Morpholino oligonucleotides (MO) are small chains of typically around 25 nucleotides complementary to specific target sites in transcribed sequences (Summerton and Weller, 1997). The MO structure is different from DNA and RNA in two distinct ways. Firstly the ribose or deoxyribose sugar is replaced with artificial morpholine rings preventing the morpholino from being recognised by endogenous enzymes and degraded. Secondly, non-ionic phosphorodiamidiate replaces the anionic phosphates, also preventing recognition by endogenous enzymes that degrade DNA and RNA. Efficient knockdown can be achieved with MOs since they bind to native nucleic acids at high affinity, but are resistant to degradation and therefore persistent in vivo (Nasevicius and Ekker, 2000; Summerton, 2007).

MOs have two modes of action either spliceosomal or translational. MOs that block an intron-exon boundary generating dysfunctional splice products are referred to as splicesomal MOs. The translational MOs sterically block the translation initiation complex, thereby preventing the translation of the target mRNA. Spliceosomal MOs are desirable in many instances because the efficiency of target knock down can be tested by RT-PCR. Translational MO knockdown efficiency is normally tested by Western blot but is dependent on a

well characterised antibody (Summerton, 1999). Despite fukutin antibodies being commercially available an antibody that is capable of detecting endogenous fukutin in fish is yet to be reported in the literature, hence a spliceosomal MO is more desirable (Draper *et al.*, 2001; Lynch *et al.*, 2012). The problem of testing MO efficacy previously occurred with the FKRP morphant fish, another dystroglycanopathy model (Thornhill *et al.*, 2008) in this case tested with a laminin overlay assay. Zebrafish injected with MO can be investigated up to 5 dpf for two main reasons. Firstly, in the UK the Home Office will not allow fish injected with MO to be kept past 5dpf. Secondly, over time the MO becomes diluted through passive diffusion and distribution amongst the increasing number of cells as the larvae develops. Concentrations after 5 dpf of MO might therefore be considered less reliable for experiments than zebrafish earlier on in the development.

A stable mutant line would circumvent the problems of transient knockdown systems. Traditional site-directed DNA recombination methodology used to create knock-out mice models unfortunatly has had limited success in zebrafish. The technology uses the flexibility of Cre-recombinase to target palindromic DNA, catalysing strand exchanges at the locus of crossover (*lox* sites; Dong and Stuart, 2004). In murine research where embryonic stem (ES) cell culture is well established there have been many models created successfully and the technology has been widely adopted, whereas culture of zebrafish ES cells has proven to be difficult. This approach therefore has not been widely adopted in zebrafish (Fan and Collodi, 2006). The zebrafish field is therefore looking towards an approach receiving increasing attention: customised zinc fingers nucleases (ZFNs), enabling the introduction of frame shift mutations at targeted genetic loci in zebrafish (Porteus and Carroll, 2005; Foley *et al.*, 2009).

1.8.1 Zinc Finger Nucleases

Zinc fingers were discovered in 1985 by Miller, McLachlan & Klug based on an observation by Roeder & Brown that 5S RNA requires RNA polymerase III and a 40kDa protein transcription factor III (TFIIIA) to initiate transcription in *Xenopus laevis* (Picard and Wegnez, 1979; Pelham and Brown, 1980; Brown, 1984). TFIIIA was found to have large repeating protein motifs and atomic absorption spectroscopy showed these to contain zinc ions. Later the zinc ion was noted to play a key role in co-ordinating the DNA binding motifs. These

binding motifs were found to be capable of binding specific DNA sequences (Klug, 2010b).

 Zinc fingers can be classified into different "fold groups" based upon the conformational structure of their back bone. The most common example is the Cys_2His_2-like zinc finger otherwise known as the classical zinc finger (zinc ribbon and treble clef are other examples). The classical zinc finger structure consists of an α-helix and an antiparallel β-sheet co-ordinating the zinc ion via two conserved cysteines and two conserved histidine residues. Cys_2His_2 zinc fingers bind nucleic acid in the major groove of DNA through the N-terminus of the α-helix (Razin *et al.*, 2012). Specificity is achieved by interaction of the DNA with side chains on the α-helix of the zinc finger. Regulation of transcription is thought to be the most important task of Cys_2His_2 zinc fingers with roles in mediating protein-protein interaction hypothesised. The first artificial application of zinc fingers was developed shortly after their discovery with an unsuccessful attempt to silence oncogenes in mice in 1994 (Choo *et al.*, 1994; Corbi *et al.*, 2004; Klug, 2010a).

 ZFNs are artificial enzymes composed of a zinc finger DNA binding domain and a Fok-I nuclease domain (Kim *et al.*, 1996; Figure 1.12). Fok-I are restriction endonucleases consisting of an N-terminal DNA-binding domain and a non-specific DNA cleavage domain at the C-terminal, found naturally occurring in *Flavobacterium okeanokoites*. The Fok-1 nuclease domain induces double stranded breaks in DNA at the site of zinc finger binding. ZFNs act as obligate heterodimers that normally require non-palindromic nine base pair (bp) target sites either side of a 5-7bp spacer region to induce double stranded DNA breaks within a gene of interest. The DNA is repaired by the endogenous process of non-homologous end-joining (Porteus and Carroll, 2005; Foley *et al.*, 2009; Maeder *et al.*, 2009; Figure 1.12 & Figure 3.1B).

The two main strategies currently being adopted to derive ZFNs are: Oligomerized Pool Engineering (OPEN) and Context Dependant Assembly (CoDA; Maeder *et al.*, 2009; Sander *et al.*, 2010). In an earlier system known as "modular assembly" each individual finger is treated as an independent unit. Zinc finger domains are now known to be dependent on their context within an array which may account for the low success rate of modular assembly. Low target binding efficacy of ZFNs produced using modular assembly meant the

approach became superseded by OPEN and CoDA (Ramirez *et al.*, 2008).
ZFNs are also commercially available through Sigma-Aldrich's CompoZr service
(Hansen *et al.*, 2012). These ZFNs are constructed based on a propriety
method developed by Sangamo Biosciences (Richmond CA, USA) and their
success rates are comparable to the OPEN protocols (Maeder *et al.*, 2009;
Remy *et al.*, 2010).
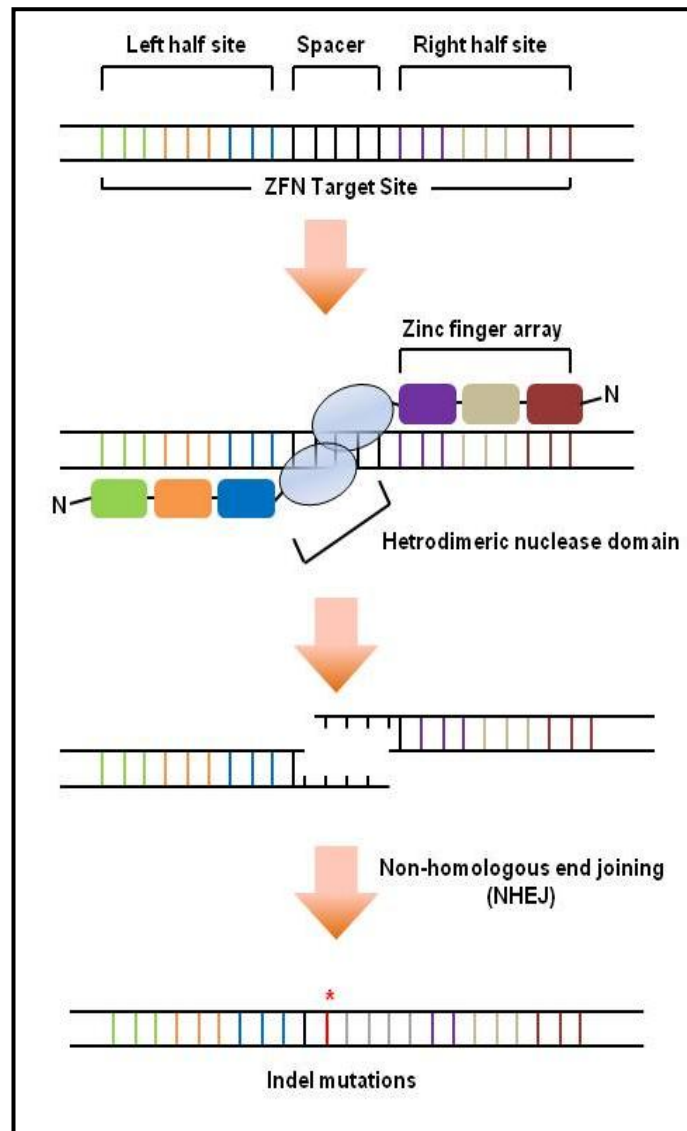
Figure 1.12: Schematics of ZFN mode of action
ZFNs are obligate heterodimers that introduce double stranded breaks between the
two target half sites. The DNA is repaired by non-homologous end joining, a process
likely to result in indel mutations (Porteus and Carroll, 2005).

Each pair of zinc fingers requires two sets of three fingers. Each set binds a 9-
bp half-site, and the pairs of ZFN binding sites are usually separated by a small
5-7bp section of DNA. With the OPEN protocol zinc finger pools are selected
from a catalogue of pools each consisting of approximately 95 fingers therefore

potentially producing a library with a complexity of 95^3 (8.5×10^6). Bacterial two-hybrid screening of the library using the target sequence cloned into a reporter vector selects for the multi-finger arrays with the highest binding affinities, maximising the probability that they function efficiently as ZFNs. The OPEN protocol therefore produces ZFNs which work well together and takes into account the context-dependent DNA binding of each finger, which is not considered in the modular assembly approach (Maeder *et al.*, 2009).

In the CoDA approach one of 319 N-terminal fingers (F1 units) and one of the 344 C-terminal fingers (F3 units) of the array are positioned either side of one of only 18 fixed (F2 units). The F1 & F3 units have been shown to function well with a particular F2 unit and therefore the CoDA protocol takes into account the context of adjacent fingers based on prior knowledge. CoDA increases the probability that a ZFN array will function with a high efficiency (Sander *et al.*, 2010). The protocol is relatively simple in comparison to OPEN, in that complex bacterial two-hybrid systems are not required (Maeder *et al.*, 2009; Figure 1.13).
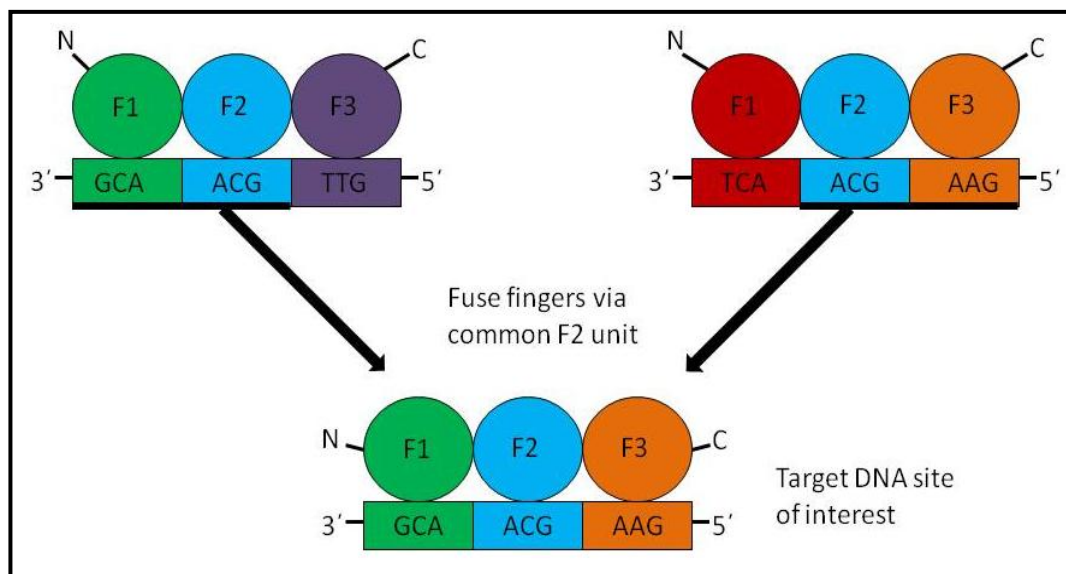
Figure 1.13: Schematic overview of CoDA ZFNs
Zinc fingers (units F1-F3) and their respective 3-bp DNA 'subsites' are shown. Two different three finger arrays, each engineered to bind different 9-bp target sites that have in common a middle F2 unit, can be used to create a three-finger array with a new specificity by joining together the F1 unit from the first array, and the F3 unit from the second array (Sander *et al.*, 2010).

The DNA sequences encoding zinc fingers from these approaches are then cloned into a vector expressing a Fok-I nuclease domain, with paired nuclease domains on each strand being required for cleavage of the DNA target. RNA

transcribed *in vitro* from the T7 RNA polymerase promoter in these vectors is injected into the embryo at the single cell stage. Mutant embryos can be screened by direct sequencing for mutations (Foley *et al.*, 2009).

1.8.2 TALENs

Transcription activator-like effector hybrid nucleases (TALENs), are similar to ZFNs in the respect they are also capable of binding to specific regions of DNA and inducing double-stranded breaks (Huang et al., 2011). The transcription activator-like proteins (TALEs) are virulence factors of phytopathogenic bacteria (*Xanthomas* genus). Once inside the cell, TALEs translocate to the nucleus, and their central repeat domain binds specific regions within the host DNA. TALEs are capable of mimicking transcription factors and re-program the host's gene expression to their advantage. The Hax3 binding domain can be manipulated to bind different DNA regions. The hybrid Hax3 can be then fused to a FokI cleavage domain, important for inducing double stranded breaks, to produce a TALEN (Wood *et al.*, 2011a). Recently the modified Goldy TALEN scaffold was combined with the addition of a single stranded nucleic acid template to refine TALEN efficacy (Bedell *et al.*, 2012). The introduction of a complementary single stranded DNA scaffold provides a template for homology directed repair (HDR). HDR uses the exogenous sequence as a template to precisely insert a desired sequence into the cut site. The template strand also reduces error arising as a result of NHEJ (Radecke *et al.*, 2010; Moore *et al.*, 2012b).

1.8.3 Chemical Mutagenesis and the Zebrafish Mutation Project

The chemical mutagen *N*-ethyl-*N*-nitrosourea (ENU) has been extensively used for mutagenesis screens in various organisms, including zebrafish. ENU can produce a mutation in approximately 1:700 gametes making it an attractive way to create mutations (Justice *et al.*, 1997). ENU is an alkylating agent, acting by transferring an ethyl group to the bases of nucleotides in DNA. However the method is random and this lack of specificity means that a large number of animals must be screened, making this approach difficult to justify for small labs (Knapik, 2000).

The Zebrafish mutation project is run by the Stemple Laboratory as part of the Wellcome Trust Sanger Institute (Hinxton, Cambridge, UK) and takes

advantage of ENU technology to create mutant zebrafish lines (Stemple, 2011). The process remains random but by creating a genotyping pipeline the project hopes to achieve a nonsense mutation in every protein coding gene in the zebrafish genome. To date >1200 nonsense and splice mutations have been identified. The exomic DNA of F1 generation fish with phenotypes are sequenced following enrichment with the Agilent Sure Select system on an Illumina Hi-seq platform. Specific alleles are then sequenced in the generated F2 by KASpar (allele specific amplification, developed by KBiosciences) to confirm any mutations (Clark *et al.*, 2011; Kettleborough *et al.*, 2011).

1.8.4 Retrovirus Strategy

An alternative strategy is the use of retroviruses as insertional mutagens. This approach uses exogenous DNA as a mutagen which also serves as a molecular tag for identifying the particular gene which when mutated has produced the phenotype. The pseudotype retrovirus is based on Moloney murine leukaemia virus and the envelope glycoprotein of the vesicular Somatitis virus. Injection into the developing embryo results in random integrations in the zebrafish genome producing chimeric fish. The insertions can be passed through the germline by inbreeding and approximately 1 in 80 embryos will have insertional mutations. The method is applicable for large scale screens as it does not rely on expensive exomic sequencing (Amsterdam *et al.*, 2011). To date only approximately 500 mutations at 350 loci have been identified which is less than by ENU based protocols.

1.8.5 Tetracycline Systems

The tetracycline Tet-on or Tet-off system is another model system gaining increasing attention to produce a conditional knock-down in zebrafish (Gossen and Bujard, 1992). Tetracycline controlled activation systems can turn on or off expression of a particular gene in a reversible manner, depending upon the concentration of tetracycline added to the aquarium water. Gene expression via a specific promoter is regulated by the tetracycline response elements (TRE's) that are bound by the tet-repressor protein, resulting in inhibition of gene expression. Tetracycline binds to the tet-repressor, resulting in de-repression of the engineered locus (Knopf *et al.*, 2010). Target gene repression is achieved by controlling the expression of a synthetic shRNA which is capable of directing the cognate mRNA from the locus of interest for degradation. Tetracycline

systems are flexible in that genes can be over or underexpressed and can be localised to a specific tissue. The system also enables control of the specific level of gene expression by means of titration of the tetracycline in the system. The major drawback in zebrafish is the low efficiency with which transgenic animals can be developed and the requirement of a closed water system in the zebrafish facility (Munoz *et al.*, 2005).

1.8.6 Binary Systems

Binary systems have been used in *Drosophila* research to regulate gene expression and are becoming available in zebrafish (Potter and Luo, 2011). The Q-transcriptional regulatory system of *Neurospora* crassa is used to produce 4 tandem, non-repetitive upstream activating sequences. These act as targets for Gal4 transcription factor, known to be less prone to transcriptional silencing over generations via methylation than other approaches such as models produced with retroviruses (Svoboda *et al.*, 2000; Munoz *et al.*, 2005).

1.9 Direction of Study

The overall aim of the project is to investigate the role of FKRP and fukutin in early zebrafish development. The aims can be split into two broad categories either resource building or hypothesis based.

Resource Building Aims:

- The project initially aims to establish the best approach to modelling fkrp and fukutin deficiency in zebrafish.
- Attempt to create an alleilic series of *fkrp* mutant lines with ZFNs.
- In parallel the project aims to investigate dystroglycanopathy using an antisense oligonucleotide morpholino (MO) strategy by knocking down fkrp, fukutin and dystroglycan.
- Characterise the phenotypes of fkrp, fukutin and dystroglycan knock downs compensating for differential efficacy of the morpholinos by controlling for the severity of the phenotype.

Thesis Hypothesis:

- The pathological features of muscle, eye and brain associated with secondary dystroglycanopathies may be attributable to pathological disturbance of basement membrane.

Chapter 2   Materials and Methods

2.1 Animal Models

2.1.1 Fish strains and maintenance

The two fish strains used in this study were the wild-type AB* strain [Zebrafish International Resource Centre (ZIRC), Oregon USA] and the transgenic line TG *(fli 1: EGFP)* expressing EGFP in the blood vessel endothelium under control of the Fli-1 promoter (Lawson and Weinstein, 2002). Males and females were paired and separated by gauze the night before embryos were required. The following morning the gauze was removed. Zebrafish embryos were collected and raised at 28.5°C in E3 medium (5mM NaCl,0.17mM KCl, 0.33mM CaCl$_2$, 0.33mM MgS0$_4$, 0.1PPM methylene blue) using established procedures and staged in hours or days post fertilisation (hpf or dpf) according to Kimmel criteria (Kimmel *et al.*, 1995). 1-2dpf embryos were dechorionated manually or bathed in 0.5 - 2 mg/ml pronase (Roche) for 5 minutes and washed several times in E3 medium. All fish, including 3-5dpf larvae, were euthanized in 4mg/ml tricaine methanesulfonate, E3 medium mix (50:50; Westerfield, 2000).

2.1.2 Criteria for the Classification of Morphant Phenotype

This section outlines the criteria for the classification of fukutin, fkrp and dystroglycan morphant zebrafish between 1-5 dpf into phenotype severity groups (Table 2.1 & Figure 2.1; Kimmel *et al.*, 1995). The zebrafish being translucent at 1dpf is a particularly attractive attribute of the system for studying dystroglycanopathy; key features have been outlined in the schematics in Figure 2.1 (Kimmel *et al.*, 1995).

Stage of Development	Time	Main Features of Period
Zygote	0 hrs	Single cell stage to first zygotic cell division. Cytoplasm moves toward animal pole forming the blastodisc (a thin layer of cells on the inside of the blastula) *N.B.* MO injection period.
Cleavage	¾ hrs	2-128 cell stage formation of three regular tiers of blastomeres.
Blastula	2 ¼ hrs	Formation of the epiblast (tissue derived from blastodisc), hypoblast (embryonic precursor of the endoderm) and embryonic axis through morphogenetic movements of involution, convergence and extension.
Gastrula	5 ¼ hrs	Germ ring and embryonic shield are at 50% epiboly (controlled movement of cells into germ layers and axis formation), visible from animal pole. Brain and notochord rudiments thicken becoming distinct structures, tail bud becoming prominent by the end of the phase.
Segmentation	$10^{1}/_{3}$ hrs	First somite furrow to 26 somites, optic vesicle and Küpffer's vesicle (epithelial ciliated sac involved in left-right signalling) start to develop at $11^{2}/_{3}$ hpf. By 16hpf otic placode (thickening of ectoderm forming sensory tissue), brain neuromeres, all begin to form and v shaped somites. Towards the end of the period muscular twitches, optic vesicle and hind brain are all visible.
Pharyngula	1 dpf	At the beginning of the phase the embryo is 1.6mm in length and 3.1mm by the end. Early touch reflex and pigmentation begin to develop. Caudal artery is almost at the end of the tail by the end of the period. Pericardium becoming prominent towards the end of the period.
Hatching	2 dpf	By the end of the period the fish are 3.5mm in length. Pigmentation and pericardium become prominent. Small mouth visible.
Early Larva	3 dpf	Phase also known as protruding mouth. Rapid growth of embryo - all systems develop further.
Mid Larva	14 dpf	6.2 mm in length, first hypural cartilage in tail fin, ossification of pharyngeal skeleton, neural maturity *i.e.* Rohon –Beard neurones replaced by dorsal root ganglia.
Juvenile	30 dpf	10 mm in length, adult fin and pigmentation patterns, lateral line shifts ventrally.
Adult	90+ dpf	18mm-500mm, earliest time to breed.

Table 2.1: Stages of zebrafish development

Table outlines prominent stages in the development of zebrafish from the single cell stage through to the fully grown adult fish. Zebrafish have an approximate life span of four years and produce high quality eggs from about six months to two years. Since temperature affects the rate of development fish are always staged according to Kimmel criteria and grown in incubators at 28°C (Kimmel *et al.*, 1995; Westerfield, 2000).
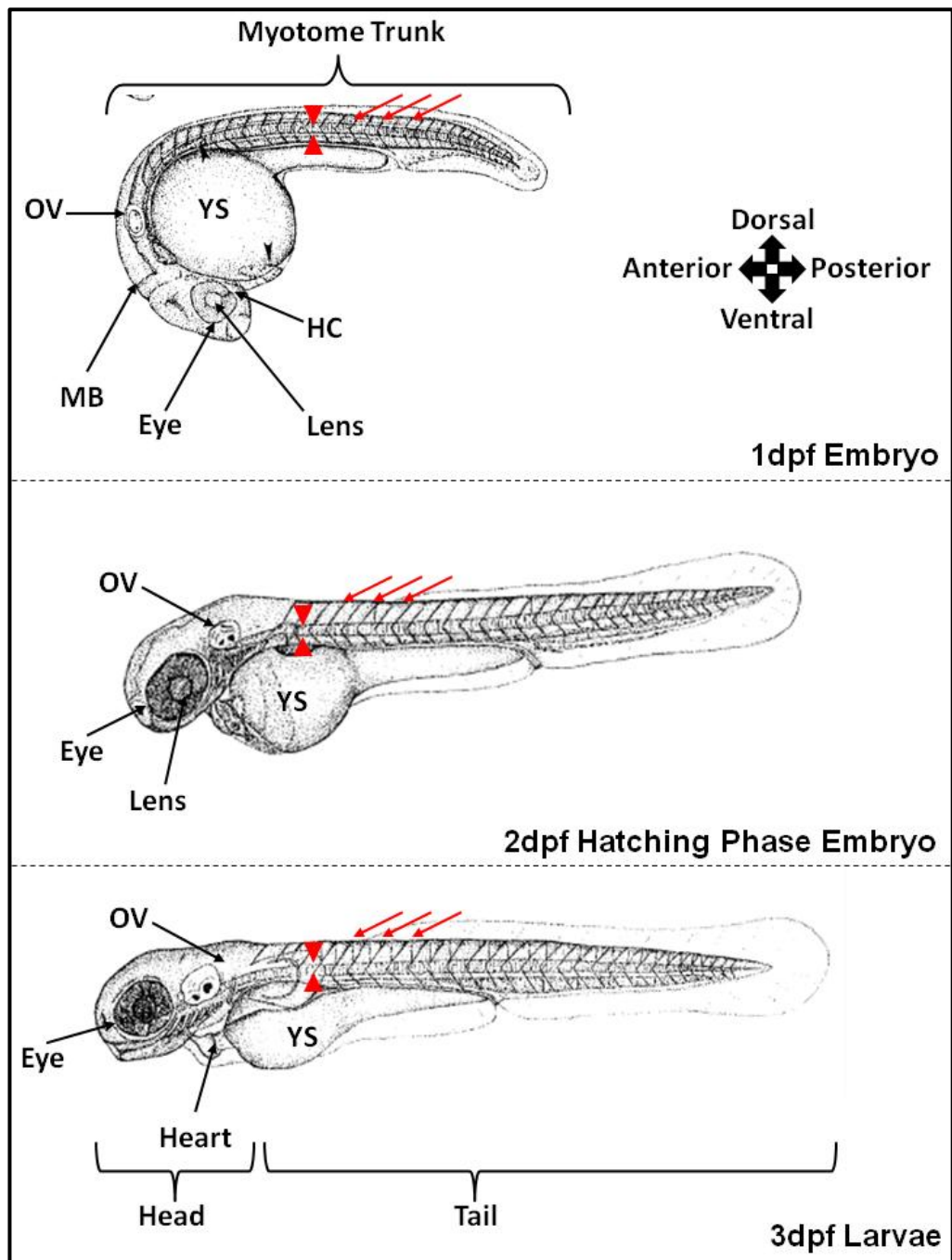
Figure 2.1: Camera lucida schematics of 1, 2 & 3dpf zebrafish
Figure shows orientation diagram of major regions *i.e.* the head, tail and myotome trunk. Trunk and tail can be used interchangeably, however it should be noted the myotome trunk is more precisely concerned with the somites and notochord whereas the tail also includes the gastrointestinal tract (Westerfield, 2000). Red arrows: somites, red triangles: notochord, MB: mid brain, HC: hyaloid canal, YS: yolk sack & OV: otic vesicle. Adapted from Kimmel *et al.*, 1995.

Anatomical structures important for investigating dystroglycanopathy have analogues in zebrafish, such as somites, mid brain and eye, and can be assessed on morphological grounds. By the beginning of the pharyngeal stage of development 1dpf, the embryonic body axis is straight and therefore even a slight effect of MO injection on tail curvature can be detected. Tail curvature is

therefore a sensitive indicator of phenotypic severity. Pigmentation begins at approximately 2dpf obscuring some of the key anatomical features from this point onwards. The tail curvature remains past 1dpf as the most suitable way to sort the embryos into phenotype categories (Table 2.2).

Phenotype	Somitic Region	Eye	Brain	Other Features
Normal	No angled curvature of somitic region	Two small round eyes with pupil present	Clear midbrain structure present at higher magnification	Embryo swims with/without stimulation (after early dechorionation)
Mild	0-15° Angle of trunk region	Small decrease in diameter but no notable shape changes	Small, no notable brain changes at higher magnification	May have cardiac oedema and swim in circles
Moderate	15-30° Angle of trunk region - may be curling to a greater degree at posterior of fish (tail).	Eye notably smaller and may have disrupted shape	Mid brain not always visible	Fasciculations regularly a feature
Severe	Tail curvature > 30° - tail often shorter in length and dorsal curvature should also be considered	Eyes often missing or very irregular in size and shape	Brain not visible	Very irregular overall in appearance on dechorionation, very unlikely to move

Table 2.2: Phenotypic classification of 1-5dpf embryos as judged under the dissecting microscope
The classification allows comparison of the phenotypes for each MO. It should be noted that for MO injected embryos the very severe embryos and no phenotype were not included in further assessment of pathology.

2.1.3 Antisense oligonucleotide morpholino preparation

Antisense morpholino oligonucleotide (MO, Gene Tools LLC) were designed to target to the putative start of translation of the zebrafish *fkrp* transcript (5´-ACTGATACGCATTATGGCTCTTGTG-3´; Thornhill *et al.*, 2008). The 30-12Apr05B *fktn* splice MO 5´-GCCCAGAAACCTCTTCAGCAGATGC-3´ is directed against the splice donor site of exon 4 in the zebrafish *fktn* gene, predicted to lead to the skipping of the exon and consequently to a frame shift that results in premature translation termination. The *dag1* translation blocking MO 5´-CATGCCTGCTTTTATTTTCCCTCGC-3´ has previously been described

(Parsons *et al.*, 2002a). The *gfat1* (glucosamine-fructose-6-phosphate aminotransferase 1) splice MO was used as described (Senderek *et al.*, 2010). The Gene Tools standard control morpholino: 5´-CCTCTTACCTCAGTTACAATTTATA-3´ was used for control MO injections. The MOs were re-suspended in 1x Danieau solution (0.4mM MgSO$_4$, 58 mM NaCl,0.7mM KCl, 5mM HEPES, 0.6 mM Ca(NO$_3$)$_2$; pH 7.6; Westerfield, 2000).

2.1.4 Glass Needle Preparation

Glass Capillaries were pulled using a P97 Flaming Brown Micropipette Puller with a heat of 695, a pull of 70 and velocity of 60. Needles were filled with injection solution using Microloader Tips (Eppendorf) and broken sequentially up the needle towards the injector using forceps under a dissecting microscope until an optimal volume was achieved on injection. Volume was judged by measuring the initial diameter of a drop of injection solution in mineral oil on a graduated microscope slide under a dissecting microscope.

2.1.5 Micro-manipulation

Individual MO MWs were calculated from sequences. MOs were diluted to 1µmol and an injection volume was calculated from a desired amount of MO *e.g.* 10ng *fkrp* MO, using the following equation:

$$Volume = Mass / Concentration$$

The volume could then be used in the following equation to derive the radius of the drop size. Diameter was obtained by doubling the result:

$$Radius = \left(V \times \frac{3}{4 \times \pi} \right)^{\frac{1}{3}}$$

10ng of *fkrp* or control MO, 2ng of 30-12Apr05B *fktn* MO and 7ng of *dag1* MO were injected into the embryos yolk sac at the one to two-cell stage, using phenol red as an injection indicator.

2.2 Molecular Biology for ZFN CoDA Protocol

2.2.1 DNA Extraction

Embryos were collected, washed several times in PBS, lysed in SDS lysis buffer (10mM Tris, pH8.0, 200mM NaCl, 10mM EDTA, 0.5% SDS and 100µg/ml Proteinase K) and incubated at 50°C overnight. Phenol-Chloroform-Isoamyl

alcohol (25:24:1 Invitrogen) was mixed with the lysates to form an emulsion and centrifuged at 14,000rpm for 5 minutes at room temperature (RT). The supernatant was mixed with 100% ethanol and centrifuged at 14,000rpm for 20 minutes at 4°C. The supernatant was completely removed and 70% ethanol was used to wash the pellet with a further spin at 14000 rpm for 10 minutes at 4°C. Samples were left to air dry at RT then left to dissolve in 20µl of EB buffer (Qiagen) for 2 hours at RT.

2.2.2 RNA Isolation

RNA was collected from approximately 30 zebrafish embryos for RT-PCR analysis. The embryos were homogenised in 200µl lysis buffer *see* 2.2.1 for further detail, 1ml of Trizol (Invitrogen) was added to lysates and incubated at RT for 1 minute then spun at 14,000rpm for 10 minutes at 4°C. 0.2ml of chloroform was added and tubes shaken vigorously by hand for 15 seconds. Samples were then incubated for 3 minutes at RT and centrifuged at 14,000rpm for 15 minutes at 4°C. The aqueous phase was transferred to an Eppendorf containing 0.5ml isopropyl alcohol, shaken by hand and incubated at RT for 10 minutes. The samples were spun at 14,000rpm for 15 minutes at 4°C and the supernatant removed. The pellet was washed in 0.5ml of 70% ethanol and centrifuged at 14,000rpm for 5 minutes at 4°C. The supernatant was removed and the pellet dried at 60°C for 10 minutes. The pellet was dissolved in 30µl of ddH$_2$O and stored at -20°C or -80°C for extended periods of time. The absorbance at 260 and 280nm was measured on a nanodrop (ND-8000, 8-Sample Spectrophotometer) to give the RNA purity and concentration.

2.2.3 First-Strand cDNA Synthesis

The isolated RNA was mixed with RNase free water, random primers (100ng/µl, Promega) and 10mM dNTPs (Fermentas). The tube was briefly centrifuged and heated to 65°C for 5 minutes, and incubated on ice for one minute. First-Strand Buffer, 0.1mM DTT, RNaseOUT Recombinant RNase inhibitor (40units/µl, Invitrogen) and Superscript III RT (200units/µl, Invitrogen) were added. The cDNA was generated by incubation at 25°C for 5 minutes then 50°C for 1 hour. The reaction was inactivated by heating to 70°C for 15 minutes. The cDNA was stored at -20°C, or used directly as a template for PCR.

2.2.4 RT-PCR

The following was made up to 50μl with dH_2O to perform PCR:

- 4μl PCR enhancer
- Template DNA 10-100ng
- 10 mM dNTPs
- 10x PCR reaction buffer
- 1μl Moltaq DNA polymerase (Moltaq)
- PCR primers to a final concentration of 50pmol/μl (Table 2.5)

After mixing and brief centrifugation, reactions were incubated in a thermal cycler (Senso Quest, Labcycler) with the parameters in Table 2.3 & Table 2.4.

Step No.	Step Name	Temperature (^{o}C)	Time
1	Initialisation	95	2 minutes
2	Denaturation	95	15 seconds
3	Annealing	55-65	1 minute
4	Elongation	72	2 minutes
5	Final Elongation	72	7 minutes
6	Hold	4	∞

Table 2.3: Standard PCR programme
Steps 2-4 were repeated 35 times.

Step No.	Step Name	Tm (^{o}C)	Time
1	Initialisation	94	2 minutes
2	Denaturation	94	10 seconds
3	Annealing	55	30 seconds
4	Elongation	68	2 minutes
5	Denaturation	94	10 seconds
6	Annealing	55	30 seconds
7	Elongation	78	20 seconds
8	Final Elongation	78	7 minutes
9	Hold	4	∞

Table 2.4: Long PCR programme
Steps 2-4 and 5-7 were repeated 9 and 19 times respectively.

Name	Gene	Sequence (5´-3´)	Tm (^{o}C)
Fukutin exon 2 FWD Fukutin exon 5 REV	*fktn(Danio rerio)*	TGTGTCGGATCGCTCTAATG CGTTAAAGCGGAACAGGAAG	57
FKRP FWD FKRP REV	*fkrp(Danio rerio)*	GCATCACTTTTGGCCAGACT TTCTCCATCATTTGCTGCTG	56
FKRP 5-1 ZFN FWD FKRP 5-1 ZFN REV	*fkrp (Danio rerio)*	TCGCGGGCTCAGCAGCAAAT ATCAGGGGGCGCCCTAAGGG	63
FKRP 5-2 ZFN FWD FKRP 5-2 ZFN REV	*fkrp (Danio rerio)*	CATCTTGTATTATGTCTCGCGGGCT AGGCCGCAGGGCTGTAAGTG	58

Table 2.5: PCR primer pairs

2.2.5 Gel Electrophoresis

1µl/ml of safe view nucleic acid stain (NBS biological) was mixed into the molten
1-2 % agarose gel in 1xTAE buffer pH8.0 (Tris base, acetic acid and
Ethylenediaminetetraacetic acid – EDTA). 5µl of PCR product was mixed with
1µl of loading dye (dH$_2$O, 15% glycerol, 0.25% bromophenol blue, 0.25% xylene
cyanol) and subjected to electrophoresis for a minimum of 30minutes at 100V
before being visualised under UV light. Gel images were captured on a
GelDoc-It 310 Imaging system (UVP).

2.2.6 Purification of Plasmids and DNA Extraction

A single colony was selected from 100µg/ml Ampicllin LB agar (10g Bacto-
tryptone, 5g yeast extract, 10g NaCl, 15g agar in 1litre dH$_2$O, sterilised by
autoclaving), incubated in 10ml LB media (10g Bacto-tryptone, 5g yeast extract,
10g NaCl, in 1litre dH$_2$O) containing 100µg/ml Ampicillin overnight at 37°C in a
shaking incubator. 1ml of the media was spun down and pellet resuspended as
per the directions of Quiagen plasmid purification kit manual (QIAprep Spin
Miniprep Kit; 27106). The final product was eluted in 20µl of EB buffer supplied
in the kit and concentration was estimated on a NanoDrop (ND-8000, 8-Sample
Spectrophotometer) and whole plasmids were sent for sequencing at Eurofins
MWG with a forward primer for each region of interest.

2.2.7 ZFN CoDA Specific Methods

The zebrafish *fkrp* transcript (NC_007126.5) was entered into ZiFit Version 3.3. The returned sequences from in the *in silico* tools for the FKRP 5-1 & 5-2 were sent for synthesis by Eurofins MWG Operon and returned in pCR2.1 vectors. The vectors were digested using XbaI and BamHI restriction enzymes and each zinc finger array was subsequently recloned into the Fok-1 nuclease containing vectors pMLM290/292. Plasmids were digested at the BamHI and XbaI restriction sites, to test whether the inserts were correctly cloned into pMLM290/292, the products were visualised on an agarose gel, and plasmidswere then sent to Eurofins MWG for sequencing, *see* section 2.2.6 and Table 2.5. To generate the mRNA the pMLM290/292 plasmids containing the correct inserts were linearised with *Pme*I. A small volume was tested by visualisation on an agarose gel.

2.2.8 Generating mRNA

All reagents in the protocols below are part of T7 Ultra mMessage mMachine kit (Ambion).

Capped Transcription Reaction Assembly

Reagents were thawed on ice, mixed by vortexing and briefly centrifuged. The transcription reaction is assembled at RT as below:

- 10µl T7 2x NTP/ARCA
- 2µl 10x T7 reaction Buffer
- 0.1-1µg linear template DNA
- dH$_2$O to a final volume of 20µl

The reaction was mixed by gentle pipetting and incubated at 37°C for 2 hours. To remove template DNA 1µl of TURBO DNase was added and incubated at 37°C for 15 minutes.

Poly (A) Tailing Procedure

The following reagents are used for the addition of poly-A tails to the mMessage mMachine T7 Ultra reaction:

- 21 µl mMessage mMachine T7 Ultra reaction
- 35 µl nuclease free water
- 20 µl 5x E-PAP Buffer
- 10 µl 25mM MnCl$_2$

- 10 µl ATP

As a control 2.5 µl was set aside and 4 µl of E-PAP was added then incubated at 37°C for 45 minutes before being returned to ice. Another 2.5 µl aliquot was kept for running on a 1% agarose gel alongside the samples without poly-A tails. The kit includes a formaldehyde based loading dye essential for accurately resolving RNA size.

Lithium Chloride Precipitation for RNA Recovery

Lithium chloride precipitation removes unincorporated nucleotides and most proteins. 50 µl of lithium chloride precipitation solution was mixed with the mMessage mMachine T7 Ultra reaction and chilled for 30 minutes at -20°C before being centrifuged at 4°C for 15 minutes at 14,000 rpm to pellet the RNA. The supernatant was removed and the pellet washed in 70% ethanol and centrifuged for 10 minutes at 4°C, 14,000rpm. The ethanol was removed and the pellet air dried until it became transparent. The pellet was resuspended in 20µl of RNAse free water (Ambion).

Micro-Injection of mRNA

2nl (300pg) of the following mixture was injected behind the cell into the yolk of a single cell staged egg.

- RNA encoding left half-site ZFN   750ng
- RNA encoding right half-site ZFN   750ng
- 1% phenol red   0.5µl
- 1x Danieau Solution   to 6µl

2.2.9 Screening Samples for Mutations

Two sets of 10 2dpf embryos were collected from the ZFN injected clutches with no discernible phenotype, *N.B.* high levels of mRNA in about a third of injected embryos creates a disrupted developmental phenotype which is undesirable for further analysis. The ten embryos were pooled and lysed for DNA extraction, as described above in section 2.2.1. The pooled DNA was amplified in a standard PCR reaction with either FKRP ZFN 5-1 or 5-2 primers (Table 2.5) and purified PCR products were cloned using the pGEM-T easy vector system, as described in the manufacturer's guidelines. The pGEM-T easy vector containing inserts was transformed into XL-1 blue E.coli cells and plated on LB *Xgal*-amp plates. 95 colonies were selected and mixed directly into PCR

mastermix on a 96 well plate. Long PCR as described above in Table 2.4, was performed to amplify the inserts, 5μl was ran on a gel to check for successful PCR reactions and sent for sequencing using MWG Eurofins plate sequencing service.

2.3 Whole-mount Antibody Immunofluorescence Staining

Embryos were fixed in 4% paraformaldehyde (PFA) in phosphate-buffered saline (PBS) overnight at 4°C and then further fixed and permeabilised in pre-cooled acetone at -20°C. Non-specific antibody binding sites were blocked in PBS containing 5% horse serum and 0.1% Tween-20 (PBST, blocking solution). Embryos were incubated overnight at 4°C in blocking solution containing either of the following primary antibodies: IIH6 (anti α-dystroglycan mouse IgM 1:50; a kind gift from Professor Kevin Campbell, University of Iowa), 43DAG (anti β-dystroglycan mouse IgG 1:50; Novocastra) and pan-laminin (anti rabbit IgG polyclonal 1:250; Sigma). The embryos were washed several times with PBST and incubated with the following secondary antibodies: Goat anti-mouse IgM Alexa Fluor 594 (Invitrogen), Goat anti-mouse IgG Alexa Fluor 594 (Invitrogen), donkey anti-rabbit IgG Fluor 594 (Invitrogen) all at a dilution of 1:500. Texas Red conjugated phalloidin 1:100 (Invitrogen) was used to label F-actin. A minimum of twenty embryos from three independent injections were stained and imaged for each individual experiment.

2.4 Cryosectioning and Immunohistochemistry

Euthanized 3dpf embryos were incubated in 4% PFA at 4°C overnight followed by three 5 minute washes in PBS. The fish were incubated in increasing concentrations of sucrose in PBS (5%, 15% & 30%) waiting each time until the fish sank to the bottom of the tube to ensure full permeation of the sucrose to the specimen. Excess sucrose was removed and fish were aligned in OCT embedding medium (RA Lamb), three on a single piece of filter paper, pre-cut into thin strips. Samples were snap frozen in pre-chilled isopentane and stored at -80°C. Embedded fish were allowed to thaw for 1 hour in the cryostat prior to sectioning (specimen -23°C and blade -21°C). The paper was removed and the specimen mounted on cork disks with OCT embedding medium. Fish were trimmed to the level of the lens by cutting in a transverse plain. Sections 8μm

thick were mounted on gelatine coated slides (0.3% gelatine, 0.1% Chromium Potassium Sulphate), slides were left overnight in a fume cupboard to dry.

A wax pen was used to draw around samples before a 1 hour incubation in either 5% horse serum in PBST or 4% bovine serum albumin (BSA) in tris-buffered saline solution containing 0.1% tween-20 (TBST). Samples were washed three times with either PBST or TBST and incubated in primary antibody: 43DAG (anti β-dystroglycan mouse IgG 1:50; Novocastra), IIH6 (anti α-dystroglycan mouse IgM 1:50) in 5% Horse serum PBST and pan-laminin (anti rabbit IgG polyclonal 1:100; Sigma) in 4% BSA PBST overnight at 4°C. Primary antibody was removed and slides washed three times in either PBST or TBST for a minimum of 5 minutes. Sections were incubated in secondary antibody: (Goat anti-mouse IgM Alexa Fluor 594, Invitrogen; 1:500, Goat anti-mouse IgG Alexa Fluor 594, Invitrogen; 1:500), in 5% Horse serum PBST (Donkey anti-rabbit IgG Fluor 594, Invitrogen; 1:250) as described above in 4% BSA PBST for 2 hours at room temperature. Samples were washed a further three times in PBST or TBST and mounted in Vectorshield without DAPI. Slides were sealed with a cover slip and clear nail varnish.

2.5 Microscopy

2.5.1 Light Microscopy

An epifluorescence stereo microscope (Leica MZ16F) was used to image live embryos. A minimum of five pictures were taken of each individual fish for each experimental group. Toluidine blue stained sections were imaged using an Axioplan-2 microscope with an Axiocam HRc camera and the Zeis Plan Neofluar 20x/0.5. The Leica DM2000 Axioplan-2 microscope with a PlanNeofluar 20x/0.5 objective and AxioCam HRM was used to capture images of immunofluorescence experiments on cryosections. Wild type fish were used to set exposure times and unstained controls were used to confirm minimal background levels in fluorescence studies.

2.5.2 Confocal Microscopy

Whole mount embryos were analysed on a Zeiss LSM 510 Meta laser scanning confocal microscope, using the Argon laser line at 488nm and the HeNe 543nm

Plan Neofluar 20x/0.5 Ph2 or Plan Neofluar 40x/1.3 Ph3 (oil) and analysed with LSM software-V4.2.0.121.

2.5.3 Electron Microscopy

Fish were washed in dH_2O and fixed immediately in 2% glutaraldehyde in 0.1M sodium cacodylate buffer (Sigma-Aldrich) overnight. The fish were subjected to three 15min washes in cacodylate buffer then stained in 1% osmium tetroxide (Agar Scientific) in dH_2O for 1 hour. The fish were washed twice in dH_2O for 15min each before being dehydrated sequentially through acetone solutions of increasing concentration (25%, 50%, 75% & twice in 100%). The samples were incubated through increasing concentrations of resin in acetone (25%, 50%, 75% & 100%; epoxy resin kit, TAAB Lab. Equip.) and left overnight on a rotator in 100% resin at RT. The samples went through a further 4 changes of resin the next day over a minimum of 5 hrs. Resin was polymerised in a $60^{\circ}C$ oven overnight.

Blocks were orientated and trimmed on a Reichert-Jung Ultracut-E microtome before cutting sections at 1µm thickness. Sections were collected on glass slides in water, dried on a heat block and stained with toluidine blue (0.5% di-sodium tetraborate, 1% toluidine blue in dH_2O and filter sterilised) for 1min on the heat block at $\sim50^{\circ}C$. Sections were mounted in DPX for imaging.

Ultrathin sections were cut to 80-110nm as judged by the colour which should be a pale gold and collected on washer grids (3mm diameter). Sections were stretched by exposing them to chloroform vapour to eliminate compression (undesirable folds) and mounted on pioloform (Agar Scientific) copper washer grids. The washer grids were prepared by dipping a slide in 0.5% pioloform in chloroform to create a film on the slide and dried in chloroform vapour. A square piece was cut in the pioloform film coating on the slide and removed by floating the square pioloform film piece onto dH_2O, the slide was discarded. Grids were placed on the pioloform film floating on the dH_2O and collected by placing parafilm on top (films and grid stick to the parafilm and can be stored in a sealed container). Grids were washed and stained on an EM AC20 (Leica UK Ltd.) in 2% aqueous uranyl acetate lead citrate (Agar Scientific).

Samples were imaged on a Phillips CM100 Compustage (FEI) Transmission Electron Microscope. Digital images were collected using an AMT CCD camera (Deben).

N.B. Most of the cutting and preparation of ultrathin sections in the project was carried out by Newcastle University Electron Microscopy Unit staff. The rest of the TEM work was carried out independently including normal microtomy and imaging.

2.6 Analysis

2.6.1 Image Analysis Software and Data Storage

Image J software was used to calculate the area of the eyes of 3 dpf larvae, derived from confocal image projection stacks of the eye vasculature (complete cross sections of the eyes; z stacks of 35 slices projected together into one image). The intersegmental vessel heights from the dorsal aorta were expressed as a proportion of total somite height as measured using Image J software. Image J was also used to measure eye size from light microscopy images and used to calculate the area of each eye of 3dpf larvae. The vertical myosepta angles were calculated using light microscopy images of 3dpf larvae of the myotome trunk region. Data was stored on a secure university server which is backed up regularly, files contained reference to magnification, date, MO and were organised accordingly in files dependent on experiment and at a higher level by technique.

2.6.2 Statistics

All basic statistical analysis including un-paired student T-tests were carried out in Excel 2007 Microsoft Office. Chi squared tests and ANOVA analysis was carried out in Minitab 16 statistical software package. To analyse variability using a one way ANOVA test, data was first checked for approximate normal distribution using a normal probability plot. Comparisons were made using Tukey's analysis.

N.B. I would like to thank Dr Peter Avery for providing his expert opinion and advice on the statistics within the thesis.

Chapter 3   Fukutin Deficient Zebrafish have a Muscle Eye Brain Phenotype

3.1. Introduction

By using zebrafish as a model for investigating FKRP and fukutin deficiency, a greater insight into the mechanism of the associated MD in humans can be gained (Fukuyama *et al.*, 1981; Takada *et al.*, 1988; Yoshioka and Kuroki, 1994; Bassett and Currie, 2003). This chapter will focus particularly on the criteria for judging the fukutin morphant phenotype and the recapitulation of the dystroglycanopathy phenotype in the zebrafish (Yoshioka and Kuroki, 1994; Hino *et al.*, 2001; Thornhill *et al.*, 2008). There is currently no single model that recapitulates human fukutin deficiency. The major drawback of the homozygous null mouse model is its inability to survive foetal development past E9.5 (Chiyonobu *et al.*, 2005; Kurahashi *et al.*, 2005). The retrotransposon knock-in fukutin mouse model, described in the introduction, survives the embryonic stage but have little in the way of pathology despite hypoglycosylation of α-dystroglycan. The fukutin chimeric mouse remains the most suitable model to investigate fukutin deficiency (Takeda *et al.*, 2003; Kanagawa *et al.*, 2009a; Taniguchi-Ikeda *et al.*, 2011). As a pilot for the use of ZFNs this chapter also describes an attempt to create a stable *fkrp* mutant line in zebrafish using the CoDA protocol.

 Here the aim is to investigate whether the dystroglycanopathy phenotype is present in fukutin knock down zebrafish, comparing the results with those published in Lin *et al.* study (Lin *et al.*, 2011). Criteria will be applied to the knock downs to attempt to align the fukutin morphants with FKRP and dystroglycan morphants. Ultimately, any similarities with other primary and secondary dystroglycanopathy models will be assessed (Heasman, 2002; Rosen *et al.*, 2009).

3.1.1 Aims

- Design ZFNs targeted at the *fkrp* locus in zebrafish.
- Assess the efficacy of ZFNs in producing mutations at the *fkrp* locus in zebrafish.
- Produce an allelic series of *fkrp* mutant zebrafish.
- To test MO that inhibit *fktn* expression and to study any associated pathology.
- To design criteria for the classification of morphant severity that is applicable for dystroglycanopathy knock down models.
- To assess the 30-12Apr05B *fktn* MO phenotype in the context of the phenotype range described in FKRP and dystroglycan knock down zebrafish.

- To assess the 30-12Apr05B *fktn* MO phenotype in the context of the muscle, eye and brain pathology observed in patients with mutations in the FKTN gene.

3.2 Results

3.2.1 CoDA Based ZFN Technology

An attempt to create an allelic series of *fkrp* mutant zebrafish was made using the CoDA protocol. Overall the protocol involved designing ZFN pairs *in silico* that targeted regions within the *fkrp* gene to be synthesized commercially. These sequences were then cloned into expression vectors that contained both the Fok-1 nuclease coding sequence and a T7 RNA polymerase initiation site. These vectors could then be linearised and used to generate mRNA, combining the pair of in vitro trasnscribed ZFNs for injection into zebrafish eggs. A selection of injected zebrafish were then screened for somatic mutations that could potentially be passed through the germline into the next generation of fish. At this stage genotype and phenotype could be defined for any mutants successfully generated (Sander *et al.*, 2010).

The zebrafish *fkrp* transcript (NC_007126.5) was entered into ZiFit Version 3.3. The programme identified two potential zinc finger pairs with five base pair spacer regions (5-1 & 5-2) and one with a seven base pair (7-1) spacer region. The first 5-1 FKRP ZFN was targeted close to the N-terminus and the 5-2 was targeted with proximity to the LiCD domain of the *fkrp* transcript. Both regions have previously been associated with mutations in the *FKRP* gene in patients (Figure 1.6; Van Reeuwijk *et al.*, 2010). The sequences for the FKRP 5-1 & 5-2 were sent for synthesis by Eurofins MWG Operon. Each zinc finger array was subsequently cloned into the Fok-1 nuclease containing pMLM290/292. Vectors were digested at the BamHI and XbaI restriction sites, to test whether the inserts were correctly cloned into pMLM290/292, the products were visualised on an agarose gel, and excised bands were then sent to Eurofins MWG for sequencing. Bands were observed at just under 300bp and sequencing confirmed the inserts were the correct sequence (Figure 3.1).
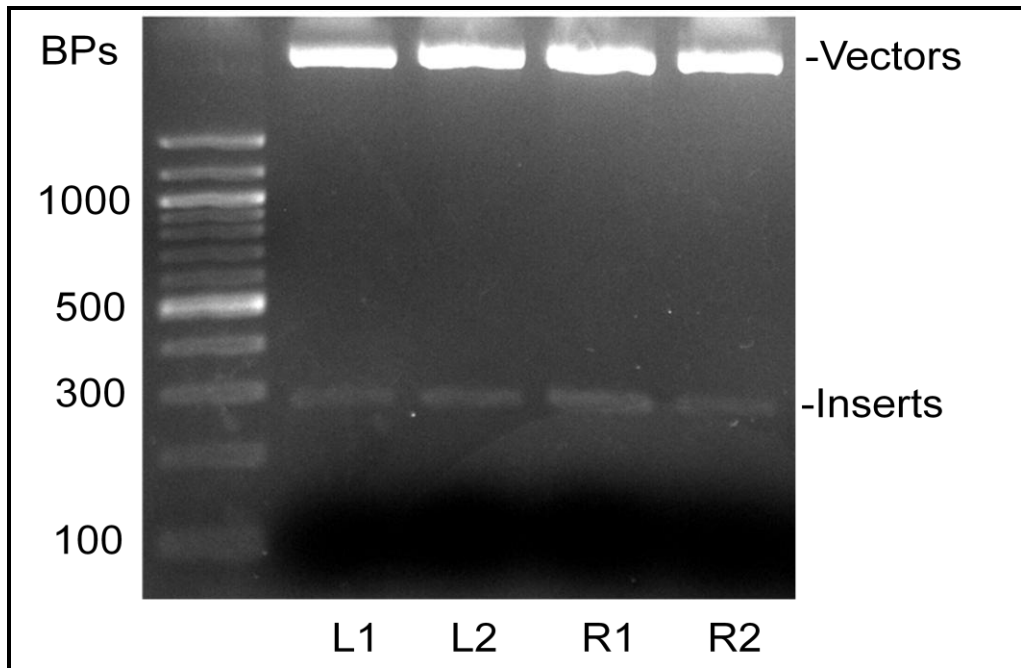
A
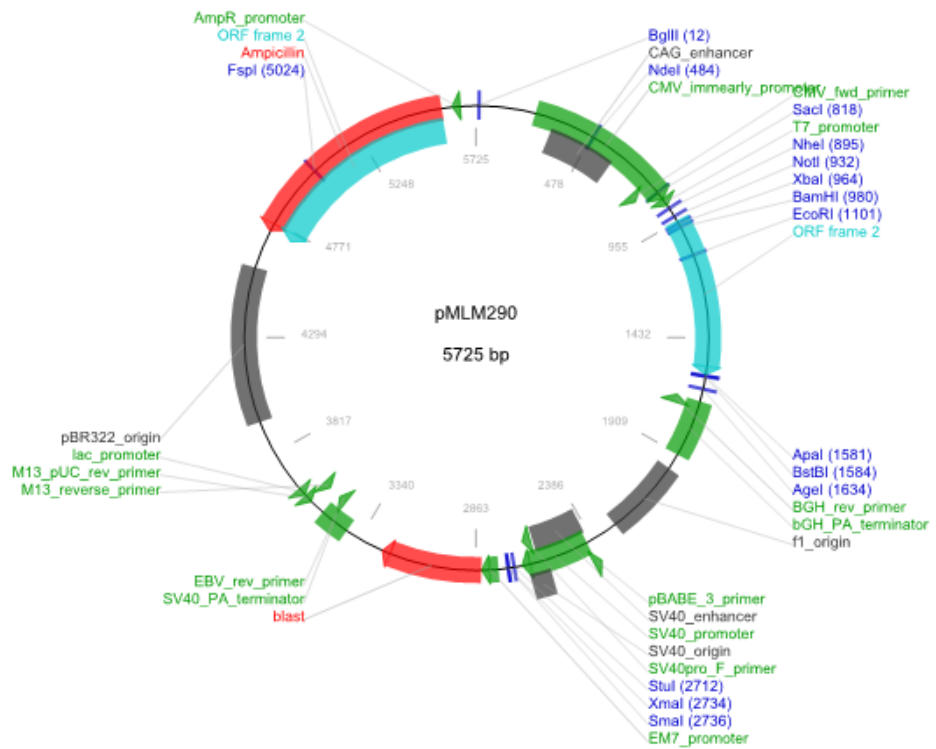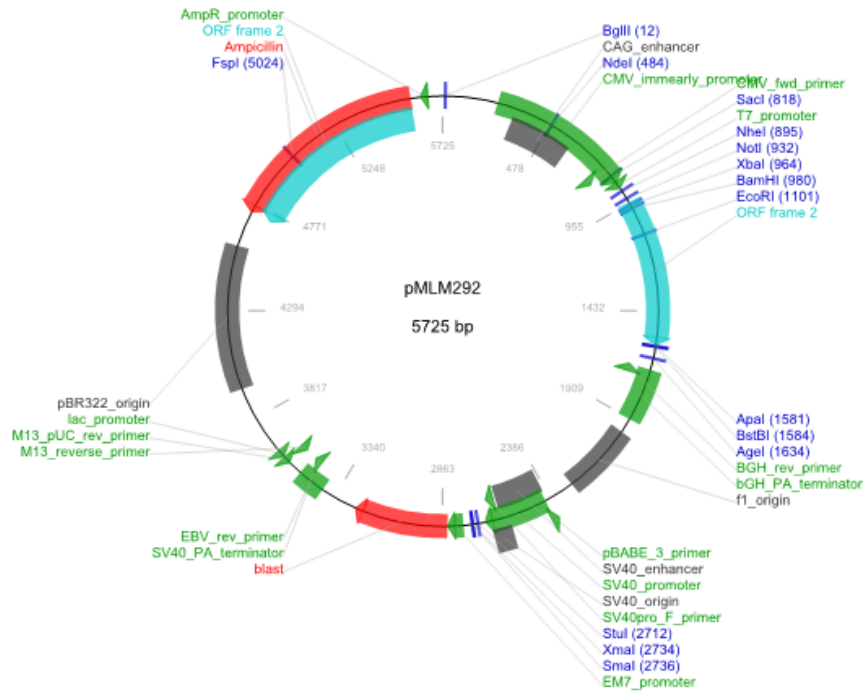
B

Figure 3.1: Digestion of pMLM290/292 vectors containing zinc finger arrays

A: Plasmids containing 5-1 (L1,R1) and 5-2 (L2,R2) ZFNs were digested with BamHI and XbaI and resolved on an agarose gel relative to a 1kb ladder. pMLM290/292 vectors are as expected above the 1kbp and inserts just below 300bps. BPs: base pairs. Vector maps for Fok-1 nuclease containing vectors pMLM290 and pMLM292. pMLM290 used for left hand ZFNs and pMLM292 for right hand ZFNs, with a 5 bp spacer region. Figures copied directly from the addgene website: [http://www.addgene.org/zfc/, accessed 4 January 2013].

Injected mRNA in zebrafish is translated by the embryonic translation machinery into the ZFN proteins. The poly-adenylation of the mRNA is an important step for several reasons including nuclear export, translation and stability. The addition of a cap to the first 5' guanine residue of the mRNA is essential for maturation of the mRNA and therefore translation. To generate the mRNA the pMLM290/292 plasmids containing the correct inserts were linearised with *Pme*I. A small volume was tested by visualisation on an agarose gel and found to be correctly linearised. Capped mRNA with poly-adenylated (poly-A) tailing was generated from the linearised pMLM290/292 vectors (Figure 3.2). The positive (+) bands represent successful mRNA creation with poly-A tails and 5' cap, the negative bands have no poly-A tailing and therefore were observed as lower molecular weight bands on the gel. A denaturing gel would give better resolution, which is not required in this instance as the step only acts as check that mRNA is created and has been fully poly-adenylated.
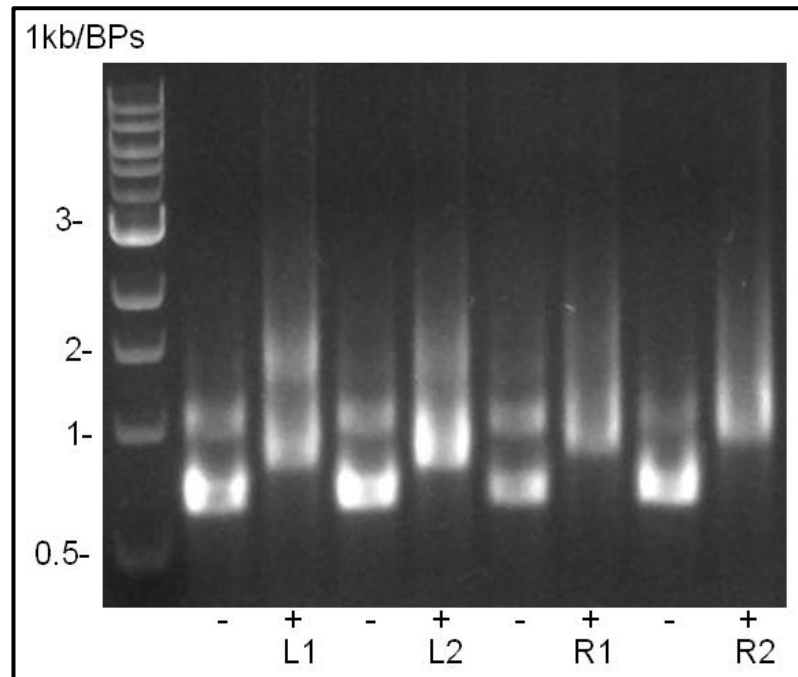
Figure 3.2: In vitro transcription reaction
Capping andadding a poly adenylated tail to mRNA greatly imporves the efficiency of mRNA translation into ZFNs. pMLM 290/292 containing ZFN inserts were linearised and mRNA is generated in vitro. mRNA before poly-A tailing **(-)** and after **(+),** 5-1 (L1,R1) and 5-2 (L2,R2) ZFNs . The generated mRNA of the two fingers was combined and injected into the zebrafish embryos.

The FKRP 5-1 and 5-2 mRNA was injected into the yolk sack close to the cell nucleus of zebrafish embryos at the single cell stage of development. The embryos were allowed to develop for 4 hours before an initial check on their viability was carried out and none of non-injected embryos were found dead at this stage. Dead embryos were found in both sets of injected embryos with 5-1 and 5-2 ZFN mRNA. At 1dpf both injected groups had higher proportions of dead embryos than the non-injected controls. The embryos that survived in the injected FKRP 5-1 and 5-2 groups could in 17% and 21% of cases respectively be seen to have an abnormal morphological phenotype in comparison to controls where no embryos had abnormal phenotypes (Table 3.1). Embryos injected with mRNA are expected to have an "RNA phenotype" (Persengiev *et al.*, 2004; Figure 3.3). The RNA phenotype can be defined as all the non-specific effects that arise from injection of concentrated mRNA. Note the straight tails of the 3dpf non-injected larvae in comparison to occasionally dorsal curvature in the tail of the injected embryos. Recent reports predict CoDA ZFNs to produce a much lower somatic mutation rate (~1.1-3.3%) in the injected embryos than previously thought (~10%; Sander *et al.*, 2010; Moore *et al.*, 2012b). The dorsal tail curvature therefore is likely to be a non-specific side

effect of mRNA injection and not as a result of inducing an indel mutation in the *fkrp* gene.

	Dead 4hpf (%)	1dpf			Total (n)
		Dead (%)	Alive (%)	Phenotype (%)	
FKRP 5-1	51 (11)	204 (46)	116 (26)	76 (17)	448
FKRP 5-2	63 (20)	116 (37)	71 (23)	62 (20)	312
Non-Injected	0 (0)	126 (21)	464 (79)	0 (0)	590

Table 3.1: Viability of fish injected with ZFNs
Viability data from injection of 300pg of FKRP 5-2 ZFN in AB[*] wild type or non-injected zebrafish embryos at 1dpf. Dead embryos were removed at 4hpf and 1dpf the remaining embryos were sequenced for mutations.
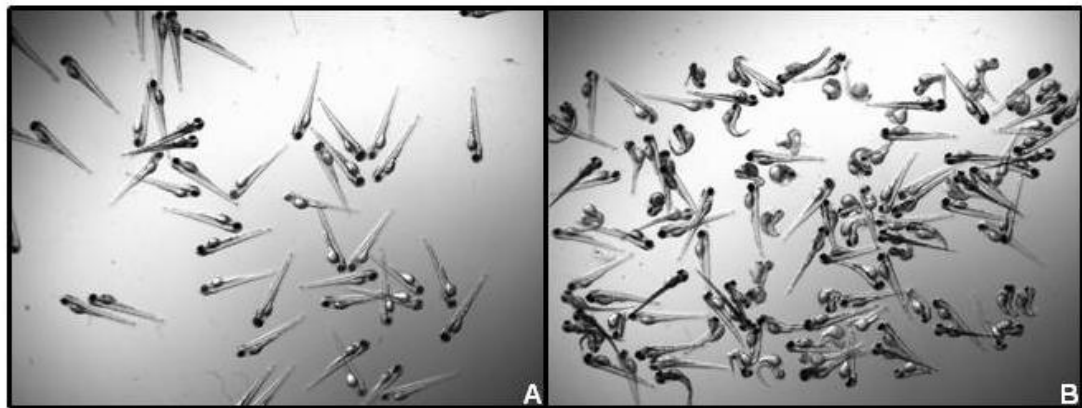
Figure 3.3: Light microscope images of wild type larvae at 3dpf
 Fish were either uninjected **(A)** or injected with 300pg of FKRP 5-2 ZFN **(B)**. Note the straight tails in the larvae in (A) and the curvature of the tail in about a third of the mRNA injected fish (B). Tail curvature is a common finding in fish injected with mRNA and is unlikely to be as a result of a mutation created by the ZFNs.

Two small clutches of 10, 2dpf embryos DNA were pooled for each ZFN pair to investigate the somatic mutation rate. Neither the 5-1 nor 5-2 ZFN pair produced an insertion or deletion within the zebrafish *fkrp* gene when the 190 samples were screened for each ZFN pair. The 50% predicted success rate discussed in the initial CoDA literature has been revised by more recent data to a much more conservative 17% (Sander *et al.*, 2010; Moore *et al.*, 2012b). Since not even a low somatic mutation rate was achieved with either pair of ZFN's, no further work was continued using ZFN technology.

3.2.3 The Zebrafish Fukutin Protein

It has previously been proposed that since fukutin and FKRP have very similar structures based on homology in the hydrophobic transmembrane spanning region and the putative catalytic domains. Here the similarities in amino acid structure are compared between species: zebrafish, human and mouse (Figure 3.4). A Database (ZDB-GENE-070410-96) search identified a single gene for *fukutin* in the zebrafish genome, encoding a 457-amino-acid polypeptide located on chromosome 5. There was 57% identity and 72% similarity of amino acid sequence between zebrafish and humans (Figure 3.5; Moore *et al.*, 2008; Drummond AJ, 2011).
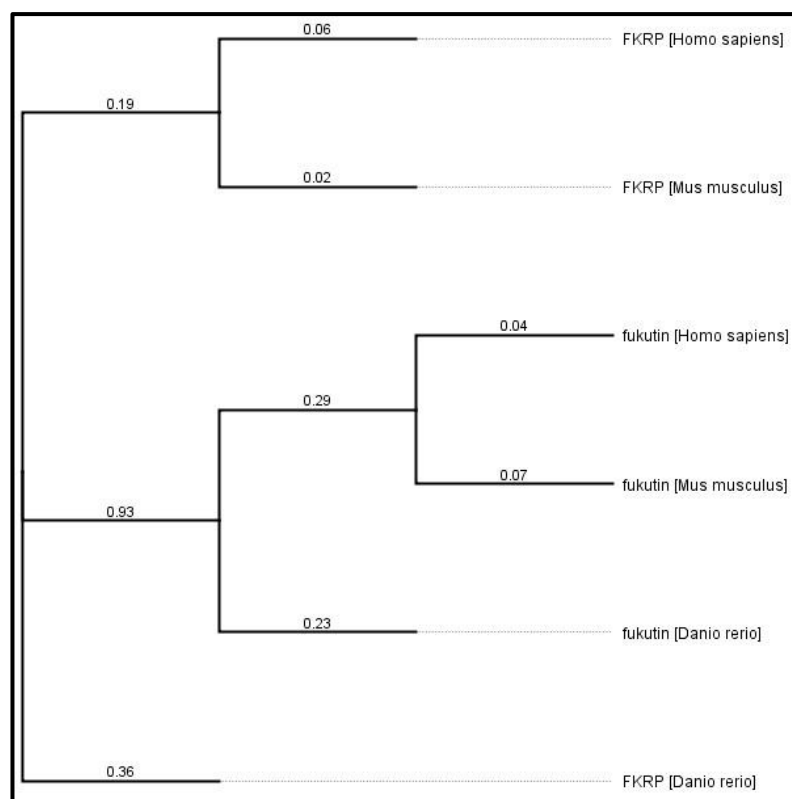
Figure 3.4: Unrooted phylogenetic tree to show the inferred genetic relationship of the fukutin and FKRP proteins in humans, mouse and zebrafish
Each node represents FKRP or fukutin in zebrafish, mice or humans. Distances are based on the amino acid sequences of each of the nodes. The distance between the fukutin nodes is smaller than that between fukutin and any FKRP node (Drummond AJ, 2011).

Figure 3.5: Comparative homology plot of Fukutin protein sequence from zebrafish and human.
Identical amino acids are on a green background, similar amino acids are on a red background. Overall, there is 57% identity and 72% similarity of amino acid sequence between zebrafish and humans.

3.2.4 Morpholino 30-12Apr05B Induces Splicing Abnormalities Leading to Truncation of Fukutin Transcript

The wild type AB line (Cha and Weinstein, 2007) was chosen to study the effects of knocking down fukutin in zebrafish. Importantly the AB line is the best characterised and most used wild type strain. A novel antisense spliceosomal MO (30-12Apr05B) targeting *fktn* at the boundary between intron 3 and exon 4 (Figure 3.6A) was designed to induce a frameshift mutation. Analysis by reverse transcriptase-polymerase chain reaction (RT-PCR) using primers in the flanking exons confirmed the ability of 30-12Apr05B to alter *fktn* mRNA splicing (Figure 3.6B). Wild type fukutin PCR products were observed in all embryos at the expected size of approximately 500bps. In the injected embryos a mis-spliced band was observed at 400bp which was not completely separated from wild type *fktn* PCR product (Figure 3.6B) and might represents a truncated form of *fktn*. Mis-spliced products were observed at 200 bp and 150 bp which were identified as representing loss of exon 4 following isolation and sequencing (Figure 3.6C-D). Previously published translation blocking MO were used to

knock down expression of FKRP and dystroglycan as previously described (Parsons *et al.*, 2002a; Thornhill *et al.*, 2008; Kawahara *et al.*, 2010; Lin *et al.*, 2011).
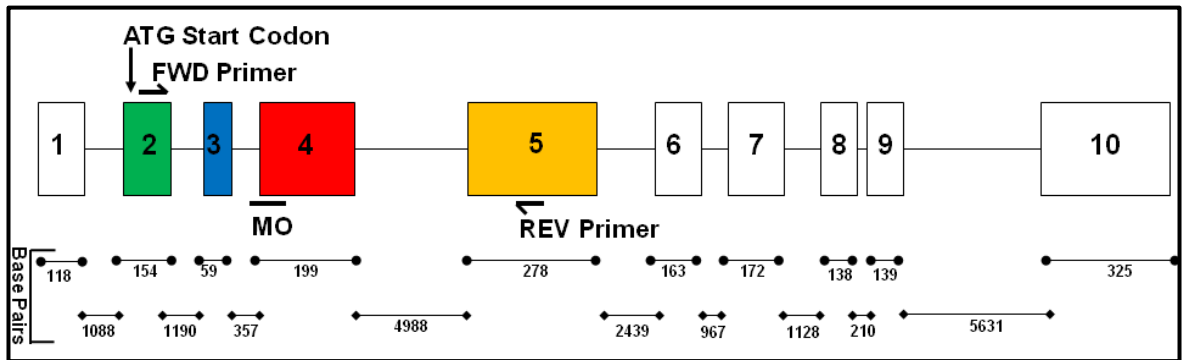
A
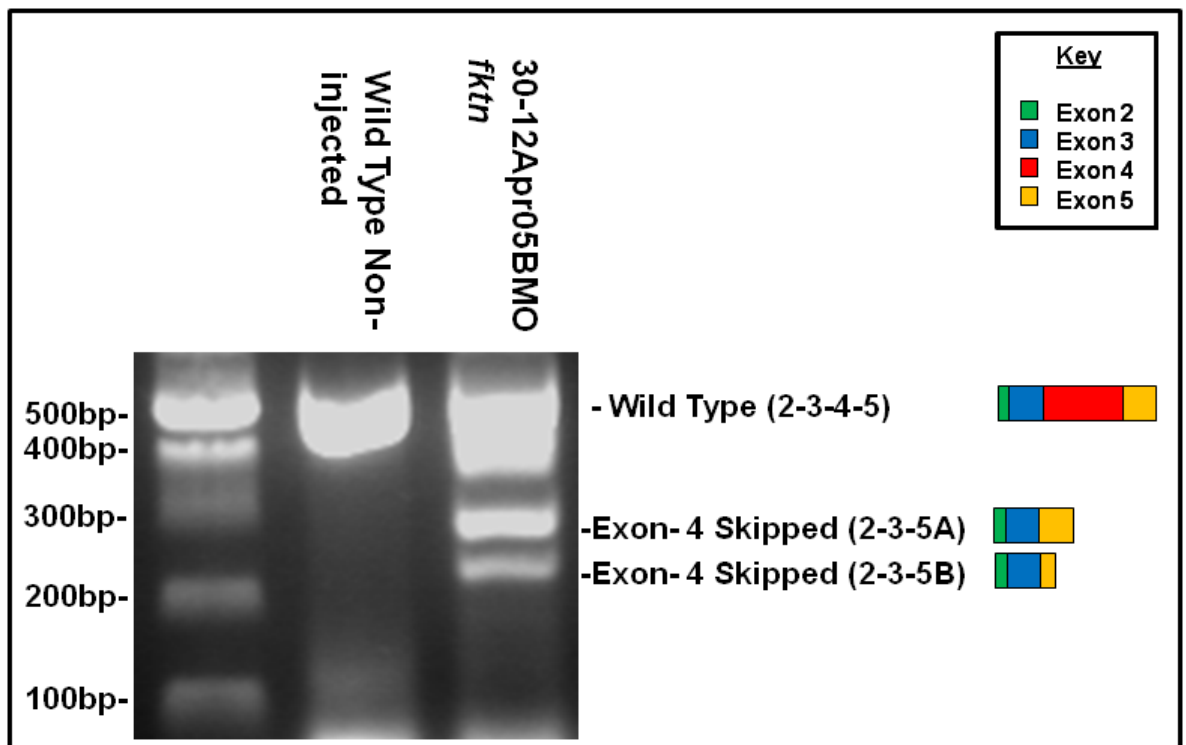
B
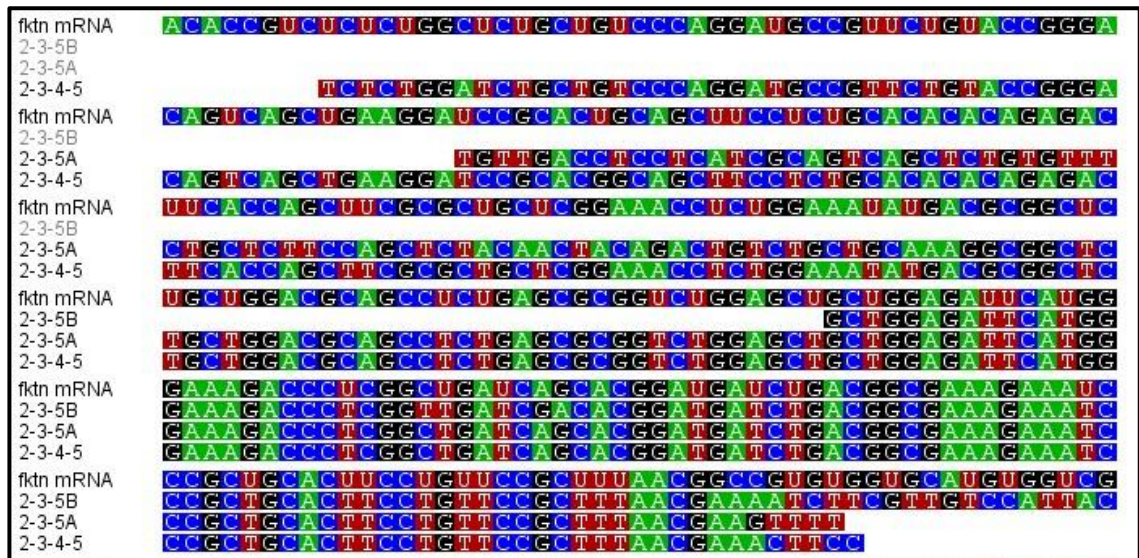
C
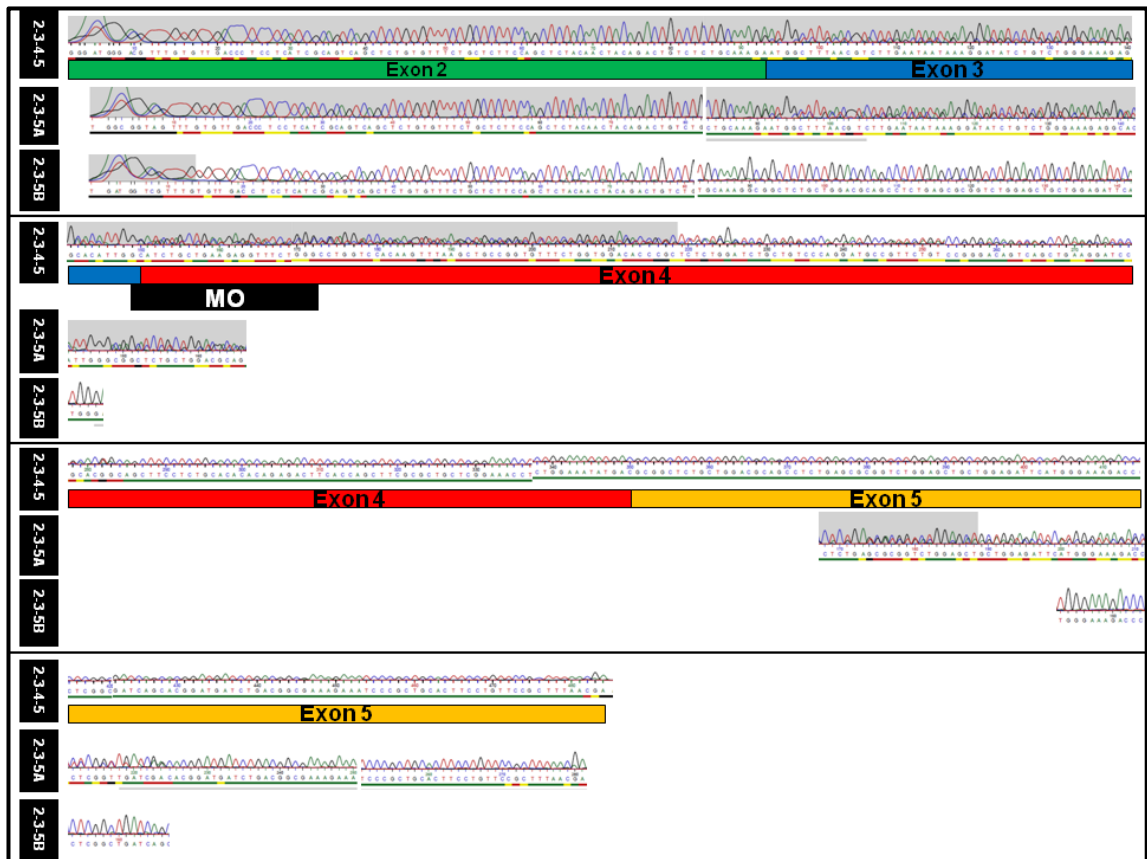
D

Figure 3.6: 30-12Apr05B-fukutin MO induces splicing aberrations in vivo
A: Diagram of the zebrafish *fktn* gene, the MO target site and the position of the primers used to verify the splicing defects induced by the MO. Boxes represent exons, the lines between the boxes represent the introns. Boxes below shows number of base pairs in exons and introns, numbers represent number of bps and correspond to box and line *fktn* gene diagram directly above them. **B:** RT-PCR of *fktn* transcripts using primers in exons on either side of the target site. The band at 500bp

corresponds to normally spliced fukutin, while the shorter fragments correspond to mis-spliced products. 2ng of 30-12Apr05B-fukutin MO was injected into the embryos and only embryos that were judged to have a phenotype at 1dpf by the criteria in Table 2.2 were used. **C:** Sequencing results of excised bands top wild type (2-3-4-5), middle (2-3-5A) and bottom (2-3-5B) refer to bands excised from gel sequence aligned with wild type *fktn* mRNA, accession number: NM_001042694. **D:** Chromatograms of splice products aligned against mRNA.

3.2.5 Optimising 30-12Apr05B-fukutin MO to Produce the Most Comprehensive Range of Morphant Phenotypes

MOs are known to produce a spectrum of phenotypes, a valuable attribute for investigating diseases that have a range of clinical severity. The severity of human dystroglycanopathies varies as a result of different mutations or combinations of mutations and heterogeneity in genetic background, see introduction Figure1.3, (Yoshioka and Kuroki, 1994; Van Reeuwijk *et al.*, 2010). The spectrum of phenotypes produced by MO occurs due to differences in site of injection within the yolk sack, concentrations of MO and factors such as individual zebrafish epigenetic heterogeneity or simply the stochastic nature of living organisms (Nechiporuk *et al.*, 1999). Criteria were designed that would aid in the classification of FKRP, fukutin and dystroglycan morphant phenotypes (Table 2.2). The mildest end of the phenotypic spectrum included fish with no visible morphological differences compared to wild type AB strain at a particular stage of development based on Kimmel criteria (Kimmel *et al.*, 1995), whilst the most severely affected fish did not survive (Thornhill *et al.*, 2008). Fish with intermediate phenotypes were grouped into mild, moderate and severe based on the criteria as outlined in Table 2.2. In most experiments the normal and lethal groups were removed from further analysis

In order to determine the optimal concentration of 30-12Apr05B fukutin MO to produce a balanced spectrum of phenotypes, a range of injection concentrations were tested. A balanced range of phenotypes is the optimal titration of phenotype to MO concentration. Fertilised eggs were collected and injected between the zygote and first cleavage phases (up to approximately 45 minutes post fertilisation). The embryos were collected at 24hpf in the pharyngeal phase and manually dechorionated. A minimum of 3 clutches were investigated for each injection concentration. A range of injection concentrations were investigated from 0.5ng-7.5ng of 30-12Apr05B fukutin MO. At the lowest concentration no abnormal phenotypes were observed, as judged by light microscopy. However, there was an increase in the number of embryos

which died (24% vs. 8% in the control; Table 3.2). At the highest MO concentration no embryos had survived by 24hpf. 1 & 3ng injection concentrations both produced a range of phenotypes, skewed to high percentages of mild phenotypes or a greater proportion of morphants at the severe end of the spectrum respectively. The 2ng injection concentration produced the most balanced range of phenotypes and was chosen for all subsequent 30-12Apr05B-fukutin MO injections (Figure 3.7). FKRP and dystroglycan MO concentrations were chosen based on previously published concentrations known to produce suitable ranges of phenotypes (Parsons *et al.*, 2002a; Thornhill *et al.*, 2008).

	Normal (%)	Mild (%)	Moderate (%)	Severe (%)	Dead 4hpf (%)	Dead 24hpf (%)	Total (n)
0.5ng	64	0	0	0	12	24	208
1ng	12	24	3	3	8	50	177
2ng	10	11	9	14	9	47	325
3ng	6	0	4	5	13	72	153
7.5ng	0	0	0	0	15	85	278
Uninjected	88	0	0	0	4	8	892

Table 3.2: Proportion of each phenotypic class following injection of a range of 30-12Apr05B-fukutin MO amounts
The amount of MO injected was calculated as outlined in the methods, *see* 2.1.3. For each MO amount phenotype severity was assessed at 24 hours post fertilisation (hpf). Morphants were assessed as in Table 2.2 and final counts are expressed as a proportion of the total. Number of dead was also recorded at 4 hpf as an indicator of survival after the injection process.
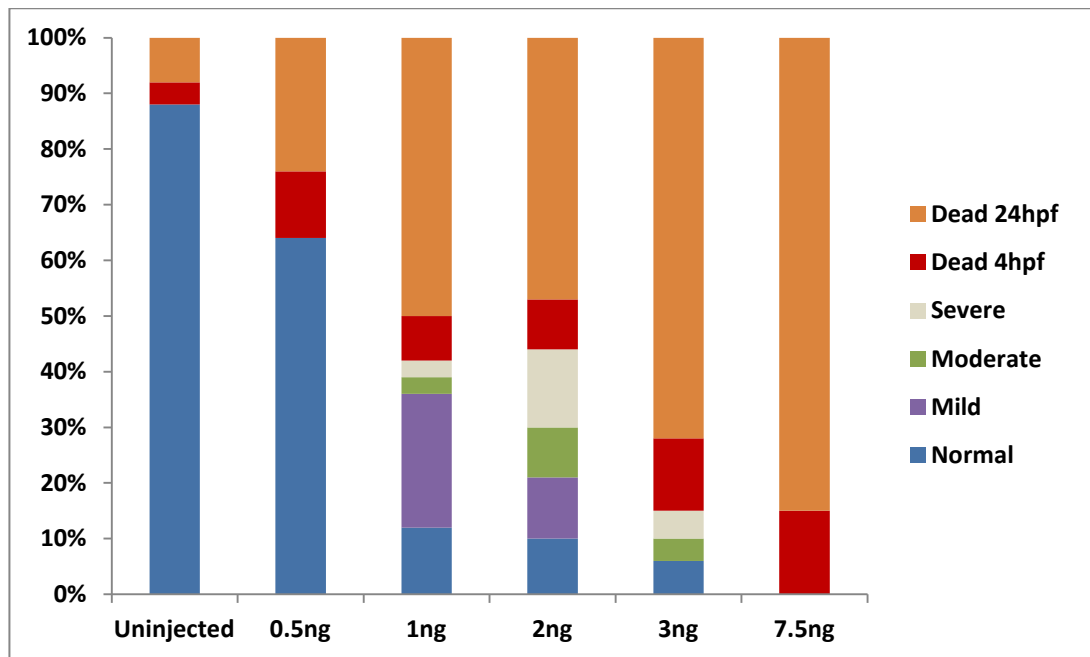
Figure 3.7: Proportion of each phenotypic class following injection of a range of 30-12Apr05B-fukutin MO amounts

The amount of MO injected was calculated as outlined in the methods, *see* 2.1.3. As the amount of MO increases the number of embryos with a more severe phenotype increases (Table 2.2) and the phenotype spectrum is skewed towards the severe phenotypic categories. Based on the most balanced and highest number of phenotype to no phenotype ratio, 2ng is the optimal amount for the 30-12Apr05B fukutin MO and was chosen for all subsequent experiments.

	Normal (%)	Mild (%)	Moderate (%)	Severe (%)	Dead (%)	Total (n)
Fukutin Mo 2ng	10	9	7	12	62	252
FKRP Mo 10ng	12	17	14	11	46	286
Dystroglycan Mo 5ng	40	9	2	3	46	384
CoMo 10ng	84	0	0	0	16	346
Uninjected	85	0	0	0	15	427

Table 3.3: The range of phenotypes induced by injection of 10ng control, 10ng FKRP, 2ng 30-12Apr05B-fukutin and 5ng dystroglycan MO

For each MO phenotype severity was assessed at 1 day post fertilisation (dpf). Morphants were assessed as in Table 2.2 and final counts are expressed as proportion of the total. The amount of MO injected was calculated as outlined in the methods, *see* 2.1.3.
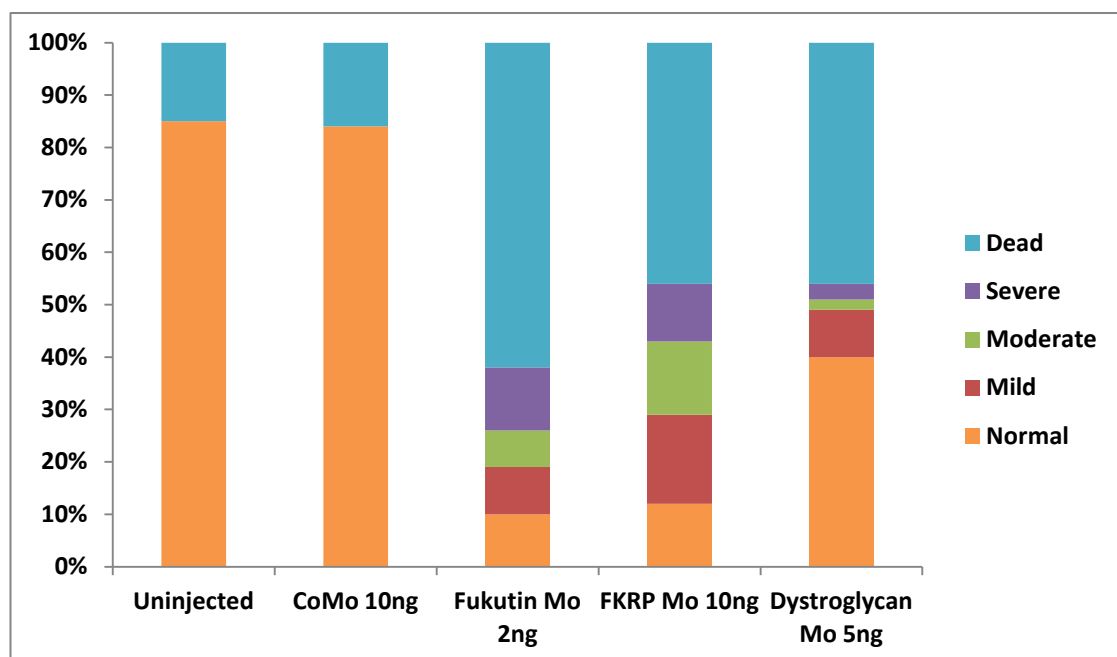
Figure 3.8: The range of phenotypes induced by injection of 10ng control, 10ng FKRP, 2ng 30-12Apr05B-fukutin and 5ng dystroglycan MO
Phenotypes were judged on morphological grounds based on Table 2.2. The range of phenotypes observed spanned embryos with a normal appearance to the most severe which were found dead at 1dpf. The amount of MO injected was calculated as outlined in the methods, *see* 2.1.3.

The proportion of embryos found dead in the control MO injected group was not significantly different from that of the uninjected controls. The FKRP and dystroglycan MO injections produced the greatest and narrowest phenotype ranges respectively. FKRP, fukutin and dystroglycan MO injected embryos all had a higher proportion of dead embryos at 1 dpf when compared to controls, indicating that mortality was due to specific effects of the MO sequence (Table 3.3 & Figure 3.8).

Phenotype ranges had previously been reported for FKRP and dystroglycan MO injections. However no criteria had been established to define each phenotype category (Thornhill *et al.*, 2008; Kawahara *et al.*, 2010). The criteria in Table 2.2 were established on the basis that difference in MO sequences will have different effects on gene expression. Redundancy and turnover of the gene will also have differential outcomes that affect the efficacy of the individual MO. A criterion allows MO concentration to be titrated against severity of phenotype. In order to compare the function of FKRP and fukutin and dystroglycan in the same molecular axis, it is desirable to knock each of them down to a similar extent. The assumption can be made that genetic pathways

are being knocked down to a similar extent, once similar phenotype ranges are achieved, by testing a range of MO concentrations. Therefore effects observed on structure are thought to be genuine and not based on individual variation amongst the MOs.

As expected, the wild type embryos showed no deviation from the normal group, but occasional mild pathological features were identified in fish in the control MO group (Table 2.2). These features are defined as non-specific effects of MO injections and have been discussed in a wide range of zebrafish MO literature (Bill *et al.*, 2009). Each of the fukutin, FKRP, and dystroglycan MO produced phenotypes that fell into each major category of the criteria at both 1 and 3 dpf ranging from normal to lethal. The mild to severe phenotypes can be seen in Figure 3.9 and Figure 3.10. A comparable range of phenotypes as observed at 1dpf is present at 3dpf for all FKRP, fukutin and dystroglycan morphants. Fukutin, FKRP and dystroglycan morphants have clear overlapping morphology, (Figure 3.9 & Figure 3.10) that can be sorted based on the criteria described in Table 2.2. The feature with the greatest utility for assessing phenotype is tail curvature. 1dpf tail curvature (Figure 3.9) correlates well with that of the 3dpf in equivalent phenotype categories across the spectrum of the FKRP, fukutin and dystroglycan morphants. Therefore the combination of tail curvature, eye, brain and other variable features was considered in the classification of the phenotype up to 1dpf. Thereafter, the tail curvature was used as the most appropriate indicator for sorting morphant fish within the phenotype spectrum.
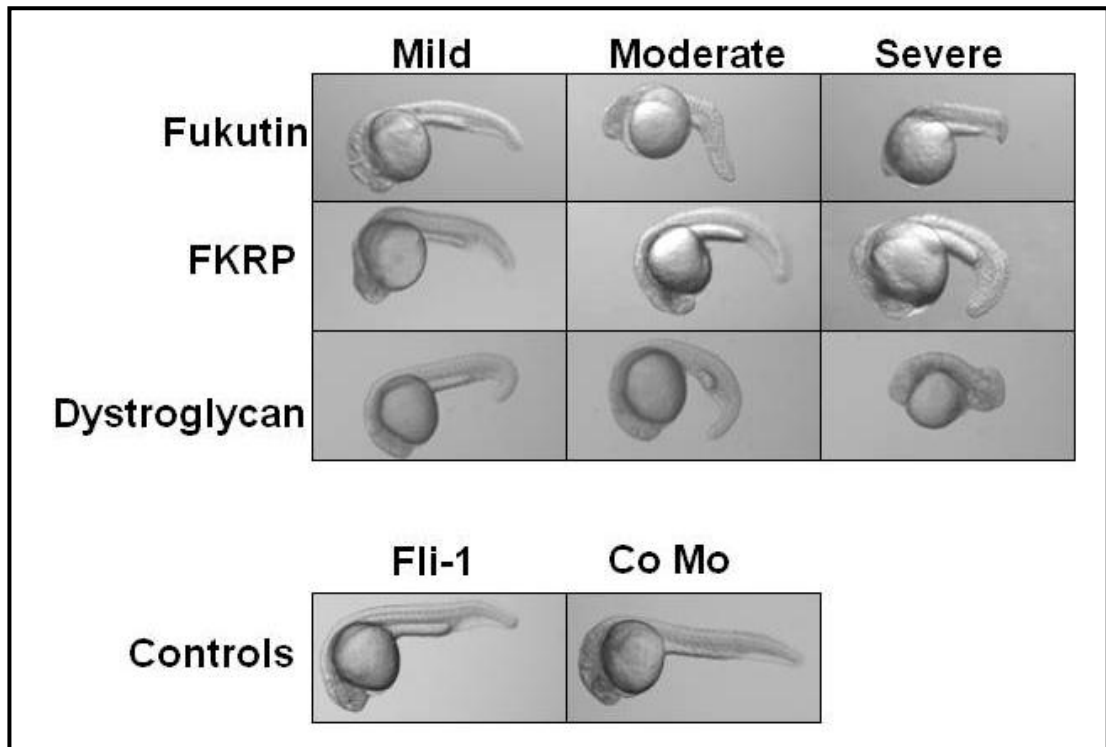
Figure 3.9: Light microscope images of embryos at 1 dpf
Embryos were either untreated or injected with MO at 10ng control & FKRP, 2ng fukutin, or 5ng dystroglycan. Embryos were staged according to Kimmel *et al.* 1995, (Table 2.1 & Figure 2.1). Embryos were sorted according to phenotypes as described in Table 2.2. The amount of MO injected was calculated as outlined in the methods, *see* 2.1.3,
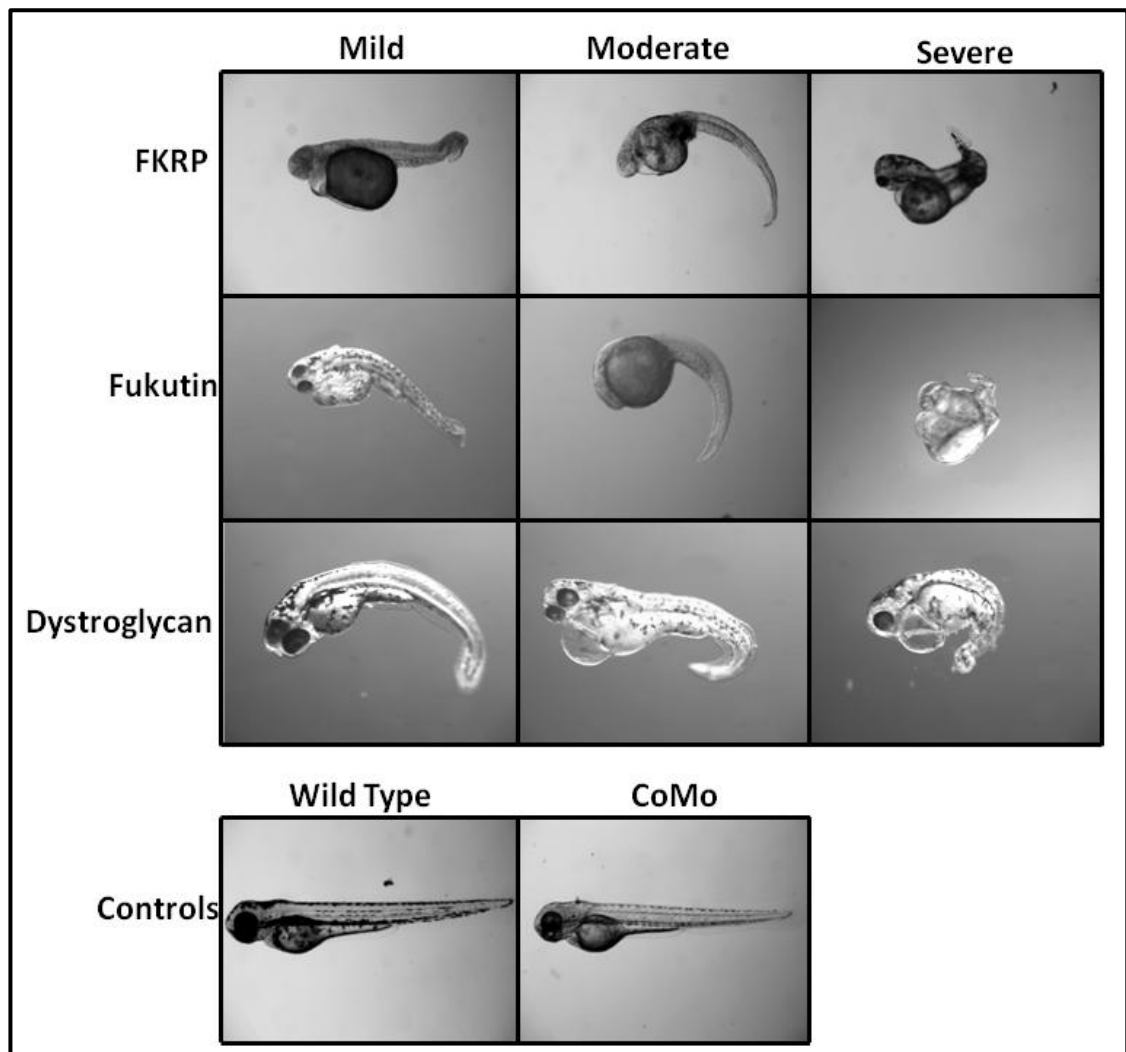
Figure 3.10: Light microscope images of larvae at 3dpf
Fish were either untreated or injected with MO at 10ng control & FKRP, 2ng 30-12Apr05B *fktn* MO, or 5ng dystroglycan. Embryos were staged according to Kimmel *et al.* 1995, (Figure 2.1 & Table 2.1). Embryos were sorted according to phenotypes as described in Table 2.2. The amount of MO injected was calculated as outlined in the methods, *see* 2.1.3,

3.2.6 30-12Apr05B- Fukutin MO Produces a Dystroglycanopathy Phenotype at 1 dpf

Morphant morphology was assessed at 1dpf to establish efficacy of the 30-12Apr05B *fktn* MO in generating a muscle, eye and brain pathology in the morphant embryos. Light microscopy was used to capture a minimum of five images of embryos within each phenotype group. Embryos were staged according to Kimmel's criteria and placed into phenotype groups according to criteria outlined in Table 2.2.

Overall, there was a clear overlap of abnormalities detected in the fukutin fish with those that had been previously described in FKRP and dystroglycan

morphants (Parsons *et al.*, 2002a; Thornhill *et al.*, 2008; Kawahara *et al.*, 2010). The morphological data suggest a slight delay in muscle, eye and brain development of morphant fukutin embryos in comparison to control injected embryos at 1dpf (Figure 3.11A-D). The muscle morphology was investigated at 1dpf, a time point prior to the development of pigmentation. The segmentation period is the key period in early muscle development occurring between the first somite furrow appearing at $10_{1/3}$ hpf and the start of the hatching period at 2dpf (Kimmel *et al.*, 1995). By 1dpf all 26 of the somites are present and are visible in the non-injected embryos (Figure 3.11A). In control embryos the somites have a "chevron" shape delineated by the vertical myosepta which is more rounded in all morphant embryos (Figure 3.11 A-D). At the severe end of all phenotypic spectra somite boundaries were no longer visible. More severely affected fish as judged by overall criteria outlined in Table 2.2, had less clearly delineated myosepta. Aberrant muscle morphology can demonstrate potential sarcolemmal instability in fukutin deficient embryos (Figure 3.11; Takeda *et al.*, 2003; Kurahashi *et al.*, 2005).

Numerical analysis of the angles inside the chevron of the vertical myosepta were measured (Figure 3.12). The angle inside the chevron was measured in controls to have a mean of (94°) in non-injected and in control MO injected (95°). The difference was found to not be significant with a student unpaired T-test between control MO and non-injected embryos. The vertical myosepta chevron angle was found to be significantly more obtuse in the FKRP (132°), fukutin (144°) and dystroglycan (131°). The FKRP, fukutin and dystroglycan morphants all were significantly more obtuse in myosepta angle than control injected embryos ($p < 1 \times 10^{-4}$ in all cases; Figure 3.11 & Figure 3.12).

A

| Whole Embryo | Myotome | Eye | Brain |

Wild Type — NC, YS, Lens, Eye, MB

Control MO — NC, YS, Lens, Eye, MB

B

| Whole Embryo | Myotome | Eye | Brain |

Fukutin Mild — YS, NC, Lens, Eye, MB

Fukutin Moderate — NC, YS, Lens, Eye, MB

Fukutin Severe — NC, YS, Eye
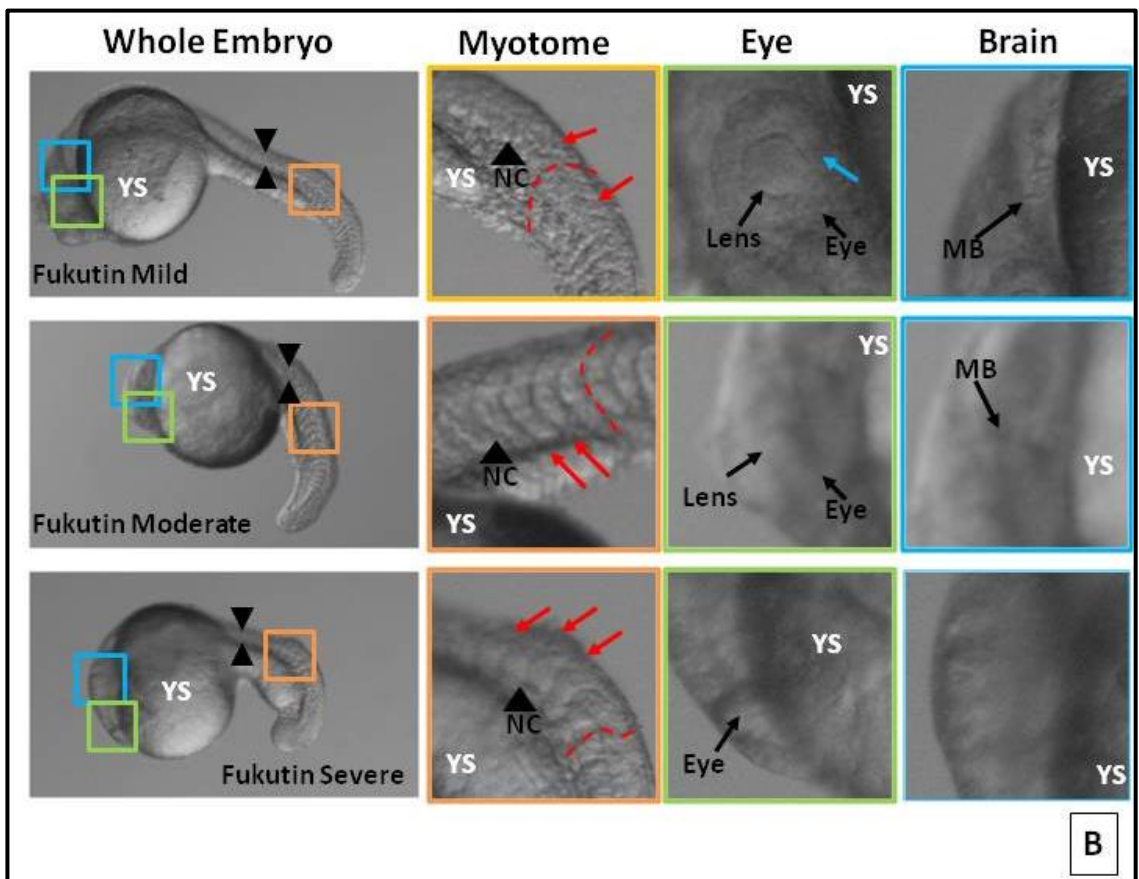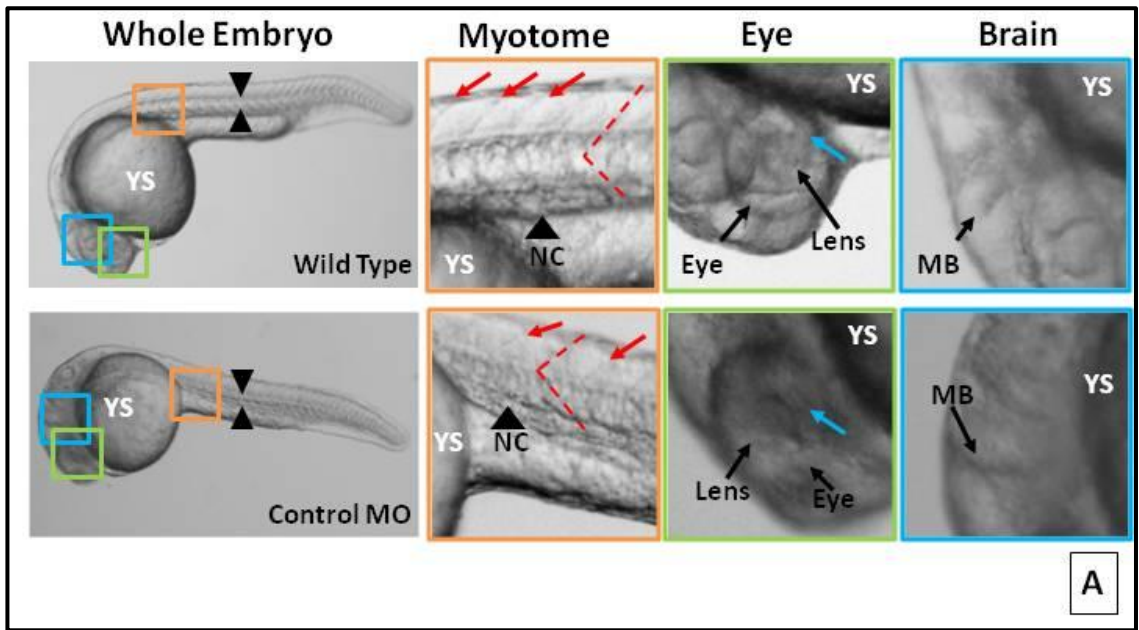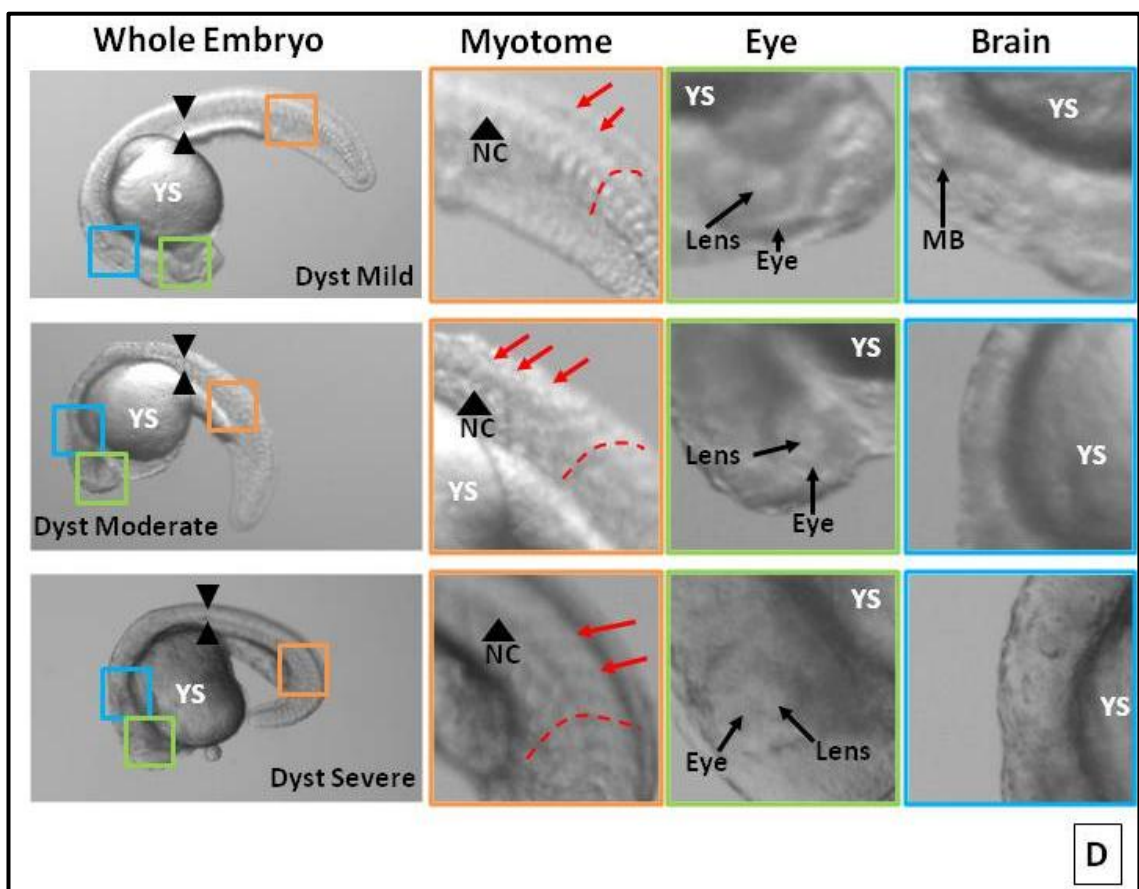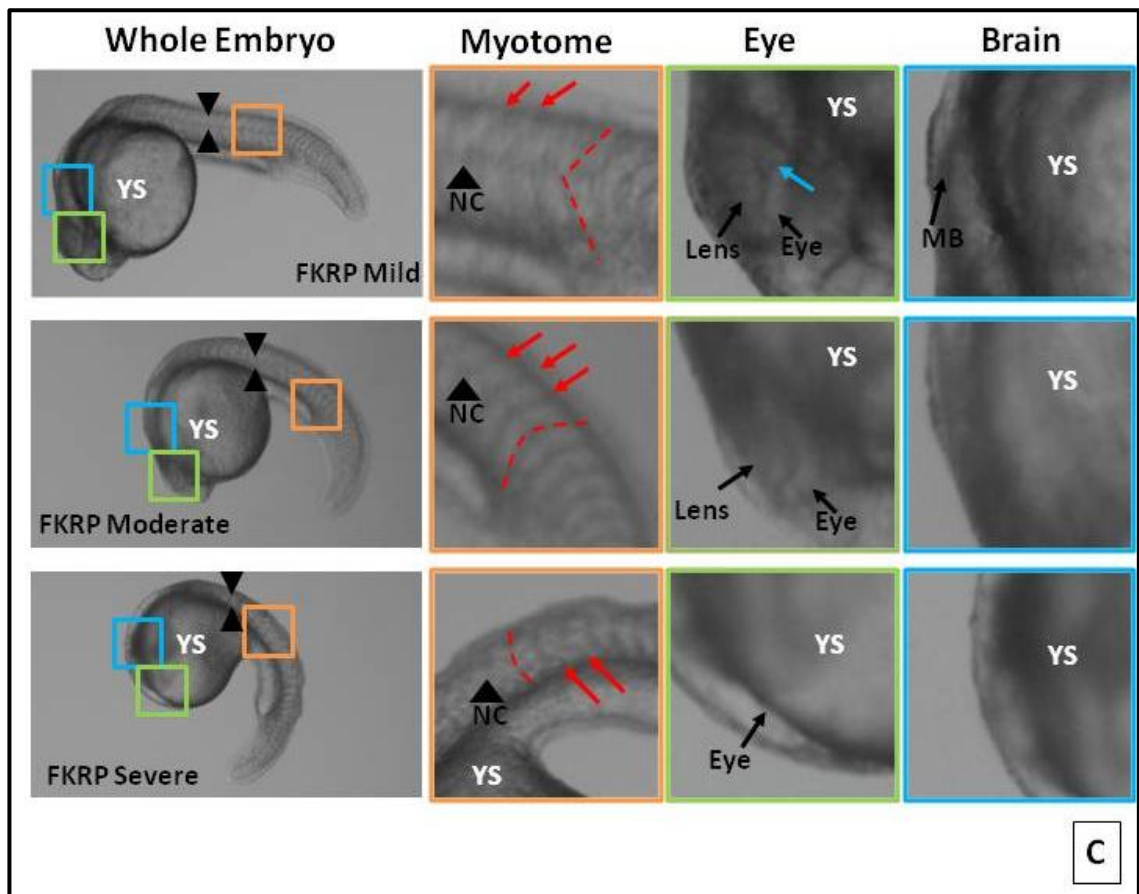
Figure 3.11: Light microscope images of embryos at 1day post fertilisation (dpf)
Morphology was investigated using light microscopy in 1dpf dechorinated embryos. Embryos were either untreated AB or injected with 10ng of control MO (A), 2ng of 30-12Apr05B-fukutin MO (B), 10ng of fkrp MO (C), 5ng of dystroglycan MO (D). Embryos were staged according to Kimmel *et al.* and phenotypes were sorted according to the criteria outlined in Table 2.2. Enlarged views of myotome (orange border), eyes (green border) and brain (blue border), it should be noted in some instances the boxes are not exactly placed due to limitations in software. Fukutin morphants have abnormal somite shape, due rounding of the vertical myosepta, outlined by red dashes and denoted by red arrows. Fukutin morphants have micropthalmia and mid brain (MB) definition loss in the most severe fukutin morphants, black triangle- NC= notochord & YS= yolk sack.

The tail curvature is indicative of the loss of sarcolemmal stability and perturbation of myosepta structure, therefore it is a good indicator of muscle pathology (Steffen *et al.*, 2007). The chorion might be accentuating the curvature of the tail in the embryos that are moving less, and further analysis of this point is required. The tail in control embryos is straight with a small ventral curvature at the most distal end of the tail at 1dpf (Figure 3.11A & Figure 3.13). The fukutin morphants in the mild phenotype category had a slight ventral curvature of their entire distal portions (Figure 3.11B & Figure 3.13). The tail curvature in the mild and moderate phenotype categories was in general more pronounced in the fukutin morphants compared to FKRP and dystroglycan morphants. The severe fukutin and dystroglycan morphants were found to have clearly abnormal body shape and much shorter tails (Figure 3.11B-D & Figure 3.13). An increasing proportion of the fukutin morphants from the mild to severe morphant phenotype had dorsal tail curvature. Embryos at the more severe end of the FKRP and dystroglycan morphant spectrum were observed to have a dorsal tail curvature (Table 3.4 & Figure 3.13). Chi-squared tests comparing number of morphant fish with a curved tail against controls found there to be significantly P-value$<1 \times 10^{-4}$, more curved tails in the combined morphant embryo group than in the combined control group.
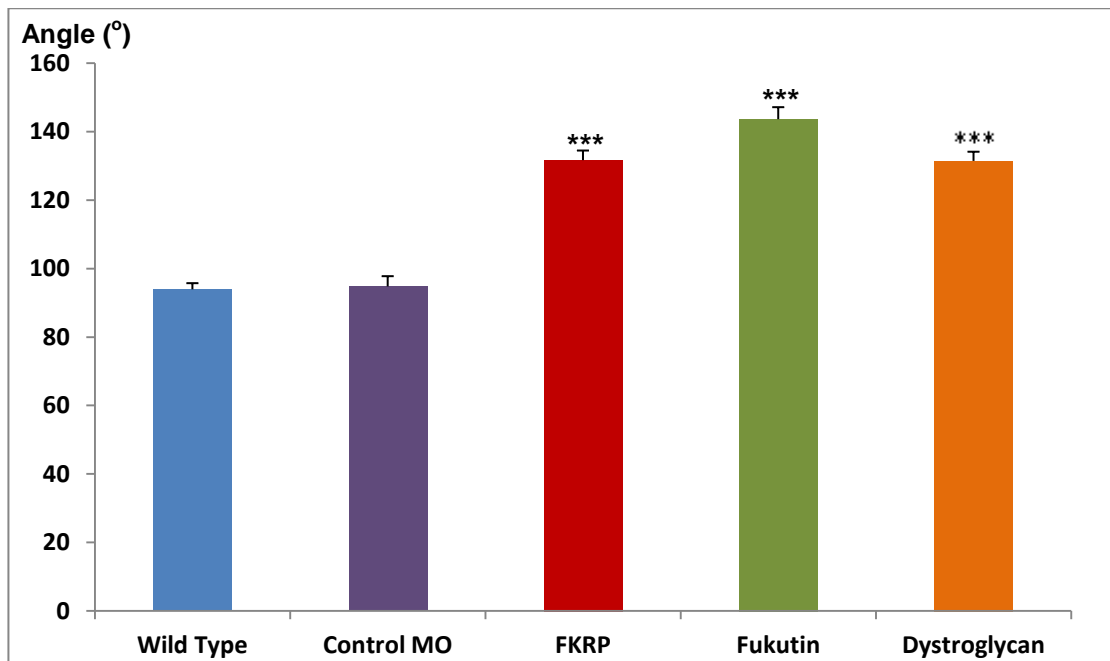
Figure 3.12: Angle of the vertical myosepta in 1dpf morphant embryos
Image-J analysis software was used to measure vertical myosepta angles of light microscopy images of 1 dpf trunks. Angle measured from where the horizontal myosepta bisects the vertical myosepta to each of the ends of the vertical myosepta at the periphery of the embryo. A minimum of five somites in threeembryos were assessed in for each morphant phenotype and grouped. Fukutin morphants were shown to have the most obtuse angled vertical myosepta when compared to dystroglycan and fkrp morphants. Morphant vertical myosepta angles were compared to control MO vertical myosepta angles using the unpaired students t-test: *** $p < 1 \times 10^{-4}$.

Studies have shown that FKRP and fukutin are important for the correct development of the glia limitans, an important basement membrane in the brain (Chiyonobu *et al.*, 2005; Kurahashi *et al.*, 2005). Loss of glia limitans integrity results in glia projecting beyond the membrane, resulting in cobblestone lissencephaly in dystroglycanopathy patients (Yoshioka and Kuroki, 1994; Satz *et al.*, 2008). Mid-brain abnormalities have been demonstrated in 1dpf zebrafish embryos (Thornhill *et al.*, 2008) and so the hypothesis is that a similar abnormality might be present in fukutin morphant embryos. The mid-brain is a defined structure visible by light microscopy as a small vertical groove posterior to the eye at 1dpf in controls (Figure 3.11A). From a morphological perspective, the fukutin knockdown embryos showed structural mid-brain abnormalities, most prominent in fish embryos with a more severe phenotype (Figure 3.11B). FKRP and dystroglycan morphants also show increasing loss of definition of the mid-brain groove with increasing severity of phenotype (Figure 3.11C-D).

	Straight (%)	Dorsal (%)	Ventral (%)	Total (n)
Wild type	100	0	0	478
Control MO	98	0	2	345
Fukutin mild	0	5	95	81
Fukutin moderate	0	36	64	76
Fukutin severe	0	53	47	50
FKRP mild	12	0	88	63
FKRP moderate	0	5	95	56
FKRP severe	0	14	86	60
Dystroglycan mild	4	0	96	46
Dystroglycan moderate	0	2	98	49
Dystroglycan severe	0	11	89	41

Table 3.4: Assessment of tail curvature in 1dpf embryos
Tail curvature was assessed to be either straight, curved dorsally or ventrally in dechorionated dystroglycanopathy morphant embryos at 1dpf.
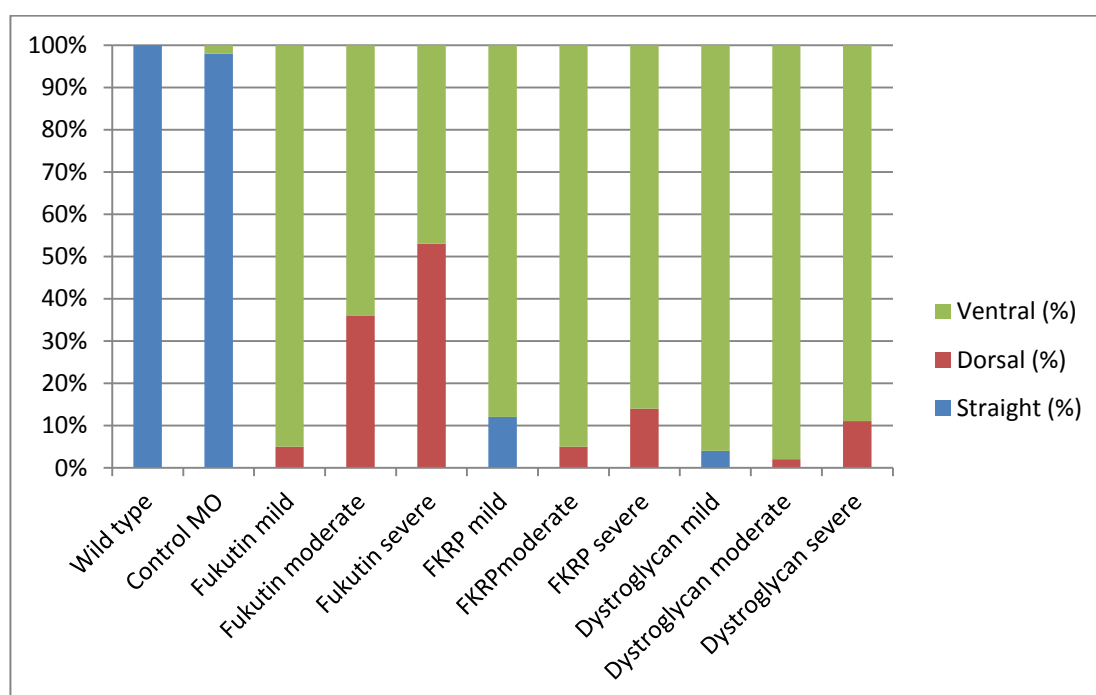
Figure 3.13: Assessment of tail curvature in 1dpf embryos
Tail curvature was assessed using light microscopy and judged to be either straight or have a ventral curvature or dorsal curvature in 1dpf dechorinated embryos. All morphants had an increased proportion of curvature in tails as would be expected when criteria in Table 2.2, are applied. Fukutin morphants had the highest proportion of dorsal tail curvature compared to dystroglycan and FKRP morphants. Dorsal and ventral tail curvature was combined and classified as abnormal tail curvature, this group was then compared against staright tails. Chi-squared analysis for each group was subsequently carried out against the control MO group and in each case was found to be $p<1 \times 10^{-4}$.

Both the fish and mouse models for FKRP deficiency have micropthalmia and morphological eye structural problems (Satz *et al.*, 2008; Thornhill *et al.*, 2008) and these abnormalities are visible at 1dpf in fukutin deficient morphants. The vertical groove in the eye known as the hyaloid canal is only found in control fish (Figure 3.11A), whilst deformed outer eye structure is found in the more severe fukutin, fkrp and dystroglycan morphants, (Figure 3.11B-D).

The notochord is an important structure during the early stages of development, providing developmental cues for zebrafish trunk morphogenesis (Stemple, 2005). A previous study identified notochord abnormalities in fkrp morphants (Thornhill *et al.*, 2008). The notochord is visible in non-injected and control MO injected embryos as a cylinder running from the mid line through the full length of the myotome (Figure 3.11A). The notochord is visible in all morphants and no noticeable structural defects were observed at this level of resolution (Figure 3.11B-D). Histological analysis is therefore required to draw firm conclusions on notochord structure.

3.2.7 2 dpf Fukutin Morphant Embryos

The main features of the 2dpf embryo period are: hatching, increase in pigmentation and the development of a visible pericardium. Based on previous studies where fkrp and dag1 expression were knocked down in zebrafish, the prediction is that the above features would also be affected by knockdown of fktn expression (Parsons *et al.*, 2002a; Thornhill *et al.*, 2008; Kawahara *et al.*, 2010).

Evaluating the pigmentation patterns of the zebrafish can help to distinguish a systemic developmental defect from a defect in a specific system. Pigmentation in the natural environment is important for camouflaging the zebrafish. At the hatching stage of development (long-pec period, 2dpf), the melanophores (equivalent to human melanocytes and expressing black pigment) are visible along the lateral stripe (Figure 3.14A-D). Melanocytes run along the dorsum of the posterior portion of wild type and control MO injected embryos. Pigmentation irregularities and delays in hatching suggest that the fukutin MO might have induced a developmental delay. The changes in melanocyte pattern might suggest the fukutin MO has affected Wnt signalling, a factor known to be important for melanocyte migration (Jin *et al.,* 2001). The somitic structure is

not visible in non-injected controls since at this stage of development pigmentation obscures these structures. Therefore it is not possible to conclude whether there is tissue specific developmental delay. It would be difficult to conclude that a change in pigmentation pattern is anything other than secondary to the overall changes to body shape of the zebrafish. Drawing firm conclusions from examining pigmentation patterns lies outside the scope of this study (Kelsh *et al.*, 1996). Using a fish line such as Golden which has significantly reduced pigmentation, would be a way to view structures unhindered by pigmentation.

The otic vesicle which is visible from 42hpf during the high-pec phase, between pharyngeal and hatching phases, can be used as a marker for normal development. At 48hpf the otic vesicle had a similar appearance (*i.e.* round structure directly posterior to the eye dorsal to the pericardium) in fukutin, FKRP and dystroglycan morphants when compared to controls. This suggests, that fukutin morphant embryos are not substantially developmentally delayed and therefore muscle, eye and brain abnormalities observed in the fukutin morphants are due to tissue specific effects of fukutin knock down (Figure 3.14A-D).

B

Whole Embryo	Head	Trunk

Fukutin Mild

Fukutin Moderate

Fukutin Severe

C

Whole Embryo	Head	Trunk

FKRP Mild

FKRP Moderate

FKRP Severe
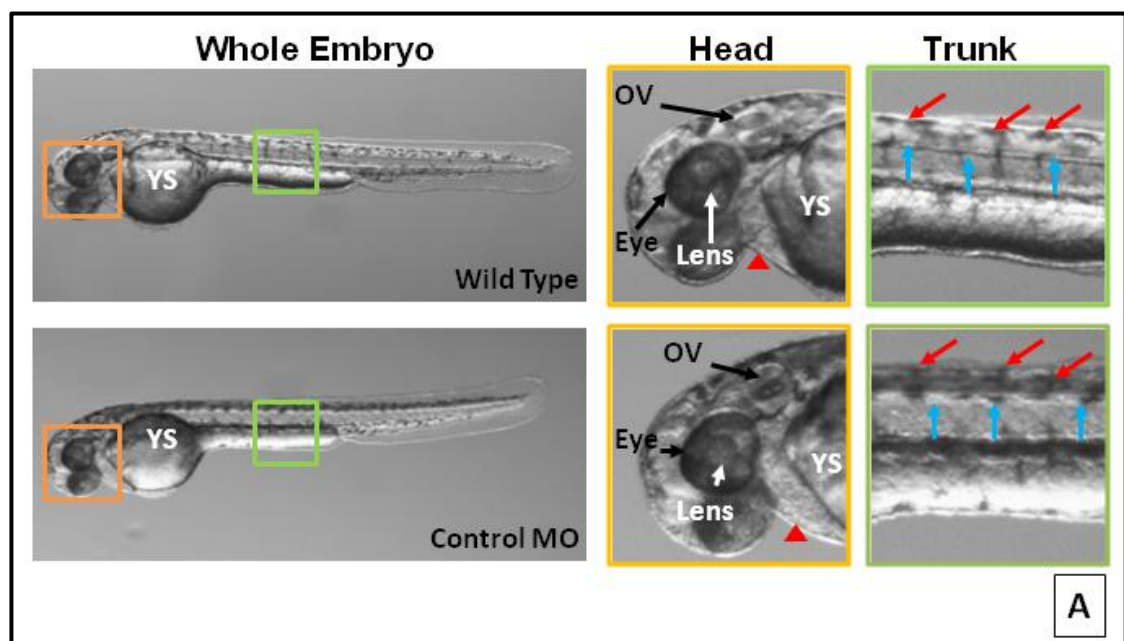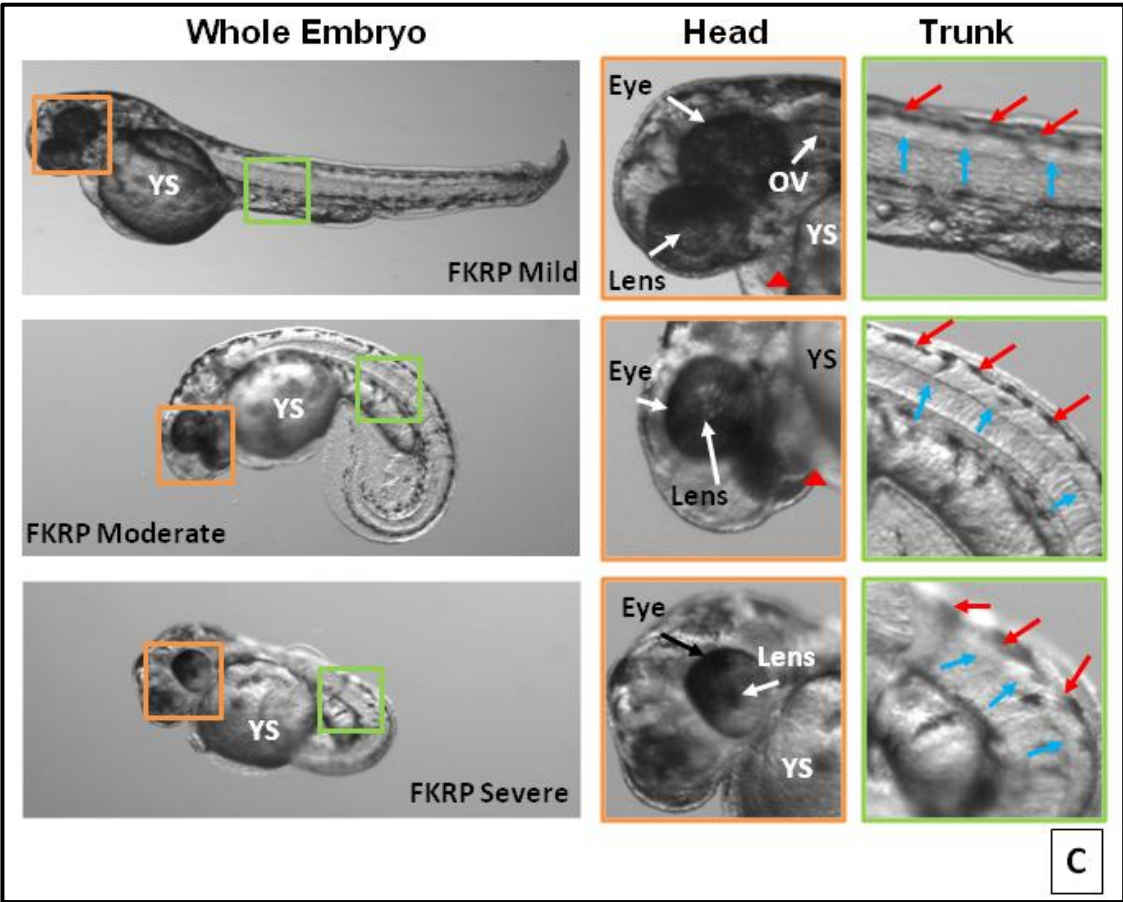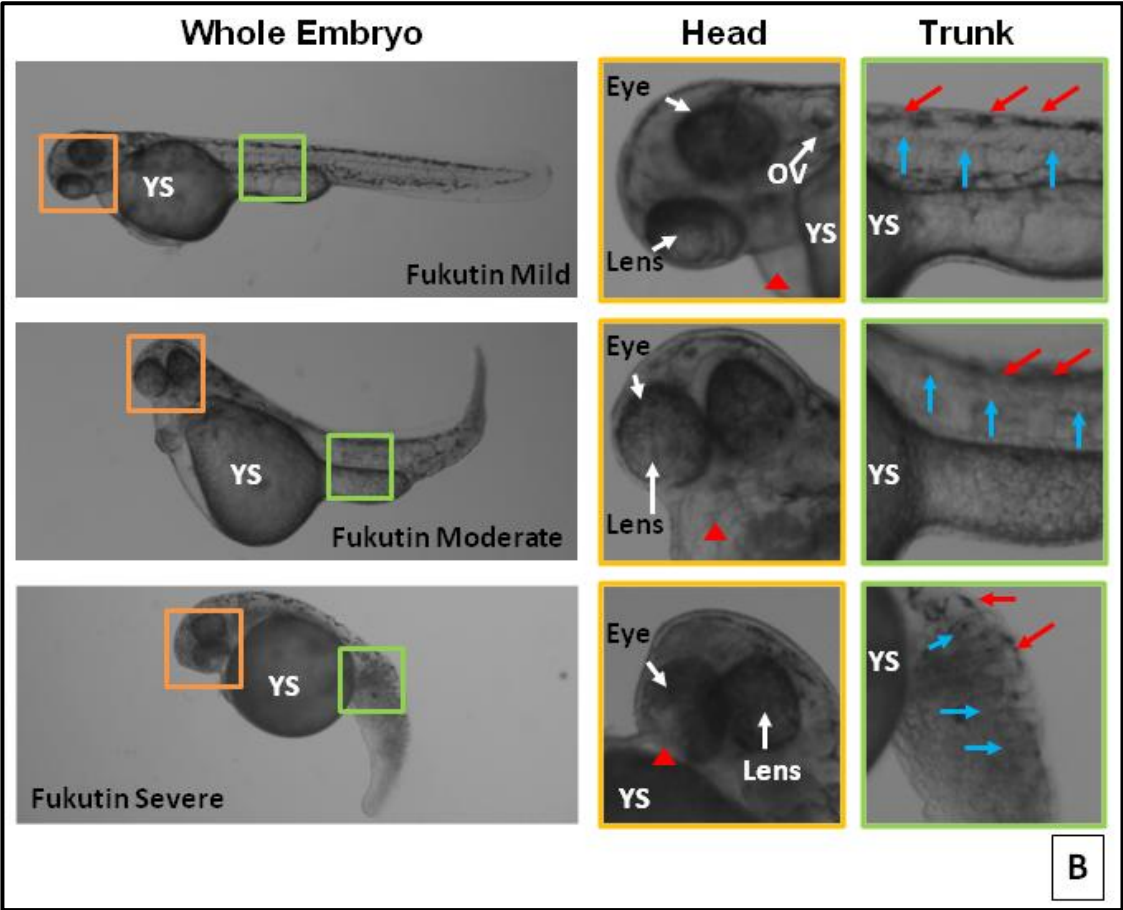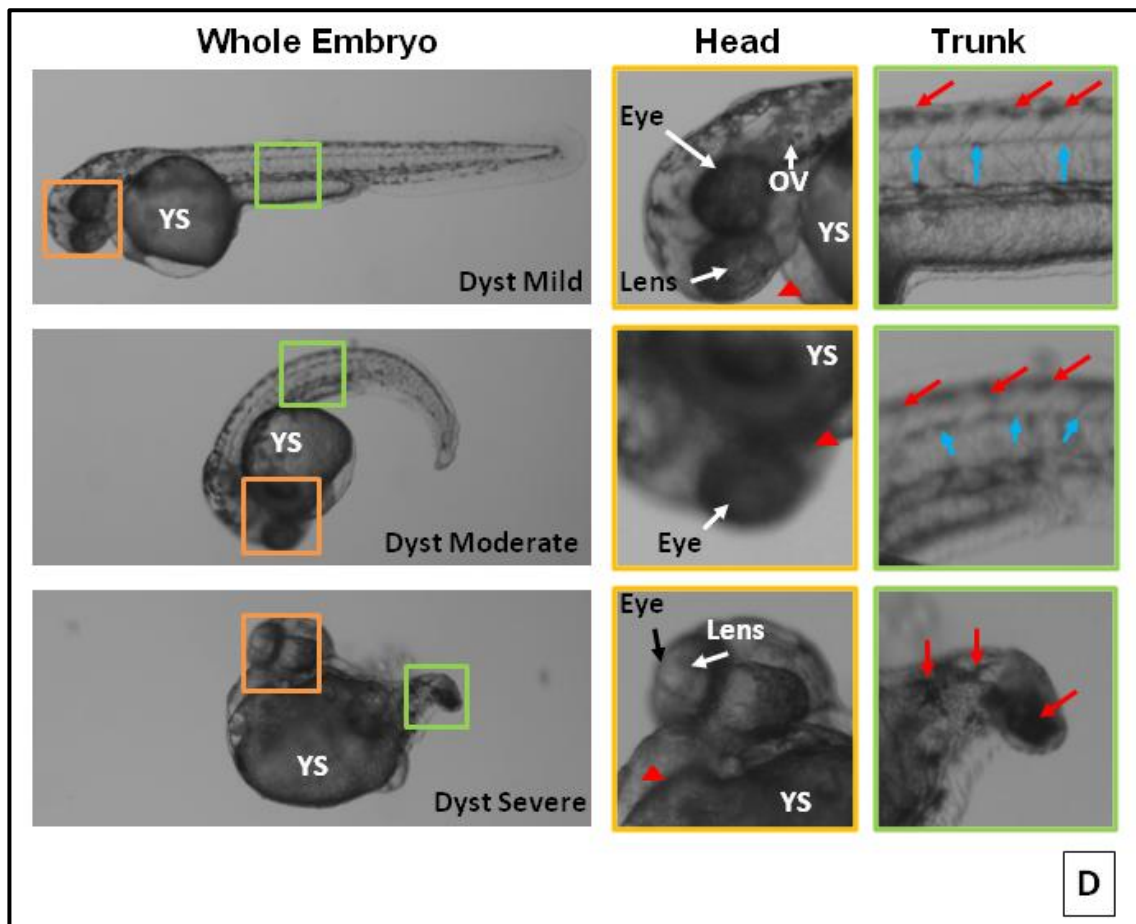
Figure 3.14: Light microscope images of embryos at 2dpf.
Morphology was investigated using light microscopy in 2dpf dechorinated embryos. Embryos were either **(A)** untreated AB or injected with 10ng of control MO **(B)** injected with 2ng of 30-12Apr05B-fukutin MO **(C)** injected with 10ng of fkrp MO or **(D)** injected with 5ng of dystroglycan MO. Embryos were staged according to Kimmel *et al.* and phenotypes were sorted according to the criteria outlined in (Table 2.2). Enlarged views of head (orange border), trunk (green border). Red triangle= pericardium, red arrows= melanocytes, blue arrows= lateral line, OV= otic vesicle, YS= yolk sack.

Hatching in embryos maintained at 28°C occurs by 2dpf and a delay in hatching is considered to represent a developmental delay. The majority (96%) of wild type and control MO injected embryos (93%) had hatched by 2dpf. 45% of the fukutin, 42% of FKRP and 49% of the dystroglycan morphants had to be manually dechorionated at 2dpf (Table 3.5 & Figure 3.15). Controls and morphants were grouped and tested against one another using a chi-squared test p< 1x10^{-3}. Providing evidence to suggest there is a significant difference in hatching at 2dpf in controls when compared to morphants. Whilst the delay in hatching suggests an overall developmental delay, it is also possible that the delay in hatching is a consequence of reduced muscle contractures. Motility is required to break out of the chorion thus the defect might be a secondary consequence to primary muscle pathology. Tail coiling is the first identifiable

muscle motor function present between 17-26hpf (Saint-Amant *et al.*, 2008). Spontaneous embryo coiling within a chorion is absent in other studies where motility is impaired (Dowling *et al.*, 2009). Inducing a developmental delay and comparing with immobilised fish, might resolve the difference between developmental delay and motility in regards to hatching.

	Wild Type	Control MO	Fukutin	FKRP	Dystroglycan
Hatched (%)	96	93	55	58	51
Unhatched (%)	4	7	45	42	49
Total (n)	240	138	101	95	135

Table 3.5: Delay in embryo hatching at 2 dpf
Light microscopy was used to investigate the hatched/unhatched status of embryos at 2dpf it would be expected that most embryos would hatch by 2dpf. Wild type, control MO, 30-12Apr05B-fukutin MO, fkrp MO and dystroglycan MO were observed to be in (unhatched) or out of their chorions (hatched) at 2dpf.
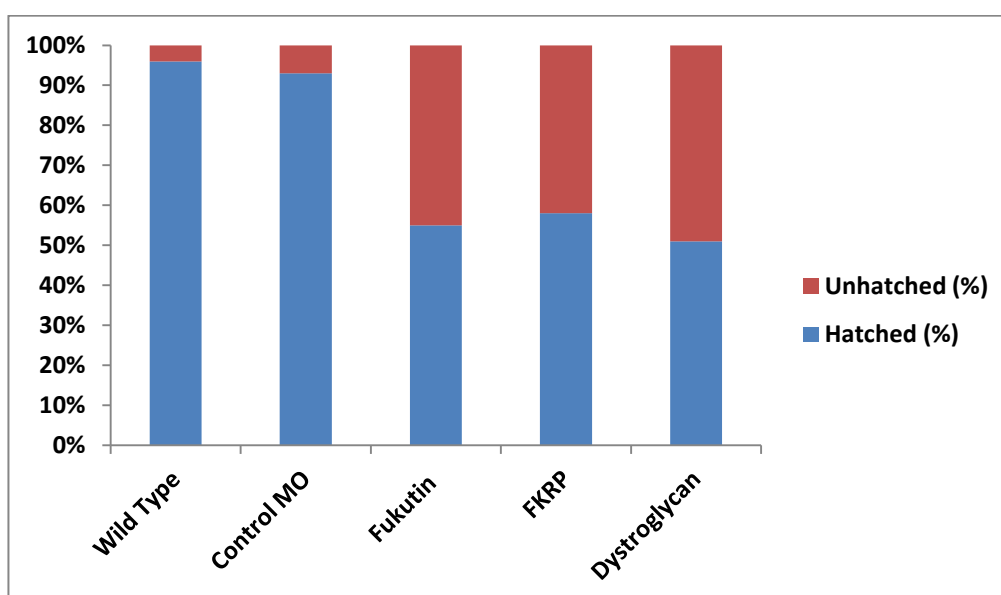
Figure 3.15: Delay in morphant embryo hatching at 2dpf
Light microscopy was used to investigate the hatched/unhatched status of embryos at 2dpf it would be expected that most embryos would hatch by 2dpf. Wild type, control MO, 30-12Apr05B-fukutin MO, fkrp MO and dystroglycan MO were observed to be in (unhatched) or out of their chorions (hatched) at 2dpf.

3.2.8 The Fukutin Morphant Larvae at 3dpf

To investigate the range of fukutin, fkrp and dystroglycan morphant phenotypes at 3dpf, light microscopy was used to image the larvae. The pathology at 3dpf may be as a result of developmental delay since at the severe end of the

morphant phenotype spectrum there were fewer somites observed in the trunk. A developmental delay would imply fkrp, fukutin and dystroglycan are important developmentally, whereas tissue specific pathology suggests an alternative mechanism. Melanophores in lateral stripe and iridiphores in the eye are present in early larval phase control embryos but are not visible in moderate or severe fukutin morphants, suggesting a possible developmental delay in the morphants (Figure 3.16A-D). The melanophores were similar to controls in all dystroglycan and most fkrp morphants. The pattern of the melanophores in the fkrp and dystroglycan morphants is likely to be as a consequence of the tail curvature and distortion rather than a primary abnormality.

The tails of the wild type and control MO injected fish are straight through their full length from the primula-16 (16mm length) stage of development at 31hpf to the protruding mouth phase at 3dpf. The mild fukutin morphants had a slight ventral tail curvature which was at a greater angle ventrally in the moderate phenotype group. The tail curvature could also be observed in fkrp and dystroglycan mild and moderate morphants. An abnormal body shape and shorter tail as consequence of fewer somites were observed at the severe end of the spectrum of all morphants. A dorsal curvature in the tail was found more often than ventral curvature in dystroglycan and fukutin morphants (Figure 3.16A-D).
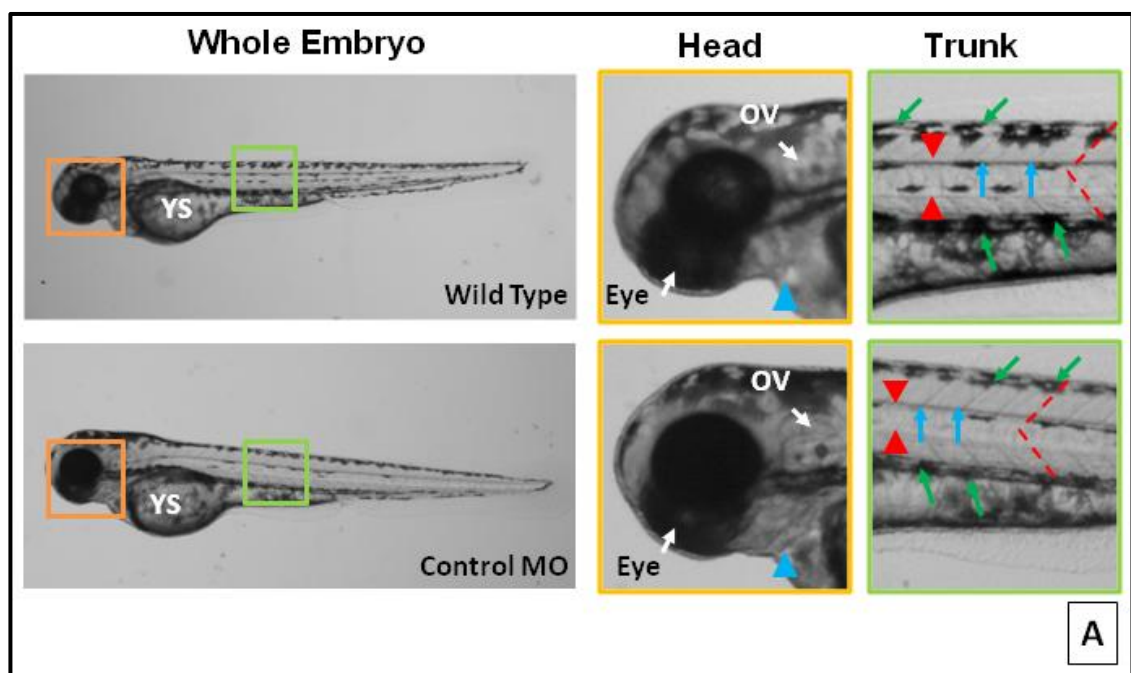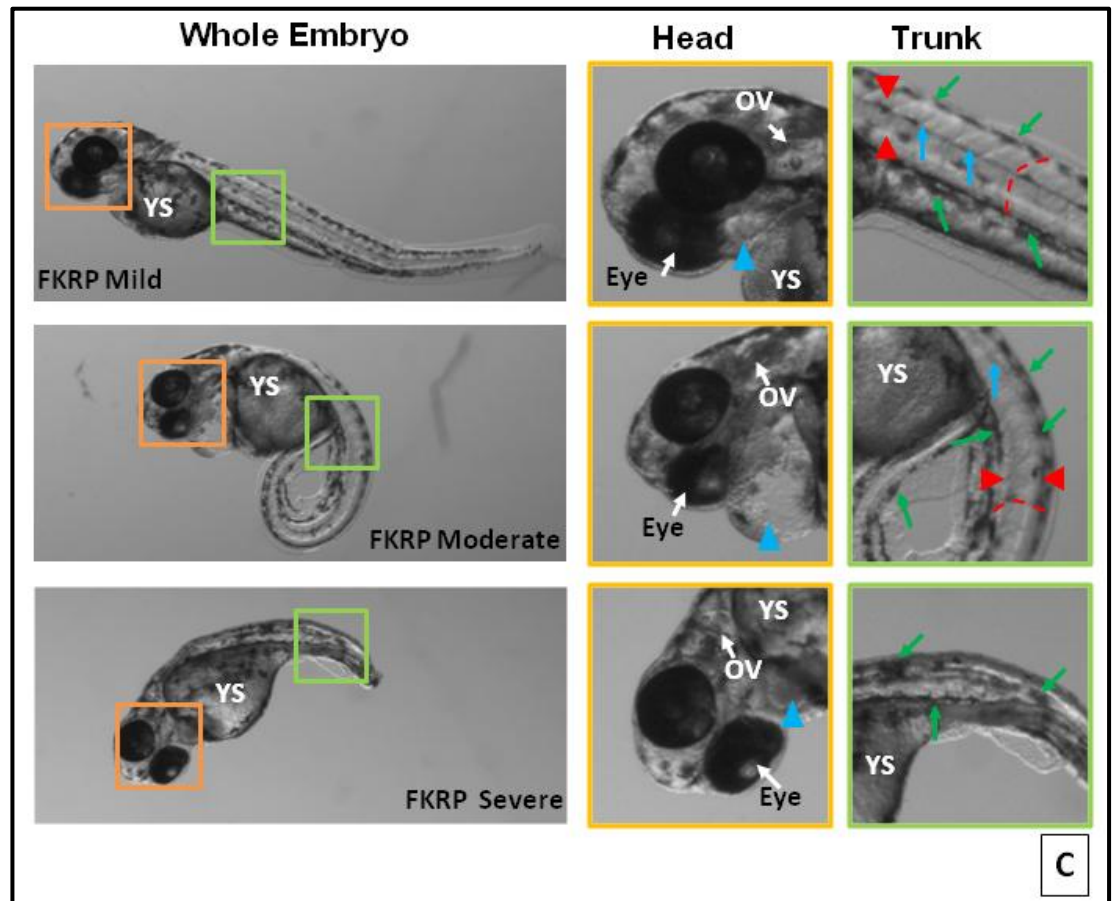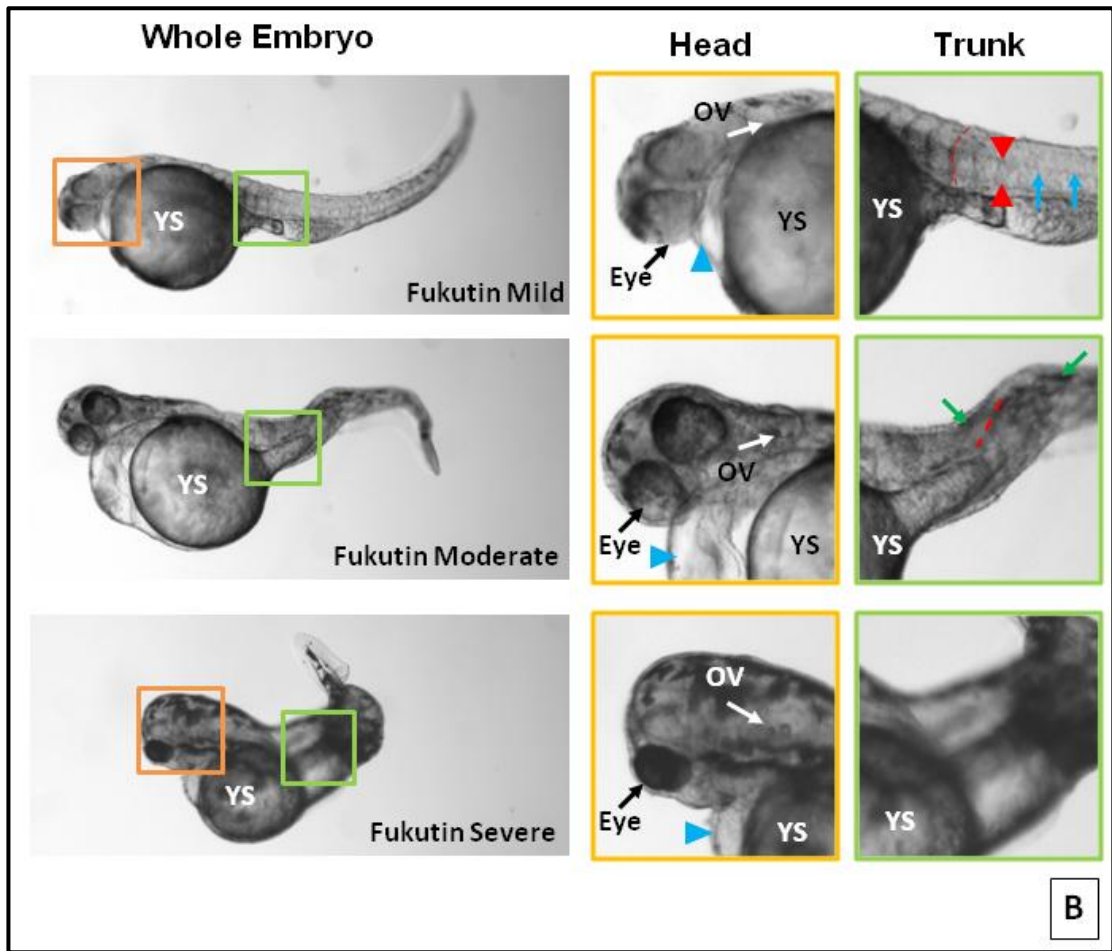
Figure 3.16: Light microscope images of larvae at 3dpf
Morphology was investigated using light microscopy in 3dpf Larvae. Larvae were either **(A)** untreated AB or injected with 10ng of control MO **(B)** injected with 2ng of 30-12Apr05B *fktn* MO **(C)** injected with 10ng of FKRP MO or **(D)** injected with 5ng of Dystroglycan MO. Embryos were staged according to Kimmel *et al.* and phenotypes were sorted according to the criteria outlined in (Table 2.2). Enlarged views of head (orange border), trunk (green border). Red triangle: notochord, blue triangle: pericardium, red dashes vertical myosepta, green arrows: melanocytes, blue arrows: lateral line, OV: otic vesicle, YS: yolk sack.

Wild type and control MO injected larvae had eyes which were round and pigmented preventing clear observations of the lens. Fukutin, fkrp and dystroglycan MO injected embryos had eyes where notable distortion to eye shape at the severe end of the phenotypic spectrum was evident. Eye area was smaller in the fukutin morphants and at the severe end of the fkrp morphant spectrum, (Figure 3.16A-D) when compared to control fish eyes. Eye area of the fukutin morphant was significantly smaller than control MO injected embryos, fkrp and dystroglycan morphants (Table 3.6 & Figure 3.17).
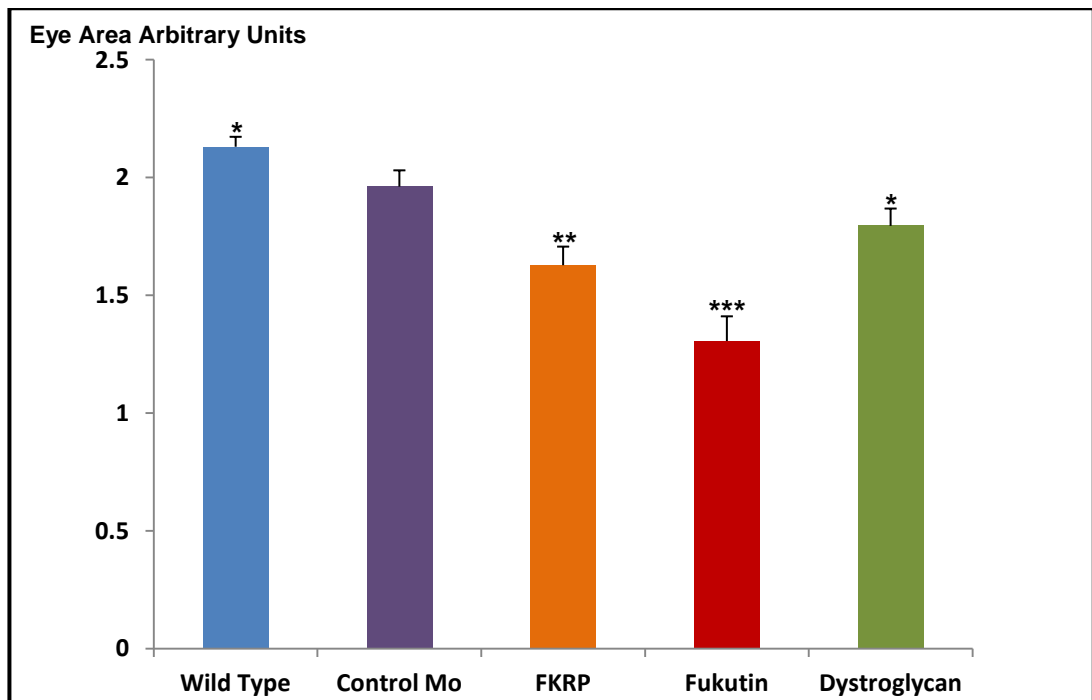
Figure 3.17: Mean eye size for 3dpf fish
Eye size was assessed on Image-J analysis software using light microscopy images of 3dpf larvae eyes and expressed in arbitrary units. A minimum of four fishfish from each of the three phenotype groups for each morphant group were assessed for eye size, phenotypes groups defined by criteria outlined in Table 2.2. Fukutin eye size was significantly smaller than control MO injected embryos, FKRP and dystroglycan morphants. Morphant eye areas were compared to the control MO eye areas using the unpaired student t-test: * p= <0.05 ** p= <1×10^{-3}, *** p= <1×10^{-4}.

Since progressive cardiac involvement is a characteristic of FCMD patients signs of cardiac failure were investigated in the morphant zebrafish (Nakanishi *et al.*, 2006). A swollen pericardium is a sign of cardiac hypertrophy and can be observed in a higher proportion of control MO injected larvae (9%) when compared to wild type larvae (0%). Therefore cardiac oedema in a small proportion of morphant fish can be considered to be a nonspecific effect of MO injection (Bill *et al.*, 2009). However, a swollen pericardium was observed in a higher proportion of the severe morphants (fukutin 42%, fkrp 37%, dystroglycan 46%). All morphants were observed to have cardiac oedema with higher frequency than observed in control injected morphants (Table 3.6, Figure 3.16A-D & Figure 3.18). Cardiac muscle is therefore also affected in dystroglycan-deficient zebrafish.

	No oedema (%)	Pericardial oedema (%)	Total (n)
Wild type	100	0	267
Control MO	91	9	124
Fukutin mild	83	17	39
Fukutin moderate	82	18	43
Fukutin severe	58	42	66
FKRP mild	85	15	45
FKRP moderate	79	21	46
FKRP severe	63	37	35
Dystroglycan mild	77	23	48
Dystroglycan moderate	78	22	27
Dystroglycan severe	54	46	31

Table 3.6: Pericardial oedema in 3dpf larvae
Pericardial oedema was judged on morphology in 3 dpf larvae in the morphant fish.
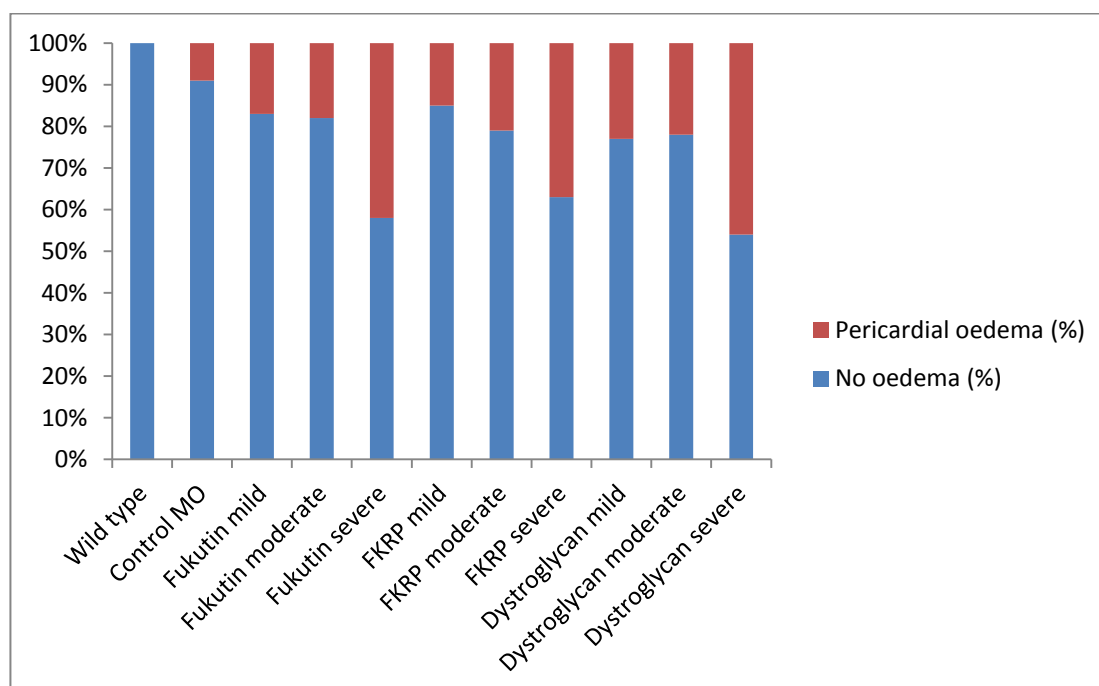
Figure 3.18: Pericardial oedema in 3dpf larvae
Pericardial oedema was judged on morphology in 3 dpf larvae in the morphant fish using images taken on light microscopy. Pericardial oedema was found in a small proportion of Control MO injected fish. The morphant fish all had a higher incidence of pericardial oedema than control MO injected larvae. The most notable pericardial oedema was observed in the morphants in the most severe phenotypic groups.

Active avoidance is a feature observed in the early larval phase of development in the majority of wild type larvae. With stimulation (a light touch of a pipette tip to the body at 3dpf) the wild type larvae swim away. A very small proportion of wild type and control MO injected larvae did not move at all in each case (n=25). Rarely, control MO were observed fasciculating (involuntary muscle contraction or relaxation) suggesting another non-specific MO effect. Swimming in circles and fasciculations are not considered normal features of development at this stage. An increasing proportion of fkrp, fukutin and dystroglycan morphants with these features were observed as the phenotypic severity increased. Fukutin morphants were observed fasciculating or swimming around in a tight circle, indicating that they have an intact peripheral nervous system, as also observed in fkrp and dystroglycan morphants (Thornhill *et al.*, 2008). The no movement phenotype also increased with increasing phenotype severity in the morphants. Consequently with increasing morphant severity the proportion of fish with a normal swim response decreased (Figure 3.19).

	No Movement	Fasciculation	Swims in Circles	Swims Away
Wild type	1	0	0	24
Control MO	1	1	0	23
Fukutin mild	3	6	14	2
Fukutin moderate	7	6	11	1
Fukutin severe	18	5	2	0
FKRP mild	4	4	7	10
FKRP moderate	7	8	8	2
FKRP severe	15	5	5	0
Dystroglycan mild	4	8	7	6
Dystroglycan moderate	9	7	8	1
Dystroglycan severe	15	4	6	0

Table 3.7: Response to touch of 3dpf larvae
Larvae were categorised as "swims away" (as expected for wild type fish as an escape mechanism), "swims around a point", fasciculates, or no movement. Morphant larvae display increasing touch response severity with severity of phenotype.
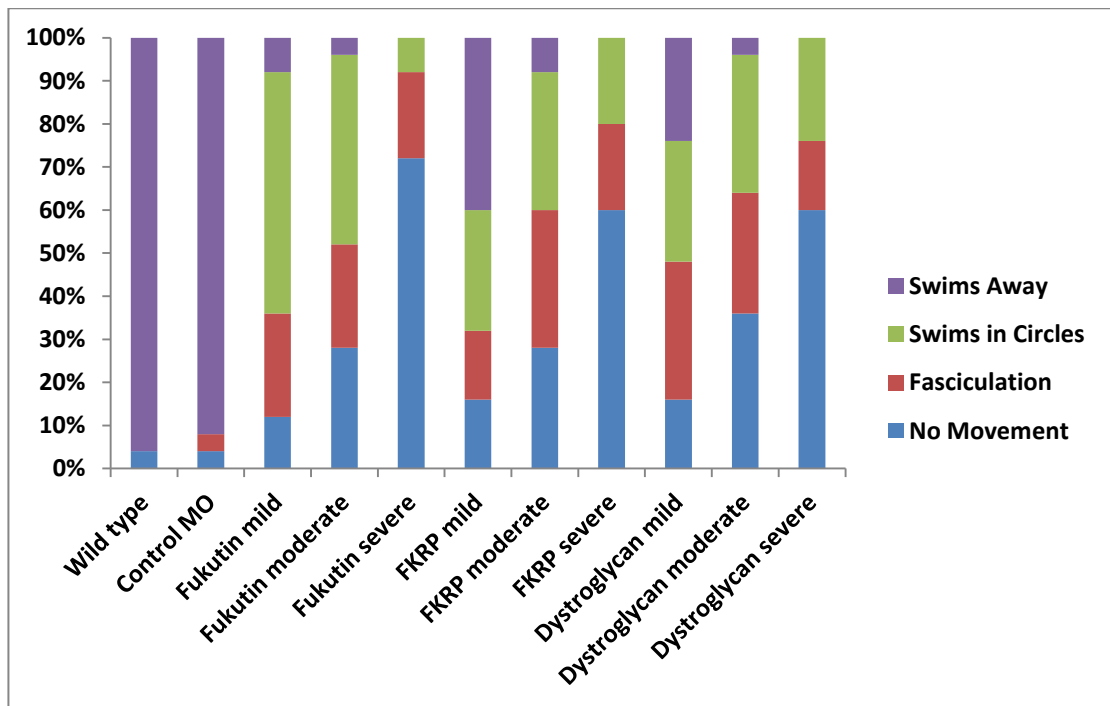
Figure 3.19: Response to touch of 3dpf larvae
3dpf larvae's movement was tested by stimulating with the point of a 10µl pipette tip. Larvae were categorised as "swims away" (as expected for wild type fish as an escape mechanism), "swims around a point", fasciculates, or no movement. Morphant larvae display increasing touch response severity with severity of phenotype.

3.2.9 The Fukutin Morphant Fish at 5dpf

The phenotype of the fukutin morphant embryos was investigated up to 5dpf and for regulatory reasons the fish were not able to be maintained past 5dpf. The morphology of 5dpf larvae was observed under light microscopy (Figure 3.20A). The 5dpf wild type larvae had a straight tail and the vertical myosepta forming the boundaries of the somites had a chevron appearance. In 5dpf fukutin morphants the tail was found to have a ventral curvature and was shortened with visible rounding of the somitic myosepta which was similar to fkrp and dystroglycan morphants (Figure 3.20B-D). The microphthalmia and cardiac oedema phenotype was also clearly present in 5dpf fukutin, fkrp and dystroglycan morphants when compared to controls (Figure 3.20A-D). The 5dpf wild type zebrafish had melanocyte pigmentation regularly spaced along the dorsum. The melanocytes of the fukutin and the more severe fkrp morphants were less regularly spaced and fewer in number than in the controls.
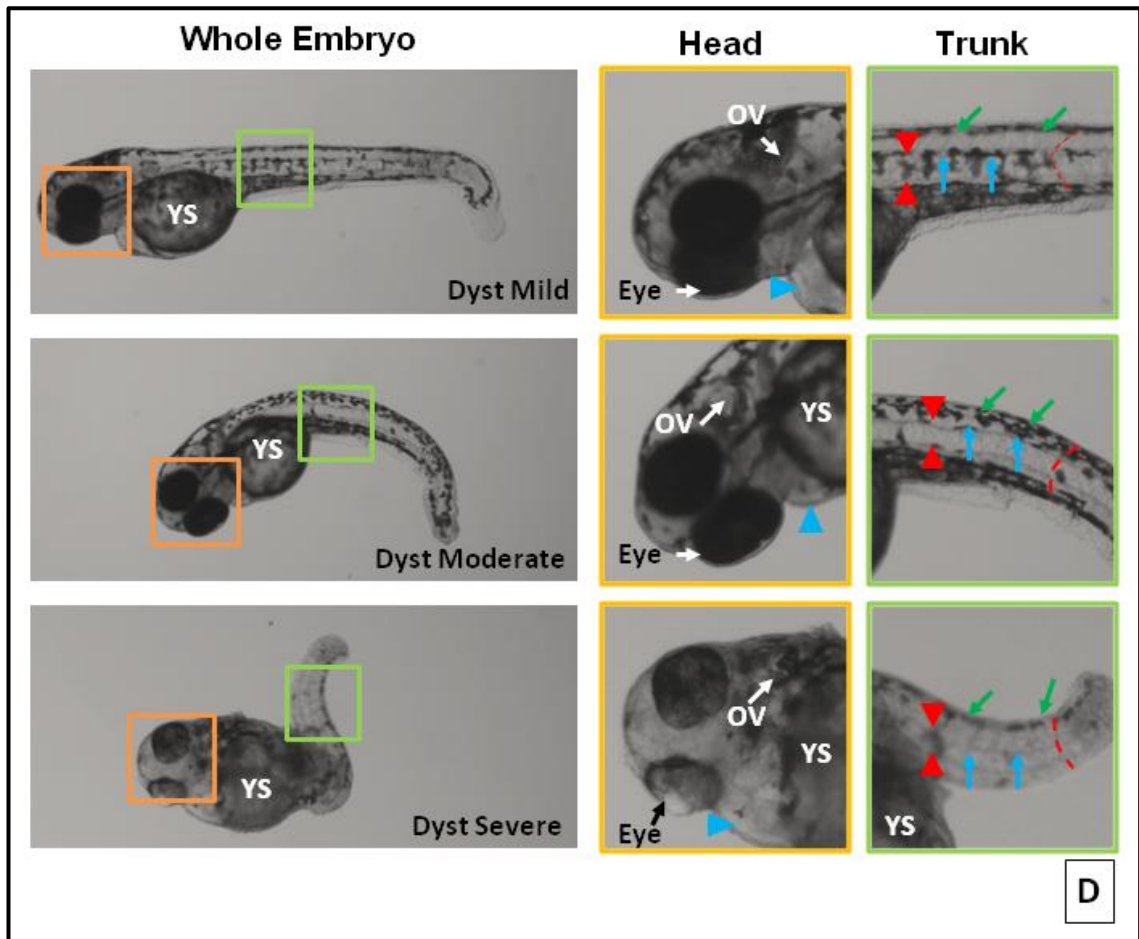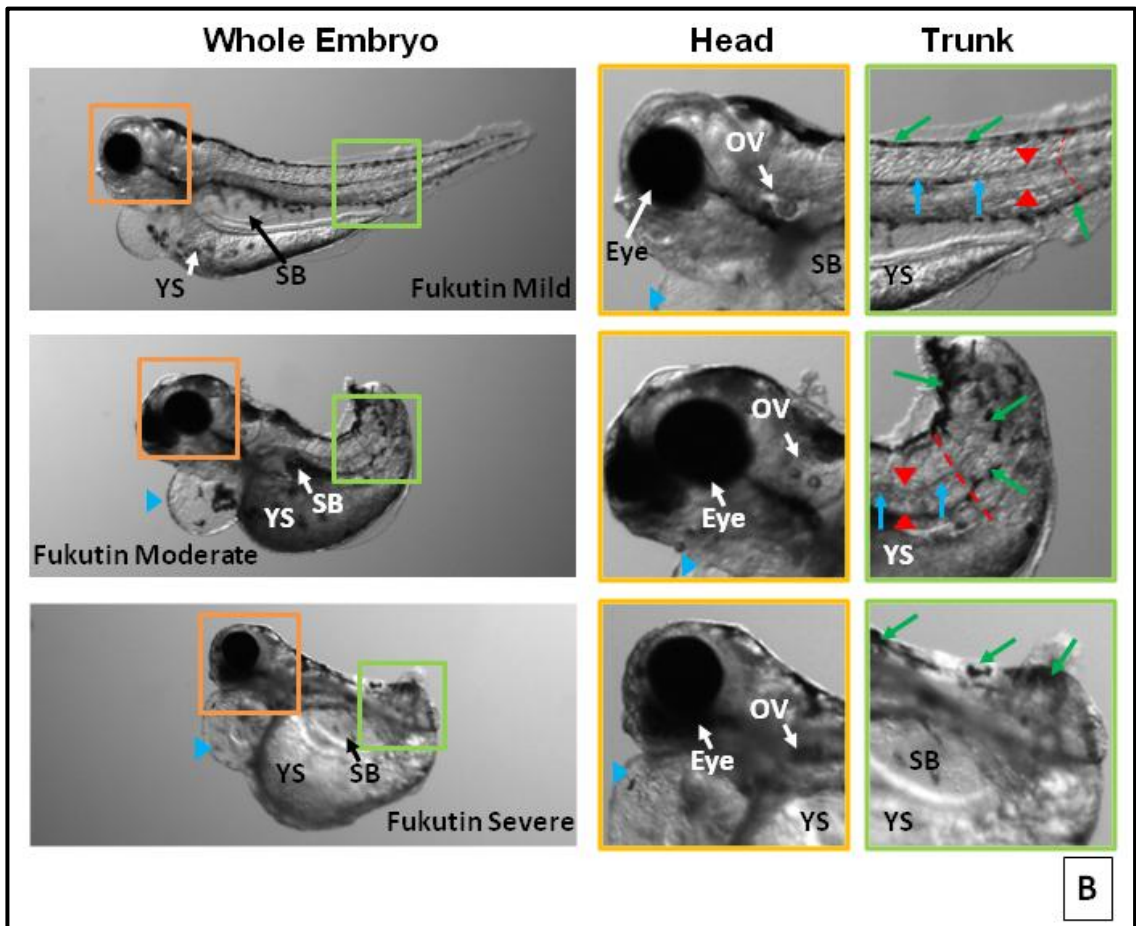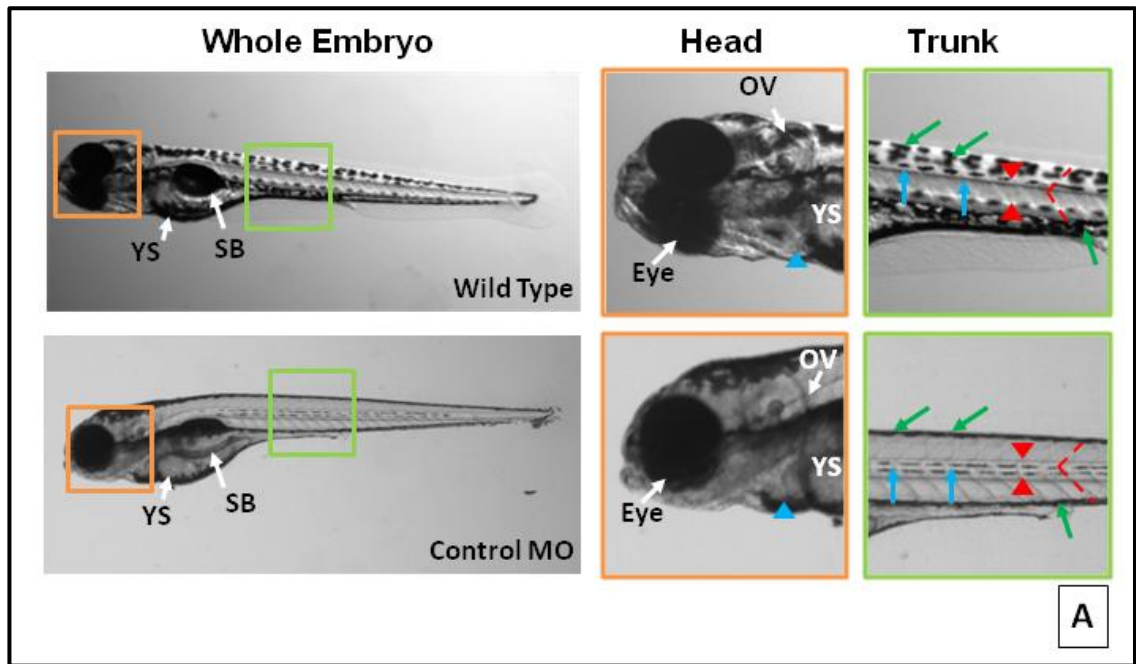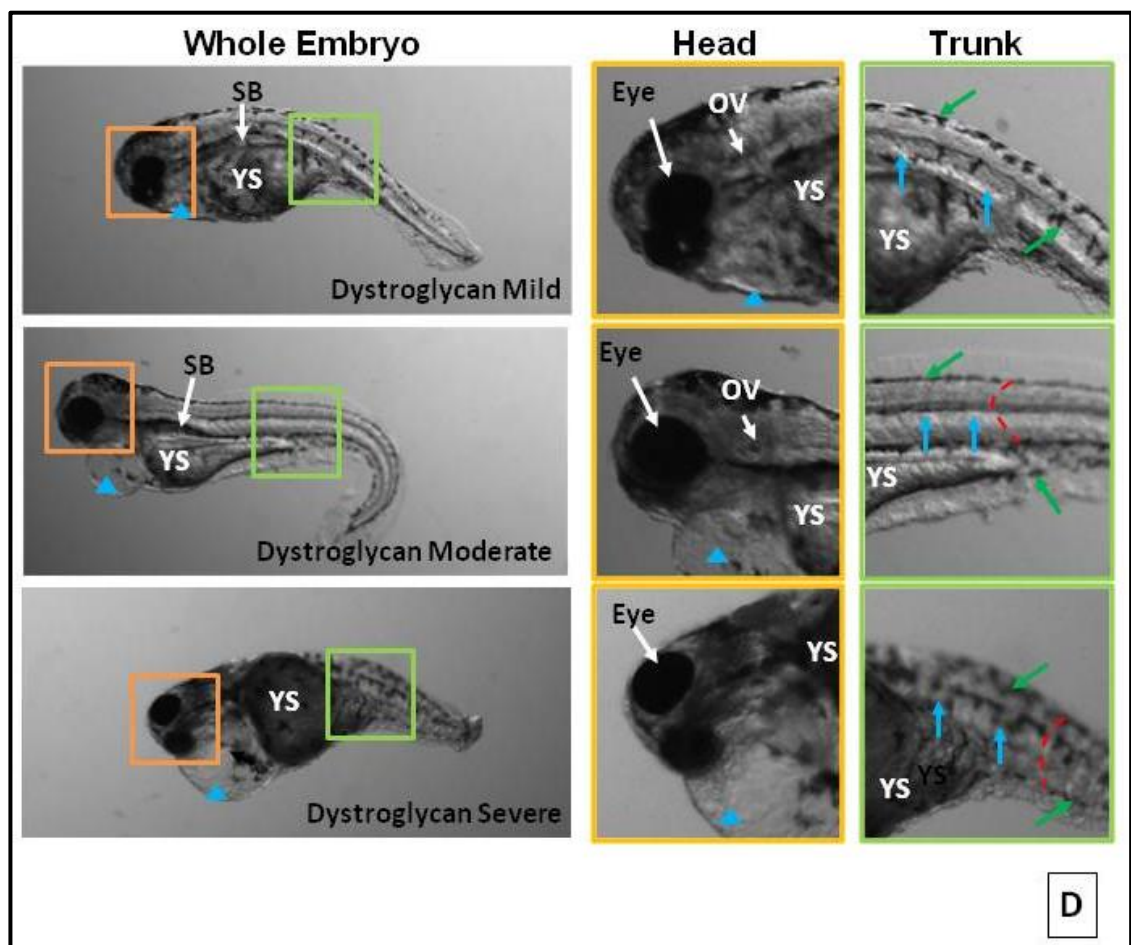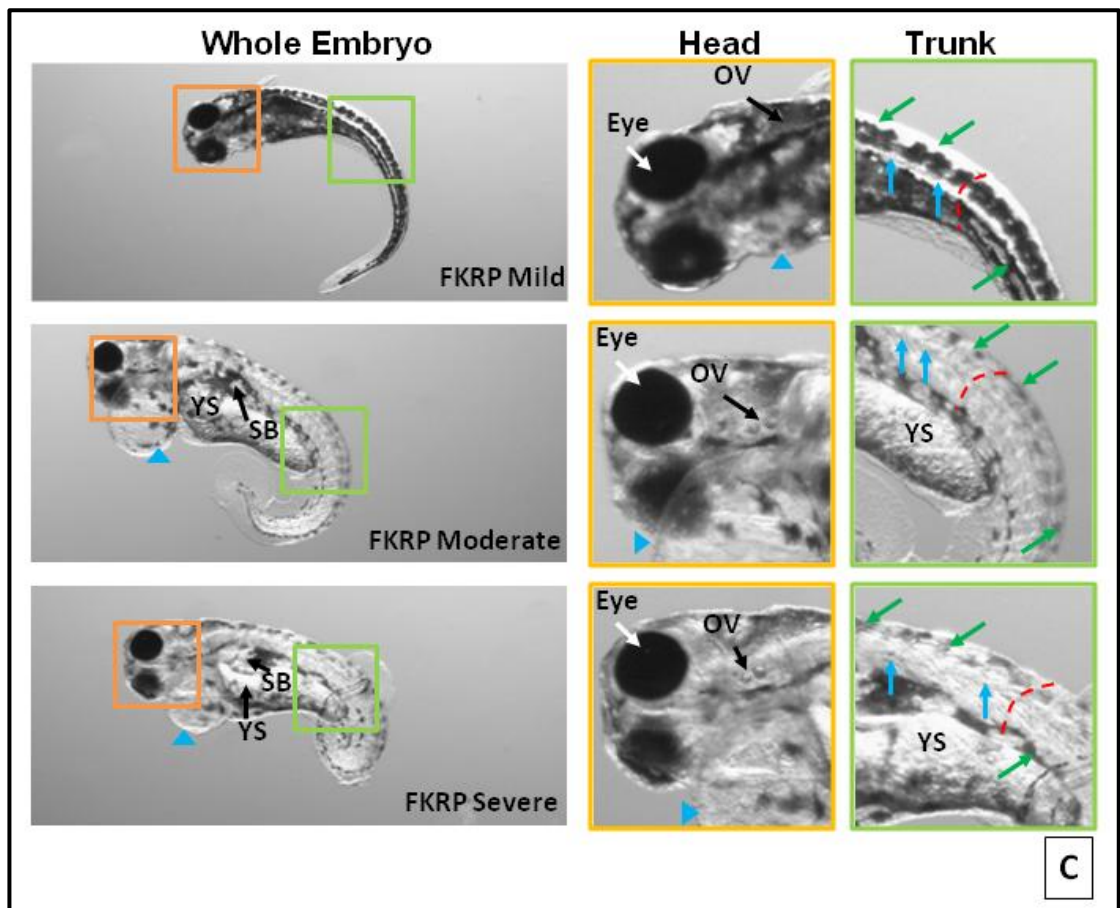
Figure 3.20: Light microscope images of phenotypes at 5dpf larvae.
Morphology was investigated using light microscopy in 5dpf larvae. Larvae were either untreated AB or injected with 10ng of control MO **(A)**, injected with 2ng of 30-12Apr05B-fukutin MO **(B)**, 10ng of fkrp MO **(C)**, 5ng of dystroglycan MO **(D)**. Larvae were staged according to Kimmel *et al.* 1995, and phenotypes were categorised according to the criteria outlined in (Table 2.2). Enlarged views of head (orange border), trunk (green border). Red triangle: notochord, blue triangle: pericardium, red dashes vertical myosepta, green arrows: melanocytes, blue arrows: lateral line, OV: otic vesicle, YS: yolk sack, SB: swim bladder.

3.3 Summary

This chapter investigated whether inhibition of fukutin function using antisense MO is associated with the dystroglycanopathy features of a muscle-eye-brain phenotype, as might be inferred from the human phenotype (Takada *et al.*, 1988; Yoshioka and Kuroki, 1994; Hino *et al.*, 2001; Toda, 2009). By testing the effect of these MO knockdowns within the confines of defined criteria, fukutin knockdown zebrafish could be compared alongside other fkrp and dystroglycan morphants without confounding effects of MO efficacy. Overall, the fukutin morphant could be validated as an appropriate model for dystroglycan glycosylation defects (Parsons *et al.*, 2002a; Bassett and Currie, 2003; Thornhill *et al.*, 2008; Kawahara *et al.*, 2010).

3.3.1 Dystroglycanopathy Specific Pathology Associated with Fukutin knockdown by MO

Overall the dystroglycanopathy phenotype cannot be distinguished between the FKRP, fukutin and dystroglycan morphants. Morphants had ventral and occasional dorsal curvature of the tail and in the most severe morphants smaller tails. Rounding of the chevron appearance of the vertical myosepta suggests sarcolemmal abnormalities, a characteristic also seen in muscle specific *filamin-c* mutant zebrafish (Ruparelia *et al.*, 2012). The micropthalmia and abnormalities in eye appearance were also observed in fkrp, fukutin and dystroglycan morphants, which correlates well with human fukutin associated MD (Yoshioka and Kuroki, 1994). Brain abnormalities in FCMD patients range from polymicrogyria to cobblestone lissencephaly. Similarly, the chimeric mice have been shown to have abnormal neuronal migration in the cerebral cortex, cerebellum and hippocampus (Takeda *et al.*, 2003; Kanagawa *et al.*, 2009b). In the fukutin, fkrp and dystroglycan knock down zebrafish the mid-brain is diminished or completely absent on morphological examination. Therefore the fukutin morphant zebrafish between 1-5dpf recapitulate fukutin deficiency in the human condition. The fukutin morphants are very similar on morphological grounds to FKRP and dystroglycan morphants suggesting that the fukutin morphant potentially has a similar pathological mechanism (Parsons *et al.*, 2002b; Takeda *et al.*, 2003; Thornhill *et al.*, 2008; Kawahara *et al.*, 2010).

While in the process of characterising this model, another study was published where fukutin and fkrp were knocked down in, and compared to, a dystroglycan

mutant line (*dag1^{hu3072}*). The fukutin spliceosomal MO targeted the intron/exon boundary of exon 2 producing a similar phenotype to that of the 30-12Apr05B *fktn* MO, described here (Lin *et al.*, 2011). Although the morphant phenotype described in Lin *et al.* show strong similarities to ours, their work mainly characterises the skeletal muscle phenotype and it is therefore complementary to our study in the full characterisation of fukutin morphant zebrafish. Lin *et al.* show that the fkrp and fukutin morphants don't accumulate Evans blue dye (EBD) in the muscle fibres suggesting an intact sarcolemma. Interestingly, this result is in contrast to the *dag1^{hu3072}* mutant fibres, suggestive of alternative mechanisms of pathology in primary to secondary dystroglycanopathy. The evidence presented indicates there might be an alternative mechanism to sarcolemmal damage in these morphants, such as the unfolded protein response (UPR). The study also found the elevated endoplasmic reticulum (ER) stress was as a direct consequence of proteins that were not folded correctly. BiP/GRP78 a chaperone of unfolded proteins was used as a marker of the UPR, was found to be increased in fkrp and fukutin knock down models. It is clear the UPR may form part of the mechanism for secondary dystroglycanopathy, however the delay in development of the notochord in the models could indicate simply a developmental delay in fukutin and fkrp fish muscle (Lin *et al.*, 2011).

3.3.2 Conclusion

The clear MEB phenotype in zebrafish where fukutin has been knocked down between 1-5dpf indicates that the MO approach is an appropriate strategy to investigate the pathology associated with fukutin deficiency (Yoshioka and Kuroki, 1994). The morphological abnormalities found in the fukutin morphants are comparable with those found in fkrp and dystroglycan morphant zebrafish (Parsons *et al.*, 2002a; Thornhill *et al.*, 2008; Kawahara *et al.*, 2010), an unsurprising result considering they have been implicated in the same biochemical pathway *i.e.* modification of mannose residues on dystroglycan (Barresi and Campbell, 2005; Kuga *et al.*, 2012a). Since the dystroglycan morphants had a very similar phenotype to both FKRP and fukutin knock down fish a more in depth histological and immunological analysis is required to distinguish the effects of each gene. It is however entirely possible that fkrp and fukutin have similar function based on the conservation of protein structure and morphology of knock downs. Both may have been conserved as different

pathways that lead to similar modification of dystroglycan, perhaps in a tissue and developmental specific fashion. Under this hypothesis subtleties in modification may act as protective mechanisms from old world adeno-viruses known to bind to dystroglycan (Manya *et al.*, 2004). In conclusion, studies based on morphological examination alone are unlikely to identify specific mechanisms for the pathology associated with 30-12Apr05B-fukutin MO knockdown and therefore inferences need to be confirmed with further detailed investigation.

Chapter 4   Abnormal Muscle and Notochord in Morphant Zebrafish

4.1 Introduction

A clear muscle pathology associated with the knock down of fukutin, fkrp and dystroglycan by MO in zebrafish between 1-5dpf, has been shown in the previous chapter. However, no perturbation in the morphant morphology was observed that would indicate any notochord pathology, contrary to expectations. Further investigation of the notochord is therefore important and is examined in more detail in this chapter. Immunohistochemical and histological analysis have been used to investigate the muscle and notochord phenotypes further. These two structures are discussed together because of their close association during development. The notochord provides developmental cues for zebrafish tail development and generation of myotome (Stemple, 2005). Specifically, loss of basement membrane stability is hypothesised to underpin tail pathology in the dystroglycanopathy morphants (Bassett *et al.*, 2003; Bassett and Currie, 2003; Thornhill *et al.*, 2008; Kawahara *et al.*, 2010).

In this chapter angiogenesis in dystroglycaonopathy will be investigated. Here the hypothesis is that correct glycosylation of α-dystroglycan is central to vascular development. This is an alternative hypothesis to the "classic vascular hypothesis in MD" which is centred on nNOS and chronic hypoxia, discussed in the introduction. For vascular endothelial cells (VEC) to succeed in migrating through the myotome they must digest the extracellular matrix (ECM). The behaviour of the VEC's is known to be influenced by various components of the ECM including integrins and laminins. Other studies have proposed dystroglycan to be present at the tip of the growing intersegmental vessels and therefore guiding angiogenesis by interacting with laminin in the surrounding ECM (Hosokawa *et al.*, 2002; Jacoby *et al.*, 2009). It would therefore seem logical to presume dystroglycan on the angiogenic growth cone, would need to be correctly glycosylated by FKRP and fukutin for the growth cone to migrate successfully across a somite.

4.1.1 Aims

- Histological assessment of muscle and notochord pathology associated with fukutin, FKRP and dystroglycan deficiency at 3dpf.
- Qualitative examination of the ultrastructure of muscle, myosepta and notochord in the FKRP, fukutin and dystroglycan morphant larvae.
- Immunohistochemical studies to examine potential molecular mechanisms of muscle pathology.

- Characterisation of the vascular phenotype of the FKRP, fukutin and dystroglycan morphant fish.

4.2 Results

4.2.1 Investigation of the Morphant Myotome from a Histological Perspective

Sections through the myotome trunk were stained with toluidine blue to investigate the phenotype of fukutin, FKRP and dystroglycan morphants from a histological perspective (Figure 4.1 & Figure 4.2). Longitudinal sections through the myotome of the trunk were cut to view muscle fibres running between the vertical myosepta. Another set of transverse sections were cut through the trunk at the level of the fifth somite to examine the muscle, horizontal myosepta, the notochord and the neural tube. The sections were cut from 3dpf larvae with a moderate phenotype. In the case of the morphants, a minimum of four embryos from two separate experiments were sectioned and the most representative image is shown.

The myosepta in zebrafish are the origin and insertion points of muscle fibres, forming boundaries between myotome segments. The vertical myosepta run from the ventral to the dorsal side of the zebrafish, the shape closely resembles a chevron when viewed on a longitudinal section of wild type and fish injected with control MO. The normal chevron appearance of the vertical myoseptum is disrupted in all morphants appearing flattened and rounded. The horizontal myoseptum runs continually from the anterior to posterior of the trunk either side of the notochord in the wild type and control injected fish. In the dystroglycan morphants disruption to the horizontal myoseptum was also visible. The fukutin and fkrp morphants appeared to have an enlarged notochord preventing clear visualisation of the horizontal myoseptum. The fkrp , fukutin and dystroglycan morphant muscle fibres all run a non-linear course or appeared in some instances to be torn. Whilst there does not seem to be an increase in fatty infiltration in the morphants, clear areas between fibres may indicate oedematous infiltration. Overall, the fukutin morphant had the more severe muscle fibre phenotype when compared to fkrp or dystroglycan morphants (Figure 4.1).
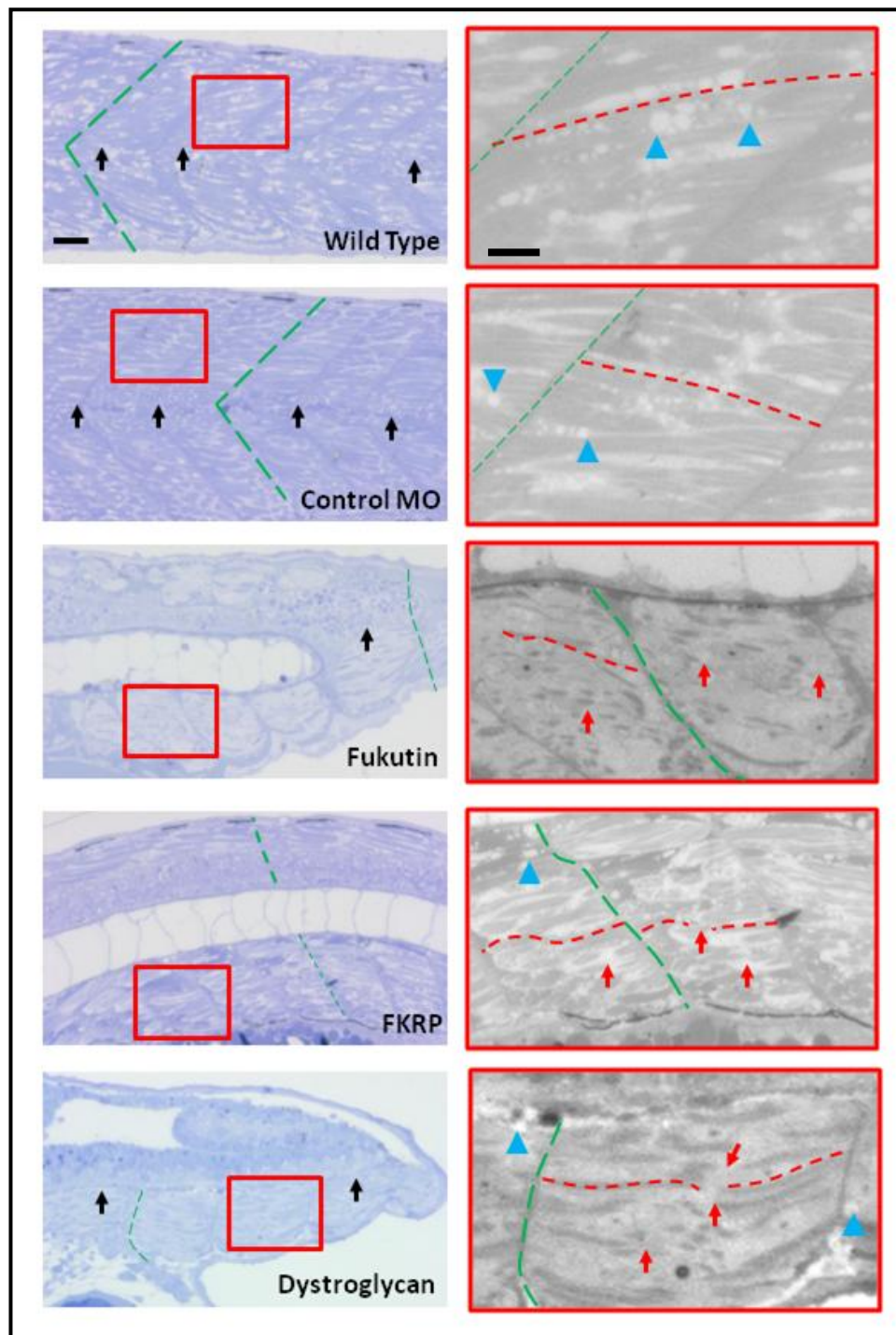
Figure 4.1: Longitudinal sections of 3dpf larvae stained with toluidine blue showing the myotome trunk

Morphants were all judged to be moderate phenotype group based on (Table 2.2). Muscle fibres in the wild type embryos run between vertical myosepta whereas in the dystroglycanopathy fish fibres were found to be disrupted. Vertical myosepta: green dashed line, muscle fibre: red dashed line, horizontal myosepta: black arrows, disrupted muscle fibre: red arrows and fat globules: blue arrow, scale bar; left = 50μm, right = 20μm.

The myotome is divided in its entirety by the horizontal myosepta in wild type

and control MO injected larvae. In fukutin and dystroglycan morphants the

horizontal myosepta are completely absent and only partially visible in the fkrp

morphants. There are two alternatives to explain this observation: it is possible that the section was cut veryclose to the centre thereforethe horizontal myosepta may be being masked by the notochord. The alternative is that the horizontal myosepta is missing, due to reduced myotome volume. In the fkrp morphants, the horizontal myosepta are visible but disrupted, suggesting that loss of the horizontal myoseptum is due to the MO knockdown, and not an artefact. The morphants all have a reduced muscle fibre density *i.e.* lower numbers of fibres per unit of area within the myotome, when compared to controls with apparent oedematous infiltration observed as clear space (Figure 4.2).

In the previous chapter the morphant notochord was indistinguishable from that of the wild type on morphological grounds despite a hypothesised disruption. In wild type and control MO injected larvae the notochord has a round appearance on sections, visible in the middle of the myotome trunk. In fkrp, fukutin and dystroglycan morphants the notochord is distorted, losing its characteristic round shape. In the dystroglycan morphants the notochord is ectopic, positioned ventrally towards the yolk sack, whereas in the fukutin and fkrp morphants the notochord has remained central (Figure 4.2). Therefore there is clear abnormal notochord pathology; however at this level of magnification it would be difficult to distinguish a primary change in notochord structure from a secondary change due to ECM disruption.

The neural tube is the larval precursor to the central nervous system. In the myotome trunk the neural tube becomes the spinal cord of the adult fish. Dystroglycan glycosylation has been implicated in synaptic plasticity and therefore an effect on the neural tube might be expected in models for dystroglycanopathy. However a more macroscopic view may argue that neural tube defects are a secondary consequence of ECM changes. The oval shaped neural tube in wild type and control larvae is located in the midline towards the dorsum, situated directly above the notochord. In the fukutin morphants the neural tube is more rounded than in controls, whereas the neural tube in fkrp morphants is irregular in shape. The dystroglycan morphant neural tube is the most severely affected with a highly abnormal shape (Figure 4.2).

Full Trunk	Notochord	Neural Tube

Wild Type — YS — NC, NT — NT, NC

Control MO — YS — NT, NC — NT, NC

Fukutin — YS — NT, NC — NT, NC

FKRP — YS — NT, NC — NT, NC

Dyst — NC — NT
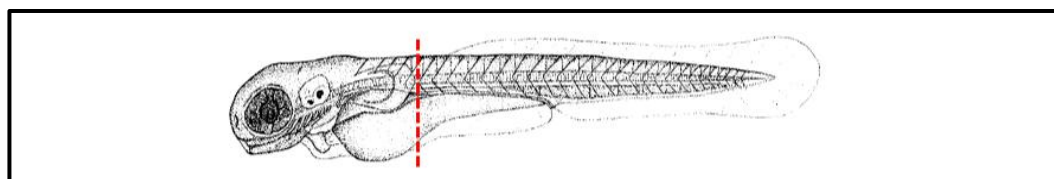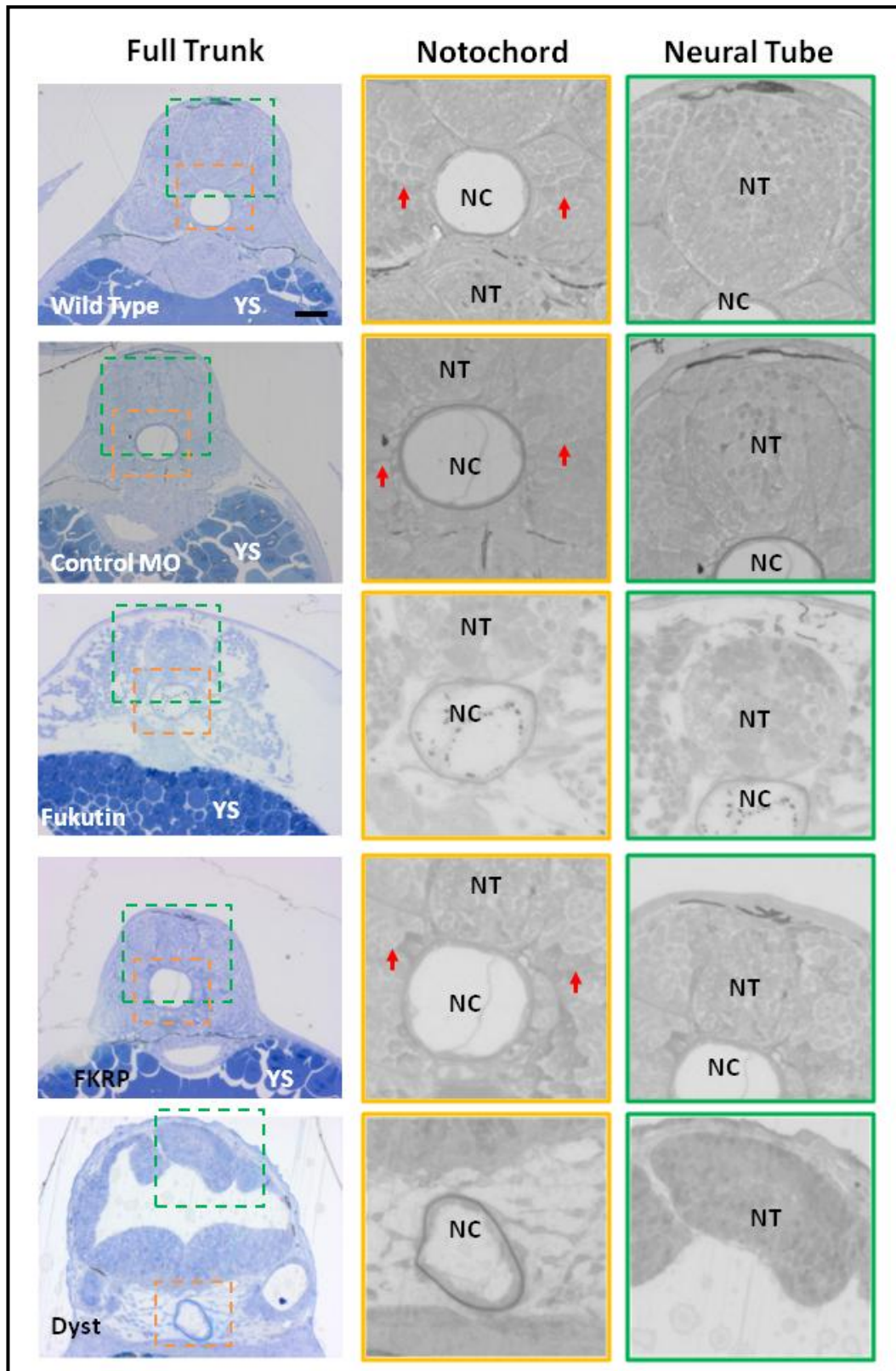
Figure 4.2: Transverse sections of 3dpf larvae stained with toluidine blue showing the myotome region.
Morphants were all judged to be in the moderate phenotype group based on Table 2.2. Notochord: NC, neural tube: NT and horizontal myosepta: red arrows, scale bar: 50µm. Bottom part of the figure shows a schematic red dotted line of where the section has been cut in the 3dpf larvae, figure adapted from kimmel *et al.* 1995.

4.2.2 Immunohistochemical Analysis of Protein Expression in Morphant Somites

The presence of glycosylated α-dystroglycan in fish embryos at 1 dpf was investigated by immunostaining with the antibody IIH6, which specifically binds to correctly glycosylated α-dystroglycan (Kuga *et al.*, 2012b). In control fish IIH6 stained the somite boundaries and horizontal myosepta with the greatest intensity. The muscle fibres that run longitudinally attaching to the vertical myosepta, were observed to have only weak IIH6 signal along the length of the fibres. In fukutin knockdown fish a similar reduction was found to that which had previously been described in the fkrp morphants (Thornhill *et al.*, 2008). Unsurprisingly, no staining was observed in the dystroglycan morphants (Parsons *et al.*, 2002a).

To examine the consequences of a reduction in glycosylation on the whole expression of the dystroglycan complex, 1 dpf embryos and morphants judged to have a phenotype of moderate severity, were immunostained with the 43DAG antibody recognising β-dystroglycan. In control embryos 43DAG stained the vertical myosepta, which have a classical chevron appearance. The horizontal myosepta running through the midline was also detected in controls. In the fukutin morphants the intensity of the staining in the myosepta was reduced, but interestingly 43DAG staining seemed reduced to a lesser extent than in the fkrp and dystroglycan morphants, where the staining was almost completely abolished (Figure 4.3).
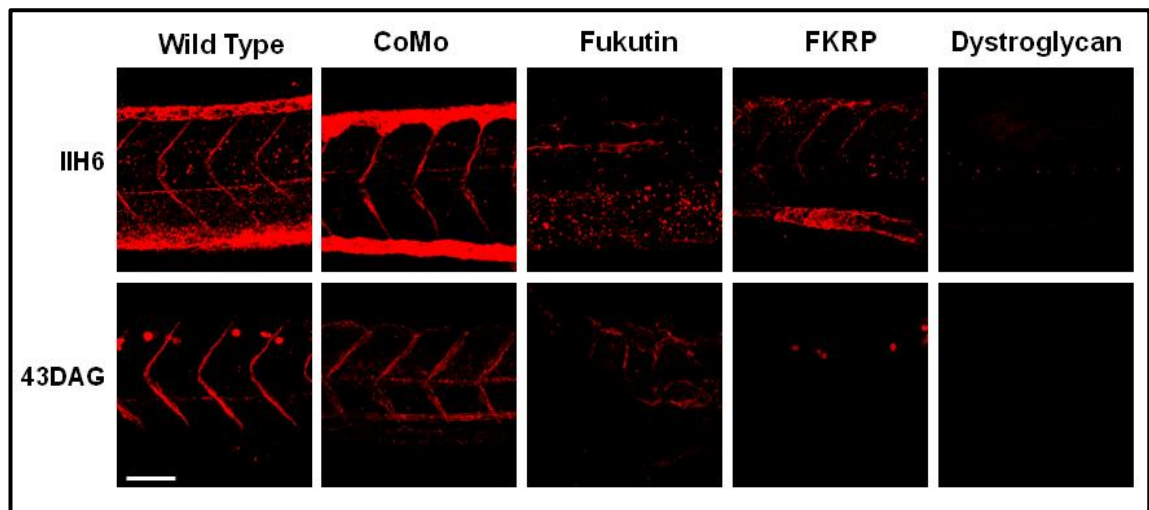
Figure 4.3: Projections from confocal microscopy through the myotome trunk of 1dpf embryos after IIH6 and 43DAG staining.
1dpf embryos were manually dechorionated and fixed before staining with IIH6 (for glycosylated dystroglycan) or 43DAG (β-dystroglycan) antibodies. White scale bar represents 80μm. Upper panel: IIH6 staining, lower panel: 43DAG. From left to right: uninjected fli-1 control, embryo injected with control MO, fukutin MO, fkrp MO and dystroglycan MO.

To investigate the consequences of knocking down fukutin and fkrp on laminin, one of the known ECM binding partners of α-dystroglycan, 1dpf embryos were immunostained with a pan-laminin antibody. The pan-laminin antibody is raised against an ECM homogenate, and therefore recognises most laminin isoforms. The classic chevron appearance of the myosepta is present when stained with the pan- laminin antibody in control fish (Figure 4.4). The myosepta of the fkrp morphants are increasingly rounded with increased severity of the phenotype. In the most severe fkrp morphants the myosepta appear to have greater width which is similar to that observed by bright field microscopy (Figure 4.1). The fukutin morphant myosepta are almost straight in all phenotype groups with very little laminin staining visible in the most severe embryos. No signal from the immunolabelling was detected in the dystroglycan morphants, suggesting laminin ligand binding to dystroglycan had been abolished, as a result of loss of dystroglycan at the vertical myosepta. Despite repeats and controls both positive and negative, the possibility that the staining did not work should be considered since laminin binding integrin-α7 should be detectable (Belkin and Stepp, 2000; Postel *et al.*, 2008; Sztal *et al.*, 2012). The specificity of the antibody should also be considered, without an antibody specifically detects laminin-α2, little in the way of conclusions can be drawn about this specific laminin chains expression at the vertical myosepta.
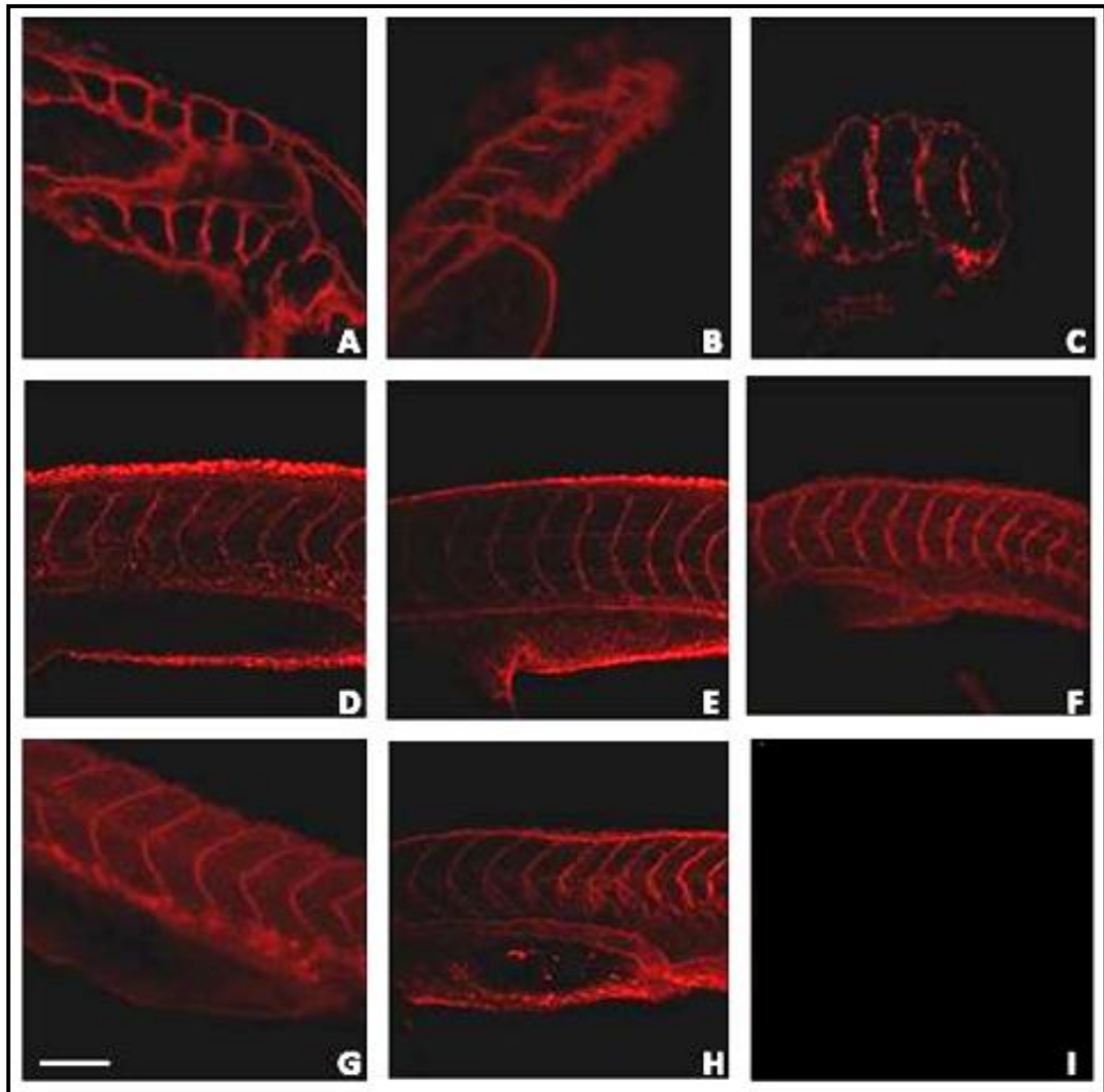
Figure 4.4: Pan-laminin staining of whole mount 1dpf embryos.
1dpf embryos were manually dechorionated and fixed before staining with a pan-laminin antibody. **(A-C)** Fukutin MO injected embryos, mild to severe phenotype, **(D-F)** fkrp MO injected embryos, **(G)** wild-type non-injected embryos, **(H)** Control MO injected embryos and **(I)** dystroglycan MO injected embryos. Scale bar: 80µm.

4.2.3 Structural Changes in Morphant Muscle Fibres

Myofibrils consist of small repeating structures known as sarcomeres contained between two zwischenscheibe (Z-lines). Surrounding each Z-line is the I-band or zone of thin filaments. The anistropic (A-band) spans the length of a full thick fibre and is contained within this band, while myosin is cross linked at the central Mittelscheibe (M-line). Transmission electron microscopy (TEM) allows the investigation of sarcomere structure at the nanometre scale and all components of the sarcomere including, can all be clearly visualised on TEM, (Figure 4.5).

Trunk muscle in zebrafish develops into dorsoventral subdivisions of epaxial/hypaxial somites (Figure 1.8), separated by the horizontal myosepta. The somites are also divided into mediolateral subdivisions of slow/fast twitch fibre territories. The process of zebrafish myogenesis is almost complete by 3dpf, with the slow twitch red fibres segregating to the periphery and the fast twitch white fibres positioned more medially. Here the hypaxial medial fast twitch fibres at 3dpf are investigated. Despite the sub populations of fast and slow twitch fibres being distinguishable there are no important physiological differences critical for development between the fibres types at this stage of development. Most of the features which distinguish fast from slow twitch fibres including ATPase reactivity and accumulation of mitochondria, occur after 3dpf. No new motor neurones will be generated after 3dpf, making this time period ideal to investigate muscle fibre structure.

Muscle fibres from wild type and control injected larvae are straight, running between vertical myosepta, filling the myotome trunk as seen in the lowest magnification part of the panel, (Figure 4.5). The fibres are surrounded by small areas of amorphous material and enclosed globules of fat, more easily seen at lower magnifications. Excessive sarcolemmal fluid and adipose globules are suggestive of muscle degeneration, indicating the muscle did develop but degenerated on movement. The morphants were all chosen from the moderate phenotype category and a minimum of three fish were imaged for each MO. The morphant muscle fibres fill less space in the myotome trunk due to reduced fibre density, most run in a non-linear fashion between myosepta. The classical chevron appearance of the vertical myosepta is also rounded in the morphants when compared to controls, as seen in the lowest magnification panel. The fatty infiltration and amorphous material is more extensive in all morphants when compared to controls. Similar to previous findings the fukutin morphant appeared to have the most severe phenotype (Figure 4.5).

At higher magnifications the sarcomere is clearly visible. In the controls the sarcomere forms regular repeating units separated by areas of ECM, sarcoplasm and mitochondria. The morphants all have torn sarcomeres around the boundaries of the fibres. Despite the torn appearance of the morphant sarcomeres the M-line and Z-lines are straight *i.e.* a normal appearance. In areas where the sarcomeres are not torn the A-band is intact, similar to controls.

The sarcomeres of the fukutin morphant have the most severe phenotype amongst the morphants with larger areas of tearing within the A-band. On occasion the morphants were observed to have enlarged mitochondria which is a non-specific sign of degenerative muscle, a feature not seen in the controls (Figure 4.5).
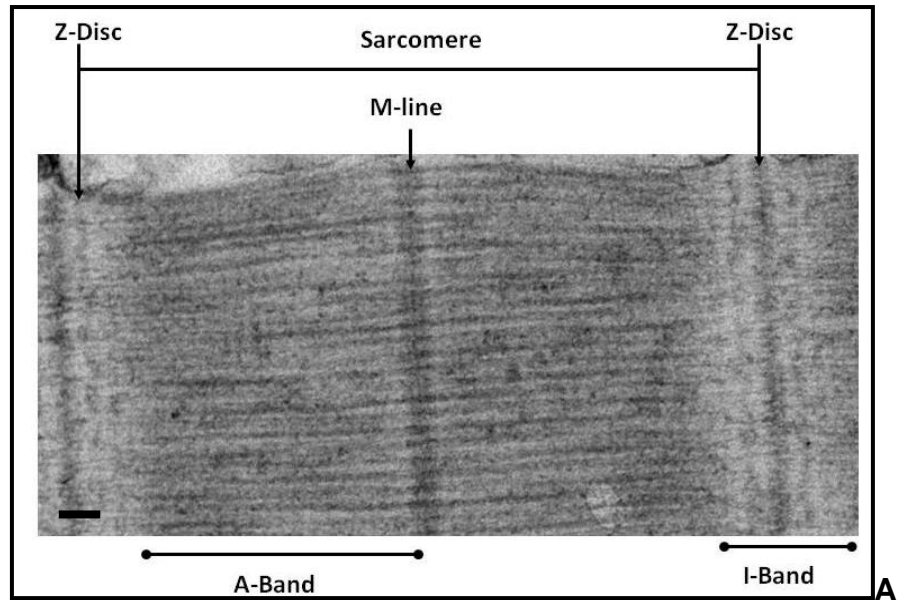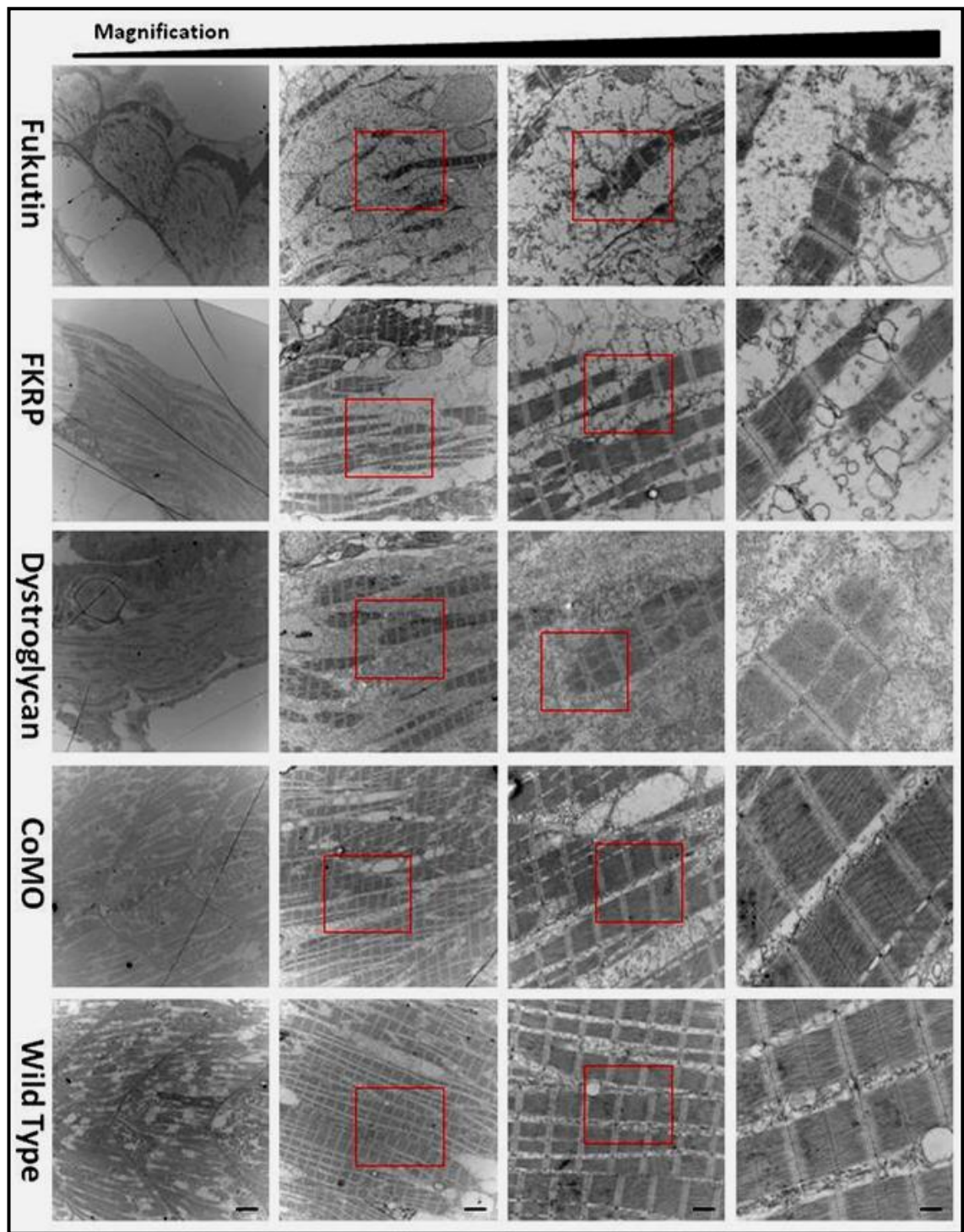
Figure 4.5: TEM of 3dpf larvea somitic muscle
A: 3dpf wild-type sarcomere structure, scale bar: 10nm. **B:** Longitudinal sections of 3dpf muscle. Lowest-highest magnification left-right, scale bars: 20μm, 2μm, 1μm & 500nm. Red square shows area of magnification. Note at lowest magnification there are some creases visible on the section which is a normal feature of TEM at low magnifications. Panels from top to bottom: larvae injected with fukutin MO, fkrp MO, dystroglycan MO, Control MO and non-injected wild type larvae.

It became clear that it was not possible to distinguish primary pathology in the myotome or vasculature from secondary changes due to structural alterations of the entire fish body. In order to control for this gfat1 protein expression was downregulated since this was known to induce a comparable bended body phenotype as observed in fukutin/fkrp morphants. The gfat1 deficient fish were shown to have muscle fibre abnormalities (Senderek *et al.*, 2010), a finding recapitulated in Figure 4.7. On closer examination the gfat1 morphants were observed to have predominantly ventral curvature of the tail enabling the classification of the *gfat1* knock down fish based on the criteria in Table 2.2. The injection of gfat1 MO produced morphants that were evenly distributed between each phenotypic category as described in Table 2.2, overall 47% of morphants and 0% of wild type controls had abnormal phenotypes (Figure 4.6). gfat1 deficient zebrafish embryos therefore have a similar morphological phenotype to the fkrp and fukutin knockdown fish (Figure 4.6). These fish were therefore used to distinguish primary events from pathology secondary to the bended body phenotype.

	No phenotype	Mild	Moderate	Severe	Dead 4hpf	Dead 24 hpf	Total (n)
GFAT1 MO	65	21	42	78	12	84	302
Wild Type	186	0	0	0	3	55	244
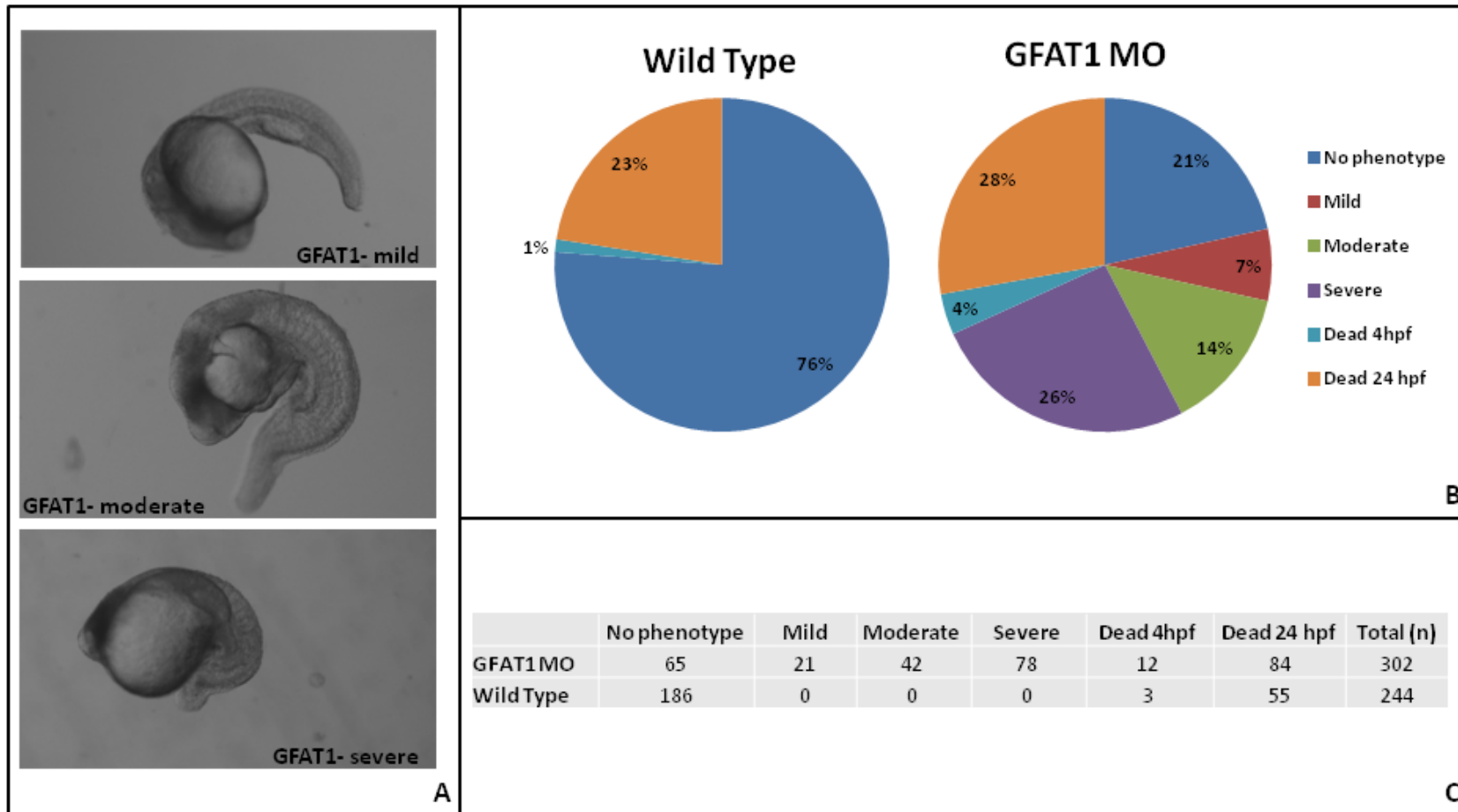
Figure 4.6: gfat1 1dpf phenotype
(A) Morphological phenotypes assessed with the muscle criteria in Table 2.2, staged using Kimmel criteria and raised as described by Westerfield. **(B)** Graphical representation of phenotype spectrum of gfat1 morphants compared to wild type control. **(C)** Table of phenotype range data of gfat1 morphants.

To determine structural changes in muscle at 1 dpf, fish were stained with phalloidin used to detect F-actin. Phalloidin is a toxin derived from *Amanita phalloides* and conjugated with a flurophore. In control fish the fibres between the vertical myosepta were straight and filled most of the myotome trunk. In mild fukutin, FKRP and dystroglycan morphant embryos muscle fibres connected with the vertical myosepta but were less linear than controls between myosepta. In the mild morphants the muscle fibres were more spaced out and thinner than in controls, while the vertical myosepta maintained their classic chevron shape. With increasing morphant severity the fibres became more distorted. In the most severe phenotypes the myosepta lost their chevron appearance and became more rounded similar to the observations reported earlier on brightfield and TEM (Figure 4.1 &Figure 3.13).
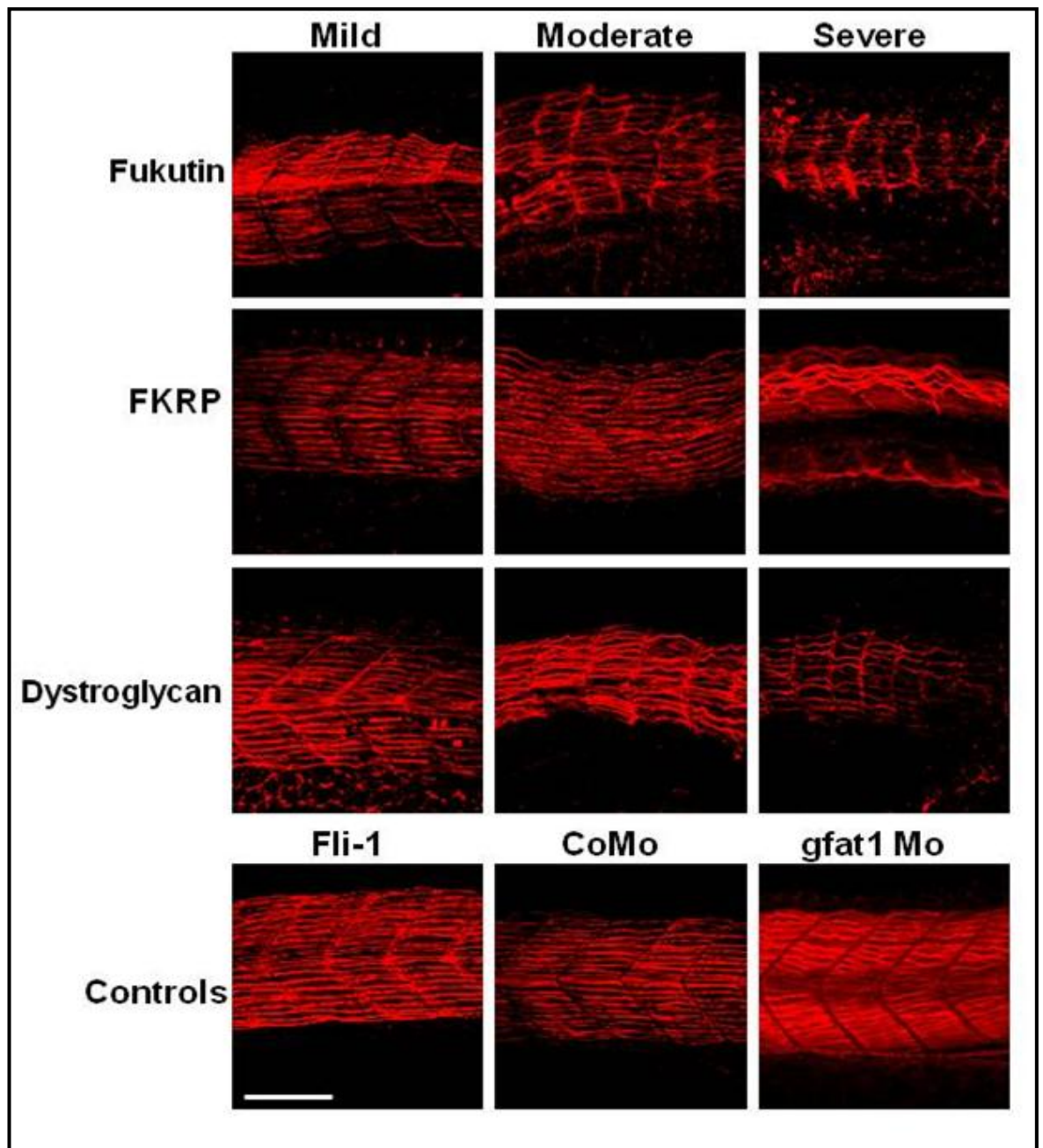
Figure 4.7: Muscle fibre F-actin staining with phalloidin
Projections from confocal microscopy through the myotome trunk of 1dpf embryos. White scale bar represents 100μm. Panels from top to bottom: embryos injected with fukutin MO, fkrp MO, dystroglycan MO. The embryos have been selected as mild, moderate or severe phenotype (from left to right). The bottom panel shows control embryos: uninjected fli-1 control, embryo injected with control MO, and embryo injected with the gfat1 MO.

4.2.4 Disrupted Sarcolemma and Myosepta in Morphant Embryos

The sarcolemma is the thin excitable membrane that encapsulates the

contractile components of striated muscle. The ECM of the sarcolemma fuses

at the ends of fibres to form tendons in humans or myosepta in fish. Disruption

to either component might be the aetiological cause of the muscle pathology in FKRP and fukutin deficient fish.

At lower magnifications in transverse sections from wild type fish the muscle fibres have a dense coverage of the myotome, running a linear course between vertical myosepta within the myotome trunk. The morphant embryos were all chosen from the moderate phenotype category and a minimum of three fish were imaged for each MO. In all the morphants there is lower muscle fibre density, similar to the longitudinal sections. In the space in which fibres would normally occupy there is amorphous material and additional adipose tissue distinguished by its globular appearance in the micrographs. Overall at lower magnifications the fukutin morphants appear to have the most severe phenotype.

Myofibrils run longitudinally in the myotome attaching to the vertical myosepta which allows transmission of force to run along the fish body. Consequently, the vertical myosepta will most likely have the greatest transmission of force as compared to the horizontal myosepta. The morphants were all chosen from the moderate phenotype category and a minimum of three fish were imaged for each MO. The vertical myosepta seen at low magnifications in control fish are straight and dark in appearance with occasional small processes. At higher magnifications the insertion of the myofibrils into the vertical myoseptum can be seen. The vertical myoseptum at lower magnifications in the morphants appears deviated from the typical chevron appearance with lower muscle fibre density surrounding it on either side. At higher magnifications the myofibrils appear to be detached from the myoseptum. The myoseptum in all morphants remains intact albeit more disorganised *i.e.* enlarged with irregular borders when compared to the control injected and wild type fish myoseptum. Finally, the myosepta in the morphants are not as dark suggesting that they may be thinner than in the controls (Figure 4.8).
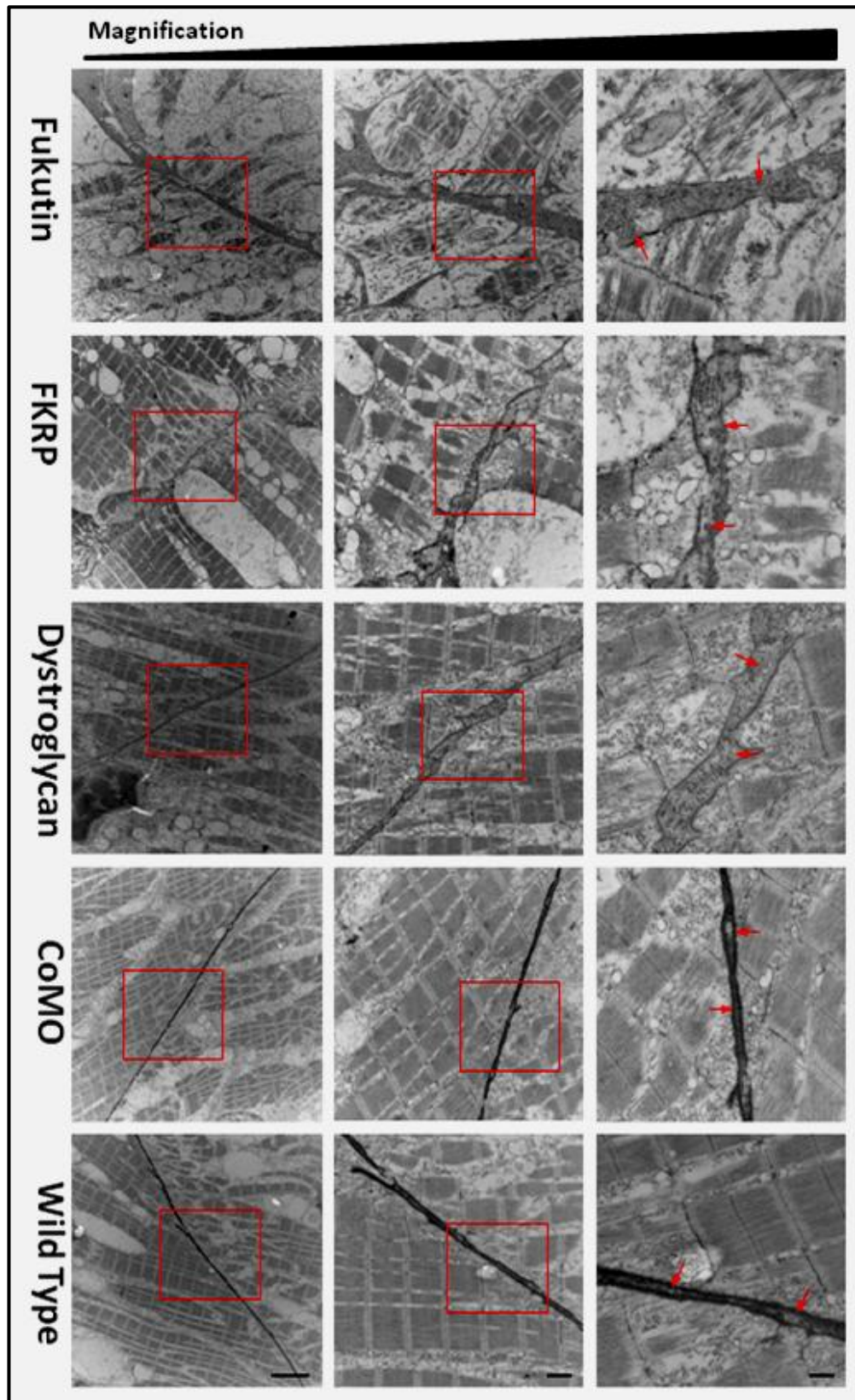
Figure 4.8: TEM of longitudinal sections from 3dpf embryos showing muscle fibre attachment to vertical myosepta

Lowest magnification is on the left, highest on the right, Scale bars: 4µm, 1µm, 500nm respectively. Red square shows area of magnification. Note at lowest magnification there are some creases visible on section a normal feature of TEM at low magnifications. Panels from top to bottom: larvae injected with fukutin MO, fkrp MO, dystroglycan MO, Control MO and non-injected larvae. Vertical myoseptum: red arrow.

4.2.5 Notochord Abnormalities in Morphants

The notochord is an essential structure for producing diffusible factors that act as molecular cues for muscle development in zebrafish (Stemple, 2005). These cues control muscle specification and guide angiogenesis in the developing embryo. Here, the notochord in particular the sheath or peri-notochord has been studied at TEM level. The peri-notochord is divided into three membranes (Figure 4.9), the outer, medial and inner basement membrane, with the medial being the largest of the three layers. The wild type notochord at low magnifications is a regular round structure. The FKRP and fukutin morphant notochords are oval in shape. The dystroglycan morphant notochord are differs from the other morphants because of the several significant irregularities in shape. The shape changes in the dystroglycan morphants are most likely due to kinks in the notochord that are observed at higher magnifications. The morphants have noticeably larger vacuoles on the basement membranes when compared to controls, perhaps suggesting an up regulation of degradation processes. At higher magnifications the three layers of the peri-notochord are all visible in the controls. All three layers are disrupted in the FKRP, fukutin and dystroglycan morphants with the most noticeable change being to the medial layer of the notochord. The medial layer of the controls is made up of tight concentric circles whereas in the morphants the medial layer is distorted with few intact concentric circles visible.
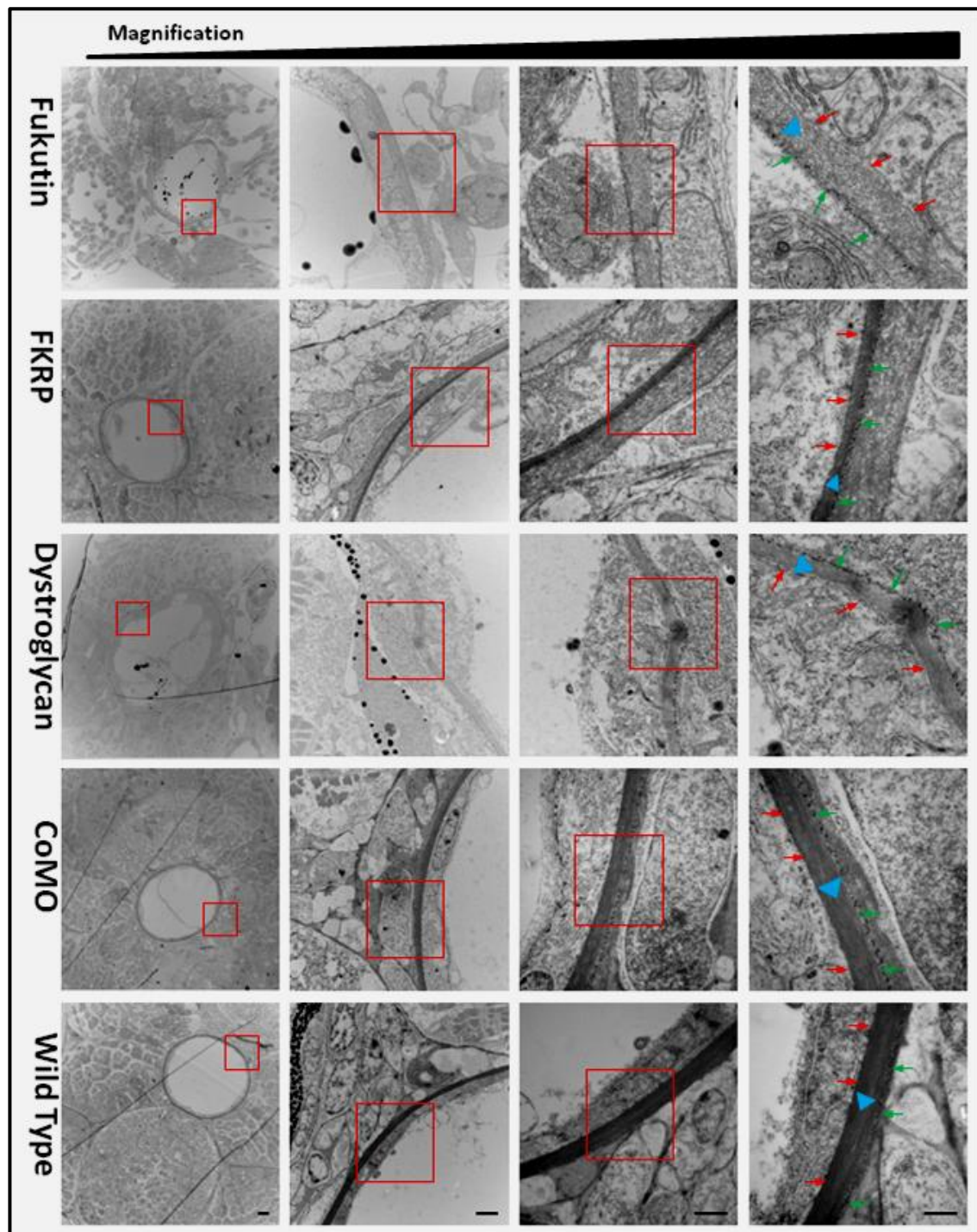
Figure 4.9: TEM of 3dpf notochord
Lowest-highest magnification left-right (transverse sections), scale Bars: 10μm, 2μm, 1μm & 500nm. Red square shows area of magnification. Panels from top to bottom: larvae injected with fukutin MO, fkrp MO, dystroglycan MO, CoMO and non-injected larvae. Peri-notochord basement membrane: red arrow, medial layer peri-notochord: blue arrow and outer layer peri-notochord green arrow.

4.2.6 Abnormal somitic vasculature in fukutin, FKRP and dystroglycan morphants

Zebrafish such as *floating head* and *no tail* have no notochord (Odenthal *et al.*, 1996) and fail to develop axial vasculature (Sumoy *et al.*, 1997). These models are thought to lack signalling cues such as vascular endothelial growth regulator that arise from the notochord (Fouquet *et al.*, 1997). Thus a potential consequence of loss of notochord structure might be abnormalities in vascular development. Fli-1 embryos were imaged using a confocal microscope to capture images of the vasculature through the myotome trunk. During the pharyngeal phase the segmental arteries of zebrafish embryos arise from the dorsal aorta, following the course of the vertical myosepta (Figure 1.7), eventually connecting with the dorsal longitudinal anastomotic vessel at 24-26 hpf (Childs *et al.*, 2002). At this developmental stage the segmental vessels of control embryos spanned from the dorsal aorta to the dorsal longitudinal anastomotic vessel in almost all cases (Figure 4.10).

In fukutin, fkrp and dystroglycan knockdowns with a mild phenotype, intersegmental vessels were unsuccessful in reaching the dorsal longitudinal anastomotic vessel pectorally at 24 hpf, (Figure 4.10A). In some instances the intersegmental vessels of the fkrp morphants branched at the tops of the segmental arteries from the midline upwards. With increasing phenotypic severity of the fukutin (10%) and FKRP (40%) morphants the intersegmental vessels were found to be missing with greater frequency (Figure 4.11). The intersegmental vessels of moderate to severe fukutin morphants were more disorganised with increasing severity of the phenotypes (Figure 4.10). The dorsal aorta in most cases was the only distinguishable vessel in the vasculature of the severe fukutin, fkrp and dystroglycan morphants within the myotome trunk region. There were several instances, where segmental artery branching occurred below the midline in the morphants with severe phenotypes. In two fukutin and one dystroglycan knockdown embryos with moderate phenotypes the vessels joined together via anastomoses in the embryo mid-line (Figure 4.10B). Despite having a bended body phenotype the vasculature in the GFAT1 morphant fish could not be distinguished from control, indicating that vascular changes were a primary pathological change.

A

Mild | Moderate | Severe

Fukutin

FKRP

Dystroglycan

Fli-1 | Co Mo | gfat1 Mo

Controls

SV
DLAV
DA
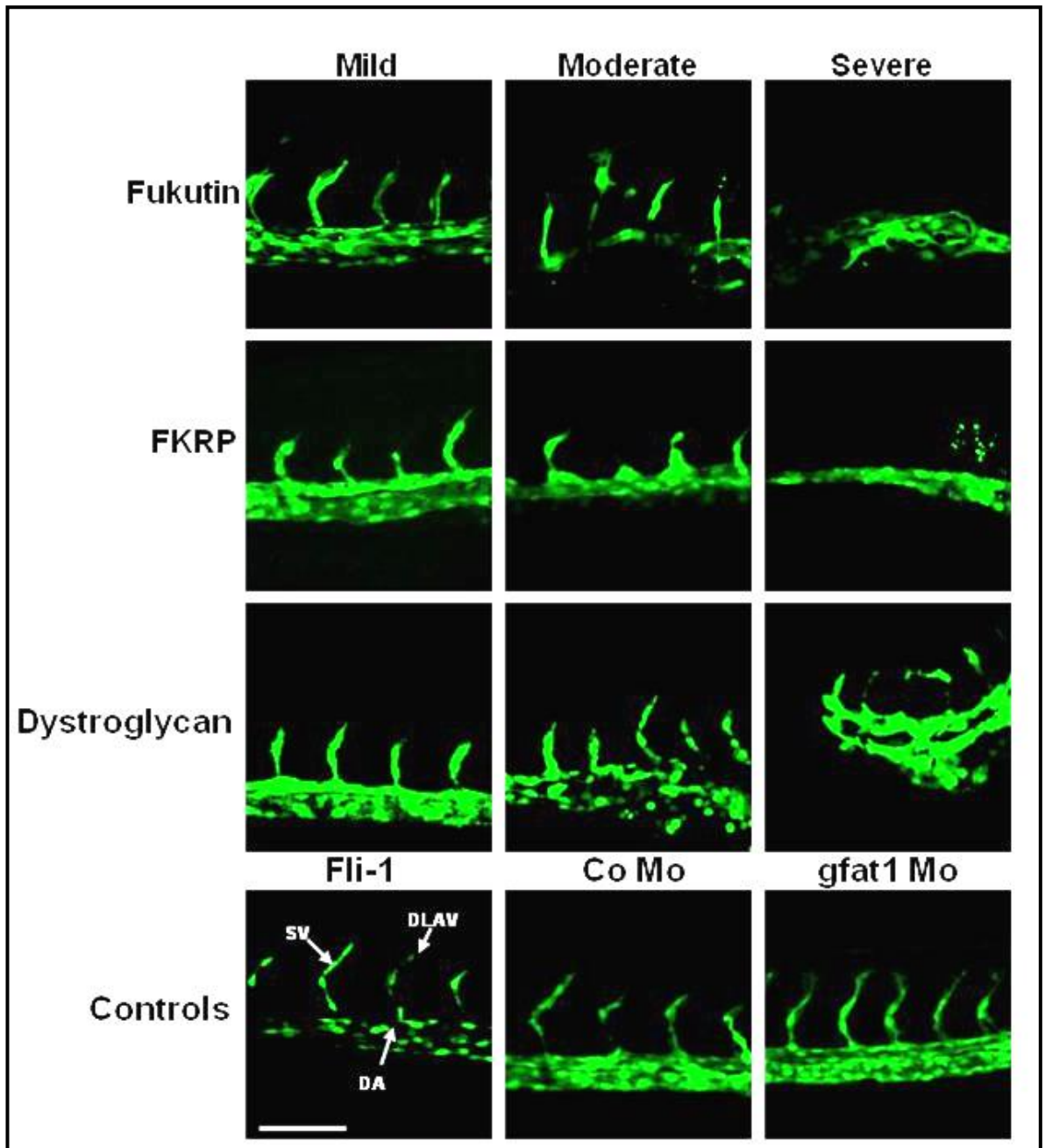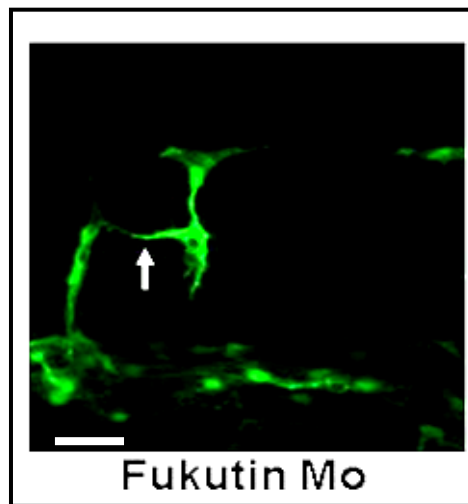
Fukutin Mo

B

Figure 4.10: Somite vasculature of 1dpf embryos detected as EGFP fluorescence in the fli-1 strain using confocal microscopy

A: The fkrp, fukutin and dystroglycan injected embryos were staged according to phenotype at 1dpf. Intersegmental vessels project from the dorsal aorta (bottom horizontal vessel) towards the dorsal longitudinal vessel at the top. White scale bar represents 100µm, SV: segmental vessel, DA: dorsal Aorta, DLAV: dorsal longitudinal anastomotic vessel. **B:** Intersegmental vessels joining in the midline of fukutin morphants: white arrow, white scale bar represents 50µm.

The vertical height of the segmental vessels above the dorsal aorta was measured and expressed as a proportion of body height and expressed as a percentage from a minimum of three independent injections for each MO. Five embryos and four intersegmental vessel heights from each injection were measured for each phenotype (Figure 4.11). All morphants segmental vessel heights were significantly smaller (P= $<1\times10^{-4}$) than observed in the controls(Tukey analysis of the one-way ANOVA). In each of the morphants phenotypic severity category there was a progressive reduction in size of segmental vessel with increasing phenotype severity. Blood vessels in the fkrp, fukutin and dystroglycan morphants were not significantly different in height across the mild phenotype category. While blood vessels in the dystroglycan morphants were significantly larger than in fkrp morphants and fukutin when moderate and severe phenotype are compared respectively, using one way ANOVA Tukey analysis.
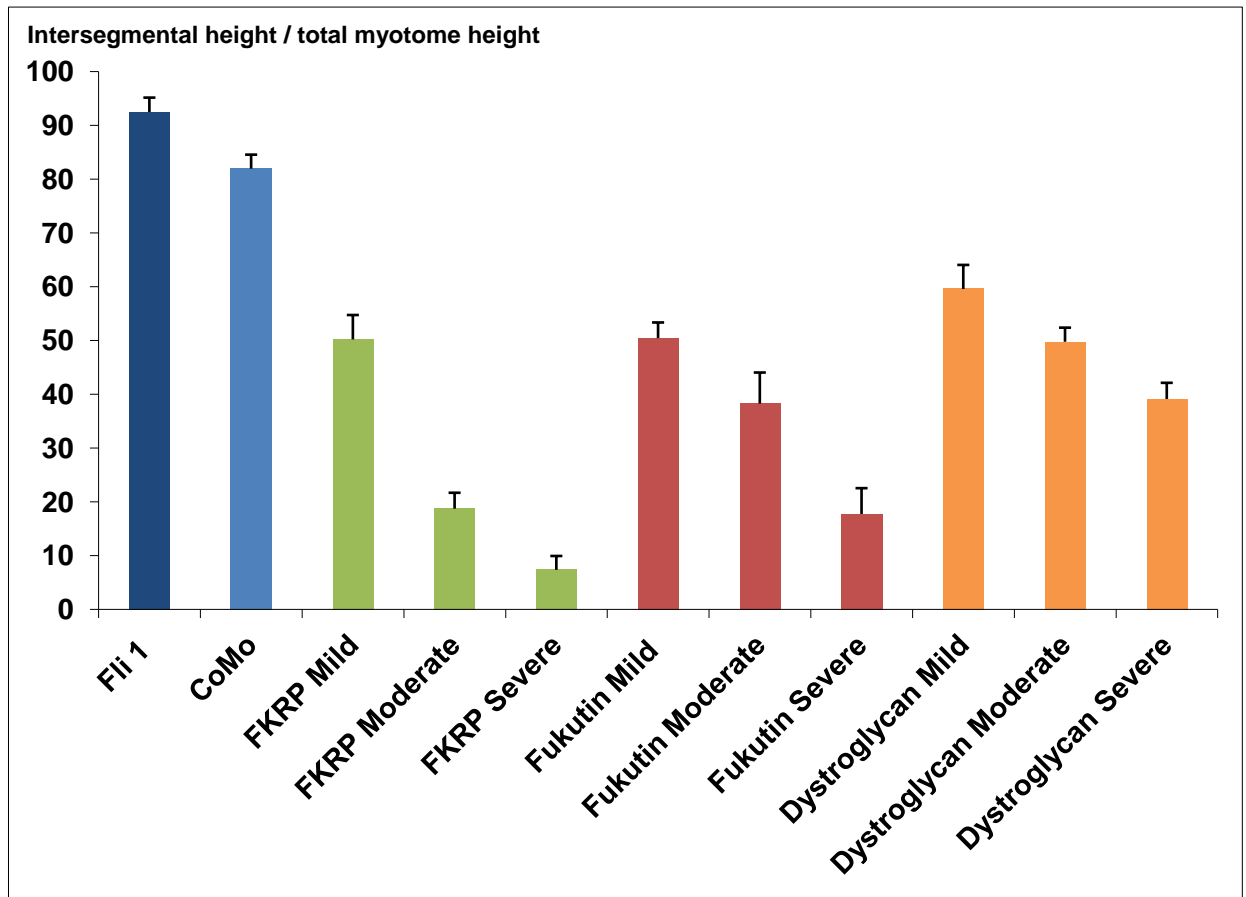
	N	Mean	Grouping		
Fli-1	20	92.48	A		
CoMo	20	81.96	A		
Dyst Mild	20	59.60	B		
Fukutin Mild	20	50.45	B	C	
FKRP Mild	20	50.20	B	C	
Dyst Mod	20	49.78	B	C	
Dyst Severe	20	39.13		C	
Fukutin Mod	20	38.28		C	
Fukutin Severe	18	19.72			D
FKRP Mod	20	18.75			D
FKRP Severe	12	12.27			D

Figure 4.11: Intersegmental blood vessel length
Measured from the dorsal aorta relative to body height at 1dpf. Graph bars represent 95% confidence interval, y-axis is a percentage of body height. The fkrp, fukutin and dystroglycan injected embryos were staged according to criteria specified in Table 2.2. One-way ANOVA with Tukey analysis is displayed in the table below the graphical representation of the data. Tukey analysis was based on the assumption the data was approximately evenly distributed and allowed variability to be assessed across morphant phenotype groups. Means that do not share a grouping are significantly different. The analysis allowed fli- and control MO to be grouped together and distinguished them from fkrp, fukutin and dystroglycan morphants, confirming that the morphants were all significantly smaller than control MO injected embryos. The analysis also shows no single morphant MO injection spectrum *i.e.* mild,

moderate severe, was significantly different from another, and while the mild and moderate categories showed substantial overlap, both were distinct from the severe category.

4.3 Discussion

Based on previous studies (Parsons *et al.*, 2002a; Thornhill *et al.*, 2008; Ackroyd *et al.*, 2009) loss of muscle integrity was hypothesised to be the key pathological cause responsible for the bent body phenotype observed in the fkrp and fukutin morphants. Muscle was therefore investigated at the structural level in order to assess this hypothesis as an aetiological cause of the bent body phenotype. As expected, morphant muscle was disrupted with detached myofibres in fkrp, fukutin and dystroglycan morphants. F-actin staining confirmed the loss of myofibres, which were sparse and deformed in the morphant embryos. Ultrastructural analysis revealed that fkrp, fukutin and dystroglycan morphants all have torn sarcomeres and loss of vertical myoseptum structure.

4.3.1 Muscle

Knock down of fukutin and fkrp using MOs was successful in reducing the levels of glycosylated α-dystroglycan in the morphants as shown by IIH6 immunostaining. A weak laminin-dystroglycan interaction may be the critical deficiency in the destabilisation of the sarcolemma, accounting for the muscle pathology of the morphants (Lin *et al.*, 2011). Work carried out previously reported the importance of correctly glycosylated α-dystroglycan for maintaining sarcolemmal stability (Reed *et al.*, 2004; Thornhill *et al.*, 2008; Lin *et al.*, 2011). Surprisingly, there was a detected concurrent reduction of β-dystroglycan immunostaining in the fkrp and fukutin morphants. The observation is in contradiction to data formerly published by (Kawahara *et al.*, 2010), but in accordance with observations in mouse models of dystroglycanopathy indicate that the structural defects caused by deficient glycosylation of α-dystroglycan may lead to misplacement of β-dystroglycan (Michele *et al.*, 2002).

Laminin was investigated as the binding partner of α-dystroglycan. However, no reduction in pan-laminin staining in the fkrp and fukutin morphants was observed. This finding is in contradiction to a previous study (Lin *et al.*, 2011), that observed a small reduction in laminin staining in fkrp and fukutin knockdowns, and in a dystroglycan mutant line. The discrepancies between results may be attributable to the sensitivity of the assay or to minor residual expression of fkrp and fukutin in the morphants analysed. The possibility of an

integrin-α7 laminin compensatory mechanism should also not be overlooked, considering the mechanism has been reported in dystroglycanopathy mice models previously (Mayer *et al.*, 1997; Sztal *et al.*, 2012).

Since no disturbances to the sarcomere could be found in the morphants beyond torn fibres, the perturbations in the sarcolemma and vertical myosepta, observed on ultrastructural examination were considered to be the basis of primary muscle pathology. The dystroglycanopathy morphant fibre damage can be attributed to loss of integrity of both the sarcolemma and vertical myosepta (Thornhill *et al.*, 2008). The *laminin-α2 & β2* mutant zebrafish *candyfloss* & *softy* mutant lines have irregular vertical myosepta borders and a similar torn sarcomere phenotype to our morphants (Hall *et al.*, 2007; Jacoby *et al.*, 2009). The mutants *bashful (*laminin-*α1)*, *grumpy* (laminin-*β1)* and *sleepy* (laminin-*γ1)* were not found to have the same muscle basement membrane pathology indicating the dystroglycan laminin-211 interaction is specific for muscle pathology (Parsons *et al.*, 2002b; Pollard *et al.*, 2006). Loss of the α-dystroglycan laminin-211, interaction may therefore be the key change responsible for the loss of the sarcolemmal interaction with the vertical myosepta in the morphants. The loss of strength in the interaction between sarcolemma and vertical myosepta results in the muscle fibre becoming susceptible to shear stress on contraction thus becoming torn. Hence tears to the sarcomere could be considered as secondary to sarcolemmal and vertical myoseptal instability.

4.3.2 Notochord

The disruption in all three layers of the tri-laminar notochord was found in fkrp, fukutin and dystroglycan morphants. Interestingly the mutants *bashful*, *grumpy* and *sleepy* all have been shown to have similar basement membrane abnormalities (Parsons *et al.*, 2002b; Pollard *et al.*, 2006). This leads to the hypothesis that it is the loss α-dystroglycan laminin-111 interaction at the notochord that is responsible for mis-localisation of the laminin-111 chains with a consequential loss of notochord basement membrane stability. Loss of notochord basement structure may prevent correct axial signalling and thereby interfere with myotome development or vascular patterning in developing zebrafish. It is also possible that loss of notochord mechanical strength is due to the perturbations in the basement membrane in the morphants, potentially

providing a mechanism for the bended body and poor locomotive function phenotypes discussed in the previous chapter (Odenthal *et al.*, 1996; Stemple *et al.*, 1996; Stemple, 2005).

4.3.3 Conclusions

Perturbations in the sarcolemma and vertical myosepta due to loss of the laminin-211 α-dystroglycan interaction is argued to be the key pathology responsible for sarcomeric tearing in the morphants (Thornhill *et al.*, 2008). The angiogenic phenotype is therefore thought to be a secondary consequence of ECM disorganisation rather than the primary cause of the muscle pathology associated with knock down of fukutin, fkrp or dystroglycan. The hypothesis is supported by previous studies (Pollard *et al.*, 2006) that suggest correct localisation of the laminin-α1 chains is essential for blood vessel and notochord development. Interestingly mutant zebrafish that don't develop notochords such as *floating head* and *no tail* fail to develop a dorsal aorta and therefore intersegmental vessel sprouting will not occur (Fouquet *et al.*, 1997). It can be postulated that lack of guidance cues as a result of perturbations in notochord may be failing to induce intersegmental vessel sprouting. When combined with rounded disorganised vertical myosepta structure intersegmental vessels fail to correctly navigate through the myotome. Therefore notochord basement membrane instability may at least in part be responsible for the bended body element of the morphant zebrafish phenotype. Whether the bended body phenotype is due to the muscle fibre tearing as a component of the pathology is yet to be confirmed.

Chapter 5   Perturbations of the Basement Membranes in the Eye of fkrp and fukutin Deficient Zebrafish

5.1 Introduction

Micropthalmia with clearly abnormal eye morphology was previously found in fkrp, fukutin and dystroglycan deficient zebrafish, see chapter 3. In this chapter the eye pathology is investigated further, to gain a better understanding of the aetiological cause of the eye abnormalities associated with fkrp and fukutin deficiency. Disruption to retinal layering was previously found in Fkrp deficient mice (Ackroyd *et al.*, 2009) and zebrafish (Thornhill *et al.*, 2008). Based on the presence of analogous structures within the human and zebrafish eye, the pathological phenotypes associated with dystroglycanopathy in both are predicted to be comparable (Hino *et al.*, 2001; Bourteel *et al.*, 2009). The eye retinal layering abnormalities in fkrp and fukutin deficiency in both systems are hypothesised to be a secondary consequence that results from disruption to basement membranes within the eye. This hypothesis is based on abnormal basement membranes found in the muscle and notochord of morphant zebrafish as discussed in the previous chapter. Angiogenesis in morphant myotome was found to be delayed, also discussed in chapter 4. Loss of vascular structure in the developing zebrafish of eye will therefore also be investigated in the fli-1 fish.

5.1.1 Aims

- To study retinal layering in 3dpf morphant larvae using histological techniques.
- Establish the most suitable time point for investigation of basement membrane pathology using TEM.
- Investigate any perturbations in basement membranes of fkrp, fukutin and dystroglycan morphant fish and characterise these at the ultrastructural level.
- Investigate abnormalities in vasculogenesis of the eye as a possible consequence of fkrp, fukutin or dystroglycan deficiency.

5.2 Results

5.2.1 Retinal Neuronal Layering and Basement Membranes are not present at 1dpf

In order to define a suitable time point for investigation of the basement membrane formation in zebrafish eyes, transverse sections of 1 dpf embryo eyes through the lens were prepared and viewed using TEM. Three eyes from 1dpf AB wild type embryos were sectioned and imaged (Figure 5.1). Neither the ILM nor ELM could be identified in the sections (Figure 5.1). The 1dpf time point was also too early to identify retinal layering, consistent with other studies (Soules and Link, 2005). The lens cells and the retinal cells could also not be distinguished from each other (Figure 5.1). The round lens structure was found anterior and ectopic to the retina. Retinal pigmented epithelium (RPE) granules could be found in low numbers at the back of the eye. No small blood vessels or erythrocytes could be identified in the eyes at 1dpf. The lack of retinal layering and ectopic lens at 1dpf, lead to further investigation of the eye being carried out at the later time point of 3dpf.
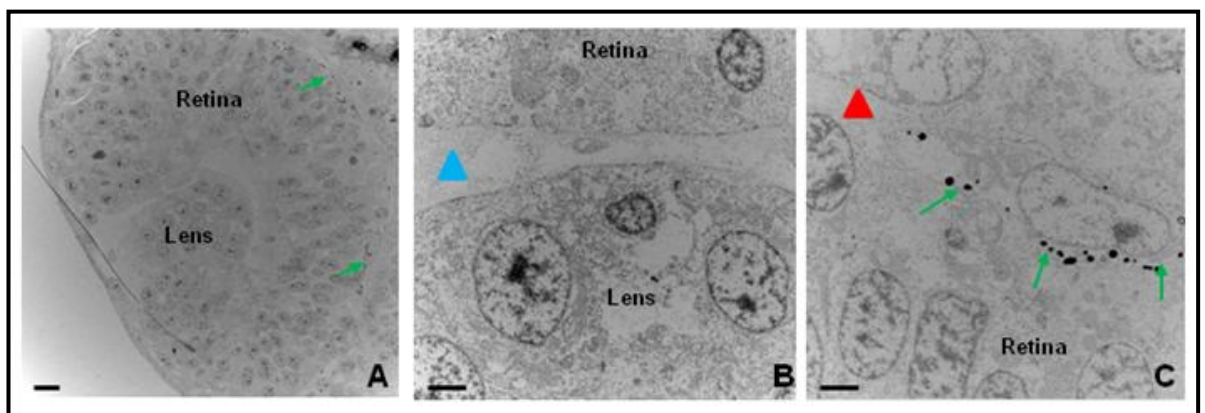
Figure 5.1: TEM micrograph in 1dpf zebrafish embryo eye.
A: Overview of eye. Note cell types are poorly differentiated in lens and retina and no retinal layering is identifiable, scale bar: 10µm. **B:** High magnification image between lens and retina, blue triangle indicates a gap between lens and retina. **C:** Posterior eye red triangle points to choroid. **B-C:** scale bar: 2µm, green arrows in **A&C** RPE.

5.2.2 Histological Assessment of the Morphant Eye Phenotype

To assess overall structure of the developing zebrafish eye transverse sections were cut through the centre of the eye in 3dpf larvae and stained with toluidine blue (Figure 5.2). Wild type and control MO injected larvae eyes were spherical in shape, with a round lens approximately one quarter of the size of total eye,

positioned anterior to the retina. The eyes were abnormal in shape in all the fkrp, fukutin and dystroglycan morphants in the moderate severity group. Dystroglycanopathy morphants and control fish lenses were comparable in shape and size. The fkrp and fukutin morphants were judged to have microphthalmia consistent with findings in chapter 3 (Figure 3.17). The fukutin and dystroglycan morphants had lenses which were ectopic *i.e.* detached from the ganglion cell layer. The finding was not recapitulated in any of the six morphant fish with a moderate fkrp phenotype, indicating that the lens attachment may be a point of divergence in the phenotypic presentation of fkrp and the other dystroglycanopathy morphants. In studies investigating wild type embryos the lens is detached up to approximately 2dpf (Dahm *et al.*, 2007), suggesting either developmental delay in the morphant eye development or disruption to lens adhesion. In wild type and control MO injected eyes there was organised retinal layering ganglion cell layer (GCL), inner plexiform layer (IPL), inner nuclear layer (INL) and the photoreceptor layer (PR) could all be identified, (Figure 5.2). Retinal layering in all morphants was disorganised (Figure 5.2), with a notably reduced retinal pigmented epithelium layer (RPE) at the back of the eye. The GCL could not be distinguished from IPL or IPL from the INL in the morphant fish. Overall the pathology was consistently most severe in the fukutin morphants.
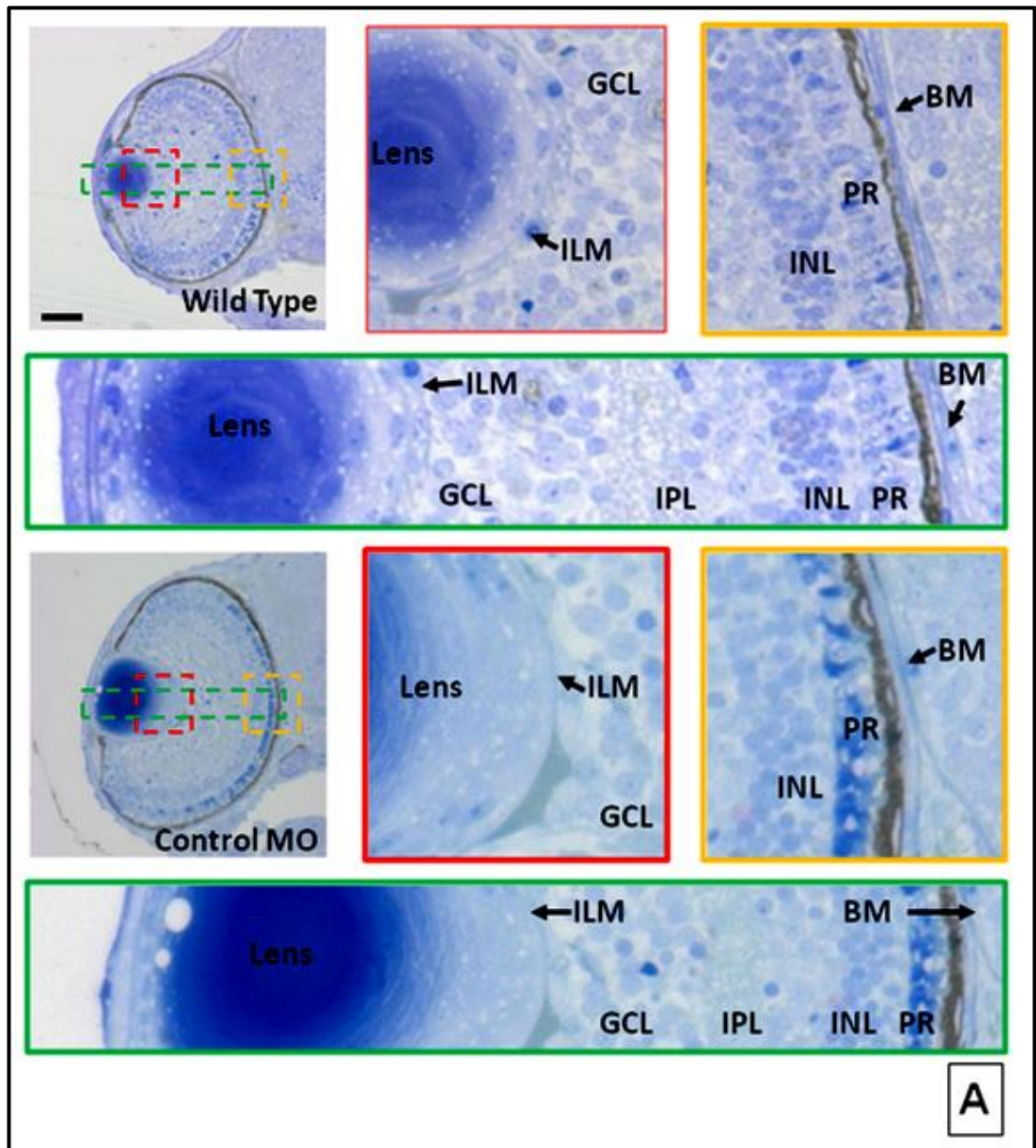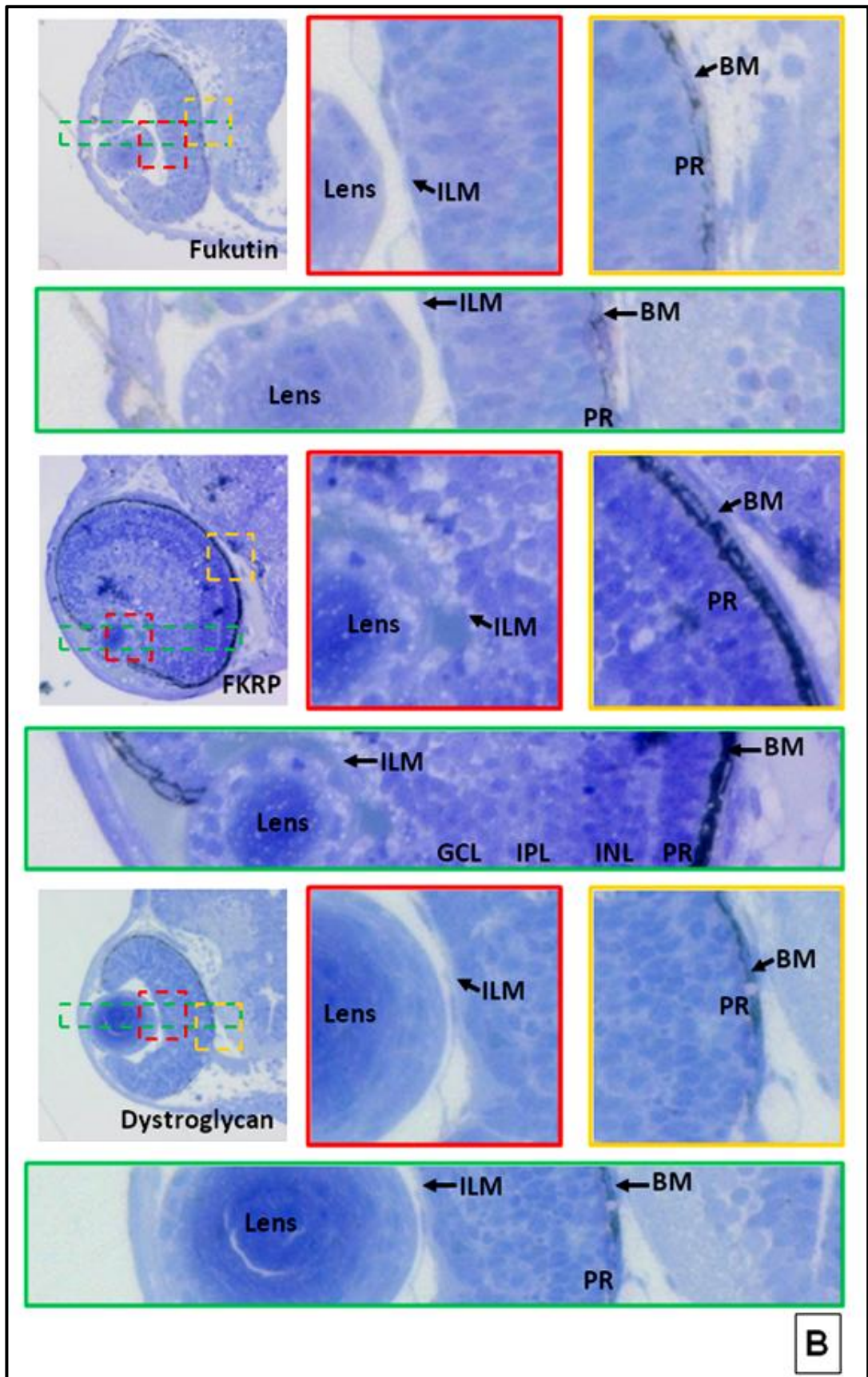
Figure 5.2: Transverse sections of the eye at 3dpf, stained with toluidine blue

Toluidine blue stain of sections allows retinal layers to be visualised and basic retinal cell morphology to be examined. Basement membranes are visble however little can

be gained about structure at low magnification (40x). Also visible is the lens and the retinal pigmented epithelium. ILM: inner limiting membrane, GCL: Ganglion Cell Layer, IPL: inner plexiform layer, INL: inner nuclear layer, PR: Photo Receptor Layer, BM: Bruch's membrane, scale bar: 20μm.

5.2.3 Immunohistochemistry of 3dpf Eye

Immunohistochemistry aided in the determination of whether there is disruption to the DGC and ECM proteins in any of the basement membranes in 3dpf dystroglycanopathy morphant zebrafish eyes. A cryosection approach was adopted to resolve the precise location of many of the proteins of interest more effectively than in wholemount studies. A minimum of three fish for each data point were transversely sectioned at the level of the mid lens. Morphants were all judged to have a moderate phenotype as described in Table 2.2.

The localisation of β-dystroglycan was used to determine whether there was any indication that there might be a mislocalisation of the DGC in the dystroglycanopathy morphant fish. β-Dystroglycan staining was strongest at the ILM, with a weaker signal strength at Bruch's membrane in the wild type fish (Figure 5.3). Specific immunofluorescence was also detected in the retinal layers in wild type fish. The fukutin morphant fish had increased intensity of staining for β-dystroglycan at the ILM and Bruch's membrane when compared to controls, a finding not observed in the fkrp morphants. As expected no specific staining was observed in the dystroglycan morphant larvae eye.

IIH6 was used to detect changes in the levels of glycosylated dystroglycan. In wild type fish IIH6 bound to the same structures as 43DAG indicating that IIH6 is unlikely to be detecting entirely unknown proteins with similar glyco-epitoptes unless the protein has an identical distribution pattern to dystroglycan in the eye. In addition to the ILM and Bruch's membrane, strong IIH6 staining was observed in two examples on the optic nerve of the wild type controls. Low IIH6 signal strength was detected in the fukutin and dystroglycan morphants at the ILM. Punctate IIH6 staining was observed in the fkrp morphant fish at the eye basement membranes.

Laminin acts as the key ligand for dystroglycan in muscle, stabilising the sarcolemma by connecting it to the ECM. A similar interaction may also be important in the eye, anchoring axons and cells to the three basement membranes. Laminin in the wild type fish was detected with equal signal

strength at the ILM and Bruch's membrane with some signal in retinal layers. The lowest signal levels were detected in the wild type embryos, while the dystroglycan morphant had the highest signal levels, perhaps suggesting laminin overexpression might be a compensatory mechanism for loss of dystroglycan in the basement membranes of the eye.

	Wild Type	Fukutin	FKRP	Dystroglycan
43 DAG				
IIH6				
Pan Laminin				
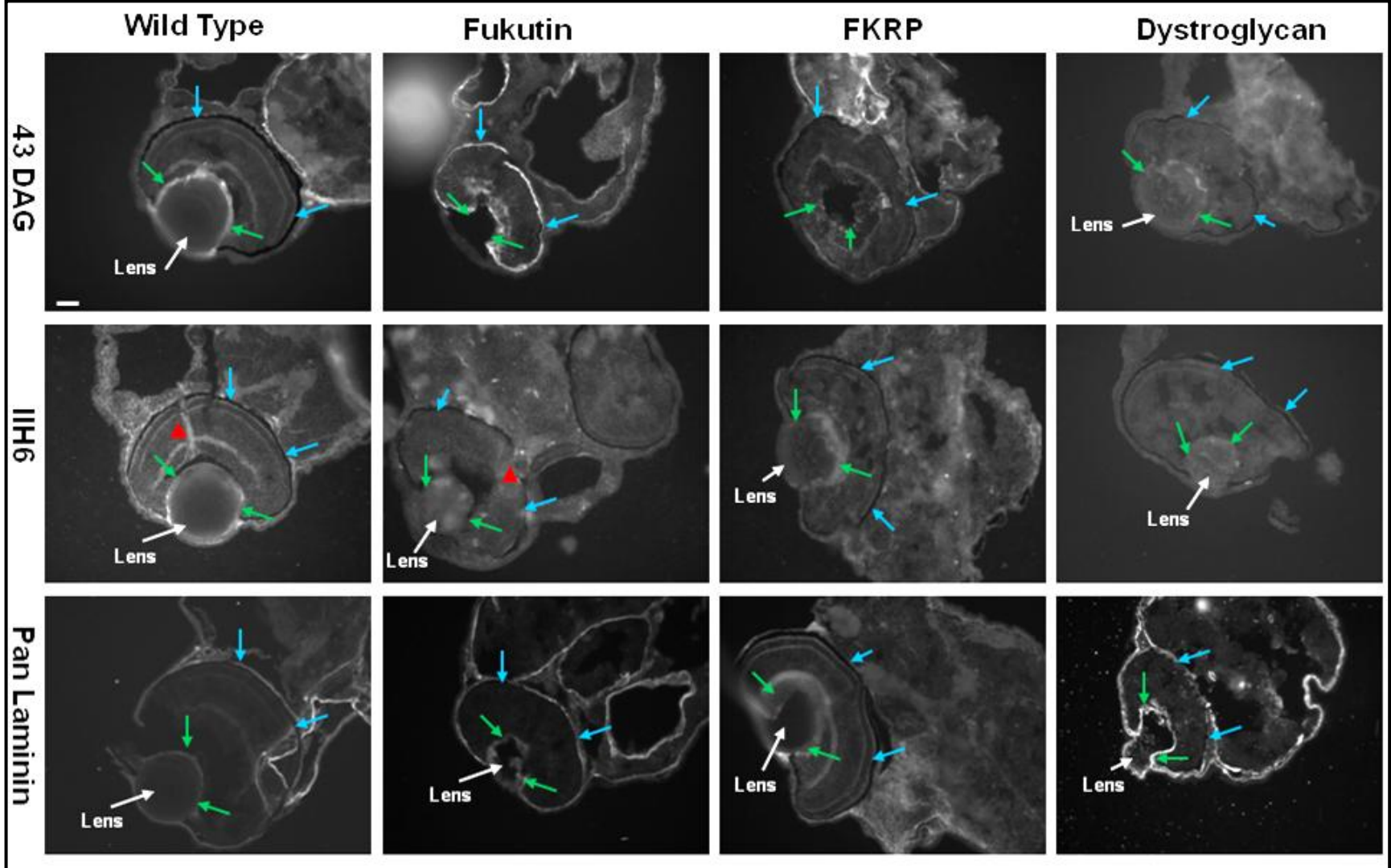
Figure 5.3: Immunostaining of cryosectioned 3dpf larval eyes
3dpf embryos were fixed and embedded in OCT, tranverse sections were cut through the eye, sections through the lens were then stained with 43DAG (β-dystroglycan), IIH6 (glycosylated dystroglycan) or pan-laminin antibody. fkrp, fukutin and dystroglycan morphants were all judged to be in the moderate phenotype group as outlined in Table 2.2. Sections were stained with either 43DAG antibody for β-dystroglycan, IIH6 for the glycosylated dystroglycan *or* pan-laminin antibody that predominantly detects laminin-111. Green arrows: ILM, blue arrows: Bruch's membrane and red triangle: optic nerve, scale bar: 20µm.

5.2.4 Analysing the Ultrastructure of the Morphant Eye

TEM was used to investigate the ILM, ELM, RPE and Bruch's membrane at the ultrastructural level in 3dpf larvae. Large overviews of the eye were imaged to assess whether the features observed on histology were still present in the eye on TEM (Figure 5.4). Wild type and control MO injected fish had spherical eyes with a round shaped lens positioned towards the front of the eye. A minimum of six larvae from each phenotype category were investigated for each morphant phenotype in addition to the controls. The eye shape in the morphants became progressively less spherical with increasing severity of phenotype. Ectopic lenses were a consistent observation in fukutin and dystroglycan morphants across all severities of phenotype, a feature only found in the fkrp morphants with the most severe phenotype. Abnormal retinal layering was observed in all morphants with the exception of the fkrp mild larvae. In general, the TEM images show a similar range of defects as observed in the toluidine blue stained sections.
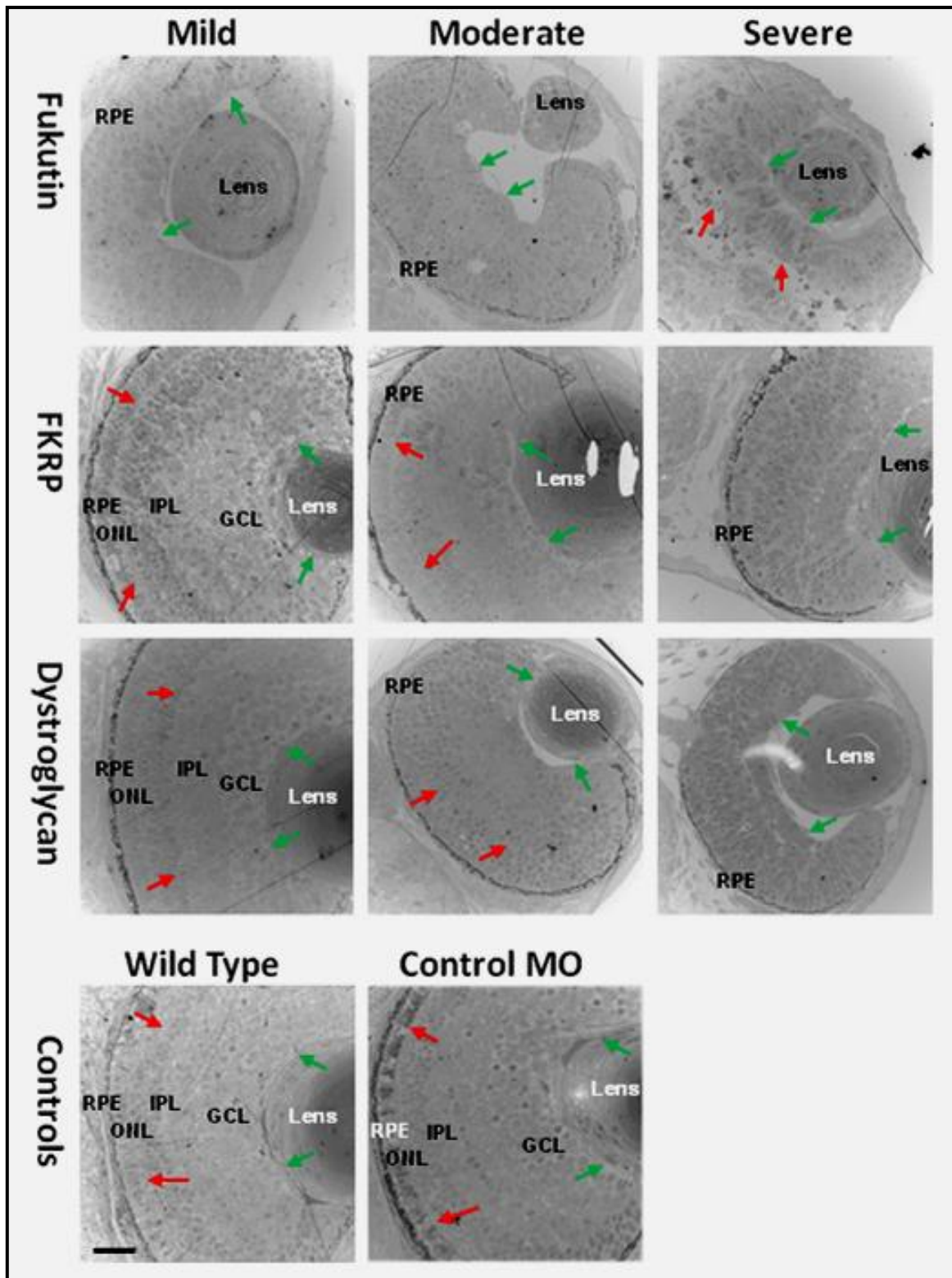
Figure 5.4: Transverse sections of the eye at 3dpf on TEM
Figure highlights similar features to Figure 5.2 including retinal layering, basement membranes, lens and retinal pigmented epithelium. Note particularly the lens dysplasia in dystroglycanopathy fish, a feature not seen in the controls. Green arrow: inner limiting membrane, GCL: Ganglion Cell Layer, IPL: inner plexiform layer, INL: inner nuclear layer, PR: photo receptor layer & red arrow: external limiting membrane. Scale bar: 20µm.

5.2.5 TEM Analysis of the ILM

To elucidate a potential mechanism leading to the ectopic lens phenotype in the fukutin and dystroglycan morphants, the ILM was investigated using high power TEM. The ILM provides a bond between the lens and the retina by connecting to the lens to the adjacent GCL. The ILM in its capacity as a basement membrane is also thought to have a role beyond structural integrity. The ILM can alter cell specification (Feitosa *et al.*, 2011), supports the avascular lens with multiple invaginations of small blood vessels (Gore *et al.*, 2012) and acts as an anchoring point for the end feet of Müller glia. The Müller glia have the important role of acting as support cells for the retinal ganglion cells (RGCs; Bringmann and Wiedemann, 2009).

The ILM is found between the GCL and lens in controls at 3dpf. The membrane is a continuous regular structure with a smooth surface and occasional invaginations of hyaloid vasculature (Figure 5.5). The small blood vessels of the ILM contain presumed blood cell progenitors circulating inside them. The blood vessels are crucial for supplying the lens with all the requirements for correct function, including delivery and removal of gases or debris. In fukutin and dystroglycan morphants the ILM is absent across all phenotype groups. The ILM is present in the fkrp morphant mild and moderate phenotypic groups but absent in the larvae with a severe phenotype. The membrane is diminished in the fkrp fish with mild and moderate phenotypes, appearing to have a rough surface on the GCL side. Interestingly, despite loss of the ILM in dystroglycan morphant fish with a mild phenotype and fkrp morphants with a severe phenotype, there are blood vessels present. The data suggests that despite a close physical association, blood vessel development does not depend directly on the ILM (Dahm *et al.*, 2007; Gore *et al.*, 2012).
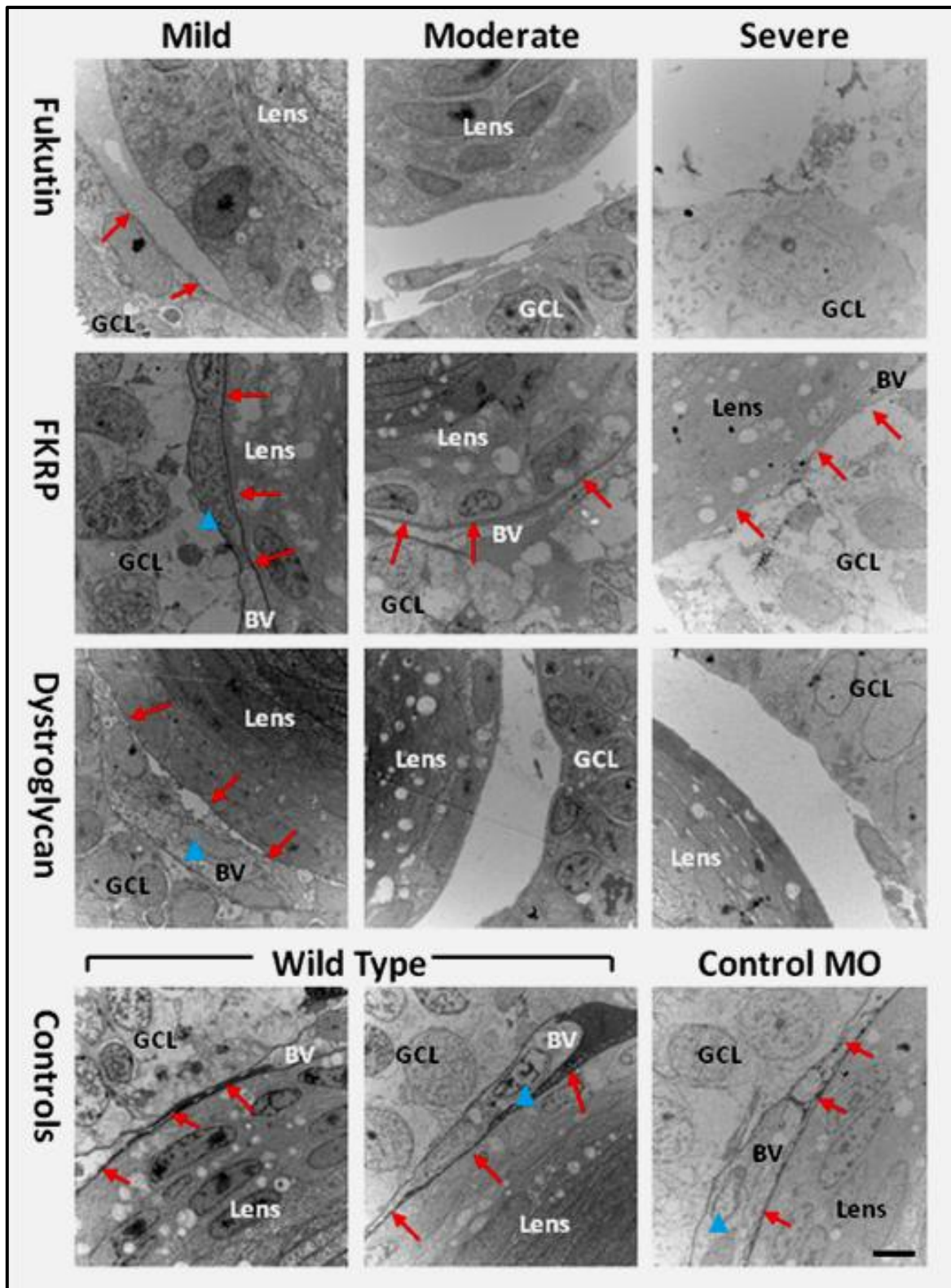
Figure 5.5: Transverse sections of the inner limiting membrane at 3dpf, TEM
Figure highlights both the ILM and the optic blood vessels that form the inner optic circle vessel that is found around the circumference of the lens. Red arrow: inner limiting membrane, Blue triangle: presumed premature erythrocyte, BV: blood vessel, GCL: ganglion cell layer, scale bar: 2µm.

5.2.6 Analysing the Ultrastructure of the ONL and ELM

The ELM was investigated because of its role in supporting the photoreceptors spanning the entirety of the posterior retina. The photoreceptors span from the outer nuclear layer (ONL) across the ELM to the INL in the control fish. The ELM in the wild type and control MO injected larvae appears as a thickening (darker layer) of the ECM that surrounds ONL cells (Figure 5.6). Unlike the Bruch's membrane and ILM the ELM is not as defined as a membrane, perhaps at 3dpf the membrane is still not fully established. The ELM is of consistent width with a rough surface on the INL side observed at the higher magnification in the wild type and control fish. A disrupted, irregular ELM was observed in dystroglycan and FKRP morphants with a mild phenotype. The ELM disruption and membrane surface irregularity increased with phenotype severity in the FKRP and dystroglycan morphants with a moderate phenotype. Fukutin morphants and dystroglycan morphants with a severe phenotype did not have a visible ELM at TEM level. ONL and INL were found to be poorly ordered in these groups surrounded by presumed oedematous infiltration. In general all morphants had poorly organised cell layering at the back of the retina.
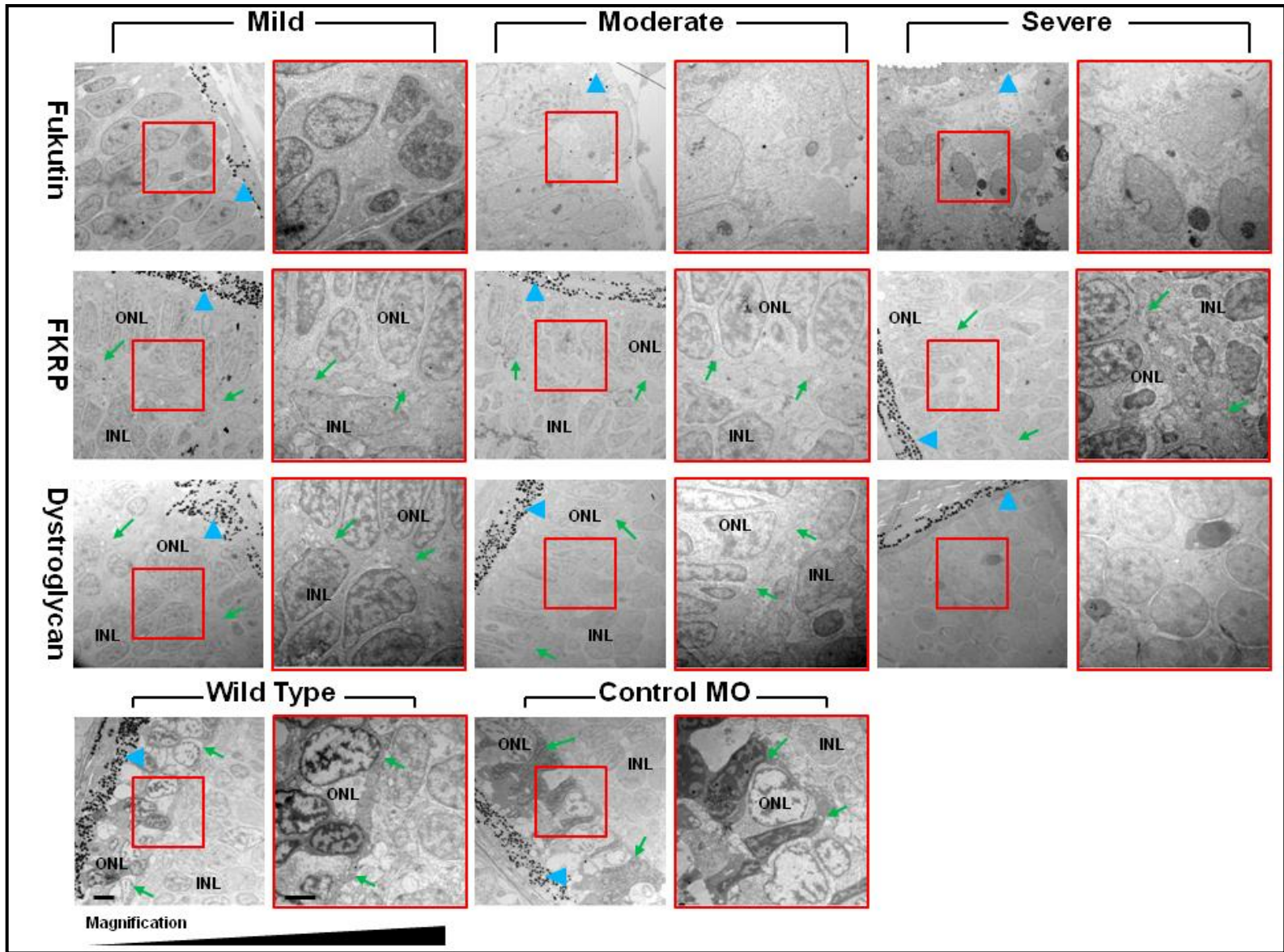
Figure 5.6: Perturbations in morphant external limiting membrane structure
TEM images from transverse sections of the eye from FKRP, fukutin, dystroglycan morphants, wild type and control injected 3 dpf larvae. No ELM was found in fukutin morphants of any phenotypic group. Blue triangle: retinal pigmented epithelial layer, green arrows: ELM, ONL: outer nuclear layer, INL: inner nuclear layer. Scale bars (bottom left panels) low magnification: 8µm, high magnification: 2µm. A minimum of five embryos for each phenotype were imaged at low and high magnifications.

5.2.7 Loss of Eye RPE in Morphants

The retinal pigmented epithelium (RPE) is attached to Bruch's basement membrane, situated between the choroid and the ELM. The main function of the RPE is to support the photoreceptors and provide cues that control the process of retinal layering. To assess the RPE in 3dpf larvae, seven fish from each phenotype group were imaged. Images were taken at three well spaced positions at the back of the retina avoiding the optic nerve or proximity to the lens. The RPE were imaged in a manner that centralised the RPE granules in the micrograph. RPE granules were counted in each micrograph and statistical analysis was carried out (Young *et al.*, 2006).

The wild type and control MO injected fish were found to have a dense concentration of RPE granules, between the choroid and the ONL (Figure 5.7). With increasing severity of the morphant phenotype there was a reduced number of RPE granules at the posterior of the eye (p $<10^{-4}$ in each case; One-way ANOVA with Tukey analysis; Figure 5.8). In the morphants with the more severe phenotype the RPE granules were found to be variable in size with a greater number of smaller granules with rougher edges when compared to the smooth edged larger granules found in the controls. In the most severe morphants the choroid appeared to have not formed correctly, suggesting FKRP, fukutin and dystroglycan deficiency in the zebrafish disrupts choroid formation.

The RPE is closely associated with a continuous Bruch's membrane in the wild type and control MO injected fish at 3 dpf (Figure 5.7). Bruch's membrane was found to be thinner with irregular perturbations in fkrp and dystroglycan morphants with a mild phenotype, when compared to controls. The Bruch's membrane is absent at the more severe end of the fkrp and dystroglycan morphant spectrum. In the fukutin morphant across the phenotype range Bruch's membrane was found to be completely abolished.
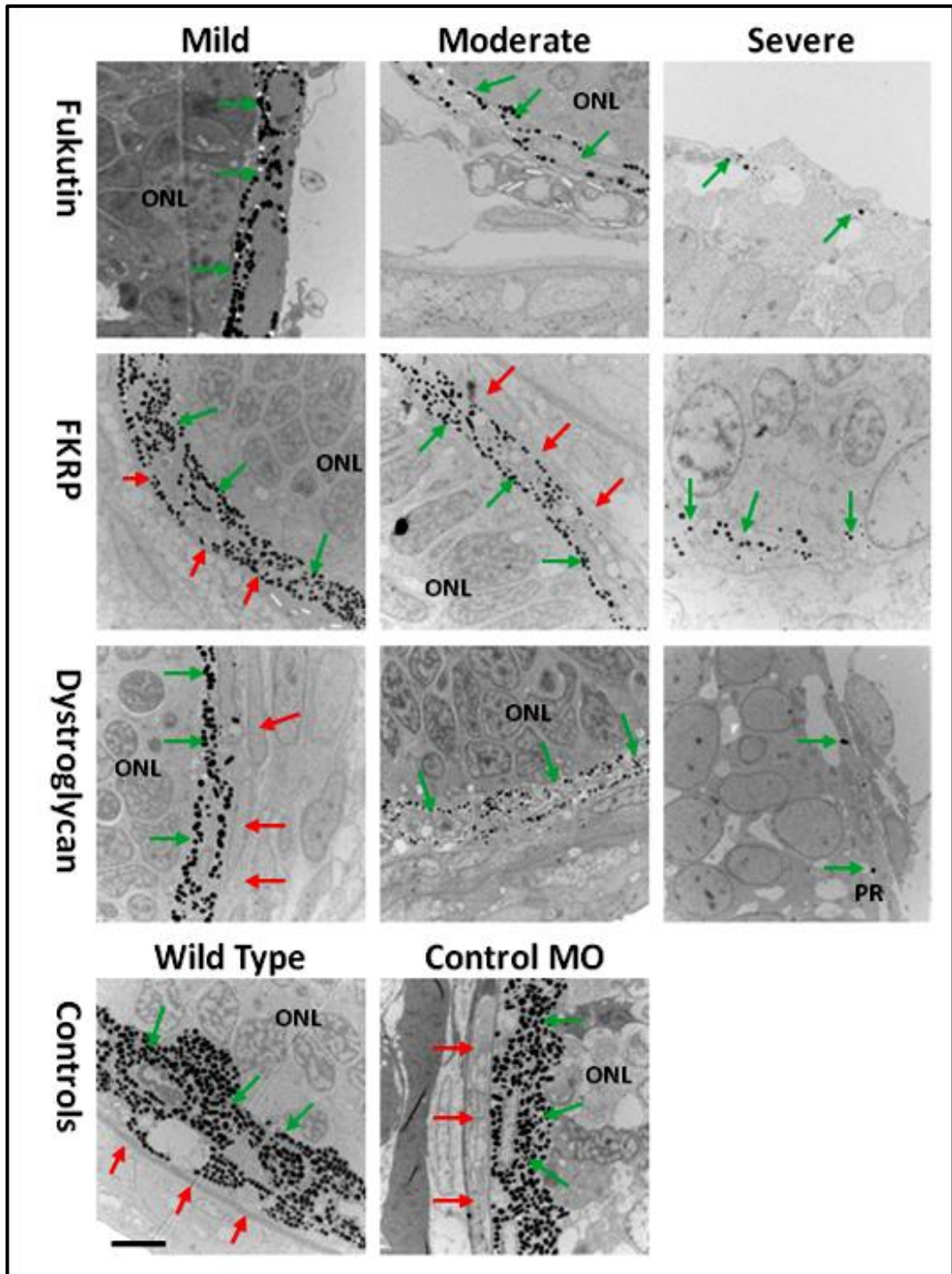
Figure 5.7: Disruption to morphant retinal pigmented epithelium layer in 3dpf larvae
Black spots (green arrows) are the pigmented granules, counts are shown in Figure 5.8. INL: inner nuclear layer, PR: photoreceptor layer, red arrows: Bruch's membrane, Scale Bar: 2μm.
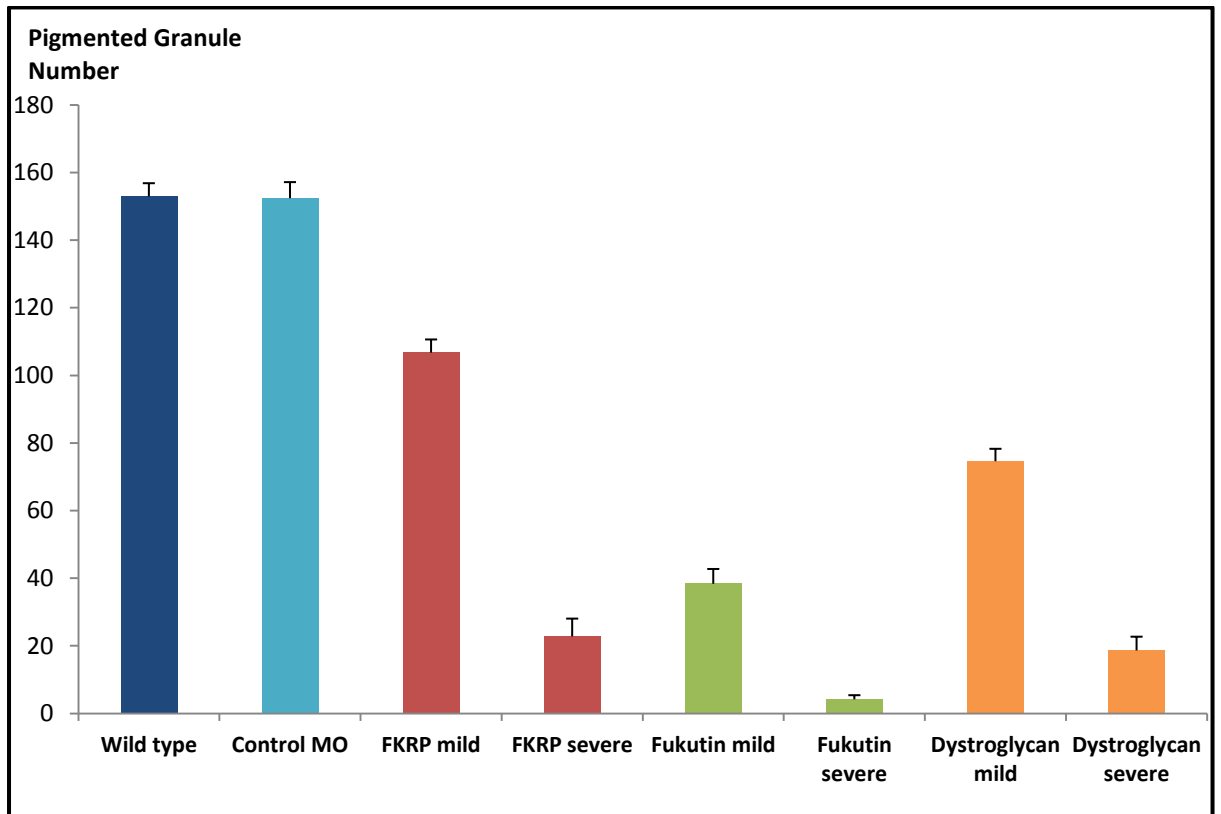
	N	Mean	Grouping	
Wild type	**15**	**152.93**	**A**	
Control MO	**21**	**152.43**	**A**	
FKRP mild	**19**	**106.74**	**B**	
Dystroglycan mild	**24**	**74.63**	**C**	
Fukutin mild	**16**	**38.38**	**D**	
FKRP severe	**15**	**22.80**	**D**	**E**
Dystroglycan severe	**15**	**18.67**		**E**
Fukutin severe	**15**	**4.20**		**E**

Figure 5.8: Reduced number of pigmented granules at Bruch's membrane in the RPE layer in 3 dpf larvae

Bars represent 95% confidence interval, results for each phenotype from minimum of three images of seven fish from a minimum of two separate experiments. Tukey analysis of the one-way ANOVA is displayed in the table below the graphical representation of the data. Tukey analysis was based on the assumption the data was approximately normally distributed and allowed variability to be assessed across morphant phenotype groups. Means that do not share a grouping are significantly different.

5.2.8   Abnormal ILM in 5dpf FKRP Morphant Larvae Eye

At 5dpf the retinal layering in the wild type fish eyes is fully established. The eye is round and the retinal layering is clearly established with defined borders (Figure 5.9). FKRP morphant fish were the only dystroglycanopathy fish investigated at 5dpf because very few fukutin or dystroglycan deficient fish survived to 5dpf. The 5dpf FKRP morphants with mild and severe phenotypes

also had round eyes and clearly demarcated retinal layering. The ILM in wild type larvae was smooth with defined membranes surrounding blood vessels which were spaced evenly around the lens. The mild FKRP morphants had no marked differences when compared to the controls. The ILM was disrupted on the GCL side in FKRP morphants with a rough surface, interestingly blood vessels could not be accurately distinguished from basement membrane on the TEM micrographs. The ELM appeared to be slightly diminished in the FKRP morphants, when compared to the controls. No differences were seen between the FKRP morphants and the wild type with respect to Bruch's membrane. There did however appear to be a reduction in number of pigmented granules in the RPE in the FKRP morphants when compared to controls. There was no statistical analysis carried out to confirm the assertion because of the limited sample size for each phenotype (n=3).
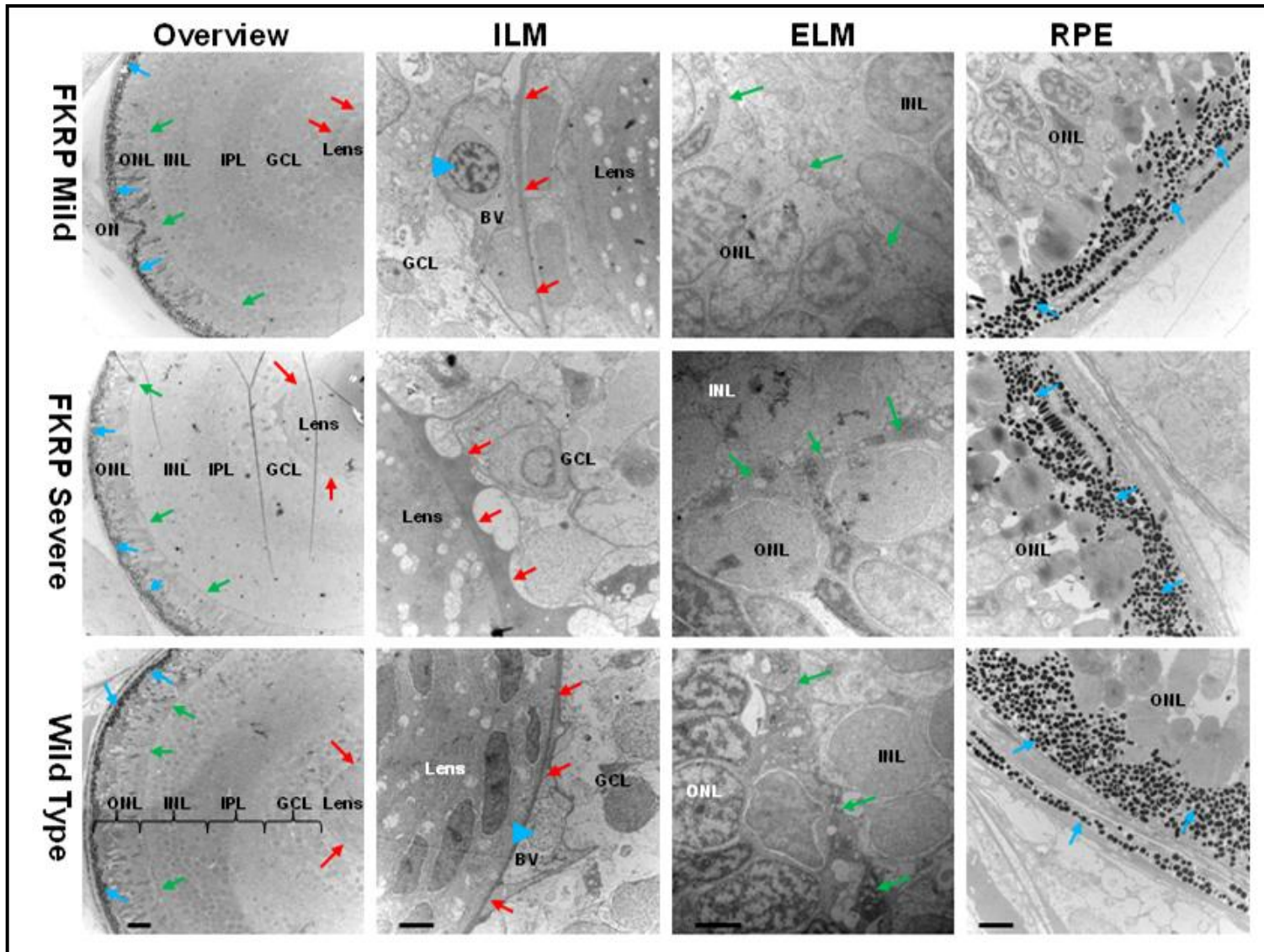
Figure 5.9: fkrp Morphant eyes at 5dpf
Red arrows: inner limiting membrane (ILM), green arrows: external limiting membranes (ELM), blue arrows: retinal pigmented epithelium (RPE), blue triangle: presumed erythrocyte, BV: Blood vessel, ONL: outer nuclear layer, INL: inner nuclear layer, IPL: inner plexiform layer, GCL: ganglion cell layer. Scale bar (left column): 10µm, scale bar right three columns: 2µm.

5.2.9 Perturbation of Eye Vasculature in fukutin and fkrp Morphant Fish

Changes in vascular development in the myotome of the morphant fish have been described in chapter 4 and in WWS patients vascular anomalies were found in the brain (Beltran-Valero de Bernabe *et al.*, 2002). It is reasonable to assume therefore that similar vascular developmental problems may persist in the eye. Similar to the previous chapter vasculature was imaged using multiple confocal images through the eye to create a projection of all the eye vasculature in a single image. The inner optic circle vessels of the wild type zebrafish form a roughly spherical shape around the perimeter of the eye at 1dpf (Figure 5.10). The inner optic circle vessels within the eyes of fkrp and fukutin morphant embryos with a mild phenotype were smaller and more oval than those in the eyes of control embryos. The eye vasculature of the fukutin and fkrp morphant zebrafish became increasingly distorted with increasing phenotype severity. In morphant embryos with the most severe phenotypes eye vasculature was deformed to an extent which was beyond being clearly identifiable as any particular vessel. Unexpectedly, the eye vasculature in dystroglycan morphant fish across all phenotype severity groups had no significant changes when compared to the control fish.
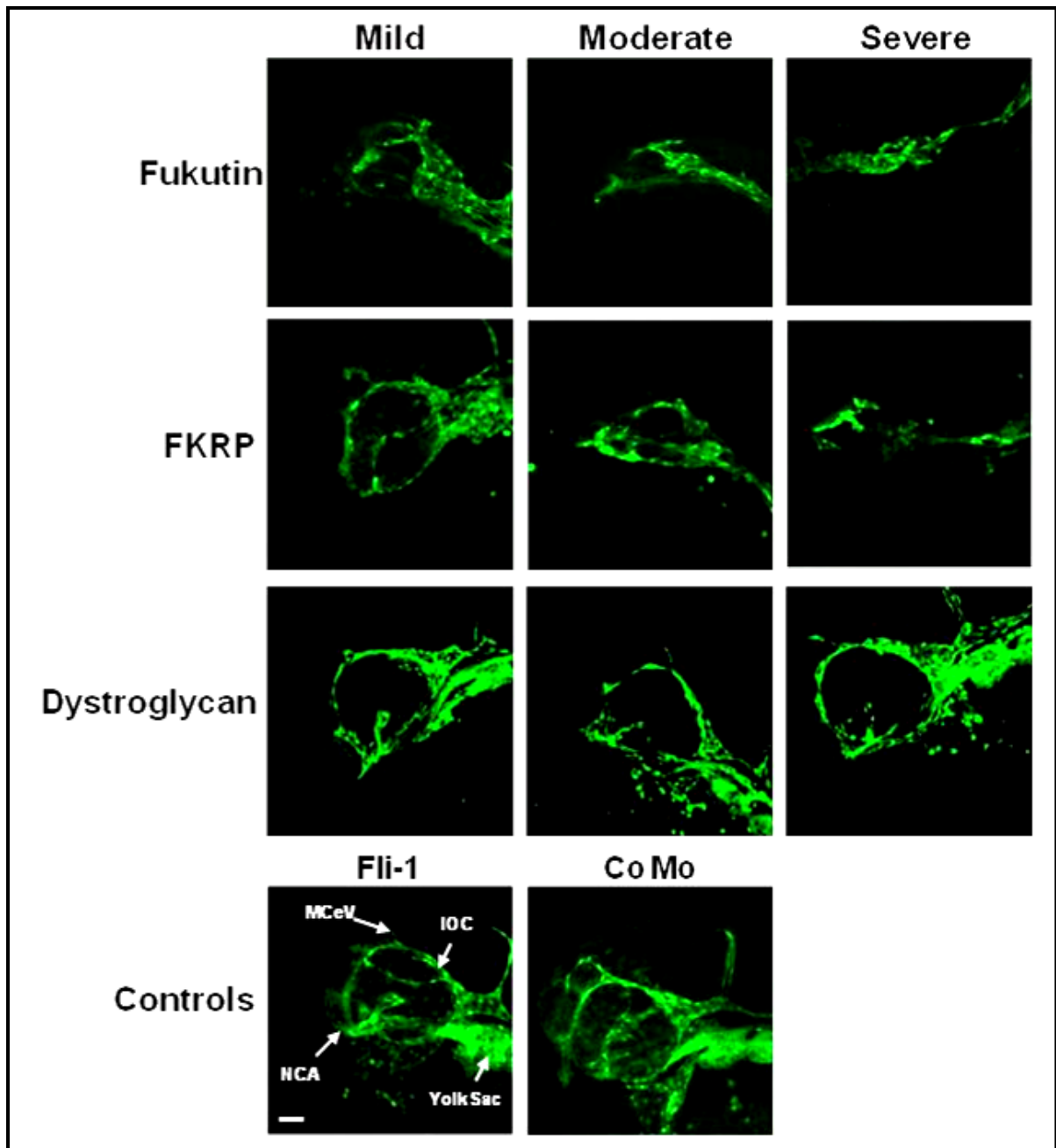
Figure 5.10: 1dpf eye vasculature of the eye
The FKRP, fukutin and dystroglycan injected embryos were staged according to phenotype at 1dpf. Micrographs through the eye were obtained on a confocal microscope and images were projected together. White scale bar: 100μm, IOC inner optic circle, MCeV middle cerebral vein & NCA naso-cillary vessel.

The eye vasculature was used as a marker of eye size at 3 dpf in the fish. The

areas of control fish eyes were measured and compared to the areas of the eyes of

the morphants. A minimum of three independent experiments were carried out for

each of the phenotypes (Table 2.2), with the exception of dystroglycan where five of

each mild, moderate and severe were combined, a minimum of ten eyes were

scanned for each phenotypic category. The eyes of control MO injected embryos had smaller mean area of eye than in the non-injected embryos however the difference was not found to be significant using Tukey analysis, suggesting that the MO had minimal non-specific effects that might affect eye development. The mean area of the mild morphant fukutin embryo eyes were significantly, see Tukey's analysis Figure 5.12, smaller than that of the control injected fish eyes (Figure 5.11). The eyes of the most severe fukutin and fkrp morphant embryos had the smallest areas and were very significantly smaller than eyes of control injected fish. The eyes of the fkrp morphant larvae were significantly larger than those found in the fukutin morphants when comparing each phenotype category. In the dystroglycan morphant fish, eye size across each phenotype group was found to be similar to that of the control MO injected and wild type fli-1 larvae.

The vasculature observed in the fli-1 fish (Figure 5.10 & Figure 5.11), can be compared to blood vessels in the ultrastructural analysis (Figure 5.1, Figure 5.5 & Figure 5.9). Despite vasculature being visible in the 1dpf fli-1 fish eye when examined using confocal microscopy (Figure 5.10), no blood vessels were detected by electron microscopy (Figure 5.1), which might indicate correct vascular specification with no associated vascular structure formation at this stage of development. By 3dpf the vasculature is visible using both confocal microscopy (Figure 5.11) and on TEM micrographs (Figure 5.5). Only small vessels are present on micrographs because the section is very thin in comparison to the confocal projections through the entire eye in the confocal micrographs which encompass most of the wild type zebrafish eye vasculature at 3dpf. However vasculature is not observed on TEM in the eyes of morphants with a severe phenotype, despite being clearly visible on confocal projection. It is possible that the marker used for vasculature (fli-1) is expressed in primordial blood vessels, and detected by fluorescence microscopy prior to their development into anatomically recognisable structures on TEM and the severe morphants are developmentally delayed. Interestingly in 5 dpf fkrp mild and occasionally in severe morphants vasculature is visible on TEM micrographs (Figure 5.9). These findings together suggest there is correct specification of vasculature with a delay in the specification of vascular epithelium structure in the morphant fish through the first five days of zebrafish development.
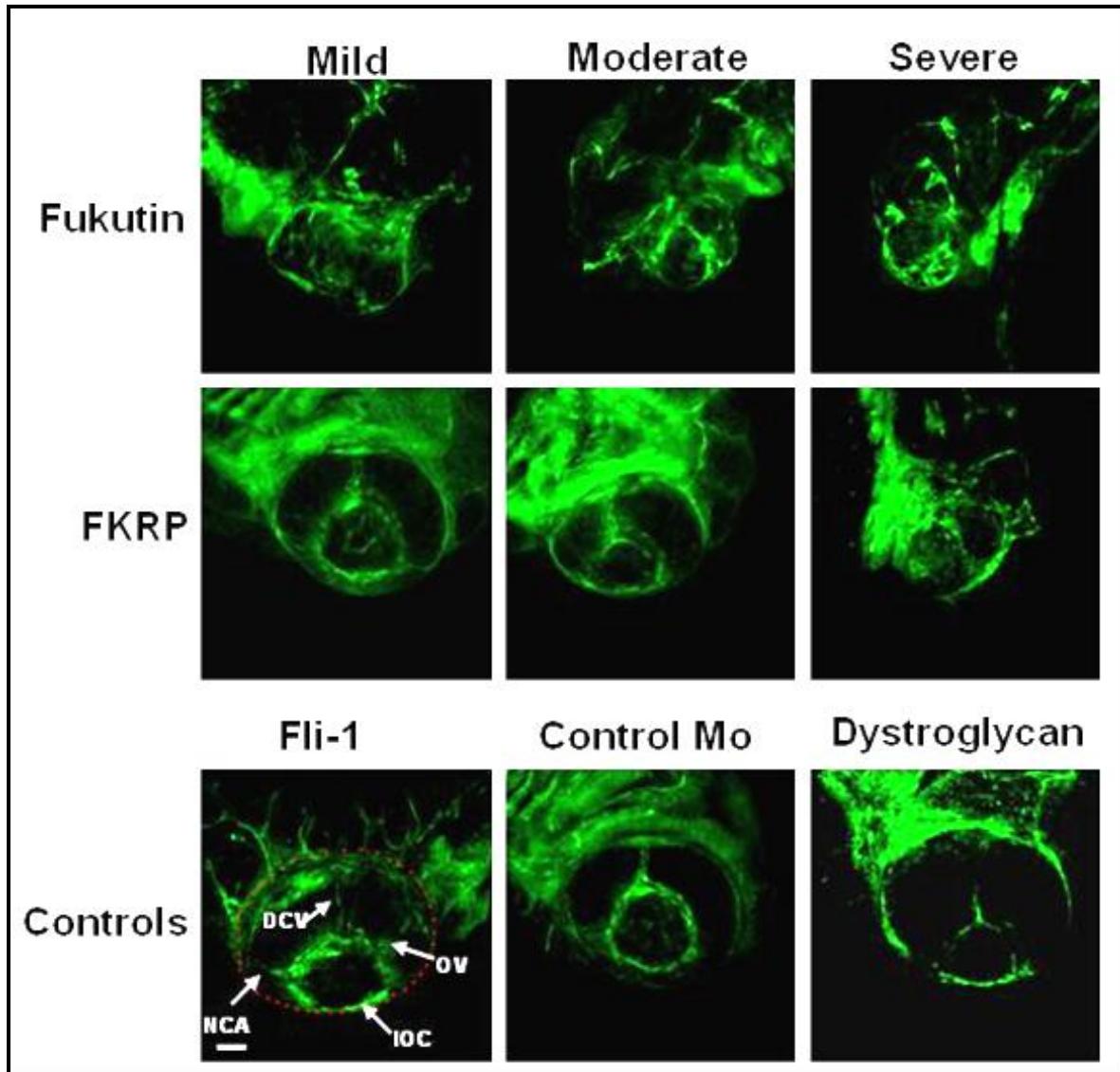
Figure 5.11: 3dpf eye vasculature using projections from confocal microscopy through the eye
Red dots show how area is calculated in Figure 5.12, IOC: inner optic circle DCV: dorsal ciliary vein, NCA: naso-cillary vessel & OV: optic vein. Scale bar: 100μm.

Eye Area Arbitrary Units
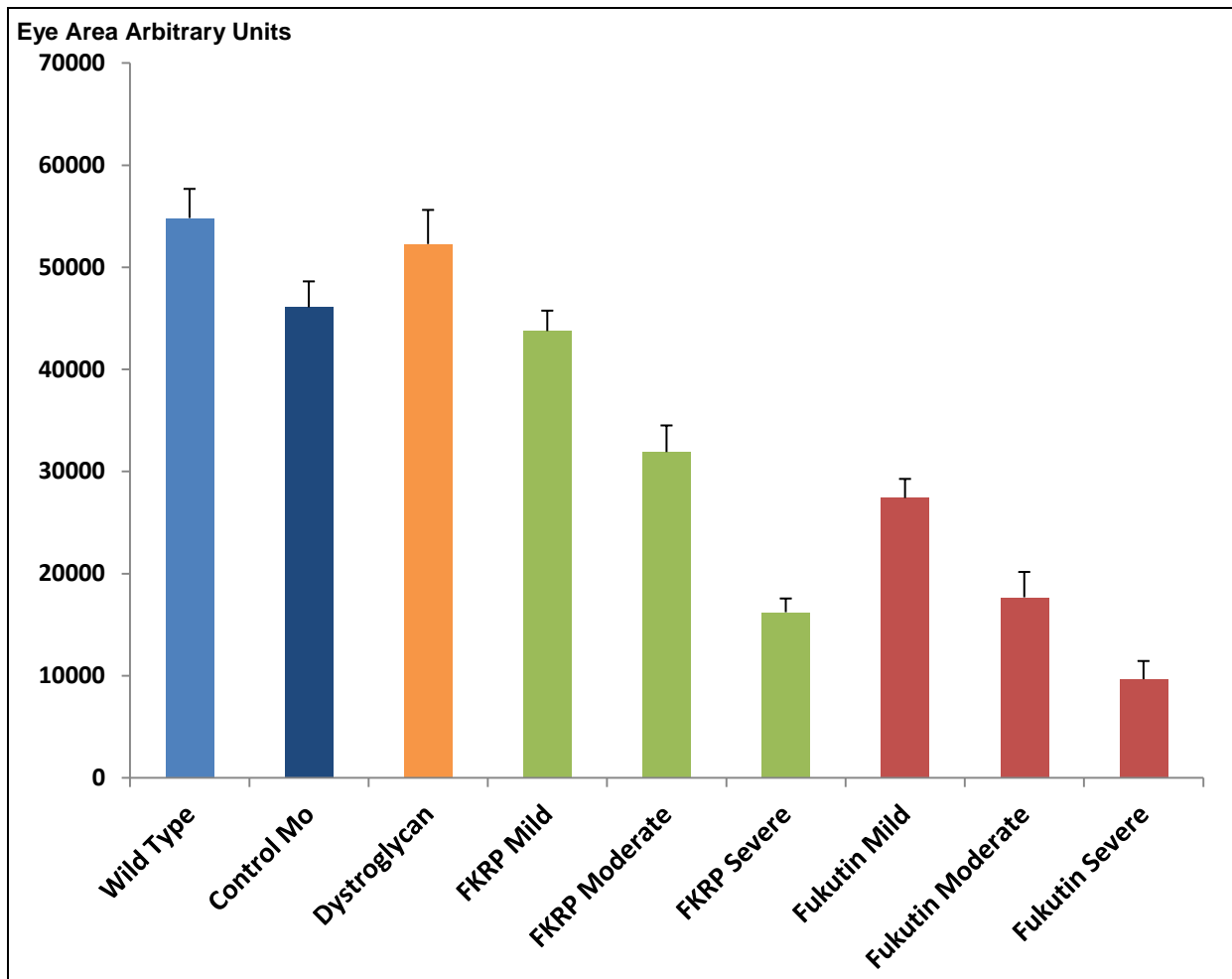
	N	Mean	Grouping				
Wild Type	21	54812	A				
Dystroglycan	13	52265	A				
Control MO	16	46072	A				
FKRP mild	10	43737	A	B			
FKRP moderate	8	31892		B	C		
Fukutin mild	15	27393			C	D	
Fukutin moderate	15	17673				D	E
FKRP severe	6	16211			C	D	E
Fukutin severe	14	9650					E

Figure 5.12: Relative area of 3dpf eye vasculature

The FKRP and fukutin injected embryos were staged according to Kimmel *et al*. 1995, Table 2.1 and morphant severity was judged as in Table 2.2. Bars represent 95% confidence interval, y-axis is in arbitrary units, results for each phenotype from minimum of three separate experiments. One-way ANOVA Tukey analysis is displayed in the table below the graphical representation of the data. Tukey analysis was based on the assumption the data was approximately normally distributed and allowed variability to be assessed across morphant phenotype groups. Means that do not share a letter are significantly different.

5.3 Summary

The microphthalmia in the fkrp, fukutin and dystroglycan morphants observed in the previous chapter is reminiscent of severe eye pathology observed in WWS. By investigating the histology of the eye at 3 dpf it is clear that there is both cellular and basement membrane pathology associated with the dystroglycanopathy morphants. Loss of retinal layering was observed in the morphant eyes on histological examination. Perturbations were also found in all the major basement membranes of the eye *i.e.* ILM, ELM and Bruch's membrane at 3dpf. This raises the important question of whether loss of retinal layering and microphthalmia are attributable to the loss of eye basement membrane structure. Interestingly ectopic lens was observed in dystroglycan and fukutin morphants which may also be a consequence of disruption to basement membranes of the eye, specifically the ILM. Finally, this data provides novel insight into how the loss of eye vascular structure in fkrp and fukutin but not dystroglycan morphants links to the ultrastructural and immunohistochemical changes.

Chapter 6   Discussion

6.1 Modelling Dystroglycanopathies using Zebrafish

By comparing dystroglycan to fkrp and fukutin deficiency in zebrafish this thesis set out to ascertain the pathological mechanism of dystroglycanopathy. Antisense MOs targeting fukutin, fkrp and dystroglycan were used throughout the thesis to knock down the fukutin and fkrp pathways to a similar extent in order to enable a meaningful comparison between phenotype of the zebrafish morphants. Dystroglycan morphants were a useful model in this study, providing confirmation that the pathology resulting from fkrp or fukutin knockdown is linked biochemically and phenotypically to dystroglycan in zebrafish. The criteria established to separate the zebrafish into phenotypic severity, outlined in Table 2.2, could be applied to other secondary dystroglycanopathy models such as POMT1, POMT2, LARGE, POMTGnT1 and ISPD in the future. Evaluating the developmental phenotype of different models with comparable severity of morphological defects allowed the identification of subtle differences in structural phenotypes by controlling for secondary effects. Since defects in primary and secondary dystroglycanopathy genes lead to severe developmental abnormalities, study of the zebrafish models, with easily accessible embryonic stages, is particularly valuable. In fact all stages of early development can be easily followed in structures of interest such as muscle, eye, brain and notochord.

Zebrafish models for other DGC components such as dystrophin (*sapje* mutant) have muscle fibre detachment from the myoseptum but no eye or brain abnormalities (Bassett *et al.*, 2003; Bassett and Currie, 2004; Guyon *et al.*, 2007). Those zebrafish mutants with mutations in proteins known to bind to α-dystroglycan such as laminin-α2 have a phenotype which resembles fukutin knockdown in terms of muscle morphology, indicating that the model is appropriate for studying fukutin deficiency (Hall *et al.*, 2007; Postel *et al.*, 2008). Laminin-α2 is a known ligand of dystroglycan in muscle. The zebrafish *candyfloss* (*caf*) mutant which has a mutation in the laminin-α2 gene has a degenerative muscle phenotype as a result of muscle detachment from the vertical myosepta (Hall *et al.*, 2007) but no observed eye and brain pathology. Interestingly the α1, β1 & γ1 laminin mutants, *bashful* (*bal*), *grumpy* (*gup*) and *sleepy* (*sly*) respectively have defects in eye development and notochord

differentiation (Parsons *et al.*, 2002b). Based on the phenotype of the fkrp, fukutin and dystroglycan morphants the muscle pathology is consistent with a failure laminin-α2 dystroglycan interaction, whereas the brain and eye pathology, which appeared more severe in fkrp and fukutin morphants than dystroglycan morphants, suggests that there may be specific pathways not dependent upon dystroglycan in relation to fkrp and fukutin function in eye and brain.

pomt 1 and pomt2 is another example of MO knock down models for the secondary dystroglycanopathy genes that produces a phenotype in zebrafish, which is similar to other secondary dystroglycanopathy models (Thornhill *et al.*, 2008; Avsar-Ban *et al.*, 2010; Kawahara *et al.*, 2010; Lin *et al.*, 2011). The pomt morphants have tail curvature and eye defects similar to that which is seen in fkrp, fukutin and dystroglycan MO knock down models. The coexpression of pomt1 and pomt2 is required for the enzymatic *O*-mannosylation of dystroglycan, and knock down of both simultaneously produces a more severe knockdown than either on their own (Avsar-Ban *et al.*, 2010). Recently Kuga *et al.* and Yoshida-Moriguchi *et al.*, showed that FKRP in addition to, fukutin and LARGE (Yoshida-Moriguchi *et al.*; Kuga *et al.*, 2012b) are all involved in the phosphorylation of the mannose residue on α-dystroglycan in muscle, eye and brain, but only to a minimal degree in lung and testis. Therefore FKRP and fukutin may need to be co-expressed for complete modification of the mannosyl residues on dystroglycan. Fukutin has also been implicated in a dimerisation with POMGnT1, supporting the theory that the secondary dystroglycanopathy proteins act in partnerships (Michele *et al.*, 2002; Manya *et al.*, 2004). Interestingly over-expression of LARGE has previously been shown to be capable of functionally bypassing fukutin and FKRP (Barresi *et al.*, 2004). This apparent functional redundancy in the enzymatic pathway for post-translational modification of dystroglycan which is not consistent with the requirement for these proteins remains intriguing.

ISPD (isoprenoid domain containing) is the protein most recently found to have a role in the modification of dystroglycan (Roscioli *et al.*, 2012; Willer *et al.*, 2012). Mutations in *ISPD* were identified by two groups simultaneously in cohorts of WWS syndrome patients whose conditions could not be attributed to mutations in the known dystroglycanopathy genes (Willer *et al.*, 2012). Knocking down *ispd* in zebrafish produced morphants with muscle, brain and

eye abnormalities (Roscioli *et al.*, 2012). Interestingly, the observed brain malformation (hydrocephalus) could be accentuated by co-injection with either fkrp or fukutin MO. Injection of 3ng each of fukutin and fkrp MO also produced hydrocephalus, a feature not seen in our morphants with a knock down of a single gene. This further indicates that the secondary dystroglycanopathy proteins may be acting cooperatively.

6.2 Analysis of the Approach to Modelling FKRP and Fukutin Deficiency

Despite several studies investigating fkrp in zebrafish there is currently no stable *fkrp* mutant fish lines. An attempt to address the problem using ZFNs with the CoDA protocol (Maeder *et al.*, 2009; Sander *et al.*, 2010) proved not to be successful in producing a mutant line. The ZFNs derived from the CoDA protocol failed to produce even a low somatic mutation rate in injected fish. If successful, the continuation of use of the ZFN technology to produce a *fukutin* mutant zebrafish line would have been feasible. Where success could be achieved in a relatively short period of time there would have been an attempt to create a fukutin morphant line with ZFNs (Porteus and Carroll, 2005).

There were no mutations reported in any embryos treated with either of the CoDA ZFN pairs investigated. Since the context of the array is only in part accounted for by the CoDA protocol, the inference that a particular array will function well together remains theoretical and may not be realised when tested. It is possible that the somatic mutation rate was too low to be detectable given the number of embryos investigated. A low somatic mutation rate would however be difficult to transfer to the next generation due to the large number of fish required in the second generation. A somatic mutation rate of approximately 10% is required to move forward with the screening protocol. No mutations were detected in either set of the 95 samples from 10 fish for the two ZFN pairs sent for sequencing. It is therefore concluded the two pairs of ZFNs tested were not working with a sufficient efficacy for further use.

Despite reaching the end of the CoDA protocol, the pairs of ZFNs derived were not effective in producing a mutation in the *fkrp* gene. CoDA is reported to have a 60-75% success rate, and it might therefore be expected that one of the two pairs of fingers would produce a mutation. There still remains a third

unexplored set of CoDA zinc fingers for the *fkrp* gene in zebrafish described by ZiFit as 7-1 because of the seven base pair spacer region. This zinc finger pair was not explored because of the requirement for a different pMLM vector. Currently only the CoDA zinc fingers with the five base pair spacer region have been investigated. The remaining 7-1 pair would be worth investigating before using alternative strategies to develop mutant zebrafish are explored (Maeder *et al.*, 2009; Sander *et al.*, 2010).

The 30-12Apr05B-fukutin MO has been shown to produce an effective knock down of *fktn* gene expression by inducing non-canonical splice variants (Nasevicius and Ekker, 2000). Despite the transient nature of the MO approach a range of fukutin morphant phenotypes were observed between 1 & 5dpf. The range of morphants effectively models the spectrum of clinical severity resulting from the variety of mutations and splice variants in the *fktn* gene (Yoshioka and Kuroki, 1994). However it is the range itself and not morphant fish within a particular severity category that is of interest, as the mechanisms which produce the spectra in fish and humans are not equivalent (Bassett and Currie, 2003).

The question of model utility is critical to assess whether any continuation of experiments with the 30-12Apr05B-fukutin MO is justified *i.e.* how useful is the fukutin knock down by MO as a model for dystroglycanopathy. By examining the phenotype up to 5dpf it is concluded that the MO is an appropriate tool for early developmental questions. However this model system is less appropriate for posing questions about the adult condition. MOs become diluted with increasing number of cells in the zebrafish resulting in re-expression, which does not recapitulate the continuing loss of muscle function with ongoing Fukutin deficiency observed in the human condition (Chiyonobu *et al.*, 2005; Kanagawa *et al.*, 2009a; Taniguchi-Ikeda *et al.*, 2011).

MO knock down is well suited to the study of congenital disorders (Bassett and Currie, 2003; Hall *et al.*, 2007; Thornhill *et al.*, 2008; Kawahara *et al.*, 2010; Lin *et al.*, 2011), although a mutant model would simultaneously eliminate non-specific effects of MO and allow studies to be carried out to investigate adult disease, and therefore a mutant line remains an important goal for zebrafish dystroglycanopathy research in the future. The Fkrp-deficient mouse that is not embryonic lethal remains the best system to investigate adult Fkrp deficiency

(Ackroyd *et al.*, 2009; Ackroyd *et al.*, 2011). The fukutin chimeric mouse remains a good alternative to zebrafish for modelling fukutin deficiency. The final consideration is what would be the best approach to produce a stable mutant zebrafish line. Since there is a range of patient phenotypes from the congenital condition to adult onset forms of fukutin associated MD, an allelic series of mutants would therefore be desirable. An allelic series of fish with equivalent mutations to those found in the human condition would be the gold standard for fukutin associated MD research in zebrafish.

 In the first chapter different strategies were considered: in the long term the zebrafish mutation project will likely produce several lines with mutations in the *fkrp* and *fukutin* genes. A mutant line is already being displayed on the ZMP website with a confirmed C>T nonsense mutation in the F2 generation in the *fkrp* gene, reported to be available as early as April 2013. In the short term the TALEN system would be a good alternative because of the specific targeted nature of the TALENs. TALENs have recently been shown to produce a higher somatic mutation rate >10% in 76% of gene loci tested whereas ZFNs produce a somatic mutation rate of <1% in 3.3% of gene loci tested (Moore *et al.*, 2012b). Therefore, there is a clear case for switching to a TALEN based approach in the future.

6.3 Mechanisms of Skeletal Muscle Pathology

The second aim was to investigate the mechanism of muscle pathology in *fkrp* and fukutin knockdown fish. Ultrastructural analysis revealed that the muscle pathology could be associated with both a disruption to the sarcolemma and fibre detachment from the vertical myoseptum. Immunostaining confirmed a hypoglycosylation of α-dystroglycan and loss of laminin at the vertical myosepta (Thornhill *et al.*, 2008). Combined with studies investigating laminin-α2 *candyfloss* zebrafish (Hall *et al.*, 2007), it was predicted that fibre detachment was as a consequence of a disrupted α-dystroglycan laminin-α2 interaction. Interestingly, studies that investigated sarcolemmal instability using Evan's blue dye did not find any dye leakage in the laminin-α2 models (Straub and Campbell, 1997). Our findings suggesting sarcolemmal damage may represent either a secondary consequence of the severe muscle damage in dystroglycanopathy or a developmental delay in the production of sarcolemma. The sarcolemmal damage remains intriguing but can be explained by the loss of

muscle fibre attachment to the vertical myoseptum. Utilizing the *sapje* DMD model zebrafish as a comparison would form a good complementary data set, since the muscle pathology in this model is thought to be entirely associated with sarcolemmal instability (Bassett *et al.*, 2003).

Interestingly muscle fibres in the *lama2 candyfloss* fish are known to fuse with the vertical myosptum correctly and therefore laminin-α2 is not required for this process (Hall *et al.*, 2007). Recent evidence suggests however that integrin-α7 is required perhaps with a laminin chain such as laminin- β2 (Jacoby *et al.*, 2009; Sztal *et al.*, 2012). Both components are known to be important for muscle fibres to form contacts with the vertical myoseptum. Therefore investigating expression and glycosylation of both laminin-β2 and integrin-α7 in early zebrafish development in dystroglycanopathy morphant fish would be the next logical step to determining the aetiological cause of the muscle pathology in fkrp and fukutin deficiency. Modification of either laminin-β2 or integrin-α7 by fkrp and fukutin has currently not been shown. The post translational modification of either component by FKRP or fukutin does not remain outside the bounds of possibility, it is however perhaps not important for their function of initial adherence of muscle fibre with myoseptum (Postel *et al.*, 2008). If fkrp and fukutin modified either laminin-β2 or integrin-α7 in any way then it would be expected that muscle fibres would not adhere to the myoseptum in our fkrp and fukutin morphant fish. Investigating muscle fibre adhesion including laminin-β2 or integrin-α7 expression to the vertical myoseptum at an earlier time point in the dystroglycanopathy fish would prove this hypothesis conclusively.

6.4 Mechanism of Eye Pathology

While zebrafish are not the best model system to study brain development since they lack much of the complexity found in mammalian brains, they are a good model system to study eye development since their eye is structurally similar to the mammalian eye. One aim of this thesis was to understand more about the underlying developmental mechanism of the eye pathology found in the fukutin and fkrp deficient zebrafish. Deficiencies in all three eye basement membranes were found, providing a basis for eye pathology in dystroglycanopathy. More work will be required to determine what the key interactions are that stabilise retinal layering to basement membranes. Preliminary examination found that a

laminin dystroglycan interaction as found in the muscle is unlikely to be responsible for maintaining cellular adhesions to basement membranes.

There is clearly a complex developmental mechanism that is responsible for establishing basement membrane structure and retinal layering in mammals and fish. The dystroglycanopathy morphant zebrafish have disrupted basement membranes and retinal layering abnormalities. The observed pathological changes in the eyes of the morphant fish may be as a result of a cascade which starts with perturbations in the posterior basement membranes *i.e.* ELM and Bruch's membrane. The important secondary change attributed to disruptions in both of the posterior eye basement membranes, could be the loss of the RPE in the morphants. The final event would be loss of retinal layering organisation as a consequence of reduced RPE density. The RPE is thought to be key in driving cellular layer organization, providing molecular cues for differentiation of the retinal layers (Strauss, 1995; Martinez-Morales *et al.*, 2004; Bharti *et al.*, 2006). Albino animals with no pigment in the RPE illustrates the hypothesised mechanism since these mice have disrupted retinal layering but intact basement membranes (Al-Hussaini *et al.*, 2008). Since it is possible to have a loss of retinal layering without a loss of basement membrane integrity, it can be assumed that disruption to the basement membranes of the eye is not sufficient on its own to cause the retinal layering abnormalities. The implication is therefore that a loss of retinal layering in the dystroglycanopathy morphants might be a secondary consequence of reduced RPE as a result of the primary aetiological perturbation to the posterior basement membranes.

Perturbations to the anterior basement membrane *i.e.* the ILM may also contribute to the overall poorly differentiated retinal layering in the dystroglycanopathy morphant fish. Recently Randlett and co-workers have shown the contact of retinal ganglion cells (RGC) with laminin at the ILM to be critical for axon guidance. Randlett and co-workers propose that axonic projections from the RGCs project from Bruch's membrane during development, connecting with the laminin at the ILM, then the axon followed by the cell body migrate towards the GCL (Randlett *et al.*, 2011). The hypothesis in our model is that dystroglycanopathy leads to disrupted retinal layering through two processes: firstly Müller glia anchoring to the ILM is disrupted as the result of loss of the α-dystroglycan laminin interaction. Secondly a reduction in correctly

glycosylated α-dystroglycan in the axonic processes of retinal ganglion cells prevents an interaction with laminin in ECM and ILM important in the guidance process of cell migration in the eye. The resultant mis-localised laminin at the ILM/ELM and incorrectly glycosylated dystroglycan results in cells failing to localise to the correct layers of the retina in fkrp and fukutin morphants. Therefore, it is the potentially loss of "driver" function from the posterior retina and loss of guidance at the anterior that contribute together to overall disorganised retinal layering, as a result of basement membrane disruption in the dystroglycanopathy fish.

The data presented in the vascular section suggests that there may be unknown proteins expressed in the eye which are subject to secondary modification by fkrp and fukutin. One potential candidate class of proteins are the major basement membrane proteins collagen. Collagen 4A1 deficiency results in iris dysplasia, vascular haemorrhaging, optic nerve cupping, corneal opacities, bupthalamos; a condition defined by enlarged eye balls and cataracts (Gould *et al.*, 2005; Van Agtmael *et al.*, 2005; Breedveld *et al.*, 2006). Mutations in human collagen 8A1-2 are the genetic basis for Fuch's corneal dystrophy (OMIM136800) and result in anterior segment dysgenesis in mice (Gottsch *et al.*, 2005; Hopfer *et al.*, 2005). Retinal detachment, high myopia and vitreoretinal degeneration are the key features of mutations in collagen 18, referred to as Knobloch syndrome in humans (OMIM 267750) and mouse models deficient in *Col18a1* have signs of age related degeneration of the eye (Sertie *et al.*, 2000; Fukai *et al.*, 2002; Ylikarppa *et al.*, 2003; Marneros and Olsen, 2005). The specific features of eye pathology associated with fkrp, fukutin and dystroglycan deficiency does not correlate with the disturbances to the eye in collagen mutant zebrafish. Despite a clear requirement for collagen in the eye the clinical phenotypes are not consistent with those seen in secondary dystroglycanopathies, and therefore do not support a collagen-dystroglycan axis. Retinal eye pathology might therefore be attributable to a more specific component within the basement membrane such as laminin.

The muscle pathology in fkrp and fukutin deficiency can be attributed to disruption to the α-dystroglycan laminin-211 interaction, important for maintenance of cell adhesion with basement membrane. It would therefore be logical to hypothesise a similar protein interaction may adhere cells to basement

membranes in the eye. Loss of fkrp and fukutin dependent secondary modification of an unknown protein with an alternative laminin chain to laminin-α2 in the classic interaction might result in loss of cell anchoring to eye basement membranes. This hypothesis is consistent with the vascular findings and supported by the nestin-Cre/DG null mouse (Satz *et al.*, 2009). Studies in the nestin-Cre/DG null mouse found that dystroglycan is required for eye development but not for the maintenance of anchoring cells at basement membranes. In the zebrafish *Laminin-α2* mutant model *candyfloss* has a muscle but no brain or eye phenotype (Hall *et al.*, 2007). Laminin-α2 is therefore an unlikely candidate as an important laminin chain in the eye.

Laminin-β2 is expressed in the eye in wild type but not the *laminin-β2* zebrafish mutant softy (Jacoby *et al.*, 2009). Despite loss of *laminin-β2* the *softy* mutants have no discernible eye phenotype. However patients with mutations in the *laminin-β2* gene have microcoria-congenital nephrosis, lens, retina, cornea and iris abnormalities referred to as Piersons syndrome (OMIM 609049) (Zenker *et al.*, 2004; Zenker *et al.*, 2005). The *laminin β1 & γ1* zebrafish mutants showed signs of ILM and lens abnormalities, however the only laminin mutant with an ectopic lens phenotype was the *laminin-α1* mutant zebrafish (Semina *et al.*, 2006; Lee and Gross, 2007). Therefore, based on the eye phenotypes of patients and animal models, laminin-α1 is the assumed candidate that is important for binding dystroglycan in the eye. The counter argument is *laminin-α1* is ubiquitously expressed and is therefore unlikely to be involved in the highly specific organisation of the eye. It is likely that more than one laminin chain interacts with dystroglycan and is important for eye development.

The clear pathology at both the anterior and posterior regions of the eye in the dystroglycan morphants, combined with dystroglycan being detectable at both the ILM and Bruch's membrane in wild type fish, suggest a role for dystroglycan across the retina. Immunostaining in the MORE-DG mouse model shows that there is role for glycosylated α-dystroglycan in the eye (Satz *et al.*, 2008). However, glycosylated α-dystroglycan is neither the most important protein for stabilising retinal cells with respect to basement membranes nor a key molecule in eye vascular development. One of the more clearly defined roles of dystroglycan is the interaction with pikachurin within ribbon synapses. Studies have shown pikachurin binding of correctly glycosylated α-dystroglycan is

important in the formation of ribbon synapses (Sato *et al.*, 2008). Recently dystroglycan clustering at the photoreceptor synaptic terminal has been shown to be dependent on pikachurin expression, which is important for proper synaptic connectivity (Sato *et al.*, 2008; Bozzi *et al.*, 2009; Omori *et al.*, 2012).

Basement membrane pathology is, at least in part, a consequence of the loss of the interaction between laminin-α1 and α-dystroglycan (Jacoby *et al.*, 2009). Based on morphant basement membrane phenotypes on TEM, laminin-α1 is clearly important for RGC migration across the retina during development. Together with a loss of RPE known to be important for driving retinal layer differentiation, laminin-α1 is evidently important in eye basement membranes. Lens ablation studies show lens and ILM together are important for invagination of vasculature into the optic cup (Semina *et al.*, 2006). A similar ectopic lens and absent ILM phenotype as observed in fkrp/fukutin morphants has been reported in *laminin-α1*deficient zebrafish embryos. This raises the question of whether there is a laminin-α1 interaction with an unknown protein requiring fukutin/fkrp for expression which forms the key axis important for driving angiogenesis since dystroglycan morphants have a normal eye vascular phenotype. This hypothesis for would support a novel axis *i.e.* fkrp, fukutin and laminin-α1 for vasculogenesis and neurogenesis in zebrafish eye development. Laminin-α1 acts as a common receptor within the basement membrane for a variety of membrane proteins. The loss of these interactions in dystroglycan morphants may occur as a result of fkrp and fukutin acting as drivers modifying independent proteins that bind laminin-α1. Processes occurring simultaneously in the eye such as neurogenesis and angiogenesis can therefore be specifically controlled by fkrp and fukutin by glycosylating different laminin binding partners at specific time points (Dahm *et al.*, 2007; Randlett *et al.*, 2011). The multiple facets of the eye pathology associated with fkrp and fukutin deficiency suggests fundamental roles for proteins modified by fkrp/fukutin in the control of eye development.

Unlike muscle, the eye phenotype cannot be attributed to a loss of α-dystroglycan interaction with laminin-α2. However, this phenotype can be hypothesised to be caused by a loss of laminin-α1 binding to other receptors present in the eye, such as integrin-α6, an integrin known to bind laminin in the eye (Hynes, 1992; van der Flier and Sonnenberg, 2001). The eye is a complex

structure and it is likely that laminins, dystroglycan and integrins are involved in an intricate interplay with many post translation modifiers such as fkrp and fukutin which are important mediators for these interactions. In conclusion, fkrp and fukutin post translational modification of dystroglycan and possibly yet to be determined proteins are important in the adherence of cellular components with basement membranes (Satz *et al.*, 2008; Bozzi *et al.*, 2009; Satz *et al.*, 2009).

6.5 Linking Vasculature and Basement Membrane Pathology

Vasculature was studied in this body of work as a hypothesised primary aetiology that might contribute to the phenotype in fkrp and fukutin deficiency. WWS Patients with *POMT1* mutations were observed to have surface vascular abnormalities on their brains, forming the initial hypothesis that vascular changes may be responsible in part for the dystroglycanopathy phenotype, (Beltran-Valero de Bernabe *et al.*, 2002). Fli-1 fish in conjunction with knock down of dystroglycanopathy genes using MOs provided a good model system to test this hypothesis.

Down-regulation of fukutin, fkrp or dystroglycan by MO was found to lead to aberrant blood vessel development in the somitic trunk of fli-1 embryos. Closer examination revealed absent or delayed growth of intersegmental vessels in the somites of all three morphants at 1dpf. These findings raised a number of questions about the primary origin of this abnormal angiogenesis. Firstly, was the vascular pathology in the dystroglycanopathy knockdown fish secondary to the observed changes in the myotome? Secondly, was myotome degradation a secondary effect of aberrant angiogenesis? A further possibility was raised, that muscle necrosis ensued as a consequence of hypoxia in somites? Finally, were both muscle and vascular development independent primary pathologies in the morphant fish which may have a currently unknown common mechanism, since ECM damage or lack of growth factors from the notochord could equally affect both processes? This raises a further question: are fkrp and fukutin involved in more global developmental events and does dystroglycan remain the sole receptor for their post translational modification?

By considering model systems without any muscle pathology and poor intersegmental growth such as the endothelial cell-specific molecule 2 (ECSM2)

and the netrin receptor UNC5B (Lu *et al.*, 2004; Ma *et al.*, 2009), it is possible to make inferences about whether poor angiogenesis is the primary aetiology responsible for the muscle damage. Based on these models it is improbable that the poor angiogenesis observed in the dystroglycanopathy models is responsible for the muscle necrosis. An analogous approach found reduced segmental vessel development without the curly tail phenotype by knocking down the myotubularin family gene *Mtmr8* in zebrafish. Interestingly despite *Mtmr8* being expressed in the mesoderm, a progenitor tissue of both muscle and endothelial cells during embryogenesis, Mtmr8 knockdown only resulted in vascular abnormalities (Mei *et al.*, 2010). Together these findings suggest that the muscle phenotype seen in the fukutin, fkrp and dystroglycan morphants was unlikely to be a secondary consequence of abnormal angiogenesis in the fish.

Turning the question around, it is possible to query whether abnormal angiogenesis seen in the somites is a secondary consequence of the muscle pathology. Vascularisation has not been studied in other zebrafish models of MD to determine whether the described vascular abnormalities are a non-specific response to muscle pathology. No vascular phenotype was observed in the somites when the ubiquitously expressed *gfat1* was down-regulated, despite the curly tail phenotype and abnormal muscle fibres. Generally vascularisation is enhanced in regenerating muscle and currently there is no evidence from patients or mouse models with MD that might suggest muscle pathology affects vascular development (Eguchi *et al.*, 2009; Senderek *et al.*, 2010).

This suggests that the disruption of somitic angiogenesis is a primary consequence of the knockdown of fukutin, fkrp or dystroglycan, and not a secondary outcome of muscle pathology (Lu *et al.*, 2004; Ma *et al.*, 2009). Considered the opposite way around aberrant angiogenesis did not result in abnormal somite or tail structure in other zebrafish models with early vascular defects. These data combined suggests that vascular and muscle pathology observed in the morphants is two distinct pathogenic consequences of dystroglycanopathy. Poor vascularisation of the eye was investigated, as one of the possible secondary consequences of loss of eye structure (Gore *et al.*, 2012).

Abnormal eye vasculature development was observed in both fkrp and fukutin knockdowns. Whereas the eyes of dystroglycan morphants had the same appearance and were of a similar size to the controls, implying that eye vascular development in zebrafish embryos and early larvae is not dependent upon dystroglycan expression. Only fkrp and fukutin morphants were found to have aberrant eye vascular development when compared to somitic vascular findings, where differences in segmental vessel height was found in all the dystroglycanopathy morphants. The implication is that fkrp and fukutin modify yet to be discovered proteins important for eye vasculature development, in contrast to vascular development in muscle where correctly glycosylated α-dystroglycan is the most important interaction for angiogenesis. The findings suggest that both fkrp and fukutin are important in vascular development, but may have distinct roles in muscle and eye maturation.

With disrupted vertical myosepta and eye basement membranes it is entirely possible that the vascular changes resulted from perturbations in basement membranes which are in analogous anatomical locations. The most likely explanation for the eye vasculature not being altered in the dystroglycan deficient fish is that FKRP and fukutin have alternative targets in the eye important for maintaining the vascular development and maintaining basement membrane integrity. The hypothesis is strengthened by findings in the Nestin/Cre DG null mouse dystroglycan mouse that found dystroglycan was important for initiating correct eye formation but is not important for its maintenance (Satz *et al.*, 2009).

6.6 Clinical Relevance

A key requirement was to test whether the MO approach related well to the clinical spectrum of disease of FKRP and fukutin deficiency. Zebrafish allow for study of early pathology in muscle and eye, and are well suited to the study of congenital conditions such as WWS (Bassett and Currie, 2003). Without a stable mutant line it would be very difficult to make any conclusions about late onset or milder conditions such as LGMD2I. In many senses this is a disappointing outcome, since the MO approach is much better system for modelling early developmental changes which may not be applicable to the later onset LGMDs. Therapy development for LGMD2I is more likely to be

successful than for the CMDs which will be much more difficult to treat due to their developmental onset (Brockington *et al.*, 2001a).

The difficulties in developing therapies for CMDs are a consequence of nature of the associated pathology which arises very early during embryonic development. Structures such as eye and brain reach full development at birth and defects are irreversible thereafter. Research into CMDs such as WWS should aim to understand the pathogenic mechanisms and to translate the findings into therapeutic strategies for milder conditions as a starting point. Attention is therefore placed into identifying the remaining causes of WWS that will be of use diagnostically. Indeed, recent findings suggest there are several causative genes for WWS that will be identified in the near future, because of the rapid progress being made in the field of next generation sequencing (Roscioli *et al.*, 2012; Willer *et al.*, 2012). The ability to diagnose these conditions may not aid their treatment but expanding patient registries are in place to enable patients to access clinical trials when they become available (Bushby *et al.*, 2009). Accurate and widespread diagnosis also enables bio-banking, retaining cell lines from these patients to be distributed to researchers who may be capable of pioneering new therapeutics.

6.7 Future Direction

Overall the project has investigated dystroglycanopathy in zebrafish in detail from a histological, ultrastructural and immunohistological perspective in muscle and eye. The notochord is an important developmental structure, clearly abnormal on ultrastructural analysis. The notochord would therefore be worth investigating further in the future for the overall understanding of developmental disturbances of the fkrp and fukutin deficient zebrafish.

There are several lines of inquiry the project could move towards. Firstly, gaining a better understanding of the mechanism of disease; finding the key proteins for maintaining cellular adhesions at basement membranes and investigating any downstream effects of fibres failing to adhere to myoseptum such as autophagy (Carmignac *et al.*, 2011). Secondly, investigating other potential targets for FKRP and fukutin; do FKRP and fukutin have any other primary targets other than α-dystroglycan? Thirdly understanding the temporal and spatial expression patterns of fkrp and fukutin in zebrafish; which might

clarify questions about overall development of muscle, eye and brain in dystroglycanopathy. Finally, developing a pharmaceutical pipeline; since adequate treatments do not currently exist for any form of dystroglycanopathy. All these approaches overlap and therefore could feed into the central understanding of the disease, progressing the overall research forward in each of the other areas. Resource building is often synonymous with progress in scientific research and therefore is considered another essential aim of any future work that might fall into each of the categories.

6.7.1 Mechanism

Understanding more about the disease mechanism of FKRP and fukutin deficiency could provide more therapeutic opportunities, such as an autophagic response (Carmignac *et al.*, 2011), tying into the translational aims of the project. The unfolded protein response is a mechanism activated to remove mis-folded or unfolded proteins by halting translation and upregulating chaperones to remove the proteins. Upregulation of the unfolded protein response may account for a part of the mechanism of the disease however it does not explain all the aberrant findings in fkrp and fukutin deficiency (Lin *et al.*, 2011). The unfolded protein response is perhaps the first attractive therapeutic avenue. However the mechanism is only the beginning of a chain of events that includes loss of correctly glycosylated α-dystroglycan binding laminin-211. How a disrupted basement membrane as a result of a reduced dystroglycan laminin interaction results in an unfolded protein response and other autophagy pathways is of key interest. It is possible autophagy is induced by either the unfolded protein response or loss of structural components. The full pathways and how they link together are currently poorly understood (Benbrook and Long, 2012).

6.7.2 Potential Targets of FKRP and Fukutin beyond Dystroglycan

The work presented in the thesis and in (Lin *et al.*, 2011), provides evidence supporting the hypothesis that other targets for FKRP and fukutin might exist. Although the brain was not investigated, it is entirely feasible that there are novel FKRP and fukutin targets in the cortex, based on the assumption that similar mechanisms guide axons through cortical layering as retinal layering. These unknown targets outwith dystroglycan may be important, for example in processes such as anchoring or guiding the optic neuronal axons. Studies in

the dystroglycan mouse suggest that dystroglycan is redundant after axons are guided through the retinal layers and not important for adhering end feet to the ILM. The implication is that FKRP and fukutin may be important for modification of the anchor protein in this instance. Alternatively, the correct glycosylation of the novel protein may be involved in providing cues that guide the axon through the ECM of the retinal layers.

The question can therefore be posed, which targets are post-translationally modified by FKRP and fukutin? Hypothetically any protein or lipid with a mannose or yet to be determined glycan residue close to its core could be phosphorylated by fukutin or FKRP. It is also not entirely clear if the other sugars in the tetramer are essential for fukutin and FKRP to have their phosphorylation activity on mannose. Conversely, the mannose residue alone may not be sufficient for phosphoryl modification of α-dystroglycan by FKRP and fukutin. Integrin is one such potential candidate based on it occupying a similar position to dystroglycan in the sarcolemma and its ability to bind with ECM laminin. In the eye integrin-α6 is known to bind laminin-111 (Belkin and Stepp, 2000), making for an attractive alternative axis to the classic dystroglycan laminin-α2 axis in the eye. The complexity of cellular layering in the eye and brain clearly require precisely controlled development, whereas muscle in comparison is a relatively simple structure but requires a strong bond between basement membrane and sarcolemma, potentially accounting for the alternative axes in eye and muscle.

6.7.3 Developing a Pharmaceutical Pipeline

Recently zebrafish have been gaining increasing popularity in drug discovery for many of their attributes that include optical transparency, low cost and ease of genetic manipulation. The approach currently adopted in MD research is to look at changes in birefringence *i.e.* a relatively fast technique for assessment of overall muscle damage, in fish myotome after treatment with chemical compound libraries, and the *sapje* fish is an example of where this technology has been employed successfully (Winder *et al.*, 2011). Normally the chemical compound libraries are drug treatments passed for use in humans either by the Federal Drug Authority in the United States of America or European Medicines Agency. Other drug screens are based on using high throughput techniques on transgenic lines and measure the amount of fluorescence change or overall

movement after treatment. Future work that investigates whether rescuing the vascular anomalies is a good assay for the whole muscle disease could potentially feed into a pharmaceutical screen for novel compounds that improve muscle pathology in dystroglycanopathy. Stable mutants crossed with TG:(Fli1:EGFP) fish could serve as model for dystroglycanopathy since there is reduced intersegmental vessel development in the mutant fish. Recovery of muscle structure could be simultaneously assessed using birefringence, previously shown in fkrp morphant fish (Thornhill *et al.*, 2008). Lead compounds and successful therapies could then be progressed to being trialled in mouse models, an organism physiologically closer to humans.

6.8 Summary

By knocking down fkrp and fukutin with MOs to a similar extent in zebrafish, with dystroglycan knock down fish used as a comparison it was possible to elucidate a great deal more about their roles in development. Each of the dystroglycanopathy morphants had a very similar morphological muscle, eye and brain phenotype observed in the fish across the first five days of development. This study was able to comprehensively associate the dystroglycanopathy pathology with loss of basement membrane structure in muscle, notochord and eye. The key axis important for maintaining muscle integrity was thought to be the α-dystroglycan laminin axis. Based on previous studies laminin-α2 was predicted to be the predominant laminin chain responsible for maintaining fibres association with the muscle specific basement membranes of the sarcolemma and myosepta. When vasculature was investigated in the eye the loss of vascular structure in the fkrp and fukutin morphants but not dystroglycan might suggest the existence of an alternative axis to the classical α-dystroglycan laminin-α2 interaction. In my opinion a novel integrin-α6 laminin-111 axis in the eye may be associated with FKRP and fukutin. Laminin and Integrin are therefore novel candidates for post-translational modification by FKRP and fukutin, currently only known to modify mannose on the dystroglycan tetramer.

References

Ackroyd, M.R., Skordis, L., Kaluarachchi, M., Godwin, J., Prior, S., Fidanboylu, M., Piercy, R.J., Muntoni, F. and Brown, S.C. (2009) 'Reduced expression of fukutin related protein in mice results in a model for fukutin related protein associated muscular dystrophies', *Brain*, 132(Pt 2), pp. 439-51.

Ackroyd, M.R., Whitmore, C., Prior, S., Kaluarachchi, M., Nikolic, M., Mayer, U., Muntoni, F. and Brown, S.C. (2011) 'Fukutin-related protein alters the deposition of laminin in the eye and brain', *J Neurosci*, 31(36), pp. 12927-35.

Adams, M.E., Kramarcy, N., Fukuda, T., Engel, A.G., Sealock, R. and Froehner, S.C. (2004) 'Structural abnormalities at neuromuscular synapses lacking multiple syntrophin isoforms', *J Neurosci*, 24(46), pp. 10302-9.

Agathon, A., Thisse, C. and Thisse, B. (2003) 'The molecular nature of the zebrafish tail organizer', *Nature*, 424(6947), pp. 448-52.

Al-Hussaini, H., Kam, J.H., Vugler, A., Semo, M. and Jeffery, G. (2008) 'Mature retinal pigment epithelium cells are retained in the cell cycle and proliferate in vivo', *Mol Vis*, 14, pp. 1784-91.

Aldridge, J., Kunkel, L., Bruns, G., Tantravahi, U., Lalande, M., Brewster, T., Moreau, E., Wilson, M., Bromley, W., Roderick, T. and et al. (1984) 'A strategy to reveal high-frequency RFLPs along the human X chromosome', *Am J Hum Genet*, 36(3), pp. 546-64.

Alvarez, Y., Cederlund, M.L., Cottell, D.C., Bill, B.R., Ekker, S.C., Torres-Vazquez, J., Weinstein, B.M., Hyde, D.R., Vihtelic, T.S. and Kennedy, B.N. (2007) 'Genetic determinants of hyaloid and retinal vasculature in zebrafish', *BMC Dev Biol*, 7, p. 114.

Amsterdam, A., Varshney, G.K. and Burgess, S.M. (2011) 'Retroviral-mediated Insertional Mutagenesis in Zebrafish', *Methods Cell Biol*, 104, pp. 59-82.

Anderson, J.E. (1991) 'Dystrophic changes in mdx muscle regenerating from denervation and devascularization', *Muscle Nerve*, 14(3), pp. 268-79.

Aravind, L. and Koonin, E.V. (1999) 'The fukutin protein family--predicted enzymes modifying cell-surface molecules', *Curr Biol*, 9(22), pp. R836-7.

Aumailley, M., Bruckner-Tuderman, L., Carter, W.G., Deutzmann, R., Edgar, D., Ekblom, P., Engel, J., Engvall, E., Hohenester, E., Jones, J.C., Kleinman, H.K., Marinkovich, M.P., Martin, G.R., Mayer, U., Meneguzzi, G., Miner, J.H., Miyazaki, K., Patarroyo, M., Paulsson, M., Quaranta, V., Sanes, J.R., Sasaki, T., Sekiguchi, K., Sorokin, L.M., Talts, J.F., Tryggvason, K., Uitto, J., Virtanen, I., von der Mark, K., Wewer, U.M., Yamada, Y. and Yurchenco, P.D. (2005) 'A simplified laminin nomenclature', *Matrix Biol*, 24(5), pp. 326-32.

Avanesov, A. and Malicki, J. (2004) 'Approaches to study neurogenesis in the zebrafish retina', *Methods Cell Biol*, 76, pp. 333-84.

Avsar-Ban, E., Ishikawa, H., Manya, H., Watanabe, M., Akiyama, S., Miyake, H., Endo, T. and Tamaru, Y. (2010) 'Protein O-mannosylation is necessary for normal embryonic development in zebrafish', *Glycobiology*, 20(9), pp. 1089-102.

Bach, J.R. (2000) 'The Duchenne de Boulogne-Meryon controversy and pseudohypertrophic muscular dystrophy', *J Hist Med Allied Sci*, 55(2), pp. 158-78.

Bajanca, F. and Thorsteinsdottir, S. (2002) 'Integrin expression patterns during early limb muscle development in the mouse', *Gene Expr Patterns*, 2(1-2), pp. 133-6.

Balci, B., Uyanik, G., Dincer, P., Gross, C., Willer, T., Talim, B., Haliloglu, G., Kale, G., Hehr, U., Winkler, J. and Topaloglu, H. (2005) 'An autosomal recessive limb girdle muscular dystrophy (LGMD2) with mild mental retardation is allelic to Walker-Warburg syndrome (WWS) caused by a mutation in the POMT1 gene', *Neuromuscul Disord*, 15(4), pp. 271-5.

Banks, G.B. and Chamberlain, J.S. (2008) 'The value of mammalian models for duchenne muscular dystrophy in developing therapeutic strategies', *Curr Top Dev Biol*, 84, pp. 431-53.

Barresi, R. and Campbell, P. (2005) 'Dystroglycan: from biosynthesis to pathogenesis of human disease', *Journal of Cell Science*, 119(2), pp. 199-2007.

Barresi, R., Michele, D.E., Kanagawa, M., Harper, H.A., Dovico, S.A., Satz, J.S., Moore, S.A., Zhang, W., Schachter, H., Dumanski, J.P., Cohn, R.D., Nishino, I. and Campbell, K.P. (2004) 'LARGE can functionally bypass alpha-dystroglycan glycosylation defects in distinct congenital muscular dystrophies', *Nat Med*, 10(7), pp. 696-703.

Bassett, D. and Currie, P.D. (2004) 'Identification of a zebrafish model of muscular dystrophy', *Clin Exp Pharmacol Physiol*, 31(8), pp. 537-40.

Bassett, D.I., Bryson-Richardson, R.J., Daggett, D.F., Gautier, P., Keenan, D.G. and Currie, P.D. (2003) 'Dystrophin is required for the formation of stable muscle attachments in the zebrafish embryo', *Development*, 130(23), pp. 5851-60.

Bassett, D.I. and Currie, P.D. (2003) 'The zebrafish as a model for muscular dystrophy and congenital myopathy', *Hum Mol Genet*, 12 Spec No 2, pp. R265-70.

Bedell, V.M., Wang, Y., Campbell, J.M., Poshusta, T.L., Starker, C.G., Krug Ii, R.G., Tan, W., Penheiter, S.G., Ma, A.C., Leung, A.Y., Fahrenkrug, S.C.,

Carlson, D.F., Voytas, D.F., Clark, K.J., Essner, J.J. and Ekker, S.C. (2012) 'In vivo genome editing using a high-efficiency TALEN system', *Nature*.

Belkin, A.M. and Stepp, M.A. (2000) 'Integrins as receptors for laminins', *Microsc Res Tech*, 51(3), pp. 280-301.

Beltran-Valero de Bernabe, D., Currier, S., Steinbrecher, A., Celli, J., van Beusekom, E., van der Zwaag, B., Kayserili, H., Merlini, L., Chitayat, D., Dobyns, W.B., Cormand, B., Lehesjoki, A.E., Cruces, J., Voit, T., Walsh, C.A., van Bokhoven, H. and Brunner, H.G. (2002) 'Mutations in the O-mannosyltransferase gene POMT1 give rise to the severe neuronal migration disorder Walker-Warburg syndrome', *Am J Hum Genet*, 71(5), pp. 1033-43.

Beltran-Valero de Bernabe, D., Voit, T., Longman, C., Steinbrecher, A., Straub, V., Yuva, Y., Herrmann, R., Sperner, J., Korenke, C., Diesen, C., Dobyns, W.B., Brunner, H.G., van Bokhoven, H., Brockington, M. and Muntoni, F. (2004) 'Mutations in the FKRP gene can cause muscle-eye-brain disease and Walker-Warburg syndrome', *J Med Genet*, 41(5), p. e61.

Benbrook, D.M. and Long, A. (2012) 'Integration of autophagy, proteasomal degradation, unfolded protein response and apoptosis', *Exp Oncol*, 34(3), pp. 286-97.

Bertini, E., D'Amico, A., Gualandi, F. and Petrini, S. (2011) 'Congenital muscular dystrophies: a brief review', *Semin Pediatr Neurol*, 18(4), pp. 277-88.

Bharti, K., Nguyen, M.T., Skuntz, S., Bertuzzi, S. and Arnheiter, H. (2006) 'The other pigment cell: specification and development of the pigmented epithelium of the vertebrate eye', *Pigment Cell Res*, 19(5), pp. 380-94.

Bill, B.R., Petzold, A.M., Clark, K.J., Schimmenti, L.A. and Ekker, S.C. (2009) 'A primer for morpholino use in zebrafish', *Zebrafish*, 6(1), pp. 69-77.

Boettiger, D. (2012) 'Mechanical control of integrin-mediated adhesion and signaling', *Curr Opin Cell Biol*.

Bogdanik, L., Framery, B., Frolich, A., Franco, B., Mornet, D., Bockaert, J., Sigrist, S.J., Grau, Y. and Parmentier, M.L. (2008) 'Muscle dystroglycan organizes the postsynapse and regulates presynaptic neurotransmitter release at the Drosophila neuromuscular junction', *PLoS One*, 3(4), p. e2084.

Bohm, S.V. and Roberts, R.G. (2009) 'Expression of members of the dystrophin, dystrobrevin, and dystrotelin superfamily', *Crit Rev Eukaryot Gene Expr*, 19(2), pp. 89-108.

Boncinelli, E. and Morgan, R. (2001) 'Downstream of Otx2, or how to get a head', *Trends Genet*, 17(11), pp. 633-6.

Bork, P., Downing, A.K., Kieffer, B. and Campbell, I.D. (1996) 'Structure and distribution of modules in extracellular proteins', *Q Rev Biophys*, 29(2), pp. 119-67.

Bourteel, H., Vermersch, P., Cuisset, J.M., Maurage, C.A., Laforet, P., Richard, P. and Stojkovic, T. (2009) 'Clinical and mutational spectrum of limb-girdle muscular dystrophy type 2I in 11 French patients', *J Neurol Neurosurg Psychiatry*, 80(12), pp. 1405-8.

Bowe, M.A., Mendis, D.B. and Fallon, J.R. (2000) 'The Small Leucine-rich Repeat Proteoglycan Biglycan Binds to α-Dystroglycan and Is Upregulated in Dystrophic Muscle' *J Cell Biology*, 148(4), pp. 801-10.

Boyd, Y. and Buckle, V.J. (1986) 'Cytogenetic heterogeneity of translocations associated with Duchenne muscular dystrophy', *Clin Genet*, 29(2), pp. 108-15.

Bozic, D., Sciandra, F., Lamba, D. and Brancaccio, A. (2004) 'The Structure of the N-terminal Region of Murine Skeletal Muscle a-Dystroglycan Discloses a Modular Architecture', *The Journal of Biological Chemistry*, 279(43), pp. 44812-44816.

Bozzi, M., Bianchi, M., Sciandra, F., Paci, M., Giardina, B., Brancaccio, A. and Cicero, D.O. (2003) 'Structural characterization by NMR of the natively unfolded extracellular domain of beta-dystroglycan: toward the identification of the binding epitope for alpha-dystroglycan', *Biochemistry*, 42(46), pp. 13717-24.

Bozzi, M., Morlacchi, S., Bigotti, M.G., Sciandra, F. and Brancaccio, A. (2009) 'Functional diversity of dystroglycan', *Matrix Biol*, 28(4), pp. 179-87.

Bozzi, M., Sciandra, F., Ferri, L., Torreri, P., Pavoni, E., Petrucci, T.C., Giardina, B. and Brancaccio, A. (2006) 'Concerted mutation of Phe residues belonging to the beta-dystroglycan ectodomain strongly inhibits the interaction with alpha-dystroglycan in vitro', *Febs J*, 273(21), pp. 4929-43.

Brancaccio, A., Schulthess, T., Gesemann, M. and Engel, J. (1995) 'Electron microscopic evidence for a mucin-like region in chick muscle alpha-dystroglycan', *FEBS Lett*, 368(1), pp. 139-42.

Brancaccio, A., Schulthess, T., Gesemann, M. and Engel, J. (1997) 'The N-terminal region of alpha-dystroglycan is an autonomous globular domain', *Eur J Biochem*, 246(1), pp. 166-72.

Breedveld, G., de Coo, I.F., Lequin, M.H., Arts, W.F., Heutink, P., Gould, D.B., John, S.W., Oostra, B. and Mancini, G.M. (2006) 'Novel mutations in three families confirm a major role of COL4A1 in hereditary porencephaly', *J Med Genet*, 43(6), pp. 490-5.

Breton, C. and Imberty, A. (1999) 'Structure/function studies of glycosyltransferases', *Curr Opin Struct Biol*, 9(5), pp. 563-71.

Bringmann, A. and Wiedemann, P. (2009) 'Involvement of Muller glial cells in epiretinal membrane formation', *Graefes Arch Clin Exp Ophthalmol*, 247(7), pp. 865-83.

Brockdorff, N., Cross, G.S., Cavanna, J.S., Fisher, E.M., Lyon, M.F., Davies, K.E. and Brown, S.D. (1987) 'The mapping of a cDNA from the human X-linked Duchenne muscular dystrophy gene to the mouse X chromosome', *Nature*, 328(6126), pp. 166-8.

Brockington, M., Blake, D.J., Brown, S.C. and Muntoni, F. (2002) 'The gene for a novel glycosyltransferase is mutated in congenital muscular dystrophy MDC1C and limb girdle muscular dystrophy 2I', *Neuromuscul Disord*, 12(3), pp. 233-4.

Brockington, M., Blake, D.J., Prandini, P., Brown, S.C., Torelli, S., Benson, M.A., Ponting, C.P., Estournet, B., Romero, N.B., Mercuri, E., Voit, T., Sewry, C.A., Guicheney, P. and Muntoni, F. (2001a) 'Mutations in the fukutin-related protein gene (FKRP) cause a form of congenital muscular dystrophy with secondary laminin alpha2 deficiency and abnormal glycosylation of alpha-dystroglycan', *Am J Hum Genet*, 69(6), pp. 1198-209.

Brockington, M., Torelli, S., Prandini, P., Boito, C., Dolatshad, N.F., Longman, C., Brown, S.C. and Muntoni, F. (2005) 'Localization and functional analysis of the LARGE family of glycosyltransferases: significance for muscular dystrophy', *Hum Mol Genet*, 14(5), pp. 657-65.

Brockington, M., Yuva, Y., Prandini, P., Brown, S.C., Torelli, S., Benson, M.A., Herrmann, R., Anderson, L.V., Bashir, R., Burgunder, J.M., Fallet, S., Romero, N., Fardeau, M., Straub, V., Storey, G., Pollitt, C., Richard, I., Sewry, C.A., Bushby, K., Voit, T., Blake, D.J. and Muntoni, F. (2001b) 'Mutations in the fukutin-related protein gene (FKRP) identify limb girdle muscular dystrophy 2I as a milder allelic variant of congenital muscular dystrophy MDC1C', *Hum Mol Genet*, 10(25), pp. 2851-9.

Broglio, L., Tentorio, M., Cotelli, M.S., Mancuso, M., Vielmi, V., Gregorelli, V., Padovani, A. and Filosto, M. (2010) 'Limb-girdle muscular dystrophy-associated protein diseases', *Neurologist*, 16(6), pp. 340-52.

Brown, C.S., Pearson, P.L., Thomas, N.S., Sarfarazi, M., Harper, P.S. and Shaw, D.J. (1985) 'Linkage analysis of a DNA polymorphism proximal to the Duchenne and Becker muscular dystrophy loci on the short arm of the X chromosome', *J Med Genet*, 22(3), pp. 179-81.

Brown, D.D. (1984) 'The role of stable complexes that repress and activate eucaryotic genes', *Cell*, 37(2), pp. 359-65.

Bulfield, G., Siller, W.G., Wight, P.A. and Moore, K.J. (1984) 'X chromosome-linked muscular dystrophy (mdx) in the mouse', *Proc Natl Acad Sci U S A*, 81(4), pp. 1189-92.

Burda, P. and Aebi, M. (1999) 'The dolichol pathway of N-linked glycosylation', *Biochim Biophys Acta*, 1426(2), pp. 239-57.

Burkin, D.J. and Kaufman, S.J. (1999) 'The alpha7beta1 integrin in muscle development and disease', *Cell Tissue Res*, 296(1), pp. 183-90.

Bushby, K. (2009) 'Diagnosis and management of the limb girdle muscular dystrophies', *Pract Neurol*, 9(6), pp. 314-23.

Bushby, K., Lynn, S. and Straub, T. (2009) 'Collaborating to bring new therapies to the patient--the TREAT-NMD model', *Acta Myol*, 28(1), pp. 12-5.

Bushby, K.M. (1994) 'The muscular dystrophies', *Baillieres Clin Neurol*, 3(2), pp. 407-30.

Calderwood, D.A., Huttenlocher, A., Kiosses, W.B., Rose, D.M., Woodside, D.G., Schwartz, M.A. and Ginsberg, M.H. (2001) 'Increased filamin binding to beta-integrin cytoplasmic domains inhibits cell migration', *Nat Cell Biol*, 3(12), pp. 1060-8.

Campanelli, J.T., Roberds, S.L., Campbell, K.P. and Scheller, R.H. (1994) 'A role for dystrophin-associated glycoproteins and utrophin in agrin-induced AChR clustering', *Cell*, 77(5), pp. 663-74.

Campbell, K.P. and Kahl, S.D. (1989) 'Association of dystrophin and an integral membrane glycoprotein', *Nature*, 338(6212), pp. 259-62.

Cao, W., Henry, M.D., Borrow, P., Yamada, H., Elder, J.H., Ravkov, E.V., Nichol, S.T., Compans, R.W., Campbell, K.P. and Oldstone, M.B. (1998) 'Identification of alpha-dystroglycan as a receptor for lymphocytic choriomeningitis virus and Lassa fever virus', *Science*, 282(5396), pp. 2079-81.

Carmignac, V., Svensson, M., Korner, Z., Elowsson, L., Matsumura, C., Gawlik, K.I., Allamand, V. and Durbeej, M. (2011) 'Autophagy is increased in laminin alpha2 chain-deficient muscle and its inhibition improves muscle morphology in a mouse model of MDC1A', *Hum Mol Genet*, 20(24), pp. 4891-902.

Carson, J.A. and Wei, L. (2000) 'Integrin signaling's potential for mediating gene expression in hypertrophying skeletal muscle', *J Appl Physiol*, 88(1), pp. 337-43.

Cazzato, G. (1968) 'Considerations about a possible role played by connective tissue proliferation and vascular disturbances in the pathogenesis of progressive muscular dystrophy', *Eur Neurol*, 1(3), pp. 158-79.

Cha, Y.R. and Weinstein, B.M. (2007) 'Visualization and experimental analysis of blood vessel formation using transgenic zebrafish', *Birth Defects Res C Embryo Today*, 81(4), pp. 286-96.

Chamberlain, J.S. and Benian, G.M. (2000) 'Muscular dystrophy: the worm turns to genetic disease', *Curr Biol*, 10(21), pp. R795-7.

Chiba, A., Matsumura, K., Yamada, H., Inazu, T., Shimizu, T., Kusunoki, S., Kanazawa, I., Kobata, A. and Endo, T. (1997) 'Structures of sialylated O-linked oligosaccharides of bovine peripheral nerve alpha-dystroglycan. The role of a novel O-mannosyl-type oligosaccharide in the binding of alpha-dystroglycan with laminin', *J Biol Chem*, 272(4), pp. 2156-62.

Childs, S., Chen, J.N., Garrity, D.M. and Fishman, M.C. (2002) 'Patterning of angiogenesis in the zebrafish embryo', *Development*, 129(4), pp. 973-82.

Chiyonobu, T., Sasaki, J., Nagai, Y., Takeda, S., Funakoshi, H., Nakamura, T., Sugimoto, T. and Toda, T. (2005) 'Effects of fukutin deficiency in the developing mouse brain', *Neuromuscul Disord*, 15(6), pp. 416-26.

Choo, Y., Sanchez-Garcia, I. and Klug, A. (1994) 'In vivo repression by a site-specific DNA-binding protein designed against an oncogenic sequence', *Nature*, 372(6507), pp. 642-5.

Chow, R.L. and Lang, R.A. (2001) 'Early eye development in vertebrates', *Annu Rev Cell Dev Biol*, 17, pp. 255-96.

Chuang, J.C. and Raymond, P.A. (2002) 'Embryonic origin of the eyes in teleost fish', *Bioessays*, 24(6), pp. 519-29.

Clark, M.D., Guryev, V., Bruijn, E., Nijman, I.J., Tada, M., Wilson, C., Deloukas, P., Postlethwait, J.H., Cuppen, E. and Stemple, D.L. (2011) 'Single nucleotide polymorphism (SNP) panels for rapid positional cloning in zebrafish', *Methods Cell Biol*, 104, pp. 219-35.

Cohn, R.D. and Campbell, K.P. (2000) 'Molecular basis of muscular dystrophies', *Muscle Nerve*, 23(10), pp. 1456-71.

Cohn, R.D., Henry, M.D., Michele, D.E., Barresi, R., Saito, F., Moore, S.A., Flanagan, J.D., Skwarchuk, M.W., Robbins, M.E., Mendell, J.R., Williamson, R.A. and Campbell, K.P. (2002) 'Disruption of DAG1 in differentiated skeletal muscle reveals a role for dystroglycan in muscle regeneration', *Cell*, 110(5), pp. 639-48.

Colombo, R., Bignamini, A.A., Carobene, A., Sasaki, J., Tachikawa, M., Kobayashi, K. and Toda, T. (2000) 'Age and origin of the FCMD 3'-untranslated-region retrotransposal insertion mutation causing Fukuyama-type congenital muscular dystrophy in the Japanese population', *Hum Genet*, 107(6), pp. 559-67.

Conte G, G.L. (1836) *Annali Clinici dell'Ospedale degl'Incurabili di Napoli*.

Corbi, N., Libri, V., Onori, A. and Passananti, C. (2004) 'Synthetic zinc finger peptides: old and novel applications', *Biochem Cell Biol*, 82(4), pp. 428-36.

Cote, P.D., Moukhles, H., Lindenbaum, M. and Carbonetto, S. (1999) 'Chimaeric mice deficient in dystroglycans develop muscular dystrophy and have disrupted myoneural synapses', *Nat Genet*, 23(3), pp. 338-42.

Cowan, J., Macdessi, J., Stark, A. and Morgan, G. (1980) 'Incidence of Duchenne muscular dystrophy in New South Wales and Australian Capital Territory', *J Med Genet*, 17(4), pp. 245-9.

Cox, G.A., Phelps, S.F., Chapman, V.M. and Chamberlain, J.S. (1993) 'New mdx mutation disrupts expression of muscle and nonmuscle isoforms of dystrophin', *Nat Genet*, 4(1), pp. 87-93.

Crosbie, R.H. (2001) 'NO vascular control in Duchenne muscular dystrophy', *Nat Med*, 7(1), pp. 27-9.

Crosbie, R.H., Lebakken, C.S., Holt, K.H., Venzke, D.P., Straub, V., Lee, J.C., Grady, R.M., Chamberlain, J.S., Sanes, J.R. and Campbell, K.P. (1999) 'Membrane targeting and stabilization of sarcospan is mediated by the sarcoglycan subcomplex', *J Cell Biol*, 145(1), pp. 153-65.

Dabire, H., Barthelemy, I., Blanchard-Gutton, N., Sambin, L., Sampedrano, C.C., Gouni, V., Unterfinger, Y., Aguilar, P., Thibaud, J.L., Ghaleh, B., Bize, A., Pouchelon, J.L., Blot, S., Berdeaux, A., Hittinger, L., Chetboul, V. and Su, J.B. (2012) 'Vascular endothelial dysfunction in Duchenne muscular dystrophy is restored by bradykinin through upregulation of eNOS and nNOS', *Basic Res Cardiol*, 107(1), p. 240.

Dahm, R., Schonthaler, H.B., Soehn, A.S., van Marle, J. and Vrensen, G.F. (2007) 'Development and adult morphology of the eye lens in the zebrafish', *Exp Eye Res*, 85(1), pp. 74-89.

Davies, K.E., Pearson, P.L., Harper, P.S., Murray, J.M., O'Brien, T., Sarfarazi, M. and Williamson, R. (1983) 'Linkage analysis of two cloned DNA sequences flanking the Duchenne muscular dystrophy locus on the short arm of the human X chromosome', *Nucleic Acids Res*, 11(8), pp. 2303-12.

de Bernabe, D.B., van Bokhoven, H., van Beusekom, E., Van den Akker, W., Kant, S., Dobyns, W.B., Cormand, B., Currier, S., Hamel, B., Talim, B., Topaloglu, H. and Brunner, H.G. (2003) 'A homozygous nonsense mutation in the fukutin gene causes a Walker-Warburg syndrome phenotype', *J Med Genet*, 40(11), pp. 845-8.

De la Porte, S., Morin, S. and Koenig, J. (1999) 'Characteristics of skeletal muscle in mdx mutant mice', *Int Rev Cytol*, 191, pp. 99-148.

Deconinck, A.E., Rafael, J.A., Skinner, J.A., Brown, S.C., Potter, A.C., Metzinger, L., Watt, D.J., Dickson, J.G., Tinsley, J.M. and Davies, K.E. (1997) 'Utrophin-dystrophin-deficient mice as a model for Duchenne muscular dystrophy', *Cell*, 90(4), pp. 717-27.

Demany, M.A. and Zimmerman, H.A. (1969) 'Progressive muscular dystrophy. Hemodynamic, angiographic, and pathologic study of a patient with myocardial involvement', *Circulation*, 40(3), pp. 377-84.

Denzer, A.J., Brandenberger, R., Gesemann, M., Chiquet, M. and Ruegg, M.A. (1997) 'Agrin binds to the nerve-muscle basal lamina via laminin', *J Cell Biol*, 137(3), pp. 671-83.

Deufel, T. and Gerbitz, K.D. (1991) 'Biochemistry and molecular genetics of muscle diseases', *Eur J Clin Chem Clin Biochem*, 29(1), pp. 13-38.

Dong, J. and Stuart, G.W. (2004) 'Transgene manipulation in zebrafish by using recombinases', *Methods Cell Biol*, 77, pp. 363-79.

Dowling, J.J., Vreede, A.P., Low, S.E., Gibbs, E.M., Kuwada, J.Y., Bonnemann, C.G. and Feldman, E.L. (2009) 'Loss of myotubularin function results in T-tubule disorganization in zebrafish and human myotubular myopathy', *PLoS Genet*, 5(2), p. e1000372.

Draper, B.W., Morcos, P.A. and Kimmel, C.B. (2001) 'Inhibition of zebrafish fgf8 pre-mRNA splicing with morpholino oligos: a quantifiable method for gene knockdown', *Genesis*, 30(3), pp. 154-6.

Drummond AJ, A.B., Buxton S, Cheung M, Cooper A, Duran C, Field M, Heled J, Kearse M, Markowitz S, Moir R, Stones-Havas S, Sturrock S, Thierer T, Wilson (2011) 'A Geneious v5.4,'.

Durbeej, M. (2010) 'Laminins', *Cell Tissue Res*, 339(1), pp. 259-68.

Durbeej, M. and Campbell, K.P. (2002) 'Muscular dystrophies involving the dystrophin-glycoprotein complex: an overview of current mouse models', *Curr Opin Genet Dev*, 12(3), pp. 349-61.

Durbeej, M., Cohn, R.D., Hrstka, R.F., Moore, S.A., Allamand, V., Davidson, B.L., Williamson, R.A. and Campbell, K.P. (2000) 'Disruption of the beta-sarcoglycan gene reveals pathogenetic complexity of limb-girdle muscular dystrophy type 2E', *Mol Cell*, 5(1), pp. 141-51.

Eguchi, S., Oshiro, N., Miyamoto, T., Yoshino, K., Okamoto, S., Ono, T., Kikkawa, U. and Yonezawa, K. (2009) 'AMP-activated protein kinase phosphorylates glutamine : fructose-6-phosphate amidotransferase 1 at Ser243 to modulate its enzymatic activity', *Genes Cells*, 14(2), pp. 179-89.

Ellertsdottir, E., Lenard, A., Blum, Y., Krudewig, A., Herwig, L., Affolter, M. and Belting, H.G. (2010) 'Vascular morphogenesis in the zebrafish embryo', *Dev Biol*, 341(1), pp. 56-65.

Emery, A.E. (1993) 'Duchenne muscular dystrophy--Meryon's disease', *Neuromuscul Disord*, 3(4), pp. 263-6.

Endo, T. (1999) 'O-mannosyl glycans in mammals', *Biochim Biophys Acta*, 1473(1), pp. 237-46.

Ervasti, J.M. and Campbell, K.P. (1991) 'Membrane organization of the dystrophin-glycoprotein complex', *Cell*, 66(6), pp. 1121-31.

Ervasti, J.M. and Campbell, K.P. (1993) 'A role for the dystrophin-glycoprotein complex as a transmembrane linker between laminin and actin', *J Cell Biol*, 122(4), pp. 809-23.

Esapa, C.T., Benson, M.A., Schroder, J.E., Martin-Rendon, E., Brockington, M., Brown, S.C., Muntoni, F., Kroger, S. and Blake, D.J. (2002) 'Functional requirements for fukutin-related protein in the Golgi apparatus', *Hum Mol Genet*, 11(26), pp. 3319-31.

Fadool, J.M. and Dowling, J.E. (2008) 'Zebrafish: a model system for the study of eye genetics', *Prog Retin Eye Res*, 27(1), pp. 89-110.

Fan, L. and Collodi, P. (2006) 'Zebrafish embryonic stem cells', *Methods Enzymol*, 418, pp. 64-77.

Favreau, C., Delbarre, E., Courvalin, J.C. and Buendia, B. (2008) 'Differentiation of C2C12 myoblasts expressing lamin A mutated at a site responsible for Emery-Dreifuss muscular dystrophy is improved by inhibition of the MEK-ERK pathway and stimulation of the PI3-kinase pathway', *Exp Cell Res*, 314(6), pp. 1392-405.

Feitosa, N.M., Richardson, R., Bloch, W. and Hammerschmidt, M. (2011) 'Basement membrane diseases in zebrafish', *Methods Cell Biol*, 105, pp. 191-222.

Foley, J.E., Maeder, M.L., Pearlberg, J., Joung, J.K., Peterson, R.T. and Yeh, J.R. (2009) 'Targeted mutagenesis in zebrafish using customized zinc-finger nucleases', *Nat Protoc*, 4(12), pp. 1855-67.

Forsberg, H., Crozet, F. and Brown, N.A. (1998) 'Waves of mouse Lunatic fringe expression, in four-hour cycles at two-hour intervals, precede somite boundary formation', *Curr Biol*, 8(18), pp. 1027-30.

Foster, H., Popplewell, L. and Dickson, G. (2012) 'Genetic therapeutic approaches for duchenne muscular dystrophy', *Hum Gene Ther*, 23(7), pp. 676-87.

Fouquet, B., Weinstein, B.M., Serluca, F.C. and Fishman, M.C. (1997) 'Vessel patterning in the embryo of the zebrafish: guidance by notochord', *Dev Biol*, 183(1), pp. 37-48.

Francke, U., Ochs, H.D., de Martinville, B., Giacalone, J., Lindgren, V., Disteche, C., Pagon, R.A., Hofker, M.H., van Ommen, G.J., Pearson, P.L. and et al. (1985) 'Minor Xp21 chromosome deletion in a male associated with expression of Duchenne muscular dystrophy, chronic granulomatous disease, retinitis pigmentosa, and McLeod syndrome', *Am J Hum Genet*, 37(2), pp. 250-67.

Froehner, S.C., Adams, M.E., Peters, M.F. and Gee, S.H. (1997) 'Syntrophins: modular adapter proteins at the neuromuscular junction and the sarcolemma', *Soc Gen Physiol Ser*, 52, pp. 197-207.

Frosk, P., Greenberg, C.R., Tennese, A.A., Lamont, R., Nylen, E., Hirst, C., Frappier, D., Roslin, N.M., Zaik, M., Bushby, K., Straub, V., Zatz, M., de Paula, F., Morgan, K., Fujiwara, T.M. and Wrogemann, K. (2005) 'The most common mutation in FKRP causing limb girdle muscular dystrophy type 2I (LGMD2I) may have occurred only once and is present in Hutterites and other populations', *Hum Mutat*, 25(1), pp. 38-44.

Fu, G., Wang, W. and Luo, B.H. (2012) 'Overview: structural biology of integrins', *Methods Mol Biol*, 757, pp. 81-99.

Fuentes-Mera, L., Rodriguez-Munoz, R., Gonzalez-Ramirez, R., Garcia-Sierra, F., Gonzalez, E., Mornet, D. and Cisneros, B. (2006) 'Characterization of a novel Dp71 dystrophin-associated protein complex (DAPC) present in the nucleus of HeLa cells: members of the nuclear DAPC associate with the nuclear matrix', *Exp Cell Res*, 312(16), pp. 3023-35.

Fuhrmann, S. (2008) 'Wnt signaling in eye organogenesis', *Organogenesis*, 4(2), pp. 60-7.

Fuhrmann, S. (2010) 'Eye morphogenesis and patterning of the optic vesicle', *Curr Top Dev Biol*, 93, pp. 61-84.

Fukai, N., Eklund, L., Marneros, A.G., Oh, S.P., Keene, D.R., Tamarkin, L., Niemela, M., Ilves, M., Li, E., Pihlajaniemi, T. and Olsen, B.R. (2002) 'Lack of collagen XVIII/endostatin results in eye abnormalities', *EMBO J*, 21(7), pp. 1535-44.

Fukuyama, Y., Osawa, M. and Suzuki, H. (1981) 'Congenital progressive muscular dystrophy of the Fukuyama type - clinical, genetic and pathological considerations', *Brain Dev*, 3(1), pp. 1-29.

Gee, S.H., Montanaro, F., Lindenbaum, M.H. and Carbonetto, S. (1994) 'Dystroglycan-alpha, a dystrophin-associated glycoprotein, is a functional agrin receptor', *Cell*, 77(5), pp. 675-86.

Gillies, A.R. and Lieber, R.L. (2011) 'Structure and function of the skeletal muscle extracellular matrix', *Muscle Nerve*, 44(3), pp. 318-31.

Gillis, J.M. (2000) 'An attempt of gene therapy in Duchenne muscular dystrophy: overexpression of utrophin in transgenic mdx mice', *Acta Neurol Belg*, 100(3), pp. 146-50.

Goder, V. and Melero, A. (2011) 'Protein O-mannosyltransferases participate in ER protein quality control', *J Cell Sci*, 124(Pt 1), pp. 144-53.

Godfrey, C., Escolar, D., Brockington, M., Clement, E.M., Mein, R., Jimenez-Mallebrera, C., Torelli, S., Feng, L., Brown, S.C., Sewry, C.A., Rutherford, M., Shapira, Y., Abbs, S. and Muntoni, F. (2006) 'Fukutin gene mutations in steroid-responsive limb girdle muscular dystrophy', *Ann Neurol*, 60(5), pp. 603-10.

Godfrey, C., Foley, A.R., Clement, E. and Muntoni, F. (2011) 'Dystroglycanopathies: coming into focus', *Curr Opin Genet Dev*, 21(3), pp. 278-85.

Gore, A.V., Monzo, K., Cha, Y.R., Pan, W. and Weinstein, B.M. (2012) 'Vascular development in the zebrafish', *Cold Spring Harb Perspect Med*, 2(5), p. a006684.

Gorecki, D.C., Derry, J.M. and Barnard, E.A. (1994) 'Dystroglycan: brain localisation and chromosome mapping in the mouse', *Hum Mol Genet*, 3(9), pp. 1589-97.

Gossen, M. and Bujard, H. (1992) 'Tight control of gene expression in mammalian cells by tetracycline-responsive promoters', *Proc Natl Acad Sci U S A*, 89(12), pp. 5547-51.

Gottsch, J.D., Zhang, C., Sundin, O.H., Bell, W.R., Stark, W.J. and Green, W.R. (2005) 'Fuchs corneal dystrophy: aberrant collagen distribution in an L450W mutant of the COL8A2 gene', *Invest Ophthalmol Vis Sci*, 46(12), pp. 4504-11.

Gould, D.B., Phalan, F.C., Breedveld, G.J., van Mil, S.E., Smith, R.S., Schimenti, J.C., Aguglia, U., van der Knaap, M.S., Heutink, P. and John, S.W. (2005) 'Mutations in Col4a1 cause perinatal cerebral hemorrhage and porencephaly', *Science*, 308(5725), pp. 1167-71.

Grady, R.M., Teng, H., Nichol, M.C., Cunningham, J.C., Wilkinson, R.S. and Sanes, J.R. (1997) 'Skeletal and cardiac myopathies in mice lacking utrophin and dystrophin: a model for Duchenne muscular dystrophy', *Cell*, 90(4), pp. 729-38.

Grewal, P.K., Holzfeind, P.J., Bittner, R.E. and Hewitt, J.E. (2001) 'Mutant glycosyltransferase and altered glycosylation of alpha-dystroglycan in the myodystrophy mouse', *Nat Genet*, 28(2), pp. 151-4.

Grindley, J.C., Davidson, D.R. and Hill, R.E. (1995) 'The role of Pax-6 in eye and nasal development', *Development*, 121(5), pp. 1433-42.

Gumerson, J.D. and Michele, D.E. (2011) 'The dystrophin-glycoprotein complex in the prevention of muscle damage', *J Biomed Biotechnol*, 2011, p. 210797.

Gupta, V., Kawahara, G., Gundry, S.R., Chen, A.T., Lencer, W.I., Zhou, Y., Zon, L.I., Kunkel, L.M. and Beggs, A.H. (2011) 'The zebrafish dag1 mutant: A novel genetic model for dystroglycanopathies', *Hum Mol Genet*.

Guyon, J.R., Mosley, A.N., Zhou, Y., O'Brien, K.F., Sheng, X., Chiang, K., Davidson, A.J., Volinski, J.M., Zon, L.I. and Kunkel, L.M. (2003) 'The dystrophin associated protein complex in zebrafish', *Hum Mol Genet*, 12(6), pp. 601-15.

Guyon, J.R., Steffen, L.S., Howell, M.H., Pusack, T.J., Lawrence, C. and Kunkel, L.M. (2007) 'Modeling human muscle disease in zebrafish', *Biochim Biophys Acta*, 1772(2), pp. 205-15.

Haenggi, T. and Fritschy, J.M. (2006) 'Role of dystrophin and utrophin for assembly and function of the dystrophin glycoprotein complex in non-muscle tissue', *Cell Mol Life Sci*, 63(14), pp. 1614-31.

Halfter, W., Willem, M. and Mayer, U. (2005) 'Basement membrane-dependent survival of retinal ganglion cells', *Invest Ophthalmol Vis Sci*, 46(3), pp. 1000-9.

Hall, H., Bozic, D., Michel, K. and Hubell, J. (2003) 'N-terminal alpha-dystroglycan binds to different extracellular matrix molecules expressed in regenerating peripheral nerves in a protein-mediated manner and promotes neurite extension of PC12 cells.', *Molecular Nueroscience*, 24, pp. 1062-1073.

Hall, T.E., Bryson-Richardson, R.J., Berger, S., Jacoby, A.S., Cole, N.J., Hollway, G.E., Berger, J. and Currie, P.D. (2007) 'The zebrafish candyfloss mutant implicates extracellular matrix adhesion failure in laminin alpha2-deficient congenital muscular dystrophy', *Proc Natl Acad Sci U S A*, 104(17), pp. 7092-7.

Hansen, K., Coussens, M.J., Sago, J., Subramanian, S., Gjoka, M. and Briner, D. (2012) 'Genome editing with CompoZr custom zinc finger nucleases (ZFNs)', *J Vis Exp*, (64), p. e3304.

Hara, Y., Balci-Hayta, B., Yoshida-Moriguchi, T., Kanagawa, M., Beltran-Valero de Bernabe, D., Gundesli, H., Willer, T., Satz, J.S., Crawford, R.W., Burden, S.J., Kunz, S., Oldstone, M.B., Accardi, A., Talim, B., Muntoni, F., Topaloglu, H., Dincer, P. and Campbell, K.P. (2011) 'A dystroglycan mutation associated with limb-girdle muscular dystrophy', *N Engl J Med*, 364(10), pp. 939-46.

Harland, R. and Gerhart, J. (1997) 'Formation and function of Spemann's organizer', *Annu Rev Cell Dev Biol*, 13, pp. 611-67.

Harper, S.Q., Crawford, R.W., DelloRusso, C. and Chamberlain, J.S. (2002) 'Spectrin-like repeats from dystrophin and alpha-actinin-2 are not functionally interchangeable', *Hum Mol Genet*, 11(16), pp. 1807-15.

Heasman, J. (2002) 'Morpholino oligos: making sense of antisense?', *Dev Biol*, 243(2), pp. 209-14.

Hehr, U., Uyanik, G., Gross, C., Walter, M.C., Bohring, A., Cohen, M., Oehl-Jaschkowitz, B., Bird, L.M., Shamdeen, G.M., Bogdahn, U., Schuierer, G., Topaloglu, H., Aigner, L., Lochmuller, H. and Winkler, J. (2007) 'Novel POMGnT1 mutations define broader phenotypic spectrum of muscle-eye-brain disease', *Neurogenetics*, 8(4), pp. 279-88.

Herson, S., Hentati, F., Rigolet, A., Behin, A., Romero, N.B., Leturcq, F., Laforet, P., Maisonobe, T., Amouri, R., Haddad, H., Audit, M., Montus, M., Masurier, C., Gjata, B., Georger, C., Cherai, M., Carlier, P., Hogrel, J.Y., Herson, A., Allenbach, Y., Lemoine, F.M., Klatzmann, D., Sweeney, H.L., Mulligan, R.C., Eymard, B., Caizergues, D., Voit, T. and Benveniste, O. (2012) 'A phase I trial of adeno-associated virus serotype 1-gamma-sarcoglycan gene therapy for limb girdle muscular dystrophy type 2C', *Brain*, 135(Pt 2), pp. 483-92.

Hewitt, J.E. (2009) 'Abnormal glycosylation of dystroglycan in human genetic disease', *Biochim Biophys Acta*, 1792(9), pp. 853-61.

Hino, N., Kobayashi, M., Shibata, N., Yamamoto, T., Saito, K. and Osawa, M. (2001) 'Clinicopathological study on eyes from cases of Fukuyama type congenital muscular dystrophy', *Brain Dev*, 23(2), pp. 97-107.

Hoffman, E.P., Brown, R.H., Jr. and Kunkel, L.M. (1987) 'Dystrophin: the protein product of the Duchenne muscular dystrophy locus', *Cell*, 51(6), pp. 919-28.

Hogan, B.L., Barlow, D.P. and Kurkinen, M. (1984) 'Reichert's membrane as a model for studying the biosynthesis and assembly of basement membrane components', *Ciba Found Symp*, 108, pp. 60-74.

Hogan, B.L., Cooper, A.R. and Kurkinen, M. (1980) 'Incorporation into Reichert's membrane of laminin-like extracellular proteins synthesized by parietal endoderm cells of the mouse embryo', *Dev Biol*, 80(2), pp. 289-300.

Hohenester, E., Tisi, D., Talts, J.F. and Timpl, R. (1999) 'The crystal structure of a laminin G-like module reveals the molecular basis of alpha-dystroglycan binding to laminins, perlecan, and agrin', *Mol Cell*, 4(5), pp. 783-92.

Holley, S.A., Geisler, R. and Nusslein-Volhard, C. (2000) 'Control of her1 expression during zebrafish somitogenesis by a delta-dependent oscillator and an independent wave-front activity', *Genes Dev*, 14(13), pp. 1678-90.

Holley, S.A. and Nusslein-Volhard, C. (2000) 'Somitogenesis in zebrafish', *Curr Top Dev Biol*, 47, pp. 247-77.

Holt, K.H., Crosbie, R.H., Venzke, D.P. and Campbell, K.P. (2000) 'Biosynthesis of dystroglycan: processing of a precursor propeptide', *FEBS Lett*, 468(1), pp. 79-83.

Hopfer, U., Fukai, N., Hopfer, H., Wolf, G., Joyce, N., Li, E. and Olsen, B.R. (2005) 'Targeted disruption of Col8a1 and Col8a2 genes in mice leads to anterior segment abnormalities in the eye', *FASEB J*, 19(10), pp. 1232-44.

Horie, M., Kobayashi, K., Takeda, S., Nakamura, Y., Lyons, G.E. and Toda, T. (2002) 'Isolation and characterization of the mouse ortholog of the Fukuyama-type congenital muscular dystrophy gene', *Genomics*, 80(5), pp. 482-6.

Hosokawa, H., Ninomiya, H., Kitamura, Y., Fujiwara, K. and Masaki, T. (2002) 'Vascular endothelial cells that express dystroglycan are involved in angiogenesis', *J Cell Sci*, 115(Pt 7), pp. 1487-96.

Huang, P., Xiao, A., Zhou, M., Zhu, Z., Lin, S. and Zhang, B. (2011) 'Heritable gene targeting in zebrafish using customized TALENs', *Nat Biotechnol*, 29(8), pp. 699-700.

Hynes, R.O. (1992) 'Integrins: versatility, modulation, and signaling in cell adhesion', *Cell*, 69(1), pp. 11-25.

Ibraghimov-Beskrovnaya, O., Ervasti, J.M., Leveille, C.J., Slaughter, C.A., Sernett, S.W. and Campbell, K.P. (1992) 'Primary structure of dystrophin-associated glycoproteins linking dystrophin to the extracellular matrix', *Nature*, 355(6362), pp. 696-702.

Ibraghimov-Beskrovnaya, O., Milatovich, A., Ozcelik, T., Yang, B., Koepnick, K., Francke, U. and Campbell, K.P. (1993) 'Human dystroglycan: skeletal muscle cDNA, genomic structure, origin of tissue specific isoforms and chromosomal localization', *Hum Mol Genet*, 2(10), pp. 1651-7.

Imperiali, M., Thoma, C., Pavoni, E., Brancaccio, A., Callewaert, N. and Oxenius, A. (2005) 'O Mannosylation of alpha-dystroglycan is essential for lymphocytic choriomeningitis virus receptor function', *J Virol*, 79(22), pp. 14297-308.

Inamori, K., Yoshida-Moriguchi, T., Hara, Y., Anderson, M.E., Yu, L. and Campbell, K.P. (2012) 'Dystroglycan function requires xylosyl- and glucuronyltransferase activities of LARGE', *Science*, 335(6064), pp. 93-6.

Inoue, S., Leblond, C.P. and Laurie, G.W. (1983) 'Ultrastructure of Reichert's membrane, a multilayered basement membrane in the parietal wall of the rat yolk sac', *J Cell Biol*, 97(5 Pt 1), pp. 1524-37.

Ishikawa-Sakurai, M., Yoshida, M., Imamura, M., Davies, K.E. and Ozawa, E. (2004) 'ZZ domain is essentially required for the physiological binding of

dystrophin and utrophin to beta-dystroglycan', *Hum Mol Genet*, 13(7), pp. 693-702.

Isogai, S., Horiguchi, M. and Weinstein, B.M. (2001) 'The vascular anatomy of the developing zebrafish: an atlas of embryonic and early larval development', *Dev Biol*, 230(2), pp. 278-301.

Jacoby, A.S., Busch-Nentwich, E., Bryson-Richardson, R.J., Hall, T.E., Berger, J., Berger, S., Sonntag, C., Sachs, C., Geisler, R., Stemple, D.L. and Currie, P.D. (2009) 'The zebrafish dystrophic mutant softy maintains muscle fibre viability despite basement membrane rupture and muscle detachment', *Development*, 136(19), pp. 3367-76.

Jarvinen, T.A., Jozsa, L., Kannus, P., Jarvinen, T.L. and Jarvinen, M. (2002) 'Organization and distribution of intramuscular connective tissue in normal and immobilized skeletal muscles. An immunohistochemical, polarization and scanning electron microscopic study', *J Muscle Res Cell Motil*, 23(3), pp. 245-54.

Jayasinha, V., Nguyen, H.H., Xia, B., Kammesheidt, A., Hoyte, K. and Martin, P.T. (2003) 'Inhibition of dystroglycan cleavage causes muscular dystrophy in transgenic mice', *Neuromuscul Disord*, 13(5), pp. 365-75.

Jerusalem, F., Engel, A.G. and Gomez, M.R. (1974) 'Duchenne dystrophy. I. Morphometric study of the muscle microvasculature', *Brain*, 97(1), pp. 115-22.

Jin, E.J., Erickson, C.A., Takada, S. and Burrus, L.W. (2001) 'Wnt and BMP signaling govern lineage segregation of melanocytes in the avian embryo', *Dev Biol*, 233(1), pp. 22-37.

Johnson, R.P. and Kramer, J.M. (2012) 'Neural maintenance roles for the matrix receptor dystroglycan and the nuclear anchorage complex in Caenorhabditis elegans', *Genetics*, 190(4), pp. 1365-77.

Jung, D., Yang, B., Meyer, J., Chamberlain, J.S. and Campbell, K.P. (1995) 'Identification and characterization of the dystrophin anchoring site on beta-dystroglycan', *J Biol Chem*, 270(45), pp. 27305-10.

Justice, M.J., Zheng, B., Woychik, R.P. and Bradley, A. (1997) 'Using targeted large deletions and high-efficiency N-ethyl-N-nitrosourea mutagenesis for functional analyses of the mammalian genome', *Methods*, 13(4), pp. 423-36.

Kanagawa, M., Nishimoto, A., Chiyonobu, T., Takeda, S., Miyagoe-Suzuki, Y., Wang, F., Fujikake, N., Taniguchi, M., Lu, Z., Tachikawa, M., Nagai, Y., Tashiro, F., Miyazaki, J., Tajima, Y., Endo, T., Kobayashi, K., Campbell, K.P. and Toda, T. (2009a) 'Residual laminin-binding activity and enhanced dystroglycan glycosylation by LARGE in novel model mice to dystroglycanopathy', *Hum Mol Genet*, 18(4), pp. 621-31.

Kanagawa, M., Nishimoto, A., Chiyonobu, T., Takeda, S., Miyagoe-Suzuki, Y., Wang, F., Fujikake, N., Taniguchi, M., Lu, Z., Tachikawa, M., Nagai, Y., Tashiro,

F., Miyazaki, J., Tajima, Y., Takeda, S., Endo, T., Kobayashi, K., Campbell, K.P. and Toda, T. (2009b) 'Residual laminin-binding activity and enhanced dystroglycan glycosylation by LARGE in novel model mice to dystroglycanopathy', *Hum Mol Genet*, 18(4), pp. 621-31.

Kanoff, R.J., Curless, R.G., Petito, C., Falcone, S., Siatkowski, R.M. and Pegoraro, E. (1998) 'Walker-Warburg syndrome: neurologic features and muscle membrane structure', *Pediatr Neurol*, 18(1), pp. 76-80.

Kaplan, J.C. (2011) 'The 2012 version of the gene table of monogenic neuromuscular disorders', *Neuromuscul Disord*, 21(12), pp. 833-61.

Kawahara, G., Guyon, J.R., Nakamura, Y. and Kunkel, L.M. (2010) 'Zebrafish models for human FKRP muscular dystrophies', *Hum Mol Genet*, 19(4), pp. 623-33.

Kelly, D., Chancellor, K., Milatovich, A., Francke, U., Suzuki, K. and Popko, B. (1994) 'Autosomal recessive neuromuscular disorder in a transgenic line of mice', *J Neurosci*, 14(1), pp. 198-207.

Kelsh, R.N., Brand, M., Jiang, Y.J., Heisenberg, C.P., Lin, S., Haffter, P., Odenthal, J., Mullins, M.C., van Eeden, F.J., Furutani-Seiki, M., Granato, M., Hammerschmidt, M., Kane, D.A., Warga, R.M., Beuchle, D., Vogelsang, L. and Nusslein-Volhard, C. (1996) 'Zebrafish pigmentation mutations and the processes of neural crest development', *Development*, 123, pp. 369-89.

Keramaris-Vrantsis, E., Lu, P.J., Doran, T., Zillmer, A., Ashar, J., Esapa, C.T., Benson, M.A., Blake, D.J., Rosenfeld, J. and Lu, Q.L. (2007) 'Fukutin-related protein localizes to the Golgi apparatus and mutations lead to mislocalization in muscle in vivo', *Muscle Nerve*, 36(4), pp. 455-65.

Kettleborough, R.N., Bruijn, E., Eeden, F., Cuppen, E. and Stemple, D.L. (2011) 'High-throughput target-selected gene inactivation in zebrafish', *Methods Cell Biol*, 104, pp. 121-7.

Kim, D.S., Hayashi, Y.K., Matsumoto, H., Ogawa, M., Noguchi, S., Murakami, N., Sakuta, R., Mochizuki, M., Michele, D.E., Campbell, K.P., Nonaka, I. and Nishino, I. (2004) 'POMT1 mutation results in defective glycosylation and loss of laminin-binding activity in alpha-DG', *Neurology*, 62(6), pp. 1009-11.

Kim, Y.G., Cha, J. and Chandrasegaran, S. (1996) 'Hybrid restriction enzymes: zinc finger fusions to Fok I cleavage domain', *Proc Natl Acad Sci U S A*, 93(3), pp. 1156-60.

Kimmel, C., Ballard, W., Kimmel, S., Ullmann, B. and Schilling, T. (1995) 'Stages of embryonic development of the zebrafish', *Developmental Dynamics*, 203, pp. 253-310.

Kimmel, C.B., Warga, R.M. and Schilling, T.F. (1990) 'Origin and organization of the zebrafish fate map', *Development*, 108(4), pp. 581-94.

Kinali, M., Arechavala-Gomeza, V., Feng, L., Cirak, S., Hunt, D., Adkin, C., Guglieri, M., Ashton, E., Abbs, S., Nihoyannopoulos, P., Garralda, M.E., Rutherford, M., McCulley, C., Popplewell, L., Graham, I.R., Dickson, G., Wood, M.J., Wells, D.J., Wilton, S.D., Kole, R., Straub, V., Bushby, K., Sewry, C., Morgan, J.E. and Muntoni, F. (2009) 'Local restoration of dystrophin expression with the morpholino oligomer AVI-4658 in Duchenne muscular dystrophy: a single-blind, placebo-controlled, dose-escalation, proof-of-concept study', *Lancet Neurol*, 8(10), pp. 918-28.

Kipling, D. (1997) 'Telomere structure and telomerase expression during mouse development and tumorigenesis', *Eur J Cancer*, 33(5), pp. 792-800.

Klug, A. (2010a) 'The discovery of zinc fingers and their applications in gene regulation and genome manipulation', *Annu Rev Biochem*, 79, pp. 213-31.

Klug, A. (2010b) 'The discovery of zinc fingers and their development for practical applications in gene regulation and genome manipulation', *Q Rev Biophys*, 43(1), pp. 1-21.

Knapik, E.W. (2000) 'ENU mutagenesis in zebrafish--from genes to complex diseases', *Mamm Genome*, 11(7), pp. 511-9.

Knopf, F., Schnabel, K., Haase, C., Pfeifer, K., Anastassiadis, K. and Weidinger, G. (2010) 'Dually inducible TetON systems for tissue-specific conditional gene expression in zebrafish', *Proc Natl Acad Sci U S A*, 107(46), pp. 19933-8.

Kobayashi, K., Nakahori, Y., Miyake, M., Matsumura, K., Kondo-Iida, E., Nomura, Y., Segawa, M., Yoshioka, M., Saito, K., Osawa, M., Hamano, K., Sakakihara, Y., Nonaka, I., Nakagome, Y., Kanazawa, I., Nakamura, Y., Tokunaga, K. and Toda, T. (1998) 'An ancient retrotransposal insertion causes Fukuyama-type congenital muscular dystrophy', *Nature*, 394(6691), pp. 388-92.

Kobayashi, Y.M., Rader, E.P., Crawford, R.W., Iyengar, N.K., Thedens, D.R., Faulkner, J.A., Parikh, S.V., Weiss, R.M., Chamberlain, J.S., Moore, S.A. and Campbell, K.P. (2008) 'Sarcolemma-localized nNOS is required to maintain activity after mild exercise', *Nature*, 456(7221), pp. 511-5.

Koch, M., Olson, P.F., Albus, A., Jin, W., Hunter, D.D., Brunken, W.J., Burgeson, R.E. and Champliaud, M.F. (1999) 'Characterization and expression of the laminin gamma3 chain: a novel, non-basement membrane-associated, laminin chain', *J Cell Biol*, 145(3), pp. 605-18.

Koenig, M. and Kunkel, L.M. (1990) 'Detailed analysis of the repeat domain of dystrophin reveals four potential hinge segments that may confer flexibility', *J Biol Chem*, 265(8), pp. 4560-6.

Kohling, R., Nischt, R., Vasudevan, A., Ho, M., Weiergraber, M., Schneider, T. and Smyth, N. (2006) 'Nidogen and nidogen-associated basement membrane proteins and neuronal plasticity', *Neurodegener Dis*, 3(1-2), pp. 56-61.

Kornegay, J.N., Childers, M.K., Bogan, D.J., Bogan, J.R., Nghiem, P., Wang, J., Fan, Z., Howard, J.F., Jr., Schatzberg, S.J., Dow, J.L., Grange, R.W., Styner, M.A., Hoffman, E.P. and Wagner, K.R. (2012) 'The paradox of muscle hypertrophy in muscular dystrophy', *Phys Med Rehabil Clin N Am*, 23(1), pp. 149-72, xii.

Kuang, W., Xu, H., Vachon, P.H. and Engvall, E. (1998) 'Disruption of the lama2 gene in embryonic stem cells: laminin alpha 2 is necessary for sustenance of mature muscle cells', *Exp Cell Res*, 241(1), pp. 117-25.

Kuga, A., Kanagawa, M., Sudo, A., Chan, Y.M., Tajiri, M., Manya, H., Kikkawa, Y., Nomizu, M., Kobayashi, K., Endo, T., Lu, Q.L., Wada, Y. and Toda, T. (2012a) 'Absence of post-phosphoryl modification in dystroglycanopathy mouse models and wild-type tissues expressing a non-laminin binding form of alpha-dystroglycan', *J Biol Chem*.

Kuga, A., Kanagawa, M., Sudo, A., Chan, Y.M., Tajiri, M., Manya, H., Kikkawa, Y., Nomizu, M., Kobayashi, K., Endo, T., Lu, Q.L., Wada, Y. and Toda, T. (2012b) 'Absence of post-phosphoryl modification in dystroglycanopathy mouse models and wild-type tissues expressing non-laminin binding form of alpha-dystroglycan', *J Biol Chem*, 287(12), pp. 9560-7.

Kuga, A., Kanagawa, M. and Toda, T. (2011) '[Recent Advances in alpha-dystroglycanopathy]', *Brain Nerve*, 63(11), pp. 1189-95.

Kunz, S., Rojek, J.M., Kanagawa, M., Spiropoulou, C.F., Barresi, R., Campbell, K.P. and Oldstone, M.B. (2005) 'Posttranslational modification of alpha-dystroglycan, the cellular receptor for arenaviruses, by the glycosyltransferase LARGE is critical for virus binding', *J Virol*, 79(22), pp. 14282-96.

Kurahashi, H., Taniguchi, M., Meno, C., Taniguchi, Y., Takeda, S., Horie, M., Otani, H. and Toda, T. (2005) 'Basement membrane fragility underlies embryonic lethality in fukutin-null mice', *Neurobiol Dis*, 19(1-2), pp. 208-17.

Kuru, S. (2011) '[Respiratory management in muscular dystrophies]', *Brain Nerve*, 63(11), pp. 1229-36.

Kwon, S.W., Kang, S.W., Kim, J.Y., Choi, E.Y., Yoon, Y.W., Park, Y.M., Ma, D.W., Chung, H., Kwon, H.M. and Rim, S.J. (2012) 'Outcomes of cardiac involvement in patients with late-stage Duchenne muscular dystrophy under management in the pulmonary rehabilitation center of a tertiary referral hospital', *Cardiology*, 121(3), pp. 186-93.

Lapidos, K.A., Kakkar, R. and McNally, E.M. (2004) 'The dystrophin glycoprotein complex: signaling strength and integrity for the sarcolemma', *Circ Res*, 94(8), pp. 1023-31.

Law, D.J., Caputo, A. and Tidball, J.G. (1995) 'Site and mechanics of failure in normal and dystrophin-deficient skeletal muscle', *Muscle Nerve*, 18(2), pp. 216-23.

Law, D.J. and Tidball, J.G. (1993) 'Dystrophin deficiency is associated with myotendinous junction defects in prenecrotic and fully regenerated skeletal muscle', *Am J Pathol*, 142(5), pp. 1513-23.

Lawson, N.D. and Weinstein, B.M. (2002) 'In vivo imaging of embryonic vascular development using transgenic zebrafish', *Dev Biol*, 248(2), pp. 307-18.

Le Rumeur, E., Winder, S.J. and Hubert, J.F. (2010) 'Dystrophin: more than just the sum of its parts', *Biochim Biophys Acta*, 1804(9), pp. 1713-22.

LeBleu, V.S., Macdonald, B. and Kalluri, R. (2007) 'Structure and function of basement membranes', *Exp Biol Med (Maywood)*, 232(9), pp. 1121-9.

Lee, J. and Gross, J.M. (2007) 'Laminin beta1 and gamma1 containing laminins are essential for basement membrane integrity in the zebrafish eye', *Invest Ophthalmol Vis Sci*, 48(6), pp. 2483-90.

Lefeber, D.J., Schonberger, J., Morava, E., Guillard, M., Huyben, K.M., Verrijp, K., Grafakou, O., Evangeliou, A., Preijers, F.W., Manta, P., Yildiz, J., Grunewald, S., Spilioti, M., van den Elzen, C., Klein, D., Hess, D., Ashida, H., Hofsteenge, J., Maeda, Y., van den Heuvel, L., Lammens, M., Lehle, L. and Wevers, R.A. (2009) 'Deficiency of Dol-P-Man synthase subunit DPM3 bridges the congenital disorders of glycosylation with the dystroglycanopathies', *Am J Hum Genet*, 85(1), pp. 76-86.

Lessman, C.A. (2011) 'The developing zebrafish (Danio rerio): a vertebrate model for high-throughput screening of chemical libraries', *Birth Defects Res C Embryo Today*, 93(3), pp. 268-80.

Liesi, P. (1990) 'Extracellular matrix and neuronal movement', *Experientia*, 46(9), pp. 900-7.

Lim, L.E. and Campbell, K.P. (1998) 'The sarcoglycan complex in limb-girdle muscular dystrophy', *Curr Opin Neurol*, 11(5), pp. 443-52.

Lin, Y.Y., White, R.J., Torelli, S., Cirak, S., Muntoni, F. and Stemple, D.L. (2011) 'Zebrafish Fukutin family proteins link the unfolded protein response with dystroglycanopathies', *Hum Mol Genet*. 20 (9) pp. 1763-75.

Liu, J., Ball, S.L., Yang, Y., Mei, P., Zhang, L., Shi, H., Kaminski, H.J., Lemmon, V.P. and Hu, H. (2006) 'A genetic model for muscle-eye-brain disease in mice

lacking protein O-mannose 1,2-N-acetylglucosaminyltransferase (POMGnT1)', *Mech Dev*, 123(3), pp. 228-40.

Lombard, J.H. (2011) 'Microcirculation in a mouse model of Duchenne muscular dystrophy: another blow to the vascular hypothesis?', *J Appl Physiol*, 110(3), pp. 587-8.

Longman, C., Brockington, M., Torelli, S., Jimenez-Mallebrera, C., Kennedy, C., Khalil, N., Feng, L., Saran, R.K., Voit, T., Merlini, L., Sewry, C.A., Brown, S.C. and Muntoni, F. (2003) 'Mutations in the human LARGE gene cause MDC1D, a novel form of congenital muscular dystrophy with severe mental retardation and abnormal glycosylation of alpha-dystroglycan', *Hum Mol Genet*, 12(21), pp. 2853-61.

Lu, X., Le Noble, F., Yuan, L., Jiang, Q., De Lafarge, B., Sugiyama, D., Breant, C., Claes, F., De Smet, F., Thomas, J.L., Autiero, M., Carmeliet, P., Tessier-Lavigne, M. and Eichmann, A. (2004) 'The netrin receptor UNC5B mediates guidance events controlling morphogenesis of the vascular system', *Nature*, 432(7014), pp. 179-86.

Lynch, T.A., Lam, L.T., Man, N.T., Kobayashi, K., Toda, T. and Morris, G.E. (2012) 'Detection of the dystroglycanopathy protein, fukutin, using a new panel of site-specific monoclonal antibodies', *Biochem Biophys Res Commun*.

Ma, F., Zhang, D., Yang, H., Sun, H., Wu, W., Gan, Y., Balducci, J., Wei, Y.Q., Zhao, X. and Huang, Y. (2009) 'Endothelial cell-specific molecule 2 (ECSM2) modulates actin remodeling and epidermal growth factor receptor signaling', *Genes Cells*, 14(3), pp. 281-93.

Maeda, Y. and Kinoshita, T. (2008) 'Dolichol-phosphate mannose synthase: structure, function and regulation', *Biochim Biophys Acta*, 1780(6), pp. 861-8.

Maeder, M.L., Thibodeau-Beganny, S., Sander, J.D., Voytas, D.F. and Joung, J.K. (2009) 'Oligomerized pool engineering (OPEN): an 'open-source' protocol for making customized zinc-finger arrays', *Nat Protoc*, 4(10), pp. 1471-501.

Mann, C.J., Honeyman, K., Cheng, A.J., Ly, T., Lloyd, F., Fletcher, S., Morgan, J.E., Partridge, T.A. and Wilton, S.D. (2001) 'Antisense-induced exon skipping and synthesis of dystrophin in the mdx mouse', *Proc Natl Acad Sci U S A*, 98(1), pp. 42-7.

Mann, C.J., Perdiguero, E., Kharraz, Y., Aguilar, S., Pessina, P., Serrano, A.L. and Munoz-Canoves, P. (2011) 'Aberrant repair and fibrosis development in skeletal muscle', *Skelet Muscle*, 1(1), p. 21.

Manya, H., Chiba, A., Yoshida, A., Wang, X., Chiba, Y., Jigami, Y., Margolis, R.U. and Endo, T. (2004) 'Demonstration of mammalian protein O-mannosyltransferase activity: coexpression of POMT1 and POMT2 required for enzymatic activity', *Proc Natl Acad Sci U S A*, 101(2), pp. 500-5.

Manzur, A.Y. and Muntoni, F. (2009) 'Diagnosis and new treatments in muscular dystrophies', *J Neurol Neurosurg Psychiatry*, 80(7), pp. 706-14.

Marneros, A.G. and Olsen, B.R. (2005) 'Physiological role of collagen XVIII and endostatin', *FASEB J*, 19(7), pp. 716-28.

Martin-Blanco, E. and Garcia-Bellido, A. (1996) 'Mutations in the rotated abdomen locus affect muscle development and reveal an intrinsic asymmetry in Drosophila', *Proc Natl Acad Sci U S A*, 93(12), pp. 6048-52.

Martinez-Morales, J.R., Rodrigo, I. and Bovolenta, P. (2004) 'Eye development: a view from the retina pigmented epithelium', *Bioessays*, 26(7), pp. 766-77.

Mayer, U. (2003) 'Integrins: redundant or important players in skeletal muscle?', *J Biol Chem*, 278(17), pp. 14587-90.

Mayer, U., Saher, G., Fassler, R., Bornemann, A., Echtermeyer, F., von der Mark, H., Miosge, N., Poschl, E. and von der Mark, K. (1997) 'Absence of integrin alpha 7 causes a novel form of muscular dystrophy', *Nat Genet*, 17(3), pp. 318-23.

McDearmon, E.L., Combs, A.C. and Ervasti, J.M. (2001) 'Differential Vicia villosa agglutinin reactivity identifies three distinct dystroglycan complexes in skeletal muscle', *J Biol Chem*, 276(37), pp. 35078-86.

McGrew, M.J., Dale, J.K., Fraboulet, S. and Pourquie, O. (1998) 'The lunatic fringe gene is a target of the molecular clock linked to somite segmentation in avian embryos', *Curr Biol*, 8(17), pp. 979-82.

Mei, J., Liu, S., Li, Z. and Gui, J.F. (2010) 'Mtmr8 is essential for vasculature development in zebrafish embryos', *BMC Dev Biol*, 10(1), p. 96.

Mendell, J.R., Boue, D.R. and Martin, P.T. (2006) 'The congenital muscular dystrophies: recent advances and molecular insights', *Pediatr Dev Pathol*, 9(6), pp. 427-43.

Mendell, J.R., Engel, W.K. and Derrer, E.C. (1972) 'Increased plasma enzyme concentrations in rats with functional ischaemia of muscle provide a possible model of Duchenne muscular dystrophy', *Nature*, 239(5374), pp. 522-4.

Mercuri, E., Brockington, M., Straub, V., Quijano-Roy, S., Yuva, Y., Herrmann, R., Brown, S.C., Torelli, S., Dubowitz, V., Blake, D.J., Romero, N.B., Estournet, B., Sewry, C.A., Guicheney, P., Voit, T. and Muntoni, F. (2003) 'Phenotypic spectrum associated with mutations in the fukutin-related protein gene', *Ann Neurol*, 53(4), pp. 537-42.

Mercuri, E., Topaloglu, H., Brockington, M., Berardinelli, A., Pichiecchio, A., Santorelli, F., Rutherford, M., Talim, B., Ricci, E., Voit, T. and Muntoni, F. (2006)

'Spectrum of brain changes in patients with congenital muscular dystrophy and FKRP gene mutations', *Arch Neurol*, 63(2), pp. 251-7.

Michele, D.E., Barresi, R., Kanagawa, M., Saito, F., Cohn, R.D., Satz, J.S., Dollar, J., Nishino, I., Kelley, R.I., Somer, H., Straub, V., Mathews, K.D., Moore, S.A. and Campbell, K.P. (2002) 'Post-translational disruption of dystroglycan-ligand interactions in congenital muscular dystrophies', *Nature*, 418(6896), pp. 417-22.

Miller, J., McLachlan, A.D. and Klug, A. (1985) 'Repetitive zinc-binding domains in the protein transcription factor IIIA from Xenopus oocytes', *EMBO J*, 4(6), pp. 1609-14.

Miyagoe-Suzuki, Y., Nakagawa, M. and Takeda, S. (2000) 'Merosin and congenital muscular dystrophy', *Microsc Res Tech*, 48(3-4), pp. 181-91.

Mohideen, M.A., Beckwith, L.G., Tsao-Wu, G.S., Moore, J.L., Wong, A.C., Chinoy, M.R. and Cheng, K.C. (2003) 'Histology-based screen for zebrafish mutants with abnormal cell differentiation', *Dev Dyn*, 228(3), pp. 414-23.

Moiseeva, E.P. (2001) 'Adhesion receptors of vascular smooth muscle cells and their functions', *Cardiovasc Res*, 52(3), pp. 372-86.

Monaco, A.P., Bertelson, C.J., Middlesworth, W., Colletti, C.A., Aldridge, J., Fischbeck, K.H., Bartlett, R., Pericak-Vance, M.A., Roses, A.D. and Kunkel, L.M. (1985) 'Detection of deletions spanning the Duchenne muscular dystrophy locus using a tightly linked DNA segment', *Nature*, 316(6031), pp. 842-5.

Monaco, A.P., Neve, R.L., Colletti-Feener, C., Bertelson, C.J., Kurnit, D.M. and Kunkel, L.M. (1986) 'Isolation of candidate cDNAs for portions of the Duchenne muscular dystrophy gene', *Nature*, 323(6089), pp. 646-50.

Moore, C.J., Goh, H.T. and Hewitt, J.E. (2008) 'Genes required for functional glycosylation of dystroglycan are conserved in zebrafish', *Genomics*, 92(3), pp. 159-67.

Moore, D.T., Nygren, P., Jo, H., Boesze-Battaglia, K., Bennett, J.S. and DeGrado, W.F. (2012a) 'Affinity of talin-1 for the beta3-integrin cytosolic domain is modulated by its phospholipid bilayer environment', *Proc Natl Acad Sci U S A*, 109(3), pp. 793-8.

Moore, F.E., Reyon, D., Sander, J.D., Martinez, S.A., Blackburn, J.S., Khayter, C., Ramirez, C.L., Joung, J.K. and Langenau, D.M. (2012b) 'Improved somatic mutagenesis in zebrafish using transcription activator-like effector nucleases (TALENs)', *PLoS One*, 7(5), p. e37877.

Moore, S.A., Saito, F., Chen, J., Michele, D.E., Henry, M.D., Messing, A., Cohn, R.D., Ross-Barta, S.E., Westra, S., Williamson, R.A., Hoshi, T. and Campbell,

K.P. (2002) 'Deletion of brain dystroglycan recapitulates aspects of congenital muscular dystrophy', *Nature*, 418(6896), pp. 422-5.

Moremen, K.W., Tiemeyer, M. and Nairn, A.V. (2012) 'Vertebrate protein glycosylation: diversity, synthesis and function', *Nat Rev Mol Cell Biol*, 13(7), pp. 448-62.

Moukhles, H., Roque, R. and Carbonetto, S. (2000) 'alpha-dystroglycan isoforms are differentially distributed in adult rat retina', *J Comp Neurol*, 420(2), pp. 182-94.

Munoz, I., Carrillo, M., Zanuy, S. and Gomez, A. (2005) 'Regulation of exogenous gene expression in fish cells: an evaluation of different versions of the tetracycline-regulated system', *Gene*, 363, pp. 173-82.

Muntoni, F., Torelli, S., Wells, D.J. and Brown, S.C. (2011) 'Muscular dystrophies due to glycosylation defects: diagnosis and therapeutic strategies', *Curr Opin Neurol*, 24(5), pp. 437-42.

Muntoni, F. and Voit, T. (2004) 'The congenital muscular dystrophies in 2004: a century of exciting progress', *Neuromuscul Disord*, 14(10), pp. 635-49.

Nakanishi, T., Sakauchi, M., Kaneda, Y., Tomimatsu, H., Saito, K., Nakazawa, M. and Osawa, M. (2006) 'Cardiac involvement in Fukuyama-type congenital muscular dystrophy', *Pediatrics*, 117(6), pp. e1187-92.

Nance, J.R., Dowling, J.J., Gibbs, E.M. and Bonnemann, C.G. (2012) 'Congenital myopathies: an update', *Curr Neurol Neurosci Rep*, 12(2), pp. 165-74.

Nasevicius, A. and Ekker, S.C. (2000) 'Effective targeted gene 'knockdown' in zebrafish', *Nat Genet*, 26(2), pp. 216-20.

Nechiporuk, A., Finney, J.E., Keating, M.T. and Johnson, S.L. (1999) 'Assessment of polymorphism in zebrafish mapping strains', *Genome Res*, 9(12), pp. 1231-8.

Negroni, E., Vallese, D., Vilquin, J.T., Butler-Browne, G., Mouly, V. and Trollet, C. (2011) 'Current advances in cell therapy strategies for muscular dystrophies', *Expert Opin Biol Ther*, 11(2), pp. 157-76.

Nicholson, L.V., Johnson, M.A., Bushby, K.M., Gardner-Medwin, D., Curtis, A., Ginjaar, I.B., den Dunnen, J.T., Welch, J.L., Butler, T.J., Bakker, E. and et al. (1993) 'Integrated study of 100 patients with Xp21 linked muscular dystrophy using clinical, genetic, immunochemical, and histopathological data. Part 2. Correlations within individual patients', *J Med Genet*, 30(9), pp. 737-44.

Nicole, S., Davoine, C.S., Topaloglu, H., Cattolico, L., Barral, D., Beighton, P., Hamida, C.B., Hammouda, H., Cruaud, C., White, P.S., Samson, D., Urtizberea,

J.A., Lehmann-Horn, F., Weissenbach, J., Hentati, F. and Fontaine, B. (2000) 'Perlecan, the major proteoglycan of basement membranes, is altered in patients with Schwartz-Jampel syndrome (chondrodystrophic myotonia)', *Nat Genet*, 26(4), pp. 480-3.

Nieves, B., Jones, C.W., Ward, R., Ohta, Y., Reverte, C.G. and LaFlamme, S.E. (2010) 'The NPIY motif in the integrin beta1 tail dictates the requirement for talin-1 in outside-in signaling', *J Cell Sci*, 123(Pt 8), pp. 1216-26.

Nishiuchi, R., Takagi, J., Hayashi, M., Ido, H., Yagi, Y., Sanzen, N., Tsuji, T., Yamada, M. and Sekiguchi, K. (2006) 'Ligand-binding specificities of laminin-binding integrins: a comprehensive survey of laminin-integrin interactions using recombinant alpha3beta1, alpha6beta1, alpha7beta1 and alpha6beta4 integrins', *Matrix Biol*, 25(3), pp. 189-97.

Noonan, D.M., Fulle, A., Valente, P., Cai, S., Horigan, E., Sasaki, M., Yamada, Y. and Hassell, J.R. (1991) 'The complete sequence of perlecan, a basement membrane heparan sulfate proteoglycan, reveals extensive similarity with laminin A chain, low density lipoprotein-receptor, and the neural cell adhesion molecule', *J Biol Chem*, 266(34), pp. 22939-47.

North, K.N. (2011) 'Clinical approach to the diagnosis of congenital myopathies', *Semin Pediatr Neurol*, 18(4), pp. 216-20.

Norwood, F.M., Harling, C., Chinnery. P.F., Eagle, M., Bushby, K. and Straub, V. (2009) 'Prevalence of genetic muscle disease in Northern England: in-depth analysis of a muscle clinic population' *Brain,* 132(11), pp. 3175-3186.

Norwood, F.L., Sutherland-Smith, A.J., Keep, N.H. and Kendrick-Jones, J. (2000) 'The structure of the N-terminal actin-binding domain of human dystrophin and how mutations in this domain may cause Duchenne or Becker muscular dystrophy', *Structure*, 8(5), pp. 481-91.

Odenthal, J., Haffter, P., Vogelsang, E., Brand, M., van Eeden, F.J., Furutani-Seiki, M., Granato, M., Hammerschmidt, M., Heisenberg, C.P., Jiang, Y.J., Kane, D.A., Kelsh, R.N., Mullins, M.C., Warga, R.M., Allende, M.L., Weinberg, E.S. and Nusslein-Volhard, C. (1996) 'Mutations affecting the formation of the notochord in the zebrafish, Danio rerio', *Development*, 123, pp. 103-15.

Olsen, B.R. (1999) 'Life without perlecan has its problems', *J Cell Biol*, 147(5), pp. 909-12.

Omori, Y., Araki, F., Chaya, T., Kajimura, N., Irie, S., Terada, K., Muranishi, Y., Tsujii, T., Ueno, S., Koyasu, T., Tamaki, Y., Kondo, M., Amano, S. and Furukawa, T. (2012) 'Presynaptic dystroglycan-pikachurin complex regulates the proper synaptic connection between retinal photoreceptor and bipolar cells', *J Neurosci*, 32(18), pp. 6126-37.

Opat, A.S., van Vliet, C. and Gleeson, P.A. (2001) 'Trafficking and localisation of resident Golgi glycosylation enzymes', *Biochimie*, 83(8), pp. 763-73.

Palmeirim, I., Henrique, D., Ish-Horowicz, D. and Pourquie, O. (1997) 'Avian hairy gene expression identifies a molecular clock linked to vertebrate segmentation and somitogenesis', *Cell*, 91(5), pp. 639-48.

Parichy, D.M. (2006) 'Evolution of danio pigment pattern development', *Heredity (Edinb)*, 97(3), pp. 200-10.

Parsons, M.J., Campos, I., Hirst, E.M. and Stemple, D.L. (2002a) 'Removal of dystroglycan causes severe muscular dystrophy in zebrafish embryos', *Development*, 129(14), pp. 3505-12.

Parsons, M.J., Pollard, S.M., Saude, L., Feldman, B., Coutinho, P., Hirst, E.M. and Stemple, D.L. (2002b) 'Zebrafish mutants identify an essential role for laminins in notochord formation', *Development*, 129(13), pp. 3137-46.

Patton, B.L., Wang, B., Tarumi, Y.S., Seburn, K.L. and Burgess, R.W. (2008) 'A single point mutation in the LN domain of LAMA2 causes muscular dystrophy and peripheral amyelination', *J Cell Sci*, 121(Pt 10), pp. 1593-604.

Paulk, A., Millard, S.S. and van Swinderen, B. (2012) 'Vision in Drosophila: Seeing the World Through a Models Eyes', *Annu Rev Entomol*. [Epub ahead of print].

Pelham, H.R. and Brown, D.D. (1980) 'A specific transcription factor that can bind either the 5S RNA gene or 5S RNA', *Proc Natl Acad Sci U S A*, 77(7), pp. 4170-4.

Persengiev, S.P., Zhu, X. and Green, M.R. (2004) 'Nonspecific, concentration-dependent stimulation and repression of mammalian gene expression by small interfering RNAs (siRNAs)', *RNA*, 10(1), pp. 12-8.

Petrof, B.J., Shrager, J.B., Stedman, H.H., Kelly, A.M. and Sweeney, H.L. (1993) 'Dystrophin protects the sarcolemma from stresses developed during muscle contraction', *Proc Natl Acad Sci U S A*, 90(8), pp. 3710-4.

Picard, B. and Wegnez, M. (1979) 'Isolation of a 7S particle from Xenopus laevis oocytes: a 5S RNA-protein complex', *Proc Natl Acad Sci U S A*, 76(1), pp. 241-5.

Pollard, S.M., Parsons, M.J., Kamei, M., Kettleborough, R.N., Thomas, K.A., Pham, V.N., Bae, M.K., Scott, A., Weinstein, B.M. and Stemple, D.L. (2006) 'Essential and overlapping roles for laminin alpha chains in notochord and blood vessel formation', *Dev Biol*, 289(1), pp. 64-76.

Pons, F., Augier, N., Heilig, R., Leger, J., Mornet, D. and Leger, J.J. (1990) 'Isolated dystrophin molecules as seen by electron microscopy', *Proc Natl Acad Sci U S A*, 87(20), pp. 7851-5.

Porteus, M.H. and Carroll, D. (2005) 'Gene targeting using zinc finger nucleases', *Nat Biotechnol*, 23(8), pp. 967-73.

Poschl, E., Schlotzer-Schrehardt, U., Brachvogel, B., Saito, K., Ninomiya, Y. and Mayer, U. (2004) 'Collagen IV is essential for basement membrane stability but dispensable for initiation of its assembly during early development', *Development*, 131(7), pp. 1619-28.

Postel, R., Vakeel, P., Topczewski, J., Knoll, R. and Bakkers, J. (2008) 'Zebrafish integrin-linked kinase is required in skeletal muscles for strengthening the integrin-ECM adhesion complex', *Dev Biol*, 318(1), pp. 92-101.

Potter, C.J. and Luo, L. (2011) 'Using the Q system in Drosophila melanogaster', *Nat Protoc*, 6(8), pp. 1105-20.

Prockop, D.J. and Kivirikko, K.I. (1995) 'Collagens: molecular biology, diseases, and potentials for therapy', *Annu Rev Biochem*, 64, pp. 403-34.

Purcell, P., Oliver, G., Mardon, G., Donner, A.L. and Maas, R.L. (2005) 'Pax6-dependence of Six3, Eya1 and Dach1 expression during lens and nasal placode induction', *Gene Expr Patterns*, 6(1), pp. 110-8.

Purslow, P.P. (2010) 'Muscle fascia and force transmission', *J Bodyw Mov Ther*, 14(4), pp. 411-7.

Purslow, P.P. and Trotter, J.A. (1994) 'The morphology and mechanical properties of endomysium in series-fibred muscles: variations with muscle length', *J Muscle Res Cell Motil*, 15(3), pp. 299-308.

Radecke, S., Radecke, F., Cathomen, T. and Schwarz, K. (2010) 'Zinc-finger nuclease-induced gene repair with oligodeoxynucleotides: wanted and unwanted target locus modifications', *Mol Ther*, 18(4), pp. 743-53.

Rambukkana, A., Yamada, H., Zanazzi, G., Mathus, T., Salzer, J.L., Yurchenco, P.D., Campbell, K.P. and Fischetti, V.A. (1998) 'Role of alpha-dystroglycan as a Schwann cell receptor for Mycobacterium leprae', *Science*, 282(5396), pp. 2076-9.

Ramirez, C.L., Foley, J.E., Wright, D.A., Muller-Lerch, F., Rahman, S.H., Cornu, T.I., Winfrey, R.J., Sander, J.D., Fu, F., Townsend, J.A., Cathomen, T., Voytas, D.F. and Joung, J.K. (2008) 'Unexpected failure rates for modular assembly of engineered zinc fingers', *Nat Methods*, 5(5), pp. 374-5.

Randlett, O., Poggi, L., Zolessi, F.R. and Harris, W.A. (2011) 'The oriented emergence of axons from retinal ganglion cells is directed by laminin contact in vivo', *Neuron*, 70(2), pp. 266-80.

Razin, S.V., Borunova, V.V., Maksimenko, O.G. and Kantidze, O.L. (2012) 'Cys2His2 Zinc Finger Protein Family: Classification, Functions, and Major Members', *Biochemistry (Mosc)*, 77(3), pp. 217-26.

Reed, P.W., Mathews, K.D., Mills, K.A. and Bloch, R.J. (2004) 'The sarcolemma in the Large(myd) mouse', *Muscle Nerve*, 30(5), pp. 585-95.

Reid, M.B. (1998) 'Role of nitric oxide in skeletal muscle: synthesis, distribution and functional importance', *Acta Physiol Scand*, 162(3), pp. 401-9.

Reifer, H. and Sobel, E. (1998) 'Contrasts in clinical presentation and genetic transmission of myotonic dystrophy', *J Am Podiatr Med Assoc*, 88(7), pp. 313-22.

Reilich, P., Krause, S., Schramm, N., Klutzny, U., Bulst, S., Zehetmayer, B., Schneiderat, P., Walter, M.C., Schoser, B. and Lochmuller, H. (2011) 'A novel mutation in the myotilin gene (MYOT) causes a severe form of limb girdle muscular dystrophy 1A (LGMD1A)', *J Neurol*, 258(8), pp. 1437-44.

Rembold, M., Loosli, F., Adams, R.J. and Wittbrodt, J. (2006) 'Individual cell migration serves as the driving force for optic vesicle evagination', *Science*, 313(5790), pp. 1130-4.

Remy, S., Tesson, L., Menoret, S., Usal, C., Scharenberg, A.M. and Anegon, I. (2010) 'Zinc-finger nucleases: a powerful tool for genetic engineering of animals', *Transgenic Res*, 19(3), pp. 363-71.

Rentschler, S., Linn, H., Deininger, K., Bedford, M.T., Espanel, X. and Sudol, M. (1999) 'The WW domain of dystrophin requires EF-hands region to interact with beta-dystroglycan', *Biol Chem*, 380(4), pp. 431-42.

Ribeiro, I., Yuan, L., Tanentzapf, G., Dowling, J.J. and Kiger, A. (2011) 'Phosphoinositide regulation of integrin trafficking required for muscle attachment and maintenance', *PLoS Genet*, 7(2), p. e1001295.

Richards, J.B. and Hemming, F.W. (1972) 'The transfer of mannose from guanosine diphosphate mannose to dolichol phosphate and protein by pig liver endoplasmic reticulum', *Biochem J*, 130(1), pp. 77-93.

Ridge, J.C., Tidball, J.G., Ahl, K., Law, D.J. and Rickoll, W.L. (1994) 'Modifications in myotendinous junction surface morphology in dystrophin-deficient mouse muscle', *Exp Mol Pathol*, 61(1), pp. 58-68.

Rocha, C.T. and Hoffman, E.P. (2010) 'Limb-girdle and congenital muscular dystrophies: current diagnostics, management, and emerging technologies', *Curr Neurol Neurosci Rep*, 10(4), pp. 267-76.

Rojek, J.M., Spiropoulou, C.F., Campbell, K.P. and Kunz, S. (2007) 'Old World and clade C New World arenaviruses mimic the molecular mechanism of receptor recognition used by alpha-dystroglycan's host-derived ligands', *J Virol*, 81(11), pp. 5685-95.

Roscioli, T., Kamsteeg, E.J., Buysse, K., Maystadt, I., van Reeuwijk, J., van den Elzen, C., van Beusekom, E., Riemersma, M., Pfundt, R., Vissers, L.E., Schraders, M., Altunoglu, U., Buckley, M.F., Brunner, H.G., Grisart, B., Zhou, H., Veltman, J.A., Gilissen, C., Mancini, G.M., Delree, P., Willemsen, M.A., Ramadza, D.P., Chitayat, D., Bennett, C., Sheridan, E., Peeters, E.A., Tan-Sindhunata, G.M., de Die-Smulders, C.E., Devriendt, K., Kayserili, H., El-Hashash, O.A., Stemple, D.L., Lefeber, D.J., Lin, Y.Y. and van Bokhoven, H. (2012) 'Mutations in ISPD cause Walker-Warburg syndrome and defective glycosylation of alpha-dystroglycan', *Nat Genet*.

Rosen, J.N., Sweeney, M.F. and Mably, J.D. (2009) 'Microinjection of zebrafish embryos to analyze gene function', *J Vis Exp*, (25).

Rowe, R.W. (1981) 'Morphology of perimysial and endomysial connective tissue in skeletal muscle', *Tissue Cell*, 13(4), pp. 681-90.

Rubenstein, J.L. and Beachy, P.A. (1998) 'Patterning of the embryonic forebrain', *Curr Opin Neurobiol*, 8(1), pp. 18-26.

Ruparelia, A.A., Zhao, M., Currie, P.D. and Bryson-Richardson, R.J. (2012) 'Characterization and investigation of zebrafish models of filamin-related myofibrillar myopathy', *Hum Mol Genet*. [Epub ahead of print].

Rush, J.S. and Waechter, C.J. (1995) 'Transmembrane movement of a water-soluble analogue of mannosylphosphoryldolichol is mediated by an endoplasmic reticulum protein', *J Cell Biol*, 130(3), pp. 529-36.

Rybakova, I.N., Amann, K.J. and Ervasti, J.M. (1996) 'A new model for the interaction of dystrophin with F-actin', *J Cell Biol*, 135(3), pp. 661-72.

Sadoulet-Puccio, H.M., Rajala, M. and Kunkel, L.M. (1997) 'Dystrobrevin and dystrophin: an interaction through coiled-coil motifs', *Proc Natl Acad Sci U S A*, 94(23), pp. 12413-8.

Saint-Amant, L., Sprague, S.M., Hirata, H., Li, Q., Cui, W.W., Zhou, W., Poudou, O., Hume, R.I. and Kuwada, J.Y. (2008) 'The zebrafish ennui behavioral mutation disrupts acetylcholine receptor localization and motor axon stability', *Dev Neurobiol*, 68(1), pp. 45-61.

Salamat, M., Gotz, W., Horster, A., Janotte, B. and Herken, R. (1993) 'Ultrastructural localization of carbohydrates in Reichert's membrane of the mouse', *Cell Tissue Res*, 272(2), pp. 375-81.

Salamat, M., Miosge, N. and Herken, R. (1995) 'Development of Reichert's membrane in the early mouse embryo', *Anat Embryol (Berl)*, 192(3), pp. 275-81.

Sander, J.D., Dahlborg, E.J., Goodwin, M.J., Cade, L., Zhang, F., Cifuentes, D., Curtin, S.J., Blackburn, J.S., Thibodeau-Beganny, S., Qi, Y., Pierick, C.J., Hoffman, E., Maeder, M.L., Khayter, C., Reyon, D., Dobbs, D., Langenau, D.M., Stupar, R.M., Giraldez, A.J., Voytas, D.F., Peterson, R.T., Yeh, J.R. and Joung, J.K. (2010) 'Selection-free zinc-finger-nuclease engineering by context-dependent assembly (CoDA)', *Nat Methods*, 8(1), pp. 67-9.

Sasaki, T., Yamada, H., Matsumura, K., Shimizu, T., Kobata, A. and Endo, T. (1998) 'Detection of O-mannosyl glycans in rabbit skeletal muscle alpha-dystroglycan', *Biochim Biophys Acta*, 1425(3), pp. 599-606.

Sato, S., Omori, Y., Katoh, K., Kondo, M., Kanagawa, M., Miyata, K., Funabiki, K., Koyasu, T., Kajimura, N., Miyoshi, T., Sawai, H., Kobayashi, K., Tani, A., Toda, T., Usukura, J., Tano, Y., Fujikado, T. and Furukawa, T. (2008) 'Pikachurin, a dystroglycan ligand, is essential for photoreceptor ribbon synapse formation', *Nat Neurosci*, 11(8), pp. 923-31.

Satz, J.S., Barresi, R., Durbeej, M., Willer, T., Turner, A., Moore, S.A. and Campbell, K.P. (2008) 'Brain and eye malformations resembling Walker-Warburg syndrome are recapitulated in mice by dystroglycan deletion in the epiblast', *J Neurosci*, 28(42), pp. 10567-75.

Satz, J.S., Philp, A.R., Nguyen, H., Kusano, H., Lee, J., Turk, R., Riker, M.J., Hernandez, J., Weiss, R.M., Anderson, M.G., Mullins, R.F., Moore, S.A., Stone, E.M. and Campbell, K.P. (2009) 'Visual impairment in the absence of dystroglycan', *J Neurosci*, 29(42), pp. 13136-46.

Saude, L., Woolley, K., Martin, P., Driever, W. and Stemple, D.L. (2000) 'Axis-inducing activities and cell fates of the zebrafish organizer', *Development*, 127(16), pp. 3407-17.

Schier, A.F. (2001) 'Axis formation and patterning in zebrafish', *Curr Opin Genet Dev*, 11(4), pp. 393-404.

Schier, A.F. and Talbot, W.S. (2005) 'Molecular genetics of axis formation in zebrafish', *Annu Rev Genet*, 39, pp. 561-613.

Schwander, M., Shirasaki, R., Pfaff, S.L. and Muller, U. (2004) 'Beta1 integrins in muscle, but not in motor neurons, are required for skeletal muscle innervation', *J Neurosci*, 24(37), pp. 8181-91.

Schwarz, F. and Aebi, M. (2011) 'Mechanisms and principles of N-linked protein glycosylation', *Curr Opin Struct Biol*, 21(5), pp. 576-82.

Sciandra, F., Bozzi, M., Bianchi, M., Pavoni, E., Giardina, B. and Brancaccio, A. (2003) 'Dystroglycan and muscular dystrophies related to the dystrophin-glycoprotein complex', *Ann Ist Super Sanita*, 39(2), pp. 173-81.

Sejerson, T. and Bushby, K. (2009) 'Standards of care for Duchenne muscular dystrophy: brief TREAT-NMD recommendations', *Adv Exp Med Biol*, 652, pp. 13-21.

Semina, E.V., Bosenko, D.V., Zinkevich, N.C., Soules, K.A., Hyde, D.R., Vihtelic, T.S., Willer, G.B., Gregg, R.G. and Link, B.A. (2006) 'Mutations in laminin alpha 1 result in complex, lens-independent ocular phenotypes in zebrafish', *Dev Biol*, 299(1), pp. 63-77.

Semmola, S. (1834) *Filiatre-Sebezio Giornale delle scienze mediche.* ch. 8, pp. 58-68.

Senderek, J., Muller, J.S., Dusl, M., Strom, T.M., Guergueltcheva, V., Diepolder, I., Laval, S.H., Maxwell, S., Cossins, J., Krause, S., Muelas, N., Vilchez, J.J., Colomer, J., Mallebrera, C.J., Nascimento, A., Nafissi, S., Kariminejad, A., Nilipour, Y., Bozorgmehr, B., Najmabadi, H., Rodolico, C., Sieb, J.P., Steinlein, O.K., Schlotter, B., Schoser, B., Kirschner, J., Herrmann, R., Voit, T., Oldfors, A., Lindbergh, C., Urtizberea, A., von der Hagen, M., Hubner, A., Palace, J., Bushby, K., Straub, V., Beeson, D., Abicht, A. and Lochmuller, H. (2010) 'Hexosamine biosynthetic pathway mutations cause neuromuscular transmission defect', *Am J Hum Genet*, 88(2), pp. 162-72.

Sertie, A.L., Sossi, V., Camargo, A.A., Zatz, M., Brahe, C. and Passos-Bueno, M.R. (2000) 'Collagen XVIII, containing an endogenous inhibitor of angiogenesis and tumor growth, plays a critical role in the maintenance of retinal structure and in neural tube closure (Knobloch syndrome)', *Hum Mol Genet*, 9(13), pp. 2051-8.

Sewry, C.A., Philpot, J., Mahony, D., Wilson, L.A., Muntoni, F. and Dubowitz, V. (1995) 'Expression of laminin subunits in congenital muscular dystrophy', *Neuromuscul Disord*, 5(4), pp. 307-16.

Sharma, A., Yu, C., Leung, C., Trane, A., Lau, M., Utokaparch, S., Shaheen, F., Sheibani, N. and Bernatchez, P. (2010) 'A new role for the muscle repair protein dysferlin in endothelial cell adhesion and angiogenesis', *Arterioscler Thromb Vasc Biol*, 30(11), pp. 2196-204.

Shih, J. and Fraser, S.E. (1996) 'Characterizing the zebrafish organizer: microsurgical analysis at the early-shield stage', *Development*, 122(4), pp. 1313-22.

Smalheiser, N. and Schwartz, N. (1987) 'Cranin: A laminin-binding protein of cell membranes', *Cell Biology*, 84, pp. 6457-6461.

Smith, K.K. and Strickland, S. (1981) 'Structural components and characteristics of Reichert's membrane, an extra-embryonic basement membrane', *J Biol Chem*, 256(9), pp. 4654-61.

Snobl, D., Binaghi, L.E. and Zenker, W. (1998) 'Microarchitecture and innervation of the human latissimus dorsi muscle', *J Reconstr Microsurg*, 14(3), pp. 171-7.

Solnica-Krezel, L. (2005) 'Conserved patterns of cell movements during vertebrate gastrulation', *Curr Biol*, 15(6), pp. R213-28.

Soules, K.A. and Link, B.A. (2005) 'Morphogenesis of the anterior segment in the zebrafish eye', *BMC Dev Biol*, 5, p. 12.

Sparks, S.E. and Escolar, D.M. (2011) 'Congenital muscular dystrophies', *Handb Clin Neurol*, 101, pp. 47-79.

Spence, H.J., Dhillon, A.S., James, M. and Winder, S.J. (2004) 'Dystroglycan, a scaffold for the ERK-MAP kinase cascade', *EMBO Rep*, 5(5), pp. 484-9.

Spiro, R.G. (1973) 'Glycoproteins', *Adv Protein Chem*, 27, pp. 349-467.

Spiro, R.G. (2002) 'Protein glycosylation: nature, distribution, enzymatic formation, and disease implications of glycopeptide bonds', *Glycobiology*, 12(4), pp. 43R-56R.

Stalnaker, S.H., Stuart, R. and Wells, L. (2011) 'Mammalian O-mannosylation: unsolved questions of structure/function', *Curr Opin Struct Biol*, 21(5), pp. 603-9.

Steffen, L.S., Guyon, J.R., Vogel, E.D., Howell, M.H., Zhou, Y., Weber, G.J., Zon, L.I. and Kunkel, L.M. (2007) 'The zebrafish runzel muscular dystrophy is linked to the titin gene', *Dev Biol*, 309(2), pp. 180-92.

Stemple, D.L. (2005) 'Structure and function of the notochord: an essential organ for chordate development', *Development*, 132(11), pp. 2503-12.

Stemple, D.L. (2011) *ZMP*. Available at: http://www.sanger.ac.uk/Projects/D_rerio/zmp/ (Accessed: 051211).

Stemple, D.L., Solnica-Krezel, L., Zwartkruis, F., Neuhauss, S.C., Schier, A.F., Malicki, J., Stainier, D.Y., Abdelilah, S., Rangini, Z., Mountcastle-Shah, E. and Driever, W. (1996) 'Mutations affecting development of the notochord in zebrafish', *Development*, 123, pp. 117-28.

Stickney, H.L., Barresi, M.J. and Devoto, S.H. (2000) 'Somite development in zebrafish', *Dev Dyn*, 219(3), pp. 287-303.

Straub, V. and Campbell, K.P. (1997) 'Muscular dystrophies and the dystrophin-glycoprotein complex', *Curr Opin Neurol*, 10(2), pp. 168-75.

Straub, V., Rafael, J.A., Chamberlain, J.S. and Campbell, K.P. (1997) 'Animal models for muscular dystrophy show different patterns of sarcolemmal disruption', *J Cell Biol*, 139(2), pp. 375-85.

Strauss, O. (1995) 'The Retinal Pigment Epithelium'. ch. 3, [available online: http://www.ncbi.nlm.nih.gov/books/NBK54392/, accesed 04/01/12]

Sugita, S., Saito, F., Tang, J., Satz, J., Campbell, K. and Sudhof, T.C. (2001) 'A stoichiometric complex of neurexins and dystroglycan in brain', *J Cell Biol*, 154(2), pp. 435-45.

Sugiyama, J., Bowen, D.C. and Hall, Z.W. (1994) 'Dystroglycan binds nerve and muscle agrin', *Neuron*, 13(1), pp. 103-15.

Summerton, J. (1999) 'Morpholino antisense oligomers: the case for an RNase H-independent structural type', *Biochim Biophys Acta*, 1489(1), pp. 141-58.

Summerton, J. and Weller, D. (1997) 'Morpholino antisense oligomers: design, preparation, and properties', *Antisense Nucleic Acid Drug Dev*, 7(3), pp. 187-95.

Summerton, J.E. (2007) 'Morpholino, siRNA, and S-DNA compared: impact of structure and mechanism of action on off-target effects and sequence specificity', *Curr Top Med Chem*, 7(7), pp. 651-60.

Sumoy, L., Keasey, J.B., Dittman, T.D. and Kimelman, D. (1997) 'A role for notochord in axial vascular development revealed by analysis of phenotype and the expression of VEGR-2 in zebrafish flh and ntl mutant embryos', *Mech Dev*, 63(1), pp. 15-27.

Sunada, Y., Bernier, S.M., Kozak, C.A., Yamada, Y. and Campbell, K.P. (1994) 'Deficiency of merosin in dystrophic dy mice and genetic linkage of laminin M chain gene to dy locus', *J Biol Chem*, 269(19), pp. 13729-32.

Sveen, M.L., Schwartz, M. and Vissing, J. (2006) 'High prevalence and phenotype-genotype correlations of limb girdle muscular dystrophy type 2I in Denmark', *Ann Neurol*, 59(5), pp. 808-15.

Svoboda, J., Hejnar, J., Geryk, J., Elleder, D. and Vernerova, Z. (2000) 'Retroviruses in foreign species and the problem of provirus silencing', *Gene*, 261(1), pp. 181-8.

Sztal, T.E., Sonntag, C., Hall, T.E. and Currie, P.D. (2012) 'Epistatic dissection of laminin-receptor interactions in dystrophic zebrafish muscle', *Hum Mol Genet*. [Epub ahead of print].

Takada, K., Nakamura, H. and Takashima, S. (1988) 'Cortical dysplasia in Fukuyama congenital muscular dystrophy (FCMD): a Golgi and angioarchitectonic analysis', *Acta Neuropathologica*, 76(2), pp. 170-8.

Takeda, S., Kondo, M., Sasaki, J., Kurahashi, H., Kano, H., Arai, K., Misaki, K., Fukui, T., Kobayashi, K., Tachikawa, M., Imamura, M., Nakamura, Y., Shimizu, T., Murakami, T., Sunada, Y., Fujikado, T., Matsumura, K., Terashima, T. and Toda, T. (2003) 'Fukutin is required for maintenance of muscle integrity, cortical histiogenesis and normal eye development', *Hum Mol Genet*, 12(12), pp. 1449-59.

Takke, C. and Campos-Ortega, J.A. (1999) 'her1, a zebrafish pair-rule like gene, acts downstream of notch signalling to control somite development', *Development*, 126(13), pp. 3005-14.

Tallquist, M.D. and Soriano, P. (2000) 'Epiblast-restricted Cre expression in MORE mice: a tool to distinguish embryonic vs. extra-embryonic gene function', *Genesis*, 26(2), pp. 113-5.

Tanabe, Y., Esaki, K. and Nomura, T. (1986) 'Skeletal muscle pathology in X chromosome-linked muscular dystrophy (mdx) mouse', *Acta Neuropathol*, 69(1-2), pp. 91-5.

Taniguchi-Ikeda, M., Kobayashi, K., Kanagawa, M., Yu, C.C., Mori, K., Oda, T., Kuga, A., Kurahashi, H., Akman, H.O., DiMauro, S., Kaji, R., Yokota, T., Takeda, S. and Toda, T. (2011) 'Pathogenic exon-trapping by SVA retrotransposon and rescue in Fukuyama muscular dystrophy', *Nature*, 478(7367), pp. 127-31.

Tawil, R. and Van Der Maarel, S.M. (2006) 'Facioscapulohumeral muscular dystrophy', *Muscle Nerve*, 34(1), pp. 1-15.

Thanh, L.T., Nguyen, T.M., Helliwell, T.R. and Morris, G.E. (1995) 'Characterization of revertant muscle fibers in Duchenne muscular dystrophy, using exon-specific monoclonal antibodies against dystrophin', *Am J Hum Genet*, 56(3), pp. 725-31.

Thomas, G.D., Shaul, P.W., Yuhanna, I.S., Froehner, S.C. and Adams, M.E. (2003) 'Vasomodulation by skeletal muscle-derived nitric oxide requires alpha-syntrophin-mediated sarcolemmal localization of neuronal Nitric oxide synthase', *Circ Res*, 92(5), pp. 554-60.

Thornhill, P., Basset, D., Lochmüller, H., Bushby, K. and Straub, V. (2008) 'Developmental defects in a zebrafish model for muscular dystrophies associated with the loss of fukutin-related protein (FKRP)', *Brain*, 131, pp. 1551-1561.

Timpl, R., Tisi, D., Talts, J.F., Andac, Z., Sasaki, T. and Hohenester, E. (2000) 'Structure and function of laminin LG modules', *Matrix Biol*, 19(4), pp. 309-17.

Tisi, D., Talts, J.F., Timpl, R. and Hohenester, E. (2000) 'Structure of the C-terminal laminin G-like domain pair of the laminin alpha2 chain harbouring binding sites for alpha-dystroglycan and heparin', *EMBO J*, 19(7), pp. 1432-40.

Toda, T. (2009) '[Pathomechanism and therapeutic strategy of Fukuyama congenital muscular dystrophy and related disorders]', *Rinsho Shinkeigaku*, 49(11), pp. 859-62.

Toda, T. and Kobayashi, K. (1999) 'Fukuyama-type congenital muscular dystrophy: the first human disease to be caused by an ancient retrotransposal integration', *J Mol Med (Berl)*, 77(12), pp. 816-23.

Toda, T., Segawa, M., Nomura, Y., Nonaka, I., Masuda, K., Ishihara, T., Sakai, M., Tomita, I., Origuchi, Y., Suzuki, M. and et al. (1993) 'Localization of a gene for Fukuyama type congenital muscular dystrophy to chromosome 9q31-33', *Nat Genet*, 5(3), pp. 283-6.

Trotter, J.A. (1993) 'Functional morphology of force transmission in skeletal muscle. A brief review', *Acta Anat (Basel)*, 146(4), pp. 205-22.

Trotter, J.A. and Purslow, P.P. (1992) 'Functional morphology of the endomysium in series fibered muscles', *J Morphol*, 212(2), pp. 109-22.

Tuckwell, D.S., Weston, S.A. and Humphries, M.J. (1993) 'Integrins: a review of their structure and mechanisms of ligand binding', *Symp Soc Exp Biol*, 47, pp. 107-36.

Vachon, P.H., Xu, H., Liu, L., Loechel, F., Hayashi, Y., Arahata, K., Reed, J.C., Wewer, U.M. and Engvall, E. (1997) 'Integrins (alpha7beta1) in muscle function and survival. Disrupted expression in merosin-deficient congenital muscular dystrophy', *J Clin Invest*, 100(7), pp. 1870-81.

Van Agtmael, T., Schlotzer-Schrehardt, U., McKie, L., Brownstein, D.G., Lee, A.W., Cross, S.H., Sado, Y., Mullins, J.J., Poschl, E. and Jackson, I.J. (2005) 'Dominant mutations of Col4a1 result in basement membrane defects which lead to anterior segment dysgenesis and glomerulopathy', *Hum Mol Genet*, 14(21), pp. 3161-8.

van der Flier, A. and Sonnenberg, A. (2001) 'Function and interactions of integrins', *Cell Tissue Res*, 305(3), pp. 285-98.

van Reeuwijk, J., Janssen, M., van den Elzen, C., Beltran-Valero de Bernabe, D., Sabatelli, P., Merlini, L., Boon, M., Scheffer, H., Brockington, M., Muntoni, F., Huynen, M.A., Verrips, A., Walsh, C.A., Barth, P.G., Brunner, H.G. and van Bokhoven, H. (2005) 'POMT2 mutations cause alpha-dystroglycan

hypoglycosylation and Walker-Warburg syndrome', *J Med Genet*, 42(12), pp. 907-12.

Van Reeuwijk, J., Olderode-Berends, M.J., Van den Elzen, C., Brouwer, O.F., Roscioli, T., Van Pampus, M.G., Scheffer, H., Brunner, H.G., Van Bokhoven, H. and Hol, F.A. (2010) 'A homozygous FKRP start codon mutation is associated with Walker-Warburg syndrome, the severe end of the clinical spectrum', *Clin Genet*, 78(3), pp. 275-81.

Verma, M., Asakura, Y., Hirai, H., Watanabe, S., Tastad, C., Fong, G.H., Ema, M., Call, J.A., Lowe, D.A. and Asakura, A. (2010) 'Flt-1 haploinsufficiency ameliorates muscular dystrophy phenotype by developmentally increased vasculature in mdx mice', *Hum Mol Genet*, 19(21), pp. 4145-59.

Vuillaumier-Barrot, S., Quijano-Roy, S., Bouchet-Seraphin, C., Maugenre, S., Peudenier, S., Van den Bergh, P., Marcorelles, P., Avila-Smirnow, D., Chelbi, M., Romero, N.B., Carlier, R.Y., Estournet, B., Guicheney, P. and Seta, N. (2009) 'Four Caucasian patients with mutations in the fukutin gene and variable clinical phenotype', *Neuromuscul Disord*, 19(3), pp. 182-8.

Walsh, M.P. (1994) 'Calmodulin and the regulation of smooth muscle contraction', *Mol Cell Biochem*, 135(1), pp. 21-41.

Walton, J.N. and Nattrass, F.J. (1954) 'On the classification, natural history and treatment of the myopathies', *Brain*, 77(2), pp. 169-231.

Wang, M.X., Murrell, D.F., Szabo, C., Warren, R.F., Sarris, M. and Murrell, G.A. (2001) 'Nitric oxide in skeletal muscle: inhibition of nitric oxide synthase inhibits walking speed in rats', *Nitric Oxide*, 5(3), pp. 219-32.

Welser, J.V., Rooney, J.E., Cohen, N.C., Gurpur, P.B., Singer, C.A., Evans, R.A., Haines, B.A. and Burkin, D.J. (2009) 'Myotendinous junction defects and reduced force transmission in mice that lack alpha7 integrin and utrophin', *Am J Pathol*, 175(4), pp. 1545-54.

Westerfield, M. (2000) *The zebrafish book. A guide for the laboratory use of zebrafish (Danio rerio).* Eugene: Univ. of Oregon Press.

Willer, T., Lee, H., Lommel, M., Yoshida-Moriguchi, T., de Bernabe, D.B., Venzke, D., Cirak, S., Schachter, H., Vajsar, J., Voit, T., Muntoni, F., Loder, A.S., Dobyns, W.B., Winder, T.L., Strahl, S., Mathews, K.D., Nelson, S.F., Moore, S.A. and Campbell, K.P. (2012) 'ISPD loss-of-function mutations disrupt dystroglycan O-mannosylation and cause Walker-Warburg syndrome', *Nat Genet*. 44(5), pp. 575-80.

Willer, T., Prados, B., Falcon-Perez, J.M., Renner-Muller, I., Przemeck, G.K., Lommel, M., Coloma, A., Valero, M.C., de Angelis, M.H., Tanner, W., Wolf, E., Strahl, S. and Cruces, J. (2004) 'Targeted disruption of the Walker-Warburg

syndrome gene Pomt1 in mouse results in embryonic lethality', *Proc Natl Acad Sci U S A*, 101(39), pp. 14126-31.

Williamson, R.A., Henry, M.D., Daniels, K.J., Hrstka, R.F., Lee, J.C., Sunada, Y., Ibraghimov-Beskrovnaya, O. and Campbell, K.P. (1997) 'Dystroglycan is essential for early embryonic development: disruption of Reichert's membrane in Dag1-null mice', *Hum Mol Genet*, 6(6), pp. 831-41.

Wilson, S.W. and Rubenstein, J.L. (2000) 'Induction and dorsoventral patterning of the telencephalon', *Neuron*, 28(3), pp. 641-51.

Winder, S.J., Hemmings, L., Maciver, S.K., Bolton, S.J., Tinsley, J.M., Davies, K.E., Critchley, D.R. and Kendrick-Jones, J. (1995) 'Utrophin actin binding domain: analysis of actin binding and cellular targeting', *J Cell Sci*, 108 (Pt 1), pp. 63-71.

Winder, S.J., Lipscomb, L., Angela Parkin, C. and Juusola, M. (2011) 'The proteasomal inhibitor MG132 prevents muscular dystrophy in zebrafish', *PLoS Curr*, 3, p. RRN1286.

Wood, A.J., Lo, T.W., Zeitler, B., Pickle, C.S., Ralston, E.J., Lee, A.H., Amora, R., Miller, J.C., Leung, E., Meng, X., Zhang, L., Rebar, E.J., Gregory, P.D., Urnov, F.D. and Meyer, B.J. (2011a) 'Targeted genome editing across species using ZFNs and TALENs', *Science*, 333(6040), p. 307.

Wood, A.J., Muller, J.S., Jepson, C.D., Laval, S.H., Lochmuller, H., Bushby, K., Barresi, R. and Straub, V. (2011b) 'Abnormal vascular development in zebrafish models for fukutin and FKRP deficiency', *Hum Mol Genet*, 20(24), pp. 4879-90.

Xie, L., Palmsten, K., MacDonald, B., Kieran, M.W., Potenta, S., Vong, S. and Kalluri, R. (2008) 'Basement membrane derived fibulin-1 and fibulin-5 function as angiogenesis inhibitors and suppress tumor growth', *Exp Biol Med (Maywood)*, 233(2), pp. 155-62.

Xu, H., Christmas, P., Wu, X.R., Wewer, U.M. and Engvall, E. (1994) 'Defective muscle basement membrane and lack of M-laminin in the dystrophic dy/dy mouse', *Proc Natl Acad Sci U S A*, 91(12), pp. 5572-6.

Yatsenko, A.S., Gray, E.E., Shcherbata, H.R., Patterson, L.B., Sood, V.D., Kucherenko, M.M., Baker, D. and Ruohola-Baker, H. (2007) 'A putative Src homology 3 domain binding motif but not the C-terminal dystrophin WW domain binding motif is required for dystroglycan function in cellular polarity in Drosophila', *J Biol Chem*, 282(20), pp. 15159-69.

Ylikarppa, R., Eklund, L., Sormunen, R., Kontiola, A.I., Utriainen, A., Maatta, M., Fukai, N., Olsen, B.R. and Pihlajaniemi, T. (2003) 'Lack of type XVIII collagen results in anterior ocular defects', *FASEB J*, 17(15), pp. 2257-9.

Yokota, T., Lu, Q.L., Morgan, J.E., Davies, K.E., Fisher, R., Takeda, S. and Partridge, T.A. (2006) 'Expansion of revertant fibers in dystrophic mdx muscles reflects activity of muscle precursor cells and serves as an index of muscle regeneration', *J Cell Sci*, 119(Pt 13), pp. 2679-87.

York, J. and Nunberg, J.H. (2006) 'Role of the stable signal peptide of Junin arenavirus envelope glycoprotein in pH-dependent membrane fusion', *J Virol*, 80(15), pp. 7775-80.

Yoshida-Moriguchi, T., Yu, L., Stalnaker, S.H., Davis, S., Kunz, S., Madson, M., Oldstone, M.B., Schachter, H., Wells, L. and Campbell, K.P. (2010) 'O-mannosyl phosphorylation of alpha-dystroglycan is required for laminin binding', *Science*, 327(5961), pp. 88-92.

Yoshioka, M. and Kuroki, S. (1994) 'Clinical spectrum and genetic studies of Fukuyama congenital muscular dystrophy', *Am J Med Genet*, 53(3), pp. 245-50.

Young, B., Lowe, J.S., Stevens, A. and Heath, J.W. (eds.) (2006) *Wheater's Functional Histology*. 5 edn. Elsevier.

Yurchenco, P.D. and Cheng, Y.S. (1994) 'Laminin self-assembly: a three-arm interaction hypothesis for the formation of a network in basement membranes', *Contrib Nephrol*, 107, pp. 47-56.

Yurchenco, P.D. and Patton, B.L. (2009) 'Developmental and pathogenic mechanisms of basement membrane assembly', *Curr Pharm Des*, 15(12), pp. 1277-94.

Zenker, M., Aigner, T., Wendler, O., Tralau, T., Muntefering, H., Fenski, R., Pitz, S., Schumacher, V., Royer-Pokora, B., Wuhl, E., Cochat, P., Bouvier, R., Kraus, C., Mark, K., Madlon, H., Dotsch, J., Rascher, W., Maruniak-Chudek, I., Lennert, T., Neumann, L.M. and Reis, A. (2004) 'Human laminin beta2 deficiency causes congenital nephrosis with mesangial sclerosis and distinct eye abnormalities', *Hum Mol Genet*, 13(21), pp. 2625-32.

Zenker, M., Pierson, M., Jonveaux, P. and Reis, A. (2005) 'Demonstration of two novel LAMB2 mutations in the original Pierson syndrome family reported 42 years ago', *Am J Med Genet A*, 138(1), pp. 73-4.

Zhang, J.R., Idanpaan-Heikkila, I., Fischer, W. and Tuomanen, E.I. (1999) 'Pneumococcal licD2 gene is involved in phosphorylcholine metabolism', *Mol Microbiol*, 31(5), pp. 1477-88.

Zhang, W., Betel, D. and Schachter, H. (2002) 'Cloning and expression of a novel UDP-GlcNAc:alpha-D-mannoside beta1,2-N-acetylglucosaminyltransferase homologous to UDP-GlcNAc:alpha-3-D-mannoside beta1,2-N-acetylglucosaminyltransferase I', *Biochem J*, 361(Pt 1), pp. 153-62.

Zhang, Z., Zhang, P. and Hu, H. (2011) 'LARGE expression augments the glycosylation of glycoproteins in addition to alpha-dystroglycan conferring laminin binding', *PLoS One*, 6(4), p. e19080.

Publications Arising From this Work

Wood, A.J., Muller, J.S., Jepson, C.D., Laval, S.H., Lochmuller, H., Bushby, K., Barresi, R. and Straub, V. (2011b) 'Abnormal vascular development in zebrafish models for fukutin and FKRP deficiency', *Hum Mol Genet*, 20(24), pp. 4879-90.